Development of pH-responsive, glycopolymer micelles for DNA delivery

Matthew J. Manganiello

A dissertation

submitted in partial fulfillment of the

requirements for the degree of

Doctor of Philosophy

University of Washington

2012

Reading Committee:

Patrick S. Stayton, Chair

Daniel M. Ratner

Kim A. Woodrow

Program Authorized to Offer Degree:

Bioengineering

University of Washington

Abstract

Development of pH-responsive, glycopolymer micelles for DNA delivery

Matthew J. Manganiello

Chair of the Supervisory Committee:
Professor Patrick S. Stayton
Bioengineering

DNA-based vaccines offer significant therapeutic potential but safe, efficacious delivery systems are still needed to enable clinical applications. Well-defined nonviral vectors, including those produced via reversible addition-fragmentation chain transfer (RAFT) polymerization, represent one approach for overcoming barriers to DNA delivery. Block copolymer micelles are an example of a complex architecture achievable by the RAFT process, adopting a core-shell morphology under physiological conditions. These polymeric nanoparticles consist of discrete segments capable of specific physicochemical and biological activities determined by their chemical composition. This thesis describes synthetic approaches focused on engineering the intra- and extracellular activity of this class of nanomaterials, with the goal of developing an in vivo DNA delivery platform. Chapter 1 focuses on how polymerization and carbohydrate chemistry techniques can be utilized to develop DNA-based cancer vaccines. Chapter 2 introduces a pH-responsive, diblock copolymer micelle platform with a tunable mode of endosomal disruption to facilitate intracellular delivery of DNA. Chapter 3 describes the synthesis of glycopolymers with carbohydrate-specific lectin-binding activity in vivo and in vitro. Chapter 4 incorporates these glycopolymer segments into a micellar architecture and evaluates the bioactivity of these materials. Chapter 5 describes analytical techniques that assess how the chemical composition of the micellar corona affects the stability and physicochemical properties of the resultant particles. Chapter 6 integrates the findings of these previous chapters into the development of glycopolymer micelles and determines their efficacy for in vivo DNA delivery.

TABLE OF CONTENTS

LIST OF FIGURES

LIST OF TABLES

ACKNOWLEDGMENTS

CHAPTER 1 – RATIONAL CARRIER DESIGN: FROM POLYMER TO DNA VACCINE

1.1. INTRODUCTION

Harnessing the body's own immune response to combat cancer represents a significant clinical opportunity but requires the development of efficacious vaccination strategies. Advances in controlled polymerization techniques, carbohydrate chemistry, and cancer immunology have enabled researchers to take a rational approach to designing complex therapeutic vaccines. The precise synthetic control afforded by these recent developments has led to the production of complex polymer architectures displaying carbohydrate-functionalities that can be tailored to suit specific biological needs. Here we describe how these inter-connected fields can be applied to the rational design of a polymer-based, glycotargeted DNA cancer vaccine.

1.2. DNA DELIVERY

Gene therapy is a powerful tool for the treatment of a variety of diseases but its clinical utility has been limited due to challenges in nucleic acid delivery [1], [2]. A commonly employed strategy involves introducing plasmid DNA (pDNA) into the nucleus of a target cell to facilitate endogenous expression of a therapeutically-relevant protein. Numerous extra- and intracellular obstacles impede the efficacious delivery of a large, polyanionic biomacromolecule such as pDNA: extracellular nuclease degradation [3], [4], anionic cell-surface proteoglycans impeding uptake [5], [6], lysosomal degradation upon cell internalization [7–9], and barriers to nuclear translocation [10], [11]. Due to the poor extracellular stability and bioavailability of pDNA, delivery systems have been required to facilitate efficacious DNA delivery.

1.2.1. Synthetic polymers for DNA delivery

The most effective delivery vectors have been viral-based; these systems exploit the pre-existing machinery viruses have established to infect cells [12]. However, non viral-vectors, while typically exhibiting low transfection activities, offer substantial advantages over their viral counterparts, most notably: scalable production, improved safety, and low immunogenicity [13]. Within this class of non-viral vectors are synthetic cationic polymers

which are capable of electrostatically condensing pDNA into particulate complexes, commonly referred to as polyplexes. Significant research has been devoted to pDNA delivery mediated by three polycations: poly(dimethylaminoethyl methacrylate) (polyDMAEMA) [14–21], poly(ethylenimine) (PEI) [22–32], and poly(L-lysine) (PLL) [33–37]. Carrier-specific delivery challenges become important to consider for polyplexes including extracellular DNA unpackaging mediated by serum proteins, soluble glycosaminoglycans, extracellular matrix proteins [38] as well as DNA decomplexation following intracellular delivery [39]. Due to the synthetic versatility of polymer-based delivery systems, design parameters can be rationally selected to address these obstacles.

1.2.2. Overcoming intracellular barriers

Difficulties in achieving high transfection activities for a pDNA delivery system can often be attributed to poor cytosolic delivery of the nucleic acid cargo [40]. Upon endocytosis, pDNA is confined to a vesicular compartment known as an endosome where it is either exocytosed back into the extracellular space or rapidly trafficked through a gradient of increasingly acidic vesicles culminating with the lysosome where degradation occurs. Viruses have evolved mechanisms to subvert this process by displaying fusogenic proteins on their viral coat [41]. These proteins undergo a pH-induced conformational change, becoming hydrophobic in response to low pH environments thereby disrupting the endosomal membranes leading to cytosolic release. Synthetic strategies have been employed to mimic this pH-responsive behavior, including the design of peptides [42] and polymers [43].

Poly(propylacrylic acid) (PPAA) exhibits similar biophysical characteristics to the viral protein hemagglutinin [41]: at physiological pH (~7.4) the polymer is partially ionized and therefore hydrophilic due to the presence of carboxylate residues and at endosomal pH (<6.6) these residues become protonated resulting in a conformational shift to a hydrophobic, membrane-destabilizing morphology. Due to these unique pH-responsive properties, this polymer has been used to facilitate the intracellular delivery of a number of biological therapeutics [44–46]. Cationic polymers also have been shown to promote cytosolic delivery albeit through a different mechanism: the "proton sponge effect". PEI, for example, exhibits the capacity to buffer endosomes: secondary and tertiary amines on the polymer become protonated during endocytotic trafficking resulting in an influx of counter ions into

the vesicle. The charge gradient across the endosomal membrane induces osmotic swelling and ultimately, perturbation of the membrane facilitating cytosolic release [47].
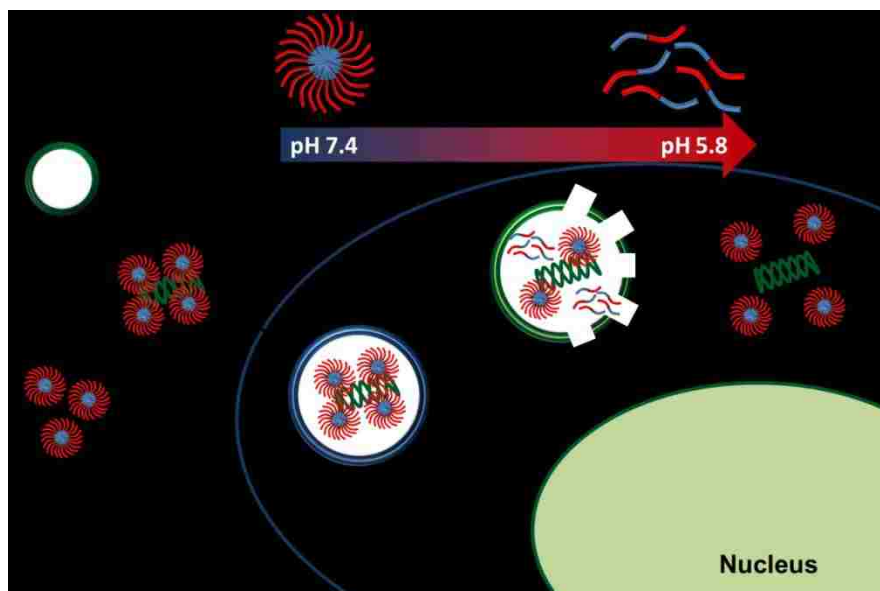
Figure 1.1. Polyplex-mediated DNA delivery by cationic micelles which become membrane-interactive upon endosomal acidification [48]. This pH-responsive endosomolytic activity is due to the exposure of hydrophobic components on the polymer when the micelle destabilizes into an unimeric conformation.

1.2.3. Reversible addition-fragmentation chain transfer (RAFT) polymerization

Rational design of polymers capable of exhibiting specific biological activities requires precise synthetic control. Traditional free radical polymerization is capable of utilizing numerous vinyl-containing monomers with unique chemical functionalities but is limited by the heterogeneity of the resultant polymers. Controlled, or "living", radical polymerization (CLRP) overcomes this issue by controlling the rate of polymer propagation. One such technique, reversible addition-fragmentation chain transfer (RAFT) polymerization [49], is a powerful tool in the field of drug delivery due to its tolerance for a broad range of monomer species and the unique pendent and terminal functionalization it affords [50]. The primary difference between RAFT and traditional free radical polymerization is the use of a chain transfer agent (CTA), which typically contains a thiocarbonylthio group. Briefly, the CTA facilitates uniform polymer chain growth by forming intermediate radicals with two propagating polymer chains. This intermediate can fragment in either direction creating an equilibrium between dormant macroCTAs and polymeric radicals. This process reduces the relative concentration of free radicals in solution, limiting termination and uncontrolled

polymer propagation. Additionally, the macroCTA exhibits a "living" character and can be isolated for subsequent block polymerizations. A wide range of chemistries can also be applied to the CTA resulting in terminal polymer functionalities [51]. Polymers prepared via RAFT can therefore exhibit complex architectures with precise molecular weights and narrow size distributions while also displaying numerous pendent and terminal chemical moieties.
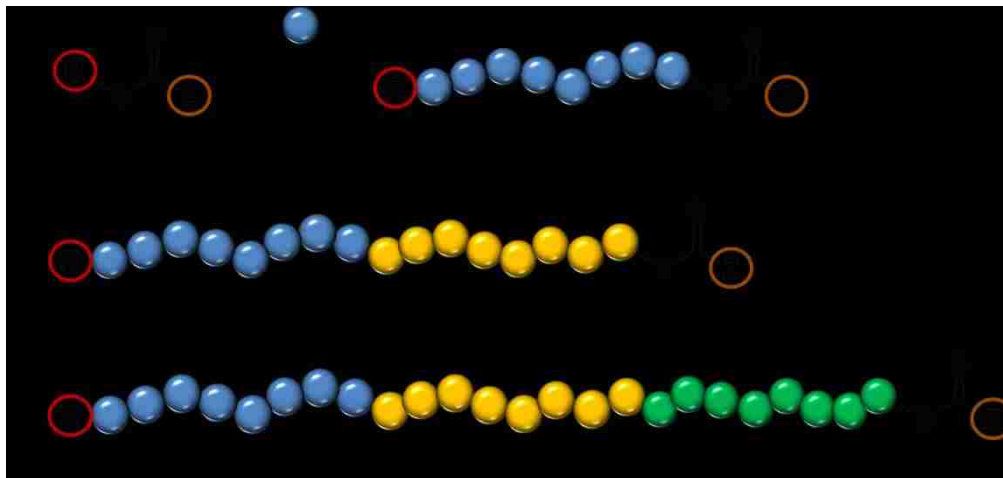
Figure 1.2. Illustration of multiblock polymers prepared via RAFT. Each block can contain monomers with unique functional groups.

1.2.4. Block copolymers for DNA delivery

Copolymers consisting of blocks with distinct functionalities have generated great interest in the DNA delivery community. Initially, these materials were explored as a means to sterically stabilize polycation-based polyplexes [52]. Kataoka et al. first examined the effect of introducing a poly(ethylene glycol) (PEG) block onto PLL and found that the block copolymer assembled into polyion complex micelles in the presence of oligonucleotides [53]. The resultant micelles displayed a PEG corona and were stable under physiological salt concentrations. This approach of producing diblock copolymers with a neutral hydrophilic and polycation component to induce stable micelle formation have been thoroughly investigated for DNA delivery applications [54].

1.2.4.1. Amphiphilic block copolymers

Amphiphilic block copolymers represent a unique polymer architecture in which one block is hydrophilic and the other is hydrophobic. In an aqueous environment these materials have

been shown to self-assemble into a core-shell micelle structure due to entropically-driven sequestration of the hydrophobic components [55]. The resultant particles are stabilized by a corona of the hydrophilic block allowing the micelles to remain soluble. Micelles prepared in this manner are considerably more stable as critical micelle concentrations (CMCs) can be as low as the μM-range; this structural property increases their clinical utility due to the inherent dilution the material would experience in a biological application [56]. Yokoyama et al. were first able to demonstrate the application of polymeric micelles for anti-cancer therapies by conjugating doxorubicin to a hydrophilic segment of a block copolymer, resulting in stable amphiphilic block copolymer micelles [57].

1.2.4.2. Stimuli-responsive cationic micelles

Cationic micelles prepared from amphiphilic block copolymers offer a means to preserve the DNA-condensing activity of the polycation while introducing a pH-sensitive functionality to overcome the endosomal/lysosomal intracellular barrier (**Figure 1**). You et al. reports on diblock copolymers consisting of pDMAEMA and poly(*N*-isopropylacrylamide) (pNIPAM) prepared via RAFT that assembled into core-shell micelles with pDMAEMA acting as the stabilizing, hydrophilic component [58]. The authors demonstrated that changing the protonation state of pDMAEMA, by adjusting the pH, affected the ability of the block to stabilize the micelle as observed by a shift in the phase transition temperature of the copolymer. A polymer similar to pDMAEMA, poly(diethylaminoethyl methacrylate) (pDEAEMA), has a predominately hydrophobic character at physiological pH while retaining a tertiary amine [59–61]. Tang et al. first demonstrated that pDEAEMA could be used to drive micelle formation of triblock copolymers in an aqueous environment and that destabilization of the particles occurred in a pH-dependent manner [62]. Research led by Irvine showed that segments of pDEAEMA in core-shell nanoparticles responded in the endosomal/lysosomal pH range by mediating cytosolic release of a membrane-impermeable dye [63]. Convertine et al. demonstrated that pDMAEMA blocked with a polyampholyte copolymer consisting of DMAEMA, PAA, and butyl methacrylate (BMA) formed stable micelles that became membrane-destabilizing at endosomal pH (<6.6) [64]; small interfering RNA (siRNA) was electrostatically adsorbed to the micelle corona and the resultant particles were shown to mediate potent knockdown of mRNA in vitro.

Figure 1.3. Mechanism of pH-responsive activity for an amphiphilic diblock copolymer [48]. Reduction in solution pH from physiological conditions promotes protonation of DEAEMA residues within the micelle core which leads to destabilization of the particulate morphology to individual solvated unimeric chains at a critical transition pH. The unimeric conformation exposes BMA residues that can interact with lipid membranes.

1.2.5. Polymer-mediated in vivo DNA delivery

Notable challenges exist in translating the high transfection efficiencies of synthetic DNA delivery systems in culture into a clinically relevant in vivo environment. The commonly employed approach of packaging DNA with cationic components is advantageous in vitro as these materials can shield the labile nucleic acid from degradation, mediate uptake through adsorptive pincocytosis, and disrupt endosomal membranes via the "proton sponge" effect [1]. However, the presence of this cationic charge becomes a liability in complex biological media as anionic extracellular proteins can interact with the positively-charged complexes, leading to DNA unpackaging or aggregation. van den Berg et al. highlighted this in vitro/in vivo discordance by demonstrating that a cationic polymer with high transfection activity in culture was only able to mediate DNA expression in vivo after PEGylation [65]. Palumbo et al. arrived at a similar finding by showing that PEGylated polyplexes can better disperse through dermal tissue and access APCs when compared to their cationic counterpart [66]. Strategies to attenuate surface charge of polyplexes and to impart cell-specific targeting are being investigated to improve the clinical potential of DNA delivery carriers for vaccine applications [67–69].

6

1.3. CARBOHYDRATES AS TARGETING LIGANDS

The targeted delivery of biologics and small molecule drugs can dramatically improve therapeutic efficacy through enhancing uptake to the specific cell type where the drug will exert maximal effect [70]. Developing targeting moieties capable of selectively recognizing particular cell types while avoiding detection and uptake towards nonspecific tissue has remained a challenge. Modification of carriers with carbohydrates offers a means to mediate drug uptake through cell-surface lectins while maintaining biocompatibility [71]. Carbohydrates are known to play roles in the cell-cell interactions of immune cells as well as marking foreign pathogens for immune cell recognition. The latter activity can be exploited to direct uptake of carriers into these immune cell populations by mimicking complex pathogenic carbohydrate structures [72].

1.3.1. Immune cell recognition by C-type lectins

C-type lectins represent a class of carbohydrate-binding proteins which depend upon Ca^{2+} ions to maintain sugar engagement [73]. All these proteins contain at least one carbohydrate recognition domain (CRD) that exhibits optimal affinity towards specific carbohydrates. Carbohydrates have a low affinity towards a single CRD, with dissociation constants in the low millimolar range [74]. Natural saccharides overcome these weak binding events by clustering multiple glycosides together, thereby allowing multivalent interactions to be made with lectins leading to a significant increase in overall affinity [75]. Carbohydrate-based ligands capable of mediating high levels of binding towards C-type lectins must be capable of multivalent CRD-engagement [76]. Dendritic cells (DCs) and macrophages express a range of C-type lectins that are able to internalize bound material [77], two of which (macrophage mannose receptor (MMR) and langerin) will be discussed in greater detail.

1.3.1.1. MMR

MMR (alternatively known as CD206) is an endocytic C-type lectin containing 8 individual CRDs [78]. Ligands capable of mediating multivalent binding through simultaneous engagement of multiple CRDs on MMR have shown to be potent facilitators of macrophage-specific uptake [79]. While mannose displays the highest affinity toward MMR CRDs, other sugars (e.g. fucose, *N*-acetylglucosamine (GlcNAc), and glucose) are additionally recognized by these lectin-like domains [80]. For oligosaccharides, the terminal sugar has

been shown to dictate the binding affinity [81]. The CRD of a related C-type lectin, the mannose binding protein (MBP), is known to exhibit the same broad carbohydrate-binding specificities due to the majority of the interaction's binding affinity being attributed to two vicinal, equatorial hydroxyl groups that are shared between different sugars [82]. MMR is found on both macrophages and subsets of DCs [83].

1.3.1.2. Langerin

Langerin (also known as CD207) is expressed predominantly on a subpopulation of skin DCs, referred to as Langerhans cells (LCs) [84]. The lectin displays high affinity for high mannose structures while also recognizing fucose and GlcNAc-containing carbohydrates [85], [86]. This receptor is primarily tasked with scavenging for foreign pathogens, e.g. viruses, which often display high mannose surface structures [87], [88]. The extracellular domain of langerin contains a single CRD while the remainder of the region mediates trimer formation [89]. Due to the low affinity of the CRD to a monosaccharide, langerin trimerization is important to generate an avidity effect by facilitating multivalent engagement of oligosaccharides [73]. Antigens internalized via langerin on LCs are capable of mediating potent CD4$^+$ and CD8$^+$ T cell responses [90], [91], an important consideration for vaccine design as will be discussed later on [92], [93].

1.3.2 RAFT Glycopolymers

Glycosylation of drug delivery systems is an attractive strategy to impart targeting specificity but can be synthetically challenging and may not facilitate multivalent lectin engagement. Synthetic glycopolymers provide a promising platform to antagonize lectin-like receptors through the presentation of multiple pendent carbohydrates (**Figure 1.2**) [71]. While such compounds have been previously synthesized to probe lectin-carbohydrate binding behavior [94], only recently have strategies to produce structurally well-defined, homogeneous glycopolymers capable of multivalent interactions been realized [95]. One technique involves the functionalization of an individual carbohydrate ring with a vinyl-containing compound resulting in a glycomonomer; subsequent free radical polymerization yields a glycopolymer with pendent carbohydrates. By combining RAFT with glycomonomer synthetic chemistry, glycopolymers with complex architectures and narrow molecular weight distributions are achievable [96]. Alternatively, post-polymerization conjugations can be

performed on non-carbohydrate RAFT polymers to yield materials bearing telechelic or pendent glycomoieties [97].

Lowe et al. first demonstrated the successful RAFT polymerization of a glycopolymer by using glucose-functionalized methacrylate monomer in aqueous conditions; the resultant material exhibited a narrow polydispersity and displayed "living" properties characteristic of the RAFT technique [98].   Since then there have been numerous reports of RAFT glycopolymers in the literature [71].   Notable among others, Albertin et al. developed hydrophilic block copolymers using an enzymatically produced glycomonomer [99], and later extended this work to create block copolymers consisting of different pendent sugar moieties [100].   Complex architectures have been demonstrated by the RAFT process including glycopolymer micelles [101], glycopolymer stars [95], multi-functional glyconanoparticles [102], and "clickable" glycopolymers [103].
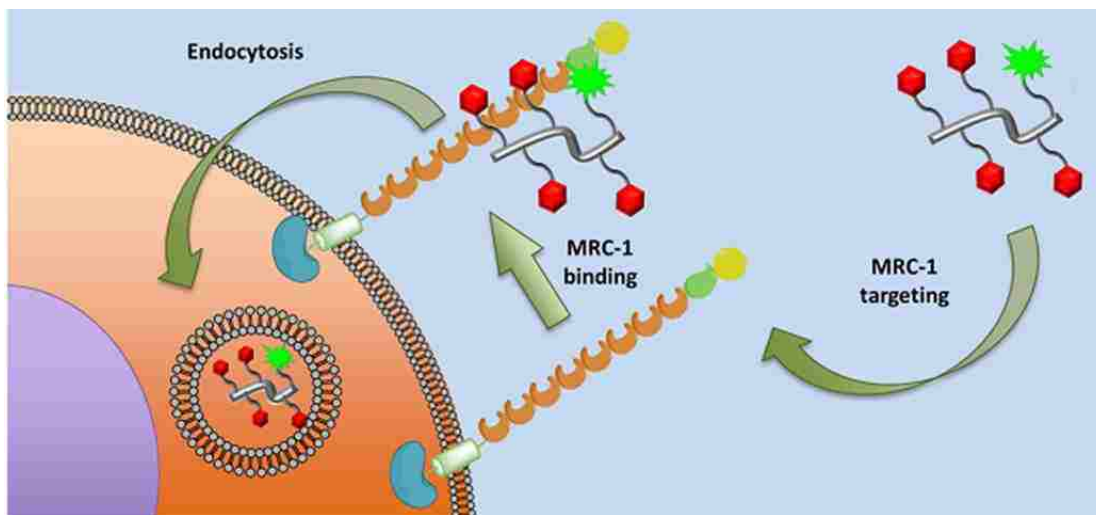
Figure 1.4. Delivery of a polymer displaying pendent carbohydrates and a fluorescent label to a MMR-expressing cell [104]. The glycopolymer is capable of multivalent engagement of the MMR CRDs leading to receptor-mediated endocytosis upon lectin binding.

1.3.3. Glycopolymer-mediated DNA delivery

The synthetic toolbox developed for the creation of multivalent carbohydrate ligands has enabled the design of targeted DNA delivery systems.   While RAFT has not been extensively utilized to produce the carbohydrate modifications, alternatively prepared glycosylated polymeric materials still have exhibited great potential for their ability to enhance internalization into select cell populations [105].   Wu et al. first reported on the

ability to modify synthetic polymers with carbohydrate moieties by demonstrating cell-specific receptor-mediated endocytosis of DNA by attaching a galactose-containing glycoprotein, asialoorosomucoid (ASOR), onto a polycation, PLL [106].   The resultant glycotargeted polyplexes exhibited preferential uptake into asialoglycoprotein receptor-positive hepatic cells.   While there have been numerous successful glycosylated gene delivery systems developed to target hepatocytes [15], [107], [108], enhancing DNA uptake into immune cells is desired for vaccination strategies. Ferkol et al. were the first to deliver DNA to murine macrophages by synthesizing a mannosylated PLL carrier [109]; similar carriers exhibited high transfection efficiency by human blood monocyte-derived macrophages [110]. Polyamidoamine-based dendrimers modified with mannose displayed high DNA transfection activity across multiple cell types [111], [112]. Hashimoto et al. was able to develop mannosylated chitosan carriers which were able to mediate high pDNA expression levels in murine peritoneal macrophages [113]. An important note from this work was the mitigation of nonspecific, polycation-mediated toxicity; this finding is often observed with reports of cationic materials that have been modified with carbohydrates [114–116].

1.4. CANCER IMMUNOTHERAPY

1.4.1. Cancer vaccine strategies

Harnessing the body's own immune system to combat cancer has been a promising strategy to address aggressive malignancies, garnering much interest in the medical community [117]. Vaccination is one route of immunotherapy that can be exploited to prime the immune system towards anti-cancer activity [118]. While tumor-associated antigens (TAAs) are continuously expressed within the tumor, the aforementioned immunosuppression prevents a viable adaptive immune response from evolving. This immune response will arise when antigen presenting cells (APCs) process antigens, either endogenously or exogenously, into peptide fragments which associate with MHCs that are ultimately presented on the cell surface. The class of the MHC determines which effector population can recognize the peptide-MHC ensemble: class I by CD8+ and class II by CD4+ T cells. Proper costimulation by the APCs will then activate the T cells towards the appropriate antigen-specific effector function. The goal of cancer vaccination is to exploit this immune machinery to develop long-lasting TAA-specific immunity by first delivering tumor-specific antigenic material to APCs [119].

While the generation of anti-tumor CD8$^+$ cytotoxic T lymphocytes (CTLs) is ultimately desirable to treat cancer, the direct activation of these cells has proven not as effective as originally envisioned [117], [119]. Understanding the intricate cooperation between multiple lymphocytes of the adaptive and innate immune response has provided insight into cancer immunotherapy: specifically, the role Th1 cells play on immunomodulating the tumor microenvironment [120]. Activated Th1 cells specific to TAAs, will accumulate at the tumor site and secrete cytokines which upregulate endogenous antigen presentation [121] and recruit innate immune cells [122]. This activity can tilt the balance from anti- to pro-inflammatory within the tumor, greatly improving the clinical outcome. Th1 cells have additionally been shown to direct the proliferation of anti-tumor CTL populations [123], [124] and drive epitope spreading [125], a phenomena which expands the antigen base for effector cells to act upon. Generating a significant TAA-specific Th1 response is therefore of great importance when developing cancer vaccination strategies.

1.4.2. DNA vaccines

Vaccines can supply antigenic material in the form of full proteins, peptides, or DNA. The latter can be advantageous as DNA has the capacity to express TAAs in the form of the full antigen or as fragments of MHC-specific peptides or domains [126]. As producing recombinant proteins and synthesizing peptides can be costly and may present stability issues, DNA becomes particularly attractive for clinical applications due to its low cost of production and scalability [127]. Multiple peptide epitopes have been encoded into a single plasmid DNA (pDNA) construct; these polyepitope pDNA are capable of eliciting broad anti-tumor specificity [128]. Once transfected into either an APC or off-target cell, DNA can provide a depot for in situ transient TAA expression with the antigen being processed endogenously by the host cell or secreted for exogenous presentation by a different cell [129].

While antigens expressed endogenously by pDNA are classically understood to present predominantly on MHC class I, and therefore elicit a predominantly CD8$^+$ T cell effector response, mechanisms of cross-presentation have been demonstrated which allow for MHC class II presentation (**Figure 1.3**) [130]. Therefore, not only can DNA vaccines promote a CD4+ T helper response, but they are known to bias activation towards a Th1 phenotype. Multiple independent studies investigating DNA vaccines administered in mice have found

11

expression of the Th1-like cytokines interleukin-2 (IL-2) and the type II interferon, interferon-γ (IFN-γ) by CD4$^+$ T cells while low levels of Th2-specific cytokine, interleukin-4 (IL-4) are observed [131–134]. These findings provide a rationale to utilize DNA vectors in cancer immunotherapy since, as described previously, eliciting potent Th1 responses can result in immunomodulation of the tumor microenvironment initiating an immunological cascade that can lead to tumor regression.
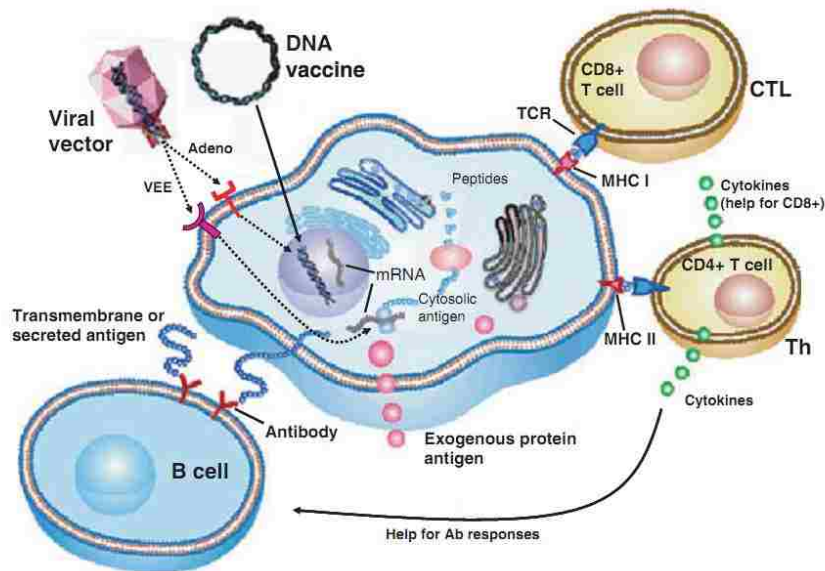
Figure 1.5. The robust immune response afforded by DNA vaccines [130]. APCs transfected with DNA vaccines can directly activate naïve CD8$^+$ (CTL) and CD4$^+$ (Th) T cells and indirectly activate B cells.

1.4.2.1. DNA vaccine clinical trails

While therapeutic DNA vaccines have been licensed for animal use, no such immunotherapy has yet advanced through human clinical trials [130]. The first DNA vaccine to enter phase I clinical trials encoded proteins from human immunodeficiency virus 1 (HIV-1) which was promptly followed by multiple vaccines against various forms of cancer and infectious diseases [135], [136]. However, this initial wave of DNA-based therapeutics exhibited relatively low immunogenicity, prompting the development of new strategies to administer the nucleic acid. These approaches have examined both the immunomodulatory aspects and the delivery challenges of DNA vaccines. As an example of these recent technologies, a successful phase I trial evaluating a trivalent influenza vaccine utilized the PMED device [137], an instrument that bombards the skin with pDNA-linked gold particles

[138]. For HIV-1 vaccines, heterologous prime-boost regimens have been explored that incorporate recombinant protein vaccines with DNA and viral vectors. A HIV-1-specific efficacy trial that showed improvement in viral acquisition protection involved priming the subject with a viral vector followed by a boost of recombinant gp120 [139]. Adjuvanting DNA-based vaccines with immunostimulatory agents has also been a promising approach to improve upon the limited immunogenicity of free DNA. A phase I HIV-1 trial investigated electroporation-mediated delivery of a DNA vaccine expressing three viral envelope proteins co-administered with the cytokine, interleukin 12 (IL-12) [140]. As of 2011, there were 43 ongoing clinical trials examining DNA vaccines with 33% of those investigating HIV and 29% targeting cancer (**Table 1.1**).

Table 1.1. Current DNA vaccine clinical trials [136].

Phase	#	Targets
I	31	HIV, influenza, HPV, cancer (metastatic breast, B cell lymphoma, prostate, colorectal), hepatitis B, hepatitis C, malaria
I/II	7	HIV, cancer (prostate, colorectal), hepatitis B, hepatitis C, HPV, malaria
II	5	HIV, Cancer (prostate, melanomal), hepatitis B

1.5. REFERENCES

[1] D. W. Pack, A. S. Hoffman, S. Pun, and P. S. Stayton, "Design and development of polymers for gene delivery.," *Nature reviews. Drug discovery*, vol. 4, no. 7, pp. 581–93, Jul. 2005.

[2] D. Schaffert and E. Wagner, "Gene therapy progress and prospects: synthetic polymer-based systems.," *Gene therapy*, vol. 15, no. 16, pp. 1131–8, Aug. 2008.

[3] P. R. Dash, V. Toncheva, E. Schacht, and L. W. Seymour, "Synthetic polymers for vectorial delivery of DNA : characterisation of polymer-DNA complexes by photon correlation spectroscopy and stability to nuclease degradation and disruption by polyanions in vitro," *Water*, vol. 48, pp. 269–276, 1997.

[4] S. Katayose and K. Kataoka, "Water-soluble polyion complex associates of DNA and poly(ethylene glycol)-poly(L-lysine) block copolymer.," *Bioconjugate chemistry*, vol. 8, no. 5, pp. 702–7, 1997.

[5] K. a Mislick and J. D. Baldeschwieler, "Evidence for the role of proteoglycans in cation-mediated gene transfer.," *Proceedings of the National Academy of Sciences of the United States of America*, vol. 93, no. 22, pp. 12349–54, Oct. 1996.

[6] D. V Schaffer and D. a Lauffenburger, "Optimization of cell surface binding enhances efficiency and specificity of molecular conjugate gene delivery.," *The Journal of biological chemistry*, vol. 273, no. 43, pp. 28004–9, Oct. 1998.

[7] H. Pollard, J. S. Remy, G. Loussouarn, S. Demolombe, J. P. Behr, and D. Escande, "Polyethylenimine but not cationic lipids promotes transgene delivery to the nucleus in mammalian cells," *The Journal of biological chemistry*, vol. 273, no. 13, pp. 7507–11, Mar. 1998.

[8]   A. Raft, D. B. Thomas, A. J. Convertine, L. J. Myrick, C. W. Scales, A. E. Smith, A. B. Lowe, Y. A. Vasilieva, N. Ayres, and C. L. Mccormick, "Kinetics and Molecular Weight Control of the Polymerization of," *Synthesis*, pp. 8941–8950, 2004.

[9]   M. L. Forrest and D. W. Pack, "On the Kinetics of Polyplex Endocytic Trafficking : Implications for Gene Delivery Vector Design," *Gene Therapy*, vol. 6, no. 1, pp. 57–66, 2002.

[10]   D. a Dean, "Import of plasmid DNA into the nucleus is sequence specific.," *Experimental cell research*, vol. 230, no. 2, pp. 293–302, Feb. 1997.

[11]   J. Vacik, B. S. Dean, W. E. Zimmer, and D. a Dean, "Cell-specific nuclear import of plasmid DNA.," *Gene therapy*, vol. 6, no. 6, pp. 1006–14, Jun. 1999.

[12]   D. Grimm and M. a Kay, "From virus evolution to vector revolution: use of naturally occurring serotypes of adeno-associated virus (AAV) as novel vectors for human gene therapy.," *Current gene therapy*, vol. 3, no. 4, pp. 281–304, Aug. 2003.

[13]   D. Luo and W. M. Saltzman, "Synthetic DNA delivery systems.," *Nature biotechnology*, vol. 18, no. 1, pp. 33–7, Jan. 2000.

[14]   P. van de Wetering, E. E. Moret, N. M. Schuurmans-Nieuwenbroek, M. J. van Steenbergen, and W. E. Hennink, "Structure-activity relationships of water-soluble cationic methacrylate/methacrylamide polymers for nonviral gene delivery.," *Bioconjugate chemistry*, vol. 10, no. 4, pp. 589–97, 1999.

[15]   D. W. Lim, Y. I. Yeom, and T. G. Park, "Poly(DMAEMA-NVP)-b-PEG-galactose as gene delivery vector for hepatocytes.," *Bioconjugate chemistry*, vol. 11, no. 5, pp. 688–95, 2000.

[16]   L. Veron, A. Ganée, C. Ladavière, and T. Delair, "Hydrolyzable p(DMAPEMA) polymers for gene delivery.," *Macromolecular bioscience*, vol. 6, no. 7, pp. 540–54, Jul. 2006.

[17]   Y. Z. You, D. S. Manickam, Q. H. Zhou, and D. D. A. Oupicky, "Reducible poly(2-dimethylaminoethyl methaerylate): Synthesis, cytotoxicity, and gene delivery activity," *Journal of Controlled Release*, vol. 122, no. 3, pp. 217–225, 2007.

[18]   R. Sharma, J. Lee, R. C. Bettencourt, C. Xiao, S. F. Konieczny, and Y.-Y. Won, "Effects of the incorporation of a hydrophobic middle block into a PEG-polycation diblock copolymer on the physicochemical and cell interaction properties of the polymer-DNA complexes.," *Biomacromolecules*, vol. 9, no. 11, pp. 3294–307, Nov. 2008.

[19]   A. J. Convertine, D. S. W. Benoit, C. L. Duvall, A. S. Hoffman, and P. S. Stayton, "Development of a novel endosomolytic diblock copolymer for siRNA delivery.," *Journal of Controlled Release*, vol. 133, no. 3, pp. 221–9, Feb. 2009.

[20]   C. Zhu, S. Jung, S. Luo, F. Meng, X. Zhu, T. G. Park, and Z. D. Zhong, "Co-delivery of siRNA and paclitaxel into cancer cells by biodegradable cationic micelles based on PDMAEMA-PCL-PDMAEMA triblock copolymers.," *Biomaterials*, vol. 31, no. 8, pp. 2408–16 ST – Co–delivery of siRNA and paclitaxel, 2010.

[21]   C. H. Zhu, S. Jung, G. Y. Si, R. Cheng, F. H. Meng, X. L. Zhu, T. G. Park, and Z. Y. Zhong, "Cationic Methacrylate Copolymers Containing Primary and Tertiary Amino Side Groups: Controlled Synthesis via RAFT Polymerization, DNA Condensation, and In Vitro Gene Transfection," *Journal of Polymer Science Part a-Polymer Chemistry*, vol. 48, no. 13, pp. 2869–2877, 2010.

[22]   Q. Peng, Z. Zhong, and R. Zhuo, "Disulfide cross-linked polyethylenimines (PEI) prepared via thiolation of low molecular weight PEI as highly efficient gene vectors.," *Bioconjugate chemistry*, vol. 19, no. 2, pp. 499–506, Feb. 2008.

[23]   S. Werth, B. Urban-Klein, L. Dai, S. Höbel, M. Grzelinski, U. Bakowsky, F. Czubayko, and A. Aigner, "A low molecular weight fraction of polyethylenimine (PEI) displays increased transfection efficiency of DNA and siRNA in fresh or lyophilized complexes.," *Journal of Controlled Release*, vol. 112, no. 2, pp. 257–70, May 2006.

[24] B. Urban-Klein, S. Werth, S. Abuharbeid, F. Czubayko, and a Aigner, "RNAi-mediated gene-targeting through systemic application of polyethylenimine (PEI)-complexed siRNA in vivo.," *Gene therapy*, vol. 12, no. 5, pp. 461–6, Mar. 2005.

[25] A. Zintchenko, A. Philipp, A. Dehshahri, and E. Wagner, "Simple modifications of branched PEI lead to highly efficient siRNA carriers with low toxicity.," *Bioconjugate chemistry*, vol. 19, no. 7, pp. 1448–55, Jul. 2008.

[26] M. S. Shim and Y. J. Kwon, "Controlled delivery of plasmid DNA and siRNA to intracellular targets using ketalized polyethylenimine.," *Biomacromolecules*, vol. 9, no. 2, pp. 444–55, Feb. 2008.

[27] O. M. Merkel, O. Germershaus, C. K. Wada, P. J. Tarcha, T. Merdan, and T. Kissel, "Integrin alphaVbeta3 targeted gene delivery using RGD peptidomimetic conjugates with copolymers of PEGylated poly(ethylene imine).," *Bioconjugate chemistry*, vol. 20, no. 6, pp. 1270–80, Jun. 2009.

[28] J. Fahrmeir, M. Gunther, N. Tietze, E. Wagner, and M. Ogris, "Electrophoretic purification of tumor-targeted polyethylenimine-based polyplexes reduces toxic side effects in vivo.," *Journal of Controlled Release*, vol. 122, no. 3, pp. 236–45, Oct. 2007.

[29] P. J. Tarcha, J. Pelisek, T. Merdan, J. Waters, K. Cheung, K. von Gersdorff, C. Culmsee, and E. Wagner, "Synthesis and characterization of chemically condensed oligoethylenimine containing beta-aminopropionamide linkages for siRNA delivery.," *Biomaterials*, vol. 28, no. 25, pp. 3731–40, Sep. 2007.

[30] L. V Christensen, C.-W. Chang, W. J. Kim, S. W. Kim, Z. Zhong, C. Lin, J. F. J. Engbersen, and J. Feijen, "Reducible poly(amido ethylenimine)s designed for triggered intracellular gene delivery.," *Bioconjugate chemistry*, vol. 17, no. 5, pp. 1233–40, 2006.

[31] Q. Peng, C. Hu, J. Cheng, Z. Zhong, and R. Zhuo, "Influence of disulfide density and molecular weight on disulfide cross-linked polyethylenimine as gene vectors.," *Bioconjugate chemistry*, vol. 20, no. 2, pp. 340–6, Feb. 2009.

[32] H. Jiang, Y.-K. Kim, R. Arote, D. Jere, J.-S. Quan, J.-H. Yu, Y.-J. Choi, J.-W. Nah, M.-H. Cho, and C.-S. Cho, "Mannosylated chitosan-graft-polyethylenimine as a gene carrier for Raw 264.7 cell targeting.," *International journal of pharmaceutics*, vol. 375, no. 1–2, pp. 133–9, Jun. 2009.

[33] C. Aral and J. Akbuga, "Preparation and in vitro transfection efficiency of chitosan microspheres containing plasmid DNA:poly(L-lysine) complexes.," *Journal of pharmacy & pharmaceutical sciences*, vol. 6, no. 3, pp. 321–6, 2003.

[34] Y. Guo, Y. Sun, J. Gu, and Y. Xu, "Capillary electrophoresis analysis of poly(ethylene glycol) and ligand-modified polylysine gene delivery vectors.," *Analytical biochemistry*, vol. 363, no. 2, pp. 204–9, Apr. 2007.

[35] T. Kawano, T. Okuda, H. Aoyagi, and T. Niidome, "Long circulation of intravenously administered plasmid DNA delivered with dendritic poly(L-lysine) in the blood flow.," *Journal of Controlled Release*, vol. 99, no. 2, pp. 329–37, Sep. 2004.

[36] T.-G. Kim, S.-Y. Kang, J.-H. Kang, M.-Y. Cho, J.-I. Kim, S.-H. Kim, and J.-S. Kim, "Gene transfer into human hepatoma cells by receptor-associated protein/polylysine conjugates.," *Bioconjugate chemistry*, vol. 15, no. 2, pp. 326–32, 2004.

[37] M. L. Read, S. Singh, Z. Ahmed, M. Stevenson, S. S. Briggs, D. Oupicky, L. B. Barrett, R. Spice, M. Kendall, M. Berry, J. a Preece, A. Logan, and L. W. Seymour, "A versatile reducible polycation-based system for efficient delivery of a broad range of nucleic acids.," *Nucleic acids research*, vol. 33, no. 9, p. e86, Jan. 2005.

[38] R. S. Burke and S. H. Pun, "Extracellular barriers to in Vivo PEI and PEGylated PEI polyplex-mediated gene delivery to the liver.," *Bioconjugate chemistry*, vol. 19, no. 3, pp. 693–704, Mar. 2008.

[39] P. Erbacher, a C. Roche, M. Monsigny, and P. Midoux, "The reduction of the positive charges of polylysine by partial gluconoylation increases the transfection efficiency of polylysine/DNA complexes.," *Biochimica et biophysica acta*, vol. 1324, no. 1, pp. 27–36, Feb. 1997.

[40]   A. El Ouahabi, M. Thiry, V. Pector, R. Fuks, J. M. Ruysschaert, and M. Vandenbranden, "Polyethylenimine but not cationic lipids promotes transgene delivery to the nucleus in mammalian cells.," *FEBS letters*, vol. 414, no. 2, pp. 187–92, Sep. 1997.

[41]   D. C. Wiley and J. J. Skehel, "The structure and function of the hemagglutinin membrane glycoprotein of influenza virus," *Annual review of biochemistry*, vol. 56, no. 1, pp. 365–394, 1987.

[42]   C. Plank, B. Oberhauser, K. Mechtler, C. Koch, and E. Wagner, "The influence of endosome-disruptive peptides on gene transfer using synthetic virus-like gene transfer systems.," *The Journal of biological chemistry*, vol. 269, no. 17, pp. 12918–24, Apr. 1994.

[43]   N. Murthy, I. Chang, P. Stayton, and A. Hoffman, "pH-sensitive hemolysis by random copolymers of alkyl acrylates and acrylic acid," in *Macromolecular Symposia*, 2001, vol. 172, no. 1, pp. 49–56.

[44]   N. Murthy, J. R. Robichaud, D. A. Tirrell, P. S. Stayton, and A. S. Hoffman, "The design and synthesis of polymers for eukaryotic membrane disruption.," *Journal of Controlled Release*, vol. 61, no. 1–2, pp. 137–43, Aug. 1999.

[45]   C. A. Lackey, O. W. Press, A. S. Hoffman, and P. S. Stayton, "A biomimetic pH-responsive polymer directs endosomal release and intracellular delivery of an endocytosed antibody complex.," *Bioconjugate chemistry*, vol. 13, no. 5, pp. 996–1001, 2002.

[46]   M. E. H. El-Sayed, A. S. Hoffman, and P. S. Stayton, "Rational design of composition and activity correlations for pH-sensitive and glutathione-reactive polymer therapeutics.," *Journal of controlled release : official journal of the Controlled Release Society*, vol. 101, no. 1–3, pp. 47–58, Jan. 2005.

[47]   O. Boussif, F. Lezoualc'h, M. a Zanta, M. D. Mergny, D. Scherman, B. Demeneix, and J. P. Behr, "A versatile vector for gene and oligonucleotide transfer into cells in culture and in vivo: polyethylenimine.," *Proceedings of the National Academy of Sciences of the United States of America*, vol. 92, no. 16, pp. 7297–301, Aug. 1995.

[48]   M. J. Manganiello, C. Cheng, A. J. Convertine, J. D. Bryers, and P. S. Stayton, "Diblock copolymers with tunable pH transitions for gene delivery.," *Biomaterials*, vol. 33, no. 7, pp. 2301–9, Mar. 2012.

[49]   J. Chiefari, Y. (Bill) Chong,, and F. Ercole, "Living free-radical polymerization by reversible addition-fragmentation chain transfer: the RAFT process," vol. 9297, no. 2, pp. 5559–5562, 1998.

[50]   A. W. York, S. E. Kirkland, and C. L. McCormick, "Advances in the synthesis of amphiphilic block copolymers via RAFT polymerization: stimuli-responsive drug and gene delivery.," *Advanced drug delivery reviews*, vol. 60, no. 9, pp. 1018–36, Jun. 2008.

[51]   C. Boyer, V. Bulmus, T. P. Davis, V. Ladmiral, J. Liu, and S. Perrier, "Bioapplications of RAFT polymerization," *Chemical Reviews*, vol. 109, no. 11, pp. 5402–5436, 2009.

[52]   K. Kataoka, a Harada, and Y. Nagasaki, "Block copolymer micelles for drug delivery: design, characterization and biological significance.," *Advanced drug delivery reviews*, vol. 47, no. 1, pp. 113–31, Mar. 2001.

[53]   K. Kataoka, H. Togawa, A. Harada, K. Yasugi, T. Matsumoto, and S. Katayose, "Spontaneous Formation of Polyion Complex Micelles with Narrow Distribution from Antisense Oligonucleotide and Cationic Block Copolymer in Physiological Saline," *Macromolecules*, vol. 29, no. 26, pp. 8556–8557, Jan. 1996.

[54]   Y. Kakizawa and K. Kataoka, "Block copolymer micelles for delivery of gene and related compounds.," *Advanced drug delivery reviews*, vol. 54, no. 2, pp. 203–22, Feb. 2002.

[55]   A. E. Smith, X. Xu, and C. L. McCormick, "Stimuli-responsive amphiphilic (co)polymers via RAFT polymerization," *Progress in Polymer Science*, vol. 35, no. 1–2, pp. 45–93, Jan. 2010.

[56]   V. P. Torchilin, "Structure and design of polymeric surfactant-based drug delivery systems.," *Journal of controlled release : official journal of the Controlled Release Society*, vol. 73, no. 2–3, pp. 137–72, Jun. 2001.

[57]   M. Yokoyama, G. S. Kwon, T. Okano, Y. Sakurai, T. Seto, and K. Kataoka, "Preparation of micelle-forming polymer-drug conjugates.," *Bioconjugate chemistry*, vol. 3, no. 4, pp. 295–301, 1992.

[58]   Y. Z. You, Q. H. Zhou, D. S. Manickam, L. Wan, G. Z. Mao, and D. Oupicky, "Dually responsive multiblock copolymers via reversible addition-fragmentation chain transfer polymerization: Synthesis of temperature- and redox-responsive copolymers of poly(N-isopropylacrylamide) and poly(2-(dimethylamino)ethyl methacrylate)," *Macromolecules*, vol. 40, pp. 8617–8624, 2007.

[59]   K. Podual, F. D. III, and N. Peppas, "Preparation and dynamic response of cationic copolymer hydrogels containing glucose oxidase," *Polymer*, vol. 41, pp. 3975–3983, 2000.

[60]   K. Podual, F. J. Doyle, and N. a Peppas, "Dynamic behavior of glucose oxidase-containing microparticles of poly(ethylene glycol)-grafted cationic hydrogels in an environment of changing pH.," *Biomaterials*, vol. 21, no. 14, pp. 1439–50, Jul. 2000.

[61]   K. Podual and N. a. Peppas, "Relaxational behavior and swelling-pH master curves of poly[(diethylaminoethyl methacrylate)-graft-(ethylene glycol)] hydrogels," *Polymer International*, vol. 54, no. 3, pp. 581–593, Mar. 2005.

[62]   Y. Tang, S. Y. Liu, S. P. Armes, and N. C. Billingham, "Solubilization and controlled release of a hydrophobic drug using novel micelle-forming ABC triblock copolymers.," *Biomacromolecules*, vol. 4, no. 6, pp. 1636–45, 2003.

[63]   Y. Hu, T. Litwin, A. R. Nagaraja, B. Kwong, J. Katz, N. Watson, and D. J. Irvine, "Cytosolic Delivery of Membrane-Impermeable Molecules in Dendritic Cells Using pH-Responsive Core-Shell Nanoparticles," *Nano Letters*, 2007.

[64]   A. J. Convertine, C. Diab, M. Prieve, A. Paschal, A. S. Hoffman, P. H. Johnson, P. S. Stayton, W. H. Street, and S. Washington, "pH-Responsive Polymeric Micelle Carriers for siRNA Drugs," *Biomacromolecules*, pp. 2904–2911, 2010.

[65]   J. H. van den Berg, K. Oosterhuis, W. E. Hennink, G. Storm, L. J. van der Aa, J. F. J. Engbersen, J. B. a G. Haanen, J. H. Beijnen, T. N. Schumacher, and B. Nuijen, "Shielding the cationic charge of nanoparticle-formulated dermal DNA vaccines is essential for antigen expression and immunogenicity.," *Journal of Controlled Release*, vol. 141, no. 2, pp. 234–40, Jan. 2010.

[66]   R. N. Palumbo, X. Zhong, D. Panus, W. Han, W. Ji, and C. Wang, "Transgene expression and local tissue distribution of naked and polymer-condensed plasmid DNA after intradermal administration in mice.," *Journal of controlled release : official journal of the Controlled Release Society*, vol. 159, no. 2, pp. 232–9, Apr. 2012.

[67]   D. Velluto, S. N. Thomas, E. Simeoni, M. a Swartz, and J. a Hubbell, "PEG-b-PPS-b-PEI micelles and PEG-b-PPS/PEG-b-PPS-b-PEI mixed micelles as non-viral vectors for plasmid DNA: tumor immunotoxicity in B16F10 melanoma.," *Biomaterials*, vol. 32, no. 36, pp. 9839–47, Dec. 2011.

[68]   W. Wijagkanalan, S. Kawakami, Y. Higuchi, F. Yamashita, and M. Hashida, "Intratracheally instilled mannosylated cationic liposome/NFκB decoy complexes for effective prevention of LPS-induced lung inflammation.," *Journal of controlled release : official journal of the Controlled Release Society*, vol. 149, no. 1, pp. 42–50, Jan. 2011.

[69]   Y. Qiao, Y. Huang, C. Qiu, X. Yue, L. Deng, Y. Wan, J. Xing, C. Zhang, S. Yuan, A. Dong, and J. Xu, "The use of PEGylated poly [2-(N,N-dimethylamino) ethyl methacrylate] as a mucosal DNA delivery vector and the activation of innate immunity and improvement of HIV-1-specific immune responses.," *Biomaterials*, vol. 31, no. 1, pp. 115–23, Jan. 2010.

[70]   T. M. Allen, "Ligand-targeted therapeutics in anticancer therapy.," *Nature reviews. Cancer*, vol. 2, no. 10, pp. 750–63, Oct. 2002.

[71]   S. R. S. Ting, G. Chen, and M. H. Stenzel, "Synthesis of glycopolymers and their multivalent recognitions with lectins," *Polymer Chemistry*, vol. 1, no. 9, p. 1392, 2010.

[72]   E. W. Adams, D. M. Ratner, P. H. Seeberger, and N. Hacohen, "Carbohydrate-mediated targeting of antigen to dendritic cells leads to enhanced presentation of antigen to T cells.," *Chembiochem : a European journal of chemical biology*, vol. 9, no. 2, pp. 294–303, Jan. 2008.

[73]   K. Drickamer, "Two distinct classes of carbohydrate-recognition domains in animal lectins.," *The Journal of biological chemistry*, vol. 263, no. 20, pp. 9557–60, Jul. 1988.

[74] R. T. Lee, K. Drickamer, and Y. C. Lee, "Multivalent Ligand Binding by Serum Protein '," *Archives of Biochemistry and Biophysics*, vol. 299, no. 1, 1992.

[75] M. Mammen, S.-K. Choi, and G. M. Whitesides, "Polyvalent Interactions in Biological Systems: Implications for Design and Use of Multivalent Ligands and Inhibitors," *Angewandte Chemie International Edition*, vol. 37, no. 20, pp. 2754–2794, Nov. 1998.

[76] R. T. Lee and Y. C. Lee, "Affinity enhancement by multivalent lectin-carbohydrate interaction.," *Glycoconjugate journal*, vol. 17, no. 7–9, pp. 543–51, 2001.

[77] C. G. Figdor, Y. van Kooyk, and G. J. Adema, "C-type lectin receptors on dendritic cells and Langerhans cells.," *Nature reviews. Immunology*, vol. 2, no. 2, pp. 77–84, Feb. 2002.

[78] M. E. Taylor, K. Bezouska, and K. Drickamer, "Contribution to ligand binding by multiple carbohydrate-recognition domains in the macrophage mannose receptor.," *The Journal of biological chemistry*, vol. 267, no. 3, pp. 1719–26, Jan. 1992.

[79] R. T. Lee and Y. C. Lee, "Affinity enhancement by multivalent lectin-carbohydrate interaction.," *Glycoconjugate journal*, vol. 17, no. 7–9, pp. 543–51, 2001.

[80] V. L. Shepherd, Y. C. Lee, P. H. Schlesinger, and P. D. Stahl, "L-Fucose-terminated glycoconjugates are recognized by pinocytosis receptors on macrophages," *Cell*, vol. 78, no. 2, pp. 1019–1022, 1981.

[81] M. E. Taylor and K. Drickamer, "Structural requirements for high affinity binding of complex ligands by the macrophage mannose receptor.," *The Journal of biological chemistry*, vol. 268, no. 1, pp. 399–404, Jan. 1993.

[82] W. I. Weis, K. Drickamer, and W. A. Hendrickson, "Structure of a C-type mannose-binding protein complexed with an oligosaccharide," *Nature*, vol. 360, no. 12, 1992.

[83] E. P. McGreal, J. L. Miller, and S. Gordon, "Ligand recognition by antigen-presenting cell C-type lectin receptors.," *Current opinion in immunology*, vol. 17, no. 1, pp. 18–24, Feb. 2005.

[84] N. S. Stambach and M. E. Taylor, "Characterization of carbohydrate recognition by langerin, a C-type lectin of Langerhans cells.," *Glycobiology*, vol. 13, no. 5, pp. 401–10, May 2003.

[85] M. a W. P. de Jong, L. E. M. Vriend, B. Theelen, M. E. Taylor, D. Fluitsma, T. Boekhout, and T. B. H. Geijtenbeek, "C-type lectin Langerin is a beta-glucan receptor on human Langerhans cells that recognizes opportunistic and pathogenic fungi.," *Molecular immunology*, vol. 47, no. 6, pp. 1216–25, Mar. 2010.

[86] R. T. Lee, T.-L. Hsu, S. K. Huang, S.-L. Hsieh, C.-H. Wong, and Y. C. Lee, "Survey of immune-related, mannose/fucose-binding C-type lectin receptors reveals widely divergent sugar-binding specificities.," *Glycobiology*, vol. 21, no. 4, pp. 512–20, Apr. 2011.

[87] R. E. Hunger, P. A. Sieling, M. T. Ochoa, M. Sugaya, A. E. Burdick, T. H. Rea, P. J. Brennan, J. T. Belisle, A. Blauvelt, S. A. Porcelli, and R. L. Modlin, "Langerhans cells utilize CD1a and langerin to efficiently present nonpeptide antigens to T cells," *Methods*, vol. 113, no. 5, 2004.

[88] T. Kawamura, M. Qualbani, E. K. Thomas, J. M. Orenstein, and a Blauvelt, "Low levels of productive HIV infection in Langerhans cell-like dendritic cells differentiated in the presence of TGF-beta1 and increased viral replication with CD40 ligand-induced maturation.," *European journal of immunology*, vol. 31, no. 2, pp. 360–8, Mar. 2001.

[89] H. Feinberg, A. S. Powlesland, M. E. Taylor, and W. I. Weis, "Trimeric structure of langerin.," *The Journal of biological chemistry*, vol. 285, no. 17, pp. 13285–93, Apr. 2010.

[90] J. Idoyaga, C. Cheong, K. Suda, N. Suda, J. Y. Kim, H. Lee, C. G. Park, and R. M. Steinman, "Cutting edge: langerin/CD207 receptor on dendritic cells mediates efficient antigen presentation on MHC I and II products in vivo.," *Journal of immunology (Baltimore, Md. : 1950)*, vol. 180, no. 6, pp. 3647–50, Mar. 2008.

[91] J. Idoyaga, A. Lubkin, C. Fiorese, M. H. Lahoud, I. Caminschi, and Y. Huang, "Comparable T helper 1 (Th1) and CD8 T-cell immunity by targeting HIV gag p24 to CD8 dendritic cells within," *PNAS*, vol. 1, pp. 1–6, 2010.

18

[92]   N. Romani, M. Thurnher, J. Idoyaga, R. M. Steinman, and V. Flacher, "Targeting of antigens to skin dendritic cells: possibilities to enhance vaccine efficacy.," *Immunology and cell biology*, vol. 88, no. 4, pp. 424–430, Apr. 2010.

[93]   V. Flacher, F. Sparber, C. H. Tripp, N. Romani, and P. Stoitzner, "Targeting of epidermal Langerhans cells with antigenic proteins: attempts to harness their properties for immunotherapy.," *Cancer immunology, immunotherapy : CII*, vol. 58, no. 7, pp. 1137–47, Jul. 2009.

[94]   C. a Hoppe and Y. C. Lee, "Accumulation of a nondegradable mannose ligand within rabbit alveolar macrophages. Receptor reutilization is independent of ligand degradation.," *Biochemistry*, vol. 23, no. 8, pp. 1723–30, Apr. 1984.

[95]   J. Bernard, X. Hao, T. P. Davis, C. Barner-Kowollik, and M. H. Stenzel, "Synthesis of various glycopolymer architectures via RAFT polymerization: from block copolymers to stars.," *Biomacromolecules*, vol. 7, no. 1, pp. 232–8, Jan. 2006.

[96]   G. Moad, A. E. Rizzardo, and S. H. T. A, "Living Radical Polymerization by the RAFT Process," *Review Literature And Arts Of The Americas*, pp. 379–410, 2005.

[97]   M. Okada, "Molecular design and syntheses of glycopolymers," *Progress in Polymer Science*, vol. 26, no. 1, pp. 67–104, Feb. 2001.

[98]   A. B. Lowe, B. S. Sumerlin, and C. L. McCormick, "The direct polymerization of 2-methacryloxyethyl glucoside via aqueous reversible addition-fragmentation chain transfer (RAFT) polymerization," *Polymer*, vol. 44, no. 22, pp. 6761–6765, Oct. 2003.

[99]   L. Albertin, C. Kohlert, M. Stenzel, L. J. R. Foster, and T. P. Davis, "Chemoenzymatic synthesis of narrow-polydispersity glycopolymers: poly(6-O-vinyladipoyl-D-glucopyranose).," *Biomacromolecules*, vol. 5, no. 2, pp. 255–60, 2004.

[100] L. Albertin, M. H. Stenzel, C. Barner-Kowollik, L. J. R. Foster, and T. P. Davis, "Well-Defined Diblock Glycopolymers from RAFT Polymerization in Homogeneous Aqueous Medium," *Macromolecules*, vol. 38, no. 22, pp. 9075–9084, Nov. 2005.

[101] N.-Y. Xiao, A.-L. Li, H. Liang, and J. Lu, "A Well-Defined Novel Aldehyde-Functionalized Glycopolymer: Synthesis, Micelle Formation, and Its Protein Immobilization," *Macromolecules*, vol. 41, no. 7, pp. 2374–2380, Apr. 2008.

[102] Z. Deng, S. Li, X. Jiang, and R. Narain, "Well-Defined Galactose-Containing Multi-Functional Copolymers and Glyconanoparticles for Biomolecular Recognition Processes," *Macromolecules*, vol. 42, no. 17, pp. 6393–6405, Sep. 2009.

[103] O. Abdelkader, S. Moebs-sanchez, Y. Queneau, J. Bernard, E. Fleury, and D. Lyon, "Generation of Well-Defined Clickable Glycopolymers from Aqueous RAFT Polymerization of Isomaltulose-Derived Acrylamides," *Polymer*, vol. 49, pp. 1309–1318, 2011.

[104] E.-H. Song, M. J. Manganiello, Y.-H. Chow, B. Ghosn, A. J. Convertine, P. S. Stayton, L. M. Schnapp, and D. M. Ratner, "In vivo targeting of alveolar macrophages via RAFT-based glycopolymers.," *Biomaterials*, vol. 33, no. 28, pp. 6889–97, Oct. 2012.

[105] H. Zhang and Y. Ma, "Recent developments in carbohydrate-decorated targeted drug/gene delivery," *Medicinal Research Reviews*, vol. 30, no. 2, pp. 270–289, 2010.

[106] G. Y. Wu and C. H. Wu, "Receptor-mediated in vitro gene transformation by a soluble DNA carrier system.," *The Journal of biological chemistry*, vol. 262, no. 10, pp. 4429–32, Apr. 1987.

[107] J. Haensler and F. C. Szoka, "Synthesis and characterization of a trigalactosylated bisacridine compound to target DNA to hepatocytes.," *Bioconjugate chemistry*, vol. 4, no. 1, pp. 85–93, 1993.

[108] X.-Q. Zhang, X.-L. Wang, P.-C. Zhang, Z.-L. Liu, R.-X. Zhuo, H.-Q. Mao, and K. W. Leong, "Galactosylated ternary DNA/polyphosphoramidate nanoparticles mediate high gene transfection efficiency in hepatocytes.," *Journal of controlled release : official journal of the Controlled Release Society*, vol. 102, no. 3, pp. 749–63, Feb. 2005.

[109] T. Ferkol, J. C. Perales, F. Mularo, and R. W. Hanson, "Receptor-mediated gene transfer into macrophages.," *Proceedings of the National Academy of Sciences of the United States of America*, vol. 93, no. 1, pp. 101–5, Jan. 1996.

[110] P. Erbacher, M. T. Bousser, J. Raimond, M. Monsigny, P. Midoux, and a C. Roche, "Gene transfer by DNA/glycosylated polylysine complexes into human blood monocyte-derived macrophages.," *Human gene therapy*, vol. 7, no. 6, pp. 721–9, Apr. 1996.

[111] K. Wada, H. Arima, T. Tsutsumi, Y. Chihara, K. Hattori, F. Hirayama, and K. Uekama, "Improvement of gene delivery mediated by mannosylated dendrimer/alpha-cyclodextrin conjugates.," *Journal of controlled release : official journal of the Controlled Release Society*, vol. 104, no. 2, pp. 397–413, May 2005.

[112] H. Arima, Y. Chihara, M. Arizono, S. Yamashita, K. Wada, F. Hirayama, and K. Uekama, "Enhancement of gene transfer activity mediated by mannosylated dendrimer/alpha-cyclodextrin conjugate (generation 3, G3).," *Journal of controlled release : official journal of the Controlled Release Society*, vol. 116, no. 1, pp. 64–74, Nov. 2006.

[113] M. Hashimoto, M. Morimoto, H. Saimoto, Y. Shigemasa, H. Yanagie, M. Eriguchi, and T. Sato, "Gene transfer by DNA/mannosylated chitosan complexes into mouse peritoneal macrophages.," *Biotechnology letters*, vol. 28, no. 11, pp. 815–21, Jun. 2006.

[114] F. Leclercq, "Synthesis of glycosylated polyethylenimine with reduced toxicity and high transfecting efficiency," *Bioorganic & Medicinal Chemistry Letters*, vol. 10, no. 11, pp. 1233–1235, Jun. 2000.

[115] H. Yan and K. Tram, "Glycotargeting to improve cellular delivery efficiency of nucleic acids.," *Glycoconjugate journal*, vol. 24, no. 2–3, pp. 107–23, Apr. 2007.

[116] Y. H. Choi, F. Liu, J. S. Park, and S. W. Kim, "Lactose-poly(ethylene glycol)-grafted poly-L-lysine as hepatoma cell-tapgeted gene carrier.," *Bioconjugate chemistry*, vol. 9, no. 6, pp. 708–18, 1998.

[117] P. Sabbatini and K. Odunsi, "Immunologic approaches to ovarian cancer treatment.," *Journal of clinical oncology : official journal of the American Society of Clinical Oncology*, vol. 25, no. 20, pp. 2884–93, Jul. 2007.

[118] A. L. Coveler and M. L. Disis, "Progress in the development of a therapeutic vaccine for breast cancer," *Therapy*, pp. 25–36, 2010.

[119] L. G. Salazar and M. L. Disis, "Cancer vaccines: the role of tumor burden in tipping the scale toward vaccine efficacy.," *Journal of Clinical Oncology*, vol. 23, no. 30, pp. 7397–8, Oct. 2005.

[120] F. Castellino and R. N. Germain, "Cooperation between CD4+ and CD8+ T cells: when, where, and how.," *Annual review of immunology*, vol. 24, pp. 519–40, Jan. 2006.

[121] A. Le Bon, N. Etchart, C. Rossmann, M. Ashton, S. Hou, D. Gewert, P. Borrow, and D. F. Tough, "Cross-priming of CD8+ T cells stimulated by virus-induced type I interferon.," *Nature immunology*, vol. 4, no. 10, pp. 1009–15, Oct. 2003.

[122] D. R. Surman, M. E. Dudley, W. W. Overwijk, and N. P. Restifo, "Cutting edge: CD4+ T cell control of CD8+ T cell reactivity to a model tumor antigen.," *Journal of immunology (Baltimore, Md. : 1950)*, vol. 164, no. 2, pp. 562–5, Jan. 2000.

[123] F. Fallarino, U. Grohmann, R. Bianchi, C. Vacca, M. C. Fioretti, and P. Puccetti, "Th1 and Th2 cell clones to a poorly immunogenic tumor antigen initiate CD8+ T cell-dependent tumor eradication in vivo.," *Journal of immunology (Baltimore, Md. : 1950)*, vol. 165, no. 10, pp. 5495–501, Nov. 2000.

[124] R. L. G. Ii, J. Lu, H. Kobayashi, R. Kennedy, and E. Celis, "Direct Costimulation of Tumor-reactive CTL by Helper T Cells Potentiate Their Proliferation , Survival , and Effector Function Direct Costimulation of Tumor-reactive CTL by Helper T Cells Potentiate Their Proliferation , Survival , and Effector Function 1," *Clinical Cancer Research*, pp. 922–931, 2002.

[125] C. L. Vanderlugt and S. D. Miller, "Epitope spreading in immune-mediated diseases: implications for immunotherapy.," *Nature reviews. Immunology*, vol. 2, no. 2, pp. 85–95, Feb. 2002.

[126] M. a Kutzler and D. B. Weiner, "DNA vaccines: ready for prime time?," *Nature reviews. Genetics*, vol. 9, no. 10, pp. 776–88, Oct. 2008.

[127] J. J. Donnelly, J. B. Ulmer, J. W. Shiver, and M. A. Liu, "Dna vaccines," *Cell*, 1997.

[128] A. Scardino, M. Alimandi, P. Correale, S. G. Smith, R. Bei, H. Firat, M. G. Cusi, O. Faure, S. Graf-Dubois, G. Cencioni, J. Marrocco, S. Chouaib, F. a Lemonnier, A. M. Jackson, and K. Kosmatopoulos, "A polyepitope DNA vaccine targeted to Her-2/ErbB-2 elicits a broad range of human and murine CTL effectors to protect against tumor challenge.," *Cancer research*, vol. 67, no. 14, pp. 7028–36, Jul. 2007.

[129] M. Michel, H. L. Davistt, M. Schleeft, M. Mancini, P. Tiollais, and R. G. Whalent, "DNA-mediated immunization to the hepatitis B surface antigen in mice: Aspects of the humoral response mimic hepatitis B viral infection in humans," *Proceedings of the National Academy of Sciences of the United States of America*, vol. 92, no. June, pp. 5307–5311, 1995.

[130] M. a Liu, "DNA vaccines: an historical perspective and view to the future.," *Immunological reviews*, vol. 239, no. 1, pp. 62–84, Jan. 2011.

[131] J. B. Ulmer, T. M. Fu, R. R. Deck, a Friedman, L. Guan, C. DeWitt, X. Liu, S. Wang, M. a Liu, J. J. Donnelly, and M. J. Caulfield, "Protective CD4+ and CD8+ T cells against influenza virus induced by vaccination with nucleoprotein DNA.," *Journal of virology*, vol. 72, no. 7, pp. 5648–53, Jul. 1998.

[132] D. M. Feltquate, S. Heaney, R. G. Webster, and H. L. Robinson, "Different T helper cell types and antibody isotypes generated by saline and gene gun DNA immunization.," *Journal of immunology (Baltimore, Md. : 1950)*, vol. 158, no. 5, pp. 2278–84, Mar. 1997.

[133] T. M. Pertmer, T. R. Roberts, and J. R. Haynes, "Influenza Virus Nucleoprotein-Specific Immunoglobulin G Subclass and Cytokine Responses Elicited by DNA Vaccination Are Dependent on the Route of Vector DNA Delivery," *Microbiology*, vol. 70, no. 9, pp. 6119–6125, 1996.

[134] C. Lekutis, J. W. Shiver, and M. A. Liu, "HIV-1 env DNA Vaccine Administered to Rhesus Monkeys Elicits MHC Class II-Restricted CD4+ T Helper Cells that Secrete IFN-y and TNF-a," *The Journal of Immunology*, 1997.

[135] R. R. MacGregor, J. D. Boyer, K. E. Ugen, K. E. Lacy, S. J. Gluckman, M. L. Bagarazzi, M. a Chattergoon, Y. Baine, T. J. Higgins, R. B. Ciccarelli, L. R. Coney, R. S. Ginsberg, and D. B. Weiner, "First human trial of a DNA-based vaccine for treatment of human immunodeficiency virus type 1 infection: safety and host response.," *The Journal of infectious diseases*, vol. 178, no. 1, pp. 92–100, Jul. 1998.

[136] B. Ferraro, M. P. Morrow, N. a Hutnick, T. H. Shin, C. E. Lucke, and D. B. Weiner, "Clinical applications of DNA vaccines: current progress.," *Clinical infectious diseases : an official publication of the Infectious Diseases Society of America*, vol. 53, no. 3, pp. 296–302, Aug. 2011.

[137] S. Jones, K. Evans, H. McElwaine-John, M. Sharpe, J. Oxford, R. Lambkin-Williams, T. Mant, A. Nolan, M. Zambon, J. Ellis, J. Beadle, and P. T. Loudon, "DNA vaccination protects against an influenza challenge in a double-blind randomised placebo-controlled phase 1b clinical trial.," *Vaccine*, vol. 27, no. 18, pp. 2506–12, Apr. 2009.

[138] M. J. Roy, M. S. Wu, L. J. Barr, J. T. Fuller, L. G. Tussey, S. Speller, J. Culp, J. K. Burkholder, W. F. Swain, R. M. Dixon, G. Widera, R. Vessey, a King, G. Ogg, a Gallimore, J. R. Haynes, and D. Heydenburg Fuller, "Induction of antigen-specific CD8+ T cells, T helper cells, and protective levels of antibody in humans by particle-mediated administration of a hepatitis B virus DNA vaccine.," *Vaccine*, vol. 19, no. 7–8, pp. 764–78, Nov. 2000.

[139] S. Rerks-Ngarm, "Vaccination with ALVAC and AIDSVAX to prevent HIV-1 infection in Thailand," *… England Journal of …*, pp. 2209–2220, 2009.

[140] "Safety and Effectiveness of PENNVAX-B Vaccine Alone, With Il-12, or IL-15 in Healthy Adults," *NIH clinicaltrials.gov*, 2012. [Online]. Available: http://clinicaltrials.gov/show/NCT00528489.

CHAPTER 2 – pH-RESPONSIVE DIBLOCK COPOLYMER MICELLES FOR PLASMID DNA DELIVERY

Matthew J. Manganiello, Connie Cheng, Anthony J. Convertine, James D. Bryers, Patrick S. Stayton

ABSTRACT

A series of diblock copolymers containing an endosomal-releasing segment composed of diethylaminoethyl methacrylate (DEAEMA) and butyl methacrylate (BMA) were synthesized via reversible addition-fragmentation chain transfer (RAFT) polymerization. The materials were designed to condense plasmid DNA (pDNA) through electrostatic interactions with a cationic poly(N,N-dimethylaminoethyl methacrylate) (pDMAEMA) first block.   The pDMAEMA was employed as a macro chain transfer agent (macroCTA) for the synthesis of a series in which the relative feed ratios of DEAEMA and BMA were systematically varied from 20% to 70% BMA. The resultant diblock copolymers exhibited low polydispersity (PDI ≤ 1.06) with similar molecular weights (M_n = 19.3 – 23.1 kDa). Dynamic light scattering (DLS) measurements in combination with ^{1}H-NMR D_2O studies demonstrated that the free copolymers assemble into core-shell micelles at physiological pH. Reduction of the solution pH to values representative of endosomal/lysosomal compartments induced an increase in the net cationic charge of the core through protonation of the DEAEMA residues. This protonation promotes micelle destabilization and exposure of the hydrophobic BMA residues that destabilize biological membranes.   The pH value at which this micelle-to-unimer transition occurred was dependent on the hydrophobic content of the copolymer, with higher BMA-containing copolymer compositions exhibiting pH-induced transitions to the membrane-destabilizing state at successively lower pH values. The ability of the diblock copolymers to deliver pDNA was subsequently investigated using a GFP expression vector in two monocyte cell lines. High levels of DNA transfection were observed for the copolymer compositions exhibiting the sharpest pH transitions and membrane destabilizing activities, demonstrating the importance of tuning the endosomal-releasing segment composition.

2.1. INTRODUCTION

Gene therapy and DNA-based vaccines offer significant therapeutic potential but safe, efficacious delivery systems are still needed to enable clinical applications [1], [2]. Cationic lipids and polymers have been extensively investigated as non-viral carriers of plasmid DNA

(pDNA) due to potential advantages in scalability of production, improved safety profile, and low immunogenicity [3–5]. Cationic polymers include poly(dimethylaminoethyl methacrylate) (pDMAEMA) [6–14], poly(ethylenimine) (PEI) [15–28], and poly(L-lysine) (PLL) [29–35]. The barrier of endosomal escape has been a special challenge for nonviral delivery systems [36], and a variety of pH-responsive polymers [37–39] and lipids [40–42] have been developed that exploit the pH gradients formed in the intracellular vesicular trafficking pathways.

Cationic micelles prepared from amphiphilic block copolymers offer a means to preserve the DNA-condensing activity of polycations while introducing pH-sensitive functionalities to overcome the endosomal/lysosomal intracellular barrier [43], [44]. Through the use of controlled radical polymerization (CRP) techniques, the synthesis of well-defined polymer architectures can be achieved. Both reversible addition-fragmentation chain transfer (RAFT) polymerization [11], [45] and atom transfer radical polymerization (ATRP) [46] have been utilized to develop such multiblock micellar systems. For example, You et al. have designed diblock copolymers consisting of pDMAEMA and poly(N-isopropylacrylamide) (pNIPAM) that assembled into core-shell micelles with pDMAEMA acting as the stabilizing, hydrophilic component [47]. The authors demonstrated that changes in the protonation state of pDMAEMA affected micelle stability as observed by a shift in the phase transition temperature. pDMAEMA exhibits a relatively low charge density, as compared to other polycations, due to the presence of a tertiary amine that is approximately 50% protonated at physiological pH although toxicity issues remain [48–52]. A similar polymer, poly(diethylaminoethyl methacrylate) (pDEAEMA), has a predominately hydrophobic character at physiological pH while retaining a tertiary amine. Tang et al. first demonstrated that pDEAEMA could be used to drive micelle formation of triblock copolymers in an aqueous environment and that destabilization of the particles occurred in a pH-dependent manner [46].

Recently, we described the synthesis of a family of diblock copolymer small-interfering RNA (siRNA) carriers composed of a positively-charged block of pDMAEMA to mediate siRNA binding and a second pH-responsive endosomal releasing block composed of DMAEMA and propylacrylic acid (PAA) in roughly equimolar ratios, and butyl methacylate (BMA) [11], [53]. These materials self-assemble to form micelles at physiological pH values, but upon

23

exposure to the low pH environment of the endosome undergo a pH-induced conformational change rendering them highly membrane destabilizing. Here, we detail the development of a class of copolymer micelles that are capable of mediating endosomal escape of plasmid DNA therapeutics. These materials incorporate DEAEMA as a pH-sensitive switch that activates hydrophobic membrane-interactive BMA residues upon exposure to low pH environments.

2.2. MATERIALS AND METHODS

2.2.1. Materials

Materials were supplied by Sigma-Aldrich (St Louis, MO) unless otherwise specified. 2,2′-Azobis(4-methoxy-2.4-dimethyl valeronitrile) (V70) and 1,1'-*Azobis*(cyclohexane-1-carbonitrile) (V40) were obtained from Wako Chemicals USA, Inc. (Richmond, VA). pDNA gWiz-GFP was obtained from Aldevron LLC (Fargo, ND). Lipofectamine 2000 (LF) was obtained from Invitrogen (Carlsbad, CA). 4-Cyano-4-(ethylsulfanylthiocarbonyl) sulfanylvpentanoic acid (ECT) was synthesized as described previously [54]. DMAEMA, DEAEMA, and BMA were distilled prior to use. RAW 264.7 (murine leukaemic monocyte macrophage cell line) (ATCC) cells were maintained in Dulbecco's Modified Eagle Medium (DMEM) High Glucose containing L-glutamine (GIBCO) supplemented with 1% penicillin-streptomycin (GIBCO) and 10% fetal bovine serum (FBS, Invitrogen), JAWSII (murine dendritic cell line) (ATCC) cells were maintained in Minimum Essential Medium α Medium (αMEM, GIBCO) supplemented with 4 mM L-glutamine (Lonza), 5 ng/ml recombinant mouse granulocyte macrophage-colony stimulating factor (Peprotech), 20% heat-inactivated FBS (GIBCO), and 1% penicillin-streptomycin, and passaged using 0.25% trypsin-EDTA (GIBCO). All cells were cultured at 37 °C and 5% CO_2.

2.2.2. Synthesis of poly(dimethylaminoethyl methacrylate) macro chain transfer agent (pDMAEMA macroCTA)

The RAFT polymerization of DMAEMA was conducted in dioxane at 30 °C under a nitrogen atmosphere for 18 h using ECT and V70 as the chain transfer agent (CTA) and radical initiator, respectively. The initial CTA to monomer molar ratio ($[CTA]_0/[M]_0$) was designed so that the theoretical M_n at 100% conversion was approximately 10,000 g/mol (degree of polymerization (DP) of 65). The initial CTA to initiator molar ratio ($[CTA]_0/[I]_0$) was 20 to 1. The resultant pDMAEMA macro chain transfer agent (macroCTA) was isolated by

precipitation into pentane. The polymer was then redissolved in acetone and subsequently precipitated into pentane (×3) and dried overnight in vacuo.

2.2.3. Block copolymerization of DEAEMA and BMA from a pDMAEMA macroCTA

The desired stoichiometric quantities of DEAEMA and BMA were added to pDMAEMA macroCTA dissolved in dioxane (57 wt% monomer and macroCTA to solvent). For all polymerizations $[M]_0/[CTA]_0$ and $[CTA]_0/[I]_0$ were 100:1 and 20:1, respectively. Following the addition of V40 the solutions were purged with nitrogen for 30 min and allowed to react at 90 °C for 6 h. The resultant diblock copolymers were isolated by precipitation into cold hexanes. The copolymers were further purified by dissolution into ethanol followed by addition into 1X DPBS (final ethanol concentration of 10 vol% and copolymer concentration of ~10 mg/mL). The copolymers were isolated from this solution via chromatographic separation with a PD-10 desalting column (GE Healthcare, Piscataway, NJ), followed by lyophilization to obtain the final copolymer. Aqueous stock solutions were prepared by dissolution of the dry copolymers in ethanol followed by dropwise addition into 10 mM, pH 7.0 sodium phosphate buffer (with 100 mM NaCl) at 2 mg/mL and 5 wt% ethanol. Both the pDMAEMA macroCTA and diblock copolymers were analyzed by ^{1}H-NMR (CDCl$_3$) spectroscopy (Bruker AV 500).

2.2.4. Gel permeation chromatography

Gel permeation chromatography (GPC) was used to determine molecular weights and polydispersities (M_w/M_n, PDI) of both the pDMAEMA macroCTA and diblock copolymer samples. SEC Tosoh TSK-GEL R-3000 and R-4000 columns (Tosoh Bioscience, Montgomeryville, PA) were connected in series to a Agilent 1200 series (Agilent Technologies, Santa Clara, CA), refractometer Optilab-rEX and triple-angle static light scattering detector miniDAWN TREOS (Wyatt Technology, Santa Barbara, CA). HPLC-grade DMF containing 0.1 wt% LiBr at 60 °C was used as the mobile phase at a flow rate of 1 mL/min. The molecular weights of each polymer were determined using a multi-detector calibration based on dn/dc values calculated separately for each homopolymer and copolymer composition.

2.2.5. Formation of copolymer/pDNA polyplexes and lipoplexes

Copolymer/pDNA polyplexes were formed by combining equal volumes of pDNA (0.1 mg/ml in molecular biology grade water) and copolymer solutions (in Dulbecco's phosphate-buffered saline, pH 7.4 (PBS)) for 30 min at room temperature. Lipoplexes were formed by combining pDNA with Lipofectamine 2000 at a 3:1 v/w LF:DNA ratio in serum-free media in accordance with the manufacturer's protocol.

2.2.6. Gel retardation assay

The charge ratio (+/-) at which the diblock copolymers mediate complete pDNA condensation was determined via a gel retardation assay. The charge ratio is the molar ratio between protonated DMAEMA tertiary amines (assuming 50% protonation at physiological pH) and phosphate groups along the pDNA backbone. Copolymer/pDNA polyplexes were formulated with 0.5 µg pDNA for 30 min followed by 30 min incubation in the presence of FBS (final FBS concentration of 10%). A 0.7% (w/v) agarose gel was loaded with each lane containing a separate treatment and subsequently run at 90V for one hour. The gels were stained with SYBR Gold prior to fluorescence visualization.

2.2.7. Dynamic light scattering (DLS)

The sizes of free diblock copolymer micelles and copolymer/pDNA polyplexes were determined by DLS measurements using a Malvern Zetasizer (Worcestershire, UK). Free copolymer measurements were performed at a polymer concentration of 100 µg/mL while polymer/pDNA particles were analyzed at a pDNA concentration of 5 µg/mL. All measurements were performed in the presence of 150 mM NaCl at 37°C. Mean diameters are reported as the number average.

2.2.8. Hemolysis assay

The potential for the free copolymer to disrupt endosomal membranes was assessed by a hemolysis assay. The protocol followed here has been described previously [38]. Briefly, polymer was incubated for one hour in the presence of erythrocytes at 20 µg/mL in 100 mM sodium phosphate buffers (supplemented with 150 mM NaCl) of varying pH (7.4, 7.0, 6.6, 6.2, and 5.8) intended to mimic the acidifying pH gradient to which endocytosed material is exposed. The extent of cell lysis (i.e. hemolytic activity) was determined by detecting the amount of released hemoglobin via absorbance measurements at 492 nm.

2.2.9. ^{1}H-NMR D$_2$O titration

^{1}H-NMR spectroscopy (Bruker AV 500, D$_2$O) was used to probe solvation of the diblock copolymer segments as a function of pH, thereby discriminating micelle and unimer conformations. Aqueous copolymer solutions were diluted into D$_2$O from ethanol stocks and titrated separately to three pD values (7.4, 6.6, and 5.8) using sodium deuteroxide and deuterium chloride. pD values were calculated using the following correlation: pD = pH · 1.06831 [55].

2.2.10. In vitro transfections

RAW 264.7 or JAWSII cell lines were seeded in 24-well plates in 1 mL complete media (2 · 10^5 cells/well in DMEM/10% FBS/antibiotics or 1.5 · 10^5 cells/well in αMEM/20% FBS/antibiotics, respectively) and cultured for 24 h to 70% confluency. Polyplexes and lipoplexes were formulated as described above. Cells were washed once with PBS and incubated with polyplexes/lipoplexes at 1 μg DNA/well in 200 μL antibiotic-free media for 4 h at 37 °C. Cells were then washed and the media replaced with 500 μL complete media for an additional 44 h prior to analysis.

2.2.11. Flow cytometry analysis of gene expression

RAW 264.7 cells were incubated for 10 min at room temperature in PBS-based cell dissociation buffer (GIBCO) and collected by vigorous washing. JAWSII cells were collected by trypsinization. Cells were resuspended in PBS containing 2% FBS and 0.2 μg/ml propidium iodide (PI, Invitrogen). GFP expression data was acquired on a BD FACscan flow cytometer (BD Biosciences). 10,000 events gated on viable PI-negative cells were collected per sample and analyzed in FlowJo (TreeStar).

2.2.12. Lactate dehydrogenase cytotoxicity assay

Cytotoxicity was evaluated by a lactate dehydrogenase (LDH) cytotoxicity detection kit (Roche). Cells were seeded at 8 x 10^4 cells/well (RAW 264.7) or 6 x 10^4 cells/well (JAWSII) in 48-well plates in 400 μL complete media and cultured for 24 h. Cells were then washed and polyplexes/lipoplexes at 0.4 μg DNA/well were added in 200 μL antibiotic-free media. Cells were incubated for 24 h, washed, then lysed in 400 μL of RIPA Lysis Buffer (Pierce) at 4 °C for at least 1 h. Lysates were diluted 2:3 in PBS in a 96-well plate (total volume 100

µL), combined with 100 µL of LDH substrate solution, incubated for 10-20 min at room temperature, and absorbance measurements recorded at 490 nm (reference 650 nm).

2.2.13. Statistical Analysis

ANOVA was used to test for treatment effects, and Tukey's test was used for post hoc pairwise comparisons between individual treatment groups.

2.3. RESULTS

2.3.1. Diblock copolymer synthesis and characterization

A series of diblock copolymers were synthesized according to **Scheme 2.1** consisting of two blocks: a DMAEMA homopolymer and a statistical copolymer composed of BMA and DEAEMA at varying monomer feed ratios, from 20% to 70% BMA. The pDMAEMA homopolymer (7,400 g/mol; DP 47) was employed as a macroCTA in the subsequent copolymer synthesis (**Table 2.1**). The diblock copolymer series exhibited low polydispersity (PDI ≤ 1.06) with similar molecular weights (M_n = 19.3 – 23.1 kDa) and compositions close to the monomer feed ratios.
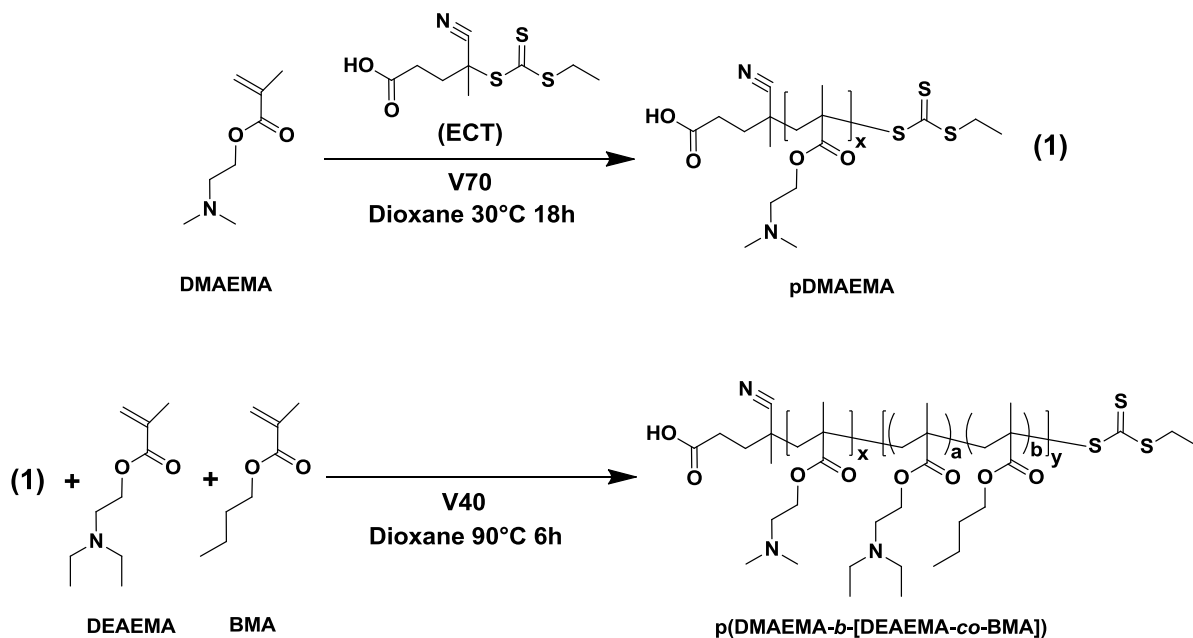
Scheme 2.1. RAFT-mediated synthesis of a diblock copolymer consisting of a cationic poly(DMAEMA) block and an endosomolytic hydrophobic block incorporating DEAEMA and BMA at varying molar feed ratios.

Table 2.1.
Molecular weights, polydispersities, and monomer compositions for polymer designs.

Polymer	Theoretical[a] % BMA 2nd block	Experimental[b] % BMA 2nd block	2nd block M_n^c (g/mol)	Total M_n^c (g/mol)	PDI[c] (M_w/M_n)
P1	20	20	12600	20000	1.06
P2	30	27	15700	23100	1.04
P3	40	39	13200	20600	1.06
P4	50	48	14700	22100	1.03
P5	60	57	13200	20600	1.03
P6	70	70	11900	19300	1.04

[a] Calculated molar feed ratio
[b] As determined by ^{1}H-NMR (CDCl$_3$) spectroscopy (Bruker AV 500)
[c] As determined by GPC.

2.3.2. pH-responsive transitions of diblock copolymers

The diblock copolymers were designed to undergo a pH-triggered phase transition, shifting the equilibrium from a micelle to unimer conformation as pH decreased. The tunability of the pH transition was controlled by varying the hydrophobic content of the second block. Particle size measurements were conducted for solutions of the diblock copolymers across a pH range of 7.4 to 5.8 (**Figure 2.1**). These pH values were selected to mimic the physiological trafficking of the materials from the extracellular space to acidic endosomal/lysosomal compartments. At physiological pH, each copolymer formed particles of approximately 20 nm in diameter. As the copolymers were exposed to more acidic conditions they were found to sharply transition to unimers. The pH at which this transition occurred was found to be strongly dependent on the relative amounts of BMA and DEAEMA present in the core. Higher BMA content shifted the transition to lower pH values. The copolymer that contained 20% BMA underwent a structural transition from micelles at pH values of 7.4 to unimers at pH 7.0 and below, while the 60% BMA copolymer transitioned at a pH values of 6.2. The copolymer with 70% BMA content did not undergo a phase transition from micelles to unimers over the pH range investigated (i.e. pH 7.4 – 5.8). The optimal pH-induced phase transition behavior was observed for the 40% BMA copolymer, where micelle-sized particles were observed at pH values near physiological conditions (i.e. pH 7.4 and 7.0) with a sharp transition to unimers at early (pH = 6.6) and late endosomal (pH 5.8) pH values.

The hemolytic activity of the diblock copolymers as a function of pH was found to be highly correlated with the intrinsic structural transition properties (**Figure 2.2**). In this assay,

human red blood cells were incubated with the copolymer in buffers over a pH range of 7.4 – 5.8. For all copolymers investigated, negligible hemolytic activity was observed at pH 7.4, which suggests that the micellar architecture does not display membrane-destabilizing segments in the necessary protonation state. The pH at which high levels of membrane destabilization were observed correlated well with the phase transition pH values determined by DLS. These studies taken together demonstrate that the highest levels of membrane destabilization occur at or below the transition pH from micelles to unimers where significant interaction of the copolymer core segment with the biological membrane is possible. Consistent with DLS measurements, the 40% BMA copolymer showed optimal pH-dependent hemolysis with a remarkably sharp transition from non-hemolytic at pH values above 7.0 to strongly membrane disruptive at pH 6.6 and below. A similar class of pH-responsive materials, methacrylic acid copolymers, also exhibit improved membrane destabilizing activity upon the incorporation of hydrophobic units, e.g. ethyl acrylate, further illustrating the importance of polymer hydrophobicity on biological activity [56].

Copolymers containing low BMA content showed negligible hemolytic activity even at pH values where the copolymers were unimers. Conversely, the copolymer with 70% BMA content does not undergo a phase transition from micelles to unimers and does not show significant hemolytic activity at any of the pH values examined. These results are consistent with our previous micellar delivery systems where a minimum hydrophobic content is required to disrupt biological membranes [11].
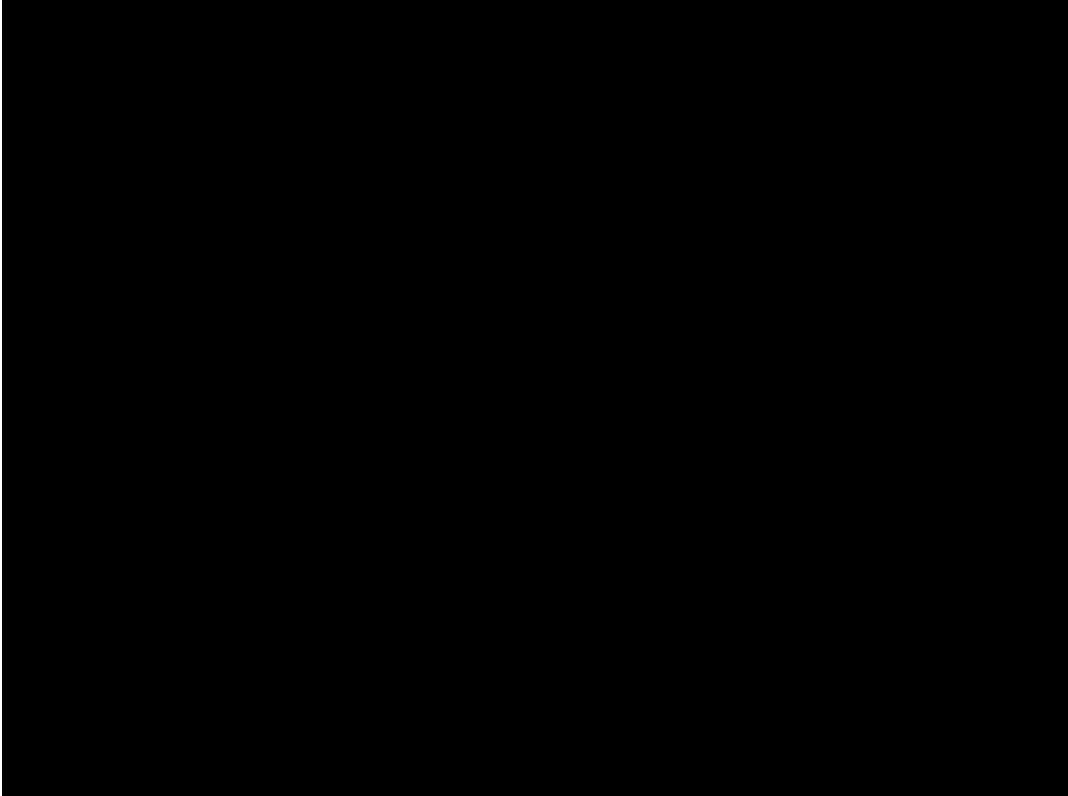
Figure 2.1. Particle size measurements of free copolymers as a function of pH via DLS. All measurements were performed at a copolymer concentration of 1 mg/mL in 100 mM sodium phosphate buffer with 150 mM NaCl. Diameter values were determined from the lognormal number average. Error bars represent the standard deviation as calculated from the polydispersity index (PDI) of the particles.
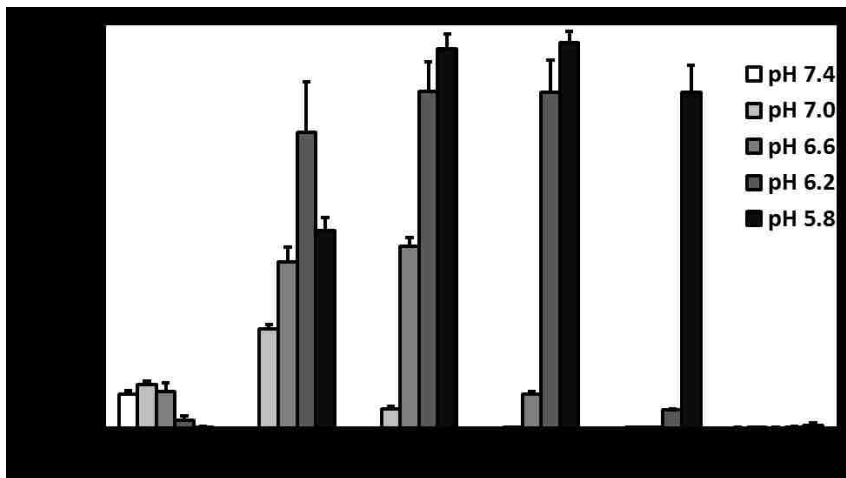
Figure 2.2. Hemolytic activity of diblock copolymers at a concentration of 20 µg/mL. Hemolytic activity is normalized relative to a positive control, 1% v/v Triton X-100, and the data represent a single experiment conducted in triplicate ± standard deviation.

31

2.3.3. ^{1}H-NMR D$_2$O titration

To further evalute the structure copolymers adopt in solution as a function of pH, ^{1}H-NMR was performed on the 40% and 70% BMA copolymer compositions and pDMAEMA homopolymer in D$_2$O at three pD values: 7.4, 6.6, and 5.8 (**Figure 2.3**). The pDMAEMA homopolymer exhibits three distinctive resonances between 2.6-4.7 ppm at pD 7.4: δ 2.8-2.9 methyl (C**H**$_3$NHC**H**$_3$), δ 3.4 methylene (C**H**$_2$NH), and δ 4.3 methylene (OC**H**$_2$). Upon decreasing the solution pD to 6.6 and 5.8, the peaks at δ 2.8-2.9 and 3.4 shift downfield to δ 3.0 and 3.6, respectively, as a result of less effective shielding of the hydrogen atoms from the electron pair of the protonated nitrogen atom [57]. At pD 7.4, the copolymer spectra resembles that of the DMAEMA homopolymer. When the pD is decreased to 6.6, a peak attributed to DEAEMA methyl protons (δ 3.3, C**H**$_3$NHC**H**$_3$) evolves for the 40% BMA composition but is absent for the 70% BMA composition suggesting solvation of the copolymer core for the former composition. At pD 5.8, this peak is present for both copolymers. These results demonstrate that the copolymers adopt a core-shell micelle conformation in an aqueous environment which destabilize in a pH-responsive, composition-dependent manner due to solvation of the core-forming segment.
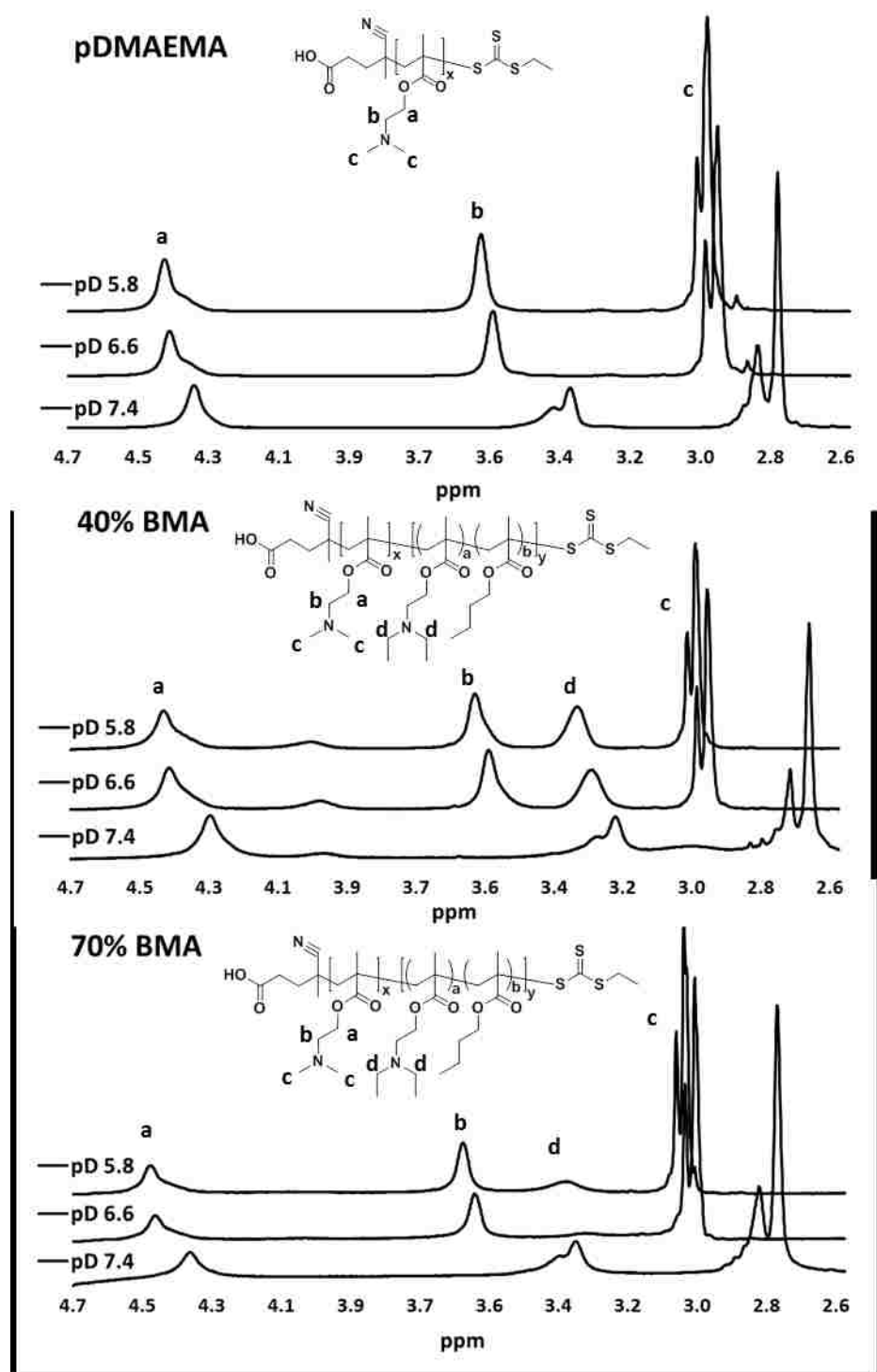
Figure 2.3. ^{1}H-NMR spectra of pDMAEMA hompolymer, 40%, and 70% BMA diblock copolymers in D$_2$O from 4.7 to 2.6 ppm at three different pD values.

2.3.4. Copolymer/pDNA polyplex characterization

The ability of the diblock copolymers to condense plasmid DNA into serum-stable nanoparticles as a function of charge ratio (+/-) was assessed by performing a gel retardation assay and by measuring particle size by dynamic light scattering (**Figure 2.4**). At all charge ratios investigated (+/- = 1 to 4), the copolymers were able to completely condense plasmid DNA. At charge ratios of 4, the following diameters (nm) were reported for copolymer compositions from 20-70% BMA, respectively: 250 ± 60, 200 ± 50, 260 ± 80, 180 ± 50, 250 ± 60, and 260 ± 80. There appeared to be no significant influence of composition on the ability of the copolymers to condense pDNA. This finding is likely a result of the common pDMAEMA condensing segment shared by the materials and provides strong evidence that the DEAEMA component does not electrostatically interact to a significant degree with the plasmid DNA at physiological pH values.
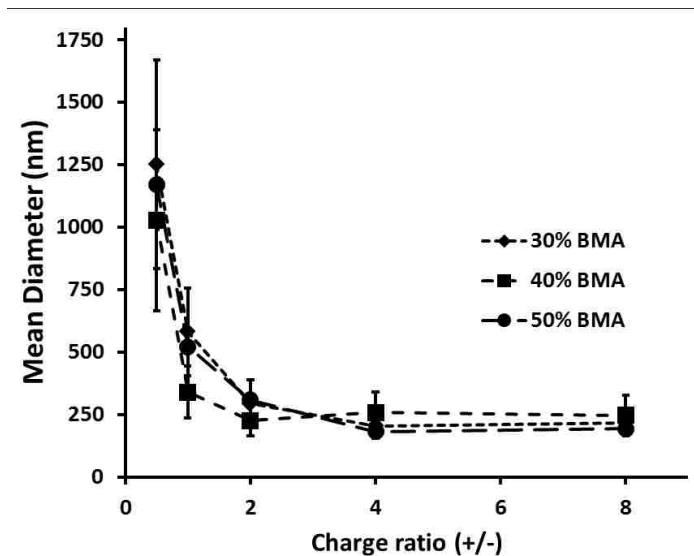
Figure 2.4. Particle size measurements of diblock copolymer/pDNA polyplexes as a function of charge ratio (+/-) by DLS. Mean diameter was determined from the lognormal size distribution. Data are compiled from one experiment with each sample run in triplicate. Error bars represent the standard deviation as calculated from the polydispersity index (PDI) of the particles.

2.3.5. Evaluation of plasmid DNA transfection activity

The transfection activities of the diblock copolymer carriers in antigen-presenting cells were evaluated in RAW 264.7 murine macrophages and JAWSII murine dendritic cells (**Figure 2.5**). Cells were treated with copolymer/DNA polyplexes formulated at theoretical charge ratios of 2 in the presence of serum (10% for RAW 264.7, 20% for JAWSII cells) and GFP expression was quantified 48 h post-transfection by flow cytometry. In RAW 264.7 cells, all

copolymers incorporating less than 60% BMA produced high transfection efficiencies comparable to or exceeding that of the commercial liposomal agent, Lipofectamine 2000. The highest efficiencies were obtained with the 30% and 40% BMA copolymers, which elicited more than double the transfection efficiency obtained using Lipofectamine (44% and 48% vs. 17%). Copolymers with 60% and 70% BMA produced very low levels of GFP expression. Absolute transfection efficiencies were lower in the JAWSII cells, but all of the copolymer carriers outperformed Lipofectamine. The 30% BMA polymer mediated the highest transfection activity with a 9-fold increase in efficiency relative to Lipofectamine. Overall, copolymers that underwent micelle to unimer transitions at endosomal pH values (20-50% BMA) were the most effective vehicles for intracellular pDNA delivery, while copolymers that remained micellar at these pH values (60-70% BMA) were deficient in mediating transfection.
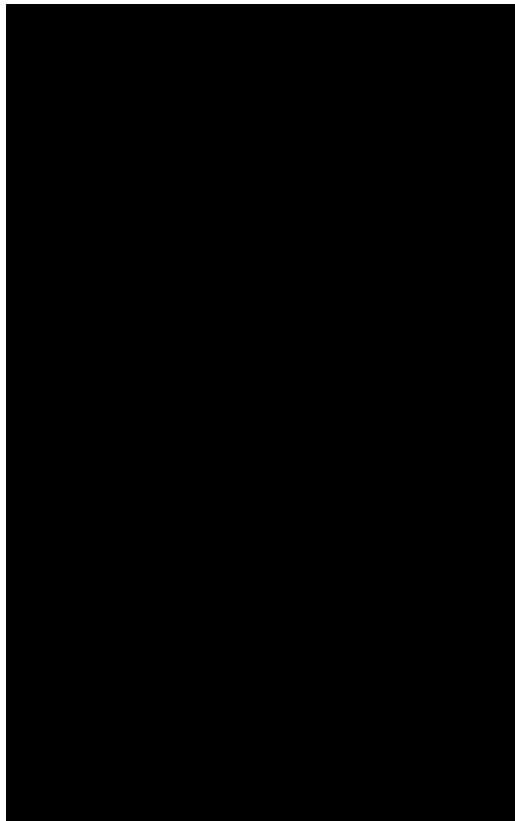
Figure 2.5. In vitro transfection efficiencies in RAW 264.7 (A) and JAWSII (B) cells. Copolymer/pDNA polyplexes were formulated at theoretical charge ratios of 2. LF corresponds to treatment with Lipofectamine/pDNA. Data are from a single experiment run in triplicate with the error bars representing the standard deviation. Statistical significance was evaluated at a level of $p < 0.05$ with the following symbols indicating significance as compared to LF, 20%, 30%, 40%, 50%, 60%, and 70% BMA copolymers, respectively: *, @, #, $, %, ^, &.

2.3.6. Copolymer/pDNA polyplex cytotoxicity

Carrier cytotoxicity was evaluated by incubating the cells with polyplex solutions for 24 h, then quantifying cell viability by measuring the total LDH content relative to untreated cells (**Figure 2.6**). All copolymer carriers displayed comparable or improved toxicity compared to Lipofectamine in both cell lines. In RAW 264.7 cells, viability was high (≥ 70%) across the series of copolymer compositions while Lipofectamine exhibited 55% cell viability. In JAWSII cells, high toxicity was observed in Lipofectamine-treated cells (<10% viability), while polyplexes were associated with moderate to low toxicity (54-85% viability). Polyplex toxicity was generally found to increase with decreasing BMA content in both cell lines, a trend that inversely follows transfection activity.
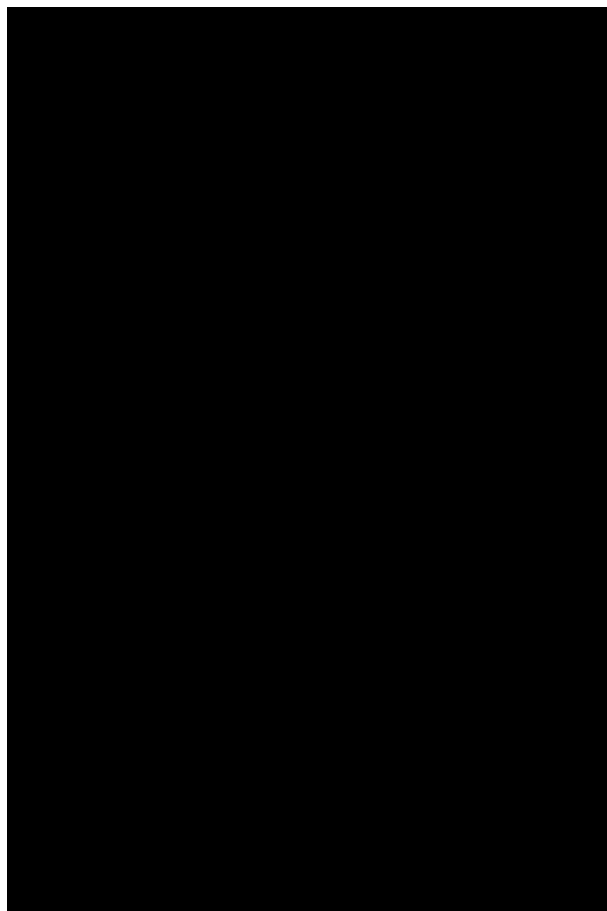
Figure 2.6. Cytotoxicity of polyplexes in RAW 264.7 (A) and JAWSII (B) cells. Polyplexes were prepared at theoretical charge ratios of 2. Data are from a single experiment run in triplicate with the error bars representing the standard deviation. Statistical significance was evaluated at a level of $p < 0.05$ with the following symbols indicating significance as compared to LF, 20%, 30%, 40%, 50%, 60%, and 70% BMA copolymers, respectively: *, @, #, $, %, ^, &.

2.4. DISCUSSION

The diblock copolymer design investigated in these studies is comprised of two distinct polymeric segments with discrete functions (**Scheme 2.1** and **Table 2.1**). The first block is a homopolymer of DMAEMA, a monomer possessing a tertiary amine that is approximately 50% protonated at physiological pH when it is within a polymeric backbone [49]. The cationic nature of this block allows for electrostatic interactions to be made with anionic phosphate groups of nucleic acids, an activity which has been demonstrated previously with DMAEMA polymers [6], [7], [9], [11]. The pDMAEMA segment also provides significant hydrophilic stabilization of the resultant polyplexes. The second block is a statistical copolymer containing DEAEMA and BMA with pH-responsive endosomolytic activity. This block is intended to possess a predominantly hydrophobic character due to the BMA component in addition to deprotonated DEAEMA residues.

The inclusion of DEAEMA in the core-forming segment serves as a pH-sensitive trigger. Upon a decrease in pH, the tertiary amine on this residue protonates to increase the positive charge density within the micelle interior. This leads to electrostatic repulsion between adjacent polymer chains, resulting in micelle destabilization once a sufficient charge density is reached. Vamvakaki et al. demonstrated that hydrophilic block copolymers containing a pDEAEMA segment lost micellar structure upon increasing the degree of amine group ionization past 10% [57]. The relative proportion of hydrophobic components and protonatable amines within the core-forming segment of our copolymer design strongly tunes micelle stability as a function of pH. As the hydrophobic content in the second block increased, greater acidic conditions were necessary to destabilize micellar particles (**Figure 2.1**). With the exception of the 70% BMA composition, all copolymers had lost particulate structure by pH 5.8.

The hemolytic activity closely correlated with the copolymer structural transition as significant red blood cell lysis was only observed at pH values where micellar particles were not detected (**Figure 2.2**). These findings are indicative of an enhanced exchange between a micelle and unimer conformation as the copolymers are exposed to acidifying conditions. At physiological pH, the copolymers were unable to mediate significant hemolysis but once exposed to pH environments supporting unimer evolution, significant lysis was observed.

The proposed core-shell micelle conformation of these copolymers was further validated by ^{1}H-NMR D_2O titration studies (**Figure 2.3**). At pD 7.4, the diblock copolymer spectra resemble that of the DMAEMA homopolymer suggesting that the pDMAEMA block forms a solvated corona while the second block is collapsed due to entropically-driven hydrophobic interactions. At an intermediate pD value of 6.6, a peak attributed to DEAEMA residues within the core block emerges in the 40% BMA copolymer but is absent in the 70% BMA copolymer. The previous DLS and hemolysis findings provide evidence that the former composition adopts a unimeric conformation in this environment while the latter retains micelle characteristics. This result confirms that solvation of the core block is driving this pH-dependent micelle destabilization into unimers.

Based on these initial findings, we anticipated that the activity of these copolymers could be exploited to facilitate intracellular delivery of pDNA by condensing the nucleic acid into serum-stable nanoparticles via electrostatic interactions with the DMAEMA homopolymer block. DLS sizing data showed that at charge ratios of 2 and greater, approximately 200 nm particles were formed for each of the copolymer compositions (**Figure 2.4**). We found that copolymer compositions that were not membrane-interactive at intermediate pH values (7.0 to 6.2) were unable to mediate significant GFP expression. Copolymers that destabilized into unimers at these pH values exhibited not only significant expression but were also more active than the commercial standard, Lipofectamine 2000. The 30% and 40% BMA compositions were found to be effective at transfecting RAW 264.7 cells while the latter copolymer had the highest activity in JAWSII cells. These findings suggest that optimizing the specific pH at which the copolymer carriers transition from inert to endosomolytic states is critical to attaining maximal transfection activity. Furthermore, the copolymer design allows for the pH-responsive profile to be modulated by adjusting the relative monomer feeds in the second block polymerization. This tunability could be advantageous in optimizing carriers for cell types that exhibit different endosomal/lysosomal pH evolution.

2.5. CONCLUSIONS

A series of diblock copolymers containing a pH-responsive endosomal-releasing segment composed of various ratios of diethylaminoethyl methacrylate (DEAEMA) and butyl methacrylate (BMA) were synthesized via reversible addition-fragmentation chain transfer (RAFT) polymerization. These diblock copolymers self-assemble into micelles at

physiological pH but undergo a pH-induced phase transition at lower pH values. The pH at which this phase transition occurs can be precisely tuned by modification of the BMA content. Diblock copolymers with 30 – 40 % BMA content exhibited phase transitions at pH values that are similar to those encountered in the early and late endosomes. These materials showed significant levels of red blood cell lysis at these pH values but negligible cell lysis under physiological conditions. High levels of DNA transfection were observed for these materials highlighting their potential to exploit unique endolysosomal trafficking pathways specific to individual cell types, thereby providing a tunable gene delivery platform.

2.6. ACKNOWLEDGEMENTS

2.7. REFERENCES

[1]   R. Mulligan, "The basic science of gene therapy," *Science*, vol. 260, 1993.

[2]   D. W. Pack, A. S. Hoffman, S. Pun, and P. S. Stayton, "Design and development of polymers for gene delivery.," *Nature reviews. Drug discovery*, vol. 4, no. 7, pp. 581–93, Jul. 2005.

[3]   D. Luo and W. M. Saltzman, "Synthetic DNA delivery systems.," *Nature biotechnology*, vol. 18, no. 1, pp. 33–7, Jan. 2000.

[4]   M. A. Mintzer and E. E. Simanek, "Nonviral vectors for gene delivery.," *Chemical reviews*, vol. 109, no. 2, pp. 259–302, Feb. 2009.

[5]   P. L. Felgner, T. R. Gadek, M. Holm, R. Roman, H. W. Chan, M. Wenz, J. P. Northrop, G. M. Ringold, and M. Danielsen, "Lipofection: a highly efficient, lipid-mediated DNA-transfection procedure.," *Proceedings of the National Academy of Sciences of the United States of America*, vol. 84, no. 21, pp. 7413–7, Nov. 1987.

[6]   P. van de Wetering, E. E. Moret, N. M. Schuurmans-Nieuwenbroek, M. J. van Steenbergen, and W. E. Hennink, "Structure-activity relationships of water-soluble cationic methacrylate/methacrylamide polymers for nonviral gene delivery.," *Bioconjugate chemistry*, vol. 10, no. 4, pp. 589–97, 1999.

[7]   D. W. Lim, Y. I. Yeom, and T. G. Park, "Poly(DMAEMA-NVP)-b-PEG-galactose as gene delivery vector for hepatocytes.," *Bioconjugate chemistry*, vol. 11, no. 5, pp. 688–95, 2000.

[8]   L. Veron, A. Ganée, C. Ladavière, and T. Delair, "Hydrolyzable p(DMAPEMA) polymers for gene delivery.," *Macromolecular bioscience*, vol. 6, no. 7, pp. 540–54, Jul. 2006.

[9]   Y. Z. You, D. S. Manickam, Q. H. Zhou, and D. D. A. Oupicky, "Reducible poly(2-dimethylaminoethyl methaerylate): Synthesis, cytotoxicity, and gene delivery activity," *Journal of Controlled Release*, vol. 122, no. 3, pp. 217–225, 2007.

[10]   R. Sharma, J. Lee, R. C. Bettencourt, C. Xiao, S. F. Konieczny, and Y.-Y. Won, "Effects of the incorporation of a hydrophobic middle block into a PEG-polycation diblock copolymer on the physicochemical and cell interaction properties of the polymer-DNA complexes.," *Biomacromolecules*, vol. 9, no. 11, pp. 3294–307, Nov. 2008.

[11]   A. J. Convertine, D. S. W. Benoit, C. L. Duvall, A. S. Hoffman, and P. S. Stayton, "Development of a novel endosomolytic diblock copolymer for siRNA delivery.," *Journal of Controlled Release*, vol. 133, no. 3, pp. 221–9, Feb. 2009.

[12]   C. H. Zhu, S. Jung, G. Y. Si, R. Cheng, F. H. Meng, X. L. Zhu, T. G. Park, and Z. Y. Zhong, "Cationic Methacrylate Copolymers Containing Primary and Tertiary Amino Side Groups: Controlled Synthesis via RAFT Polymerization, DNA Condensation, and In Vitro Gene Transfection," *Journal of Polymer Science Part a-Polymer Chemistry*, vol. 48, no. 13, pp. 2869–2877, 2010.

[13]   L. Tao, W. C. Chou, B. H. Tan, and T. P. Davis, "DNA polyplexes formed using PEGylated biodegradable hyperbranched polymers.," *Macromolecular bioscience*, vol. 10, no. 6, pp. 632–7, Jun. 2010.

[14]   E. Mastrobattista, R. H. Kapel, M. H. Eggenhuisen, P. J. Roholl, D. J. Crommelin, W. E. Hennink, and G. Storm, "Lipid-coated polyplexes for targeted gene delivery to ovarian carcinoma cells.," *Cancer gene therapy*, vol. 8, no. 6, pp. 405–13, Jun. 2001.

[15]   Q. Peng, Z. Zhong, and R. Zhuo, "Disulfide cross-linked polyethylenimines (PEI) prepared via thiolation of low molecular weight PEI as highly efficient gene vectors.," *Bioconjugate chemistry*, vol. 19, no. 2, pp. 499–506, Feb. 2008.

[16]   S. Werth, B. Urban-Klein, L. Dai, S. Höbel, M. Grzelinski, U. Bakowsky, F. Czubayko, and A. Aigner, "A low molecular weight fraction of polyethylenimine (PEI) displays increased transfection efficiency of DNA and siRNA in fresh or lyophilized complexes.," *Journal of Controlled Release*, vol. 112, no. 2, pp. 257–70, May 2006.

[17]   M. S. Shim and Y. J. Kwon, "Controlled delivery of plasmid DNA and siRNA to intracellular targets using ketalized polyethylenimine.," *Biomacromolecules*, vol. 9, no. 2, pp. 444–55, Feb. 2008.

[18]   O. M. Merkel, O. Germershaus, C. K. Wada, P. J. Tarcha, T. Merdan, and T. Kissel, "Integrin alphaVbeta3 targeted gene delivery using RGD peptidomimetic conjugates with copolymers of PEGylated poly(ethylene imine).," *Bioconjugate chemistry*, vol. 20, no. 6, pp. 1270–80, Jun. 2009.

[19]   J. Fahrmeir, M. Gunther, N. Tietze, E. Wagner, and M. Ogris, "Electrophoretic purification of tumor-targeted polyethylenimine-based polyplexes reduces toxic side effects in vivo.," *Journal of Controlled Release*, vol. 122, no. 3, pp. 236–45, Oct. 2007.

[20]   L. V Christensen, C.-W. Chang, W. J. Kim, S. W. Kim, Z. Zhong, C. Lin, J. F. J. Engbersen, and J. Feijen, "Reducible poly(amido ethylenimine)s designed for triggered intracellular gene delivery.," *Bioconjugate chemistry*, vol. 17, no. 5, pp. 1233–40, 2006.

[21]   Q. Peng, C. Hu, J. Cheng, Z. Zhong, and R. Zhuo, "Influence of disulfide density and molecular weight on disulfide cross-linked polyethylenimine as gene vectors.," *Bioconjugate chemistry*, vol. 20, no. 2, pp. 340–6, Feb. 2009.

[22]   H. Jiang, Y.-K. Kim, R. Arote, D. Jere, J.-S. Quan, J.-H. Yu, Y.-J. Choi, J.-W. Nah, M.-H. Cho, and C.-S. Cho, "Mannosylated chitosan-graft-polyethylenimine as a gene carrier for Raw 264.7 cell targeting.," *International journal of pharmaceutics*, vol. 375, no. 1–2, pp. 133–9, Jun. 2009.

[23]   M. Ogris, S. Brunner, S. Schüller, R. Kircheis, and E. Wagner, "PEGylated DNA/transferrin-PEI complexes: reduced interaction with blood components, extended circulation in blood and potential for systemic gene delivery.," *Gene therapy*, vol. 6, no. 4, pp. 595–605, Apr. 1999.

[24]   W. T. Godbey, K. K. Wu, and a G. Mikos, "Tracking the intracellular path of poly(ethylenimine)/DNA complexes for gene delivery.," *Proceedings of the National Academy of Sciences of the United States of America*, vol. 96, no. 9, pp. 5177–81, Apr. 1999.

[25]   R. S. Burke and S. H. Pun, "Extracellular barriers to in Vivo PEI and PEGylated PEI polyplex-mediated gene delivery to the liver.," *Bioconjugate chemistry*, vol. 19, no. 3, pp. 693–704, Mar. 2008.

[26]   Z. Zhong, J. Feijen, M. C. Lok, W. E. Hennink, L. V Christensen, J. W. Yockman, Y.-H. Kim, and S. W. Kim, "Low molecular weight linear polyethylenimine-b-poly(ethylene glycol)-b-polyethylenimine triblock copolymers: synthesis, characterization, and in vitro gene transfer properties.," *Biomacromolecules*, vol. 6, no. 6, pp. 3440–8, 2005.

[27]   O. Boussif, F. Lezoualc'h, M. a Zanta, M. D. Mergny, D. Scherman, B. Demeneix, and J. P. Behr, "A versatile vector for gene and oligonucleotide transfer into cells in culture and in vivo: polyethylenimine.," *Proceedings of the National Academy of Sciences of the United States of America*, vol. 92, no. 16, pp. 7297–301, Aug. 1995.

[28]   H. Pollard, J. S. Remy, G. Loussouarn, S. Demolombe, J. P. Behr, and D. Escande, "Polyethylenimine but not cationic lipids promotes transgene delivery to the nucleus in mammalian cells.," *The Journal of biological chemistry*, vol. 273, no. 13, pp. 7507–11, Mar. 1998.

[29]   C. Aral and J. Akbuga, "Preparation and in vitro transfection efficiency of chitosan microspheres containing plasmid DNA:poly(L-lysine) complexes.," *Journal of pharmacy & pharmaceutical sciences*, vol. 6, no. 3, pp. 321–6, 2003.

[30]   Y. Guo, Y. Sun, J. Gu, and Y. Xu, "Capillary electrophoresis analysis of poly(ethylene glycol) and ligand-modified polylysine gene delivery vectors.," *Analytical biochemistry*, vol. 363, no. 2, pp. 204–9, Apr. 2007.

[31]   T. Kawano, T. Okuda, H. Aoyagi, and T. Niidome, "Long circulation of intravenously administered plasmid DNA delivered with dendritic poly(L-lysine) in the blood flow.," *Journal of Controlled Release*, vol. 99, no. 2, pp. 329–37, Sep. 2004.

[32]   T.-G. Kim, S.-Y. Kang, J.-H. Kang, M.-Y. Cho, J.-I. Kim, S.-H. Kim, and J.-S. Kim, "Gene transfer into human hepatoma cells by receptor-associated protein/polylysine conjugates.," *Bioconjugate chemistry*, vol. 15, no. 2, pp. 326–32, 2004.

[33]   Y. H. Choi, F. Liu, J. S. Park, and S. W. Kim, "Lactose-poly(ethylene glycol)-grafted poly-L-lysine as hepatoma cell-tapgeted gene carrier.," *Bioconjugate chemistry*, vol. 9, no. 6, pp. 708–18, 1998.

[34]   P. Midoux and M. Monsigny, "Efficient gene transfer by histidylated polylysine/pDNA complexes.," *Bioconjugate chemistry*, vol. 10, no. 3, pp. 406–11, 1999.

[35]   Y. H. Choi, F. Liu, J. S. Kim, Y. K. Choi, J. S. Park, and S. W. Kim, "Polyethylene glycol-grafted poly-L-lysine as polymeric gene carrier.," *Journal of Controlled Release*, vol. 54, no. 1, pp. 39–48, Jun. 1998.

[36]   M. L. Forrest and D. W. Pack, "On the Kinetics of Polyplex Endocytic Trafficking : Implications for Gene Delivery Vector Design," *Gene Therapy*, vol. 6, no. 1, pp. 57–66, 2002.

[37]   J. L. Thomas and D. A. Tirrell, "Polyelectrolyte-sensitized phospholipid vesicles," *Accounts of Chemical Research*, vol. 25, no. 8, pp. 336–342, Aug. 1992.

[38]   N. Murthy, J. R. Robichaud, D. A. Tirrell, P. S. Stayton, and A. S. Hoffman, "The design and synthesis of polymers for eukaryotic membrane disruption.," *Journal of Controlled Release*, vol. 61, no. 1–2, pp. 137–43, Aug. 1999.

[39]   C. A. Lackey, O. W. Press, A. S. Hoffman, and P. S. Stayton, "A biomimetic pH-responsive polymer directs endosomal release and intracellular delivery of an endocytosed antibody complex.," *Bioconjugate chemistry*, vol. 13, no. 5, pp. 996–1001, 2002.

[40]   V. P. Torchilin, "Recent advances with liposomes as pharmaceutical carriers.," *Nature reviews. Drug discovery*, vol. 4, no. 2, pp. 145–60, Feb. 2005.

[41]   S. Simões, J. N. Moreira, C. Fonseca, N. Düzgüneş, and M. C. P. de Lima, "On the formulation of pH-sensitive liposomes with long circulation times.," *Advanced drug delivery reviews*, vol. 56, no. 7, pp. 947–65, Apr. 2004.

[42]   C. Y. Wang and L. Huang, "pH-sensitive immunoliposomes mediate target-cell-specific delivery and controlled expression of a foreign gene in mouse.," *Proceedings of the National Academy of Sciences of the United States of America*, vol. 84, no. 22, pp. 7851–5, Nov. 1987.

[43]   B. Pitard, O. Aguerre, M. Airiau, a M. Lachagès, T. Boukhnikachvili, G. Byk, C. Dubertret, C. Herviou, D. Scherman, J. F. Mayaux, and J. Crouzet, "Virus-sized self-assembling lamellar complexes between plasmid DNA and cationic

micelles promote gene transfer.," *Proceedings of the National Academy of Sciences of the United States of America*, vol. 94, no. 26, pp. 14412–7, Dec. 1997.

[44] Y. Kakizawa and K. Kataoka, "Block copolymer micelles for delivery of gene and related compounds.," *Advanced drug delivery reviews*, vol. 54, no. 2, pp. 203–22, Feb. 2002.

[45] C. Zhu, S. Jung, S. Luo, F. Meng, X. Zhu, T. G. Park, and Z. D. Zhong, "Co-delivery of siRNA and paclitaxel into cancer cells by biodegradable cationic micelles based on PDMAEMA-PCL-PDMAEMA triblock copolymers.," *Biomaterials*, vol. 31, no. 8, pp. 2408–16 ST – Co–delivery of siRNA and paclitaxel, 2010.

[46] Y. Tang, S. Y. Liu, S. P. Armes, and N. C. Billingham, "Solubilization and controlled release of a hydrophobic drug using novel micelle-forming ABC triblock copolymers.," *Biomacromolecules*, vol. 4, no. 6, pp. 1636–45, 2003.

[47] Y. Z. You, Q. H. Zhou, D. S. Manickam, L. Wan, G. Z. Mao, and D. Oupicky, "Dually responsive multiblock copolymers via reversible addition-fragmentation chain transfer polymerization: Synthesis of temperature- and redox-responsive copolymers of poly(N-isopropylacrylamide) and poly(2-(dimethylamino)ethyl methacrylate)," *Macromolecules*, vol. 40, pp. 8617–8624, 2007.

[48] P. van de Wetering, J.-Y. Cherng, H. Talsma, and W. E. Hennink, "Relation between transfection efficiency and cytotoxicity of poly(2-(dimethylamino)ethyl methacrylate)/plasmid complexes," *Journal of Controlled Release*, vol. 49, no. 1, pp. 59–69, Nov. 1997.

[49] P. van de Wetering, N. J. Zuidam, M. J. van Steenbergen, O. a. G. J. van der Houwen, W. J. M. Underberg, and W. E. Hennink, "A Mechanistic Study of the Hydrolytic Stability of Poly(2-(dimethylamino)ethyl methacrylate)," *Macromolecules*, vol. 31, no. 23, pp. 8063–8068, Nov. 1998.

[50] T. Reschel, C. Konák, D. Oupický, L. W. Seymour, and K. Ulbrich, "Physical properties and in vitro transfection efficiency of gene delivery vectors based on complexes of DNA with synthetic polycations.," *Journal of controlled release : official journal of the Controlled Release Society*, vol. 81, no. 1–2, pp. 201–17, May 2002.

[51] R. A. Jones, M. H. Poniris, and M. R. Wilson, "pDMAEMA is internalised by endocytosis but does not physically disrupt endosomes.," *Journal of Controlled Release*, vol. 96, no. 3, pp. 379–91, May 2004.

[52] A. M. Funhoff, C. F. van Nostrum, M. C. Lok, J. A. W. Kruijtzer, D. J. A. Crommelin, and W. E. Hennink, "Cationic polymethacrylates with covalently linked membrane destabilizing peptides as gene delivery vectors.," *Journal of Controlled Release*, vol. 101, no. 1–3, pp. 233–46, Jan. 2005.

[53] A. J. Convertine, C. Diab, M. Prieve, A. Paschal, A. S. Hoffman, P. H. Johnson, P. S. Stayton, W. H. Street, and S. Washington, "pH-Responsive Polymeric Micelle Carriers for siRNA Drugs," *Biomacromolecules*, pp. 2904–2911, 2010.

[54] G. Moad, Y. K. Chong, A. Postma, E. Rizzardo, and S. H. Thang, "Advances in RAFT polymerization: the synthesis of polymers with defined end-groups," *Polymer*, vol. 46, no. 19, pp. 8458–8468, Sep. 2005.

[55] A. Kręzel and W. Bal, "A formula for correlating pKa values determined in D2O and H2O," *Journal of Inorganic Biochemistry*, vol. 98, no. 1, pp. 161–166, Jan. 2004.

[56] M. Yessine, M. Lafleur, C. Meier, H. Petereit, and J. Leroux, "Characterization of the membrane-destabilizing properties of different pH-sensitive methacrylic acid copolymers," *Biochimica et Biophysica Acta (BBA)*, vol. 1613, no. 1–2, pp. 28–38, Jun. 2003.

[57] M. Vamvakaki, D. Palioura, a. Spyros, S. P. Armes, and S. H. Anastasiadis, "Dynamic Light Scattering vs 1 H NMR Investigation of pH-Responsive Diblock Copolymers in Water," *Macromolecules*, vol. 39, no. 15, pp. 5106–5112, Jul. 2006.

CHAPTER 3 – GLYCOPOLYMERS EXHIBITING LECTIN-SPECIFIC, RECEPTOR-MEDIATED UPTAKE

Matthew J. Manganiello*, Eun-Ho Song*, Yu-Hua Chow*, Anthony J. Convertine, Bilal Ghosn, Lynn M. Schnapp, Patrick S. Stayton, Daniel M. Ratner

*These authors contributed equally to this work.

ABSTRACT

Targeting cell populations via endogenous carbohydrate receptors is an appealing approach for drug delivery. PENDENTHowever, to be effective, this strategy requires the production of high affinity carbohydrate ligands capable of engaging with specific cell-surface lectins. To develop materials that exhibit high affinity towards these receptors, we synthesized glycopolymers displaying pendent carbohydrate moieties from carbohydrate-functionalized monomer precursors via reversible addition-fragmentation chain transfer (RAFT) polymerization. These glycopolymers were fluorescently labeled and used to determine macrophage-specific targeting both in vitro and in vivo. Mannose- and N-acetylglucosamine-containing glycopolymers were shown to specifically target mouse bone marrow-derived macrophages (BMDMs) in vitro in a dose-dependent manner as compared to a galactose-containing glycopolymer (30- and 19-fold higher uptake, respectively). In addition, upon macrophage differentiation, the mannose glycopolymer exhibited enhanced uptake in M2-polarized macrophages, an anti-inflammatory macrophage phenotype prevalent in injured tissue. This carbohydrate-specific uptake was retained in vivo, as alveolar macrophages demonstrated 6-fold higher internalization of mannose glycopolymer, as compared to galactose, following intratracheal administration in mice. We have shown the successful synthesis of a class of functional RAFT glycopolymers capable of macrophage-type specific uptake both in vitro and in vivo, with significant implications for the design of future targeted drug delivery systems.

3.1. INTRODUCTION

The targeted delivery of small molecule drugs and biologics continues to be a major objective towards improving therapeutic efficiency through the mitigation of off-target effects and reduction in required dose [1]. However, few delivery carriers are capable of recognizing cell-specific ligands while avoiding nonspecific cellular uptake. To overcome this

limitation, carbohydrate-based materials have been investigated due to their biocompatibility, target specificity, and ability to facilitate receptor-mediated uptake through cell-surface lectins (carbohydrate-binding proteins) [2,3].

Macrophages are an attractive therapeutic target because they play an important role in the inflammatory response and wound healing [4]. A number of macrophage subsets have been described that are associated with distinct phenotypes. Classically activated macrophages (M1) are critical for host defense whereas alternatively activated macrophages (M2) are important in injury resolution and wound healing. In response to acute injury, the predominant macrophage phenotype is pro-inflammatory (M1). However, an overexuberant M1 macrophage response can result in collateral tissue damage and impaired wound healing. Likewise, while M2 macrophages are important for appropriate wound healing, excess M2 response can result in tissue fibrosis. Indeed, dysregulated macrophage function is associated with a wide range of conditions including chronic ulcers, allergic asthma, atherosclerosis, autoimmune disorders, and fibrotic diseases [4]. Therefore, developing a drug delivery platform capable of directly targeting and modulating polarized macrophages has important therapeutic implications, for example, targeting of alveolar macrophage represents a promising strategy for addressing pulmonary inflammatory conditions [5,6].

Carbohydrates are known to play a significant role in the inflammatory response through mediating cell-cell recognition of immune cells, including macrophages [7]. Macrophages are a promising target for carbohydrate-based therapeutics as they express carbohydrate binding receptors which internalize bound material via receptor-mediated endocytosis [8]. One such carbohydrate binding receptor is the macrophage mannose receptor, an endocytic protein that is highly expressed on macrophages, including the alveolar macrophage [9]. The mannose receptor mediates the uptake and internalization of extracellular ligands including potentially harmful extracellular glycoproteins with terminal mannose, fucose, or *N*-acetylglucosamine, and pathogens with high densities of mannose on their surface [10,11]. The murine mannose receptor, MRC-1 (CD206), contains eight extracellular C-type lectin-like domains (CTLDs) [12]. Simple monosaccharides exhibit low affinities towards single MRC-1 CTLDs, with dissociation constants in the low millimolar range [13]. Many natural glycans enhance these weak binding events by clustering multiple glycosides together, thereby allowing multivalent interactions to be made with a multidomain lectin receptor (e.g.

the mannose receptor) leading to a significant increase in overall avidity [14]. Ligands capable of exhibiting this multivalent behavior through simultaneous engagement of multiple CTLDs on the mannose receptor are potent facilitators of macrophage-specific uptake [15]. While mannose displays the highest affinity toward mannose receptor CTLDs, other sugars (e.g. fucose, *N*-acetylglucosamine and glucose) are also recognized by these lectin-like domains [16].

Through the presentation of multiple pendent carbohydrates, synthetic glycopolymers provide a promising platform to facilitate mannose receptor-mediated binding and subsequent endocytosis [2]. While such compounds have been previously synthesized to probe lectin-carbohydrate binding behavior [17], only recently have structurally well-defined, homogeneous glycopolymers capable of multivalent interactions been successfully prepared [18]. For example, multivalent glycopolymers can be synthesized via the functionalization of an individual monosaccharide with a vinyl-containing compound resulting in a glycomonomer [19]. These glycomonomers can be polymerized through free radical polymerization to yield a glycopolymer with pendent carbohydrates [20,21]. Use of reversible addition-fragmentation chain transfer (RAFT) polymerization for this glycopolymer synthesis offers precise control over the reaction, resulting in predictable molecular weights, narrow molecular weight distributions, and the ability to develop complex polymer architectures [22]. Lowe et al. first demonstrated the successful RAFT polymerization of a glycomonomer by using glucose-functionalized methacrylate monomer in aqueous conditions; the resultant material exhibited a low polydispersity and displayed "living" properties characteristic of the RAFT technique [19]. Additionally, through the modification of the chain transfer agent (CTA) and the incorporation of comonomers, facile telechelic and pendent polymer functionalization is achievable [23-25]. By combining the versatility of the RAFT process with carbohydrate synthetic techniques, structurally complex glycosylated materials capable of mimicking the multivalent binding activity of biological carbohydrate compounds can be realized., e.g. glycopolymer micelles [25,26], stars [18], nanoparticles [27,28], "clickable" constructs [23] [29-31], and glycosylated block copolymers [26] [32-34]. By displaying multiple functional carbohydrates, these materials can be used to target specific cell populations via carbohydrate-dependent uptake mechanisms, allowing for the design of diagnostic and therapeutic glycosylated constructs.

Glycosylation of drug delivery vehicles has been explored as a means to access alveolar macrophages in vivo, a cell implicated in the pathogenesis of pulmonary conditions [6]. Chono et al. demonstrated that mannosylating liposomes enhanced their uptake by rat alveolar macrophages in vivo following intratracheal administration, work which has been extended by Wijagkanalan et al. [35-37]. In light of this previous work, there has yet to be a study systemically evaluating the uptake of well-defined, multivalent carbohydrate materials by macrophages both in vitro and in pulmonary tissue. Herein, we describe the synthesis of glycomonomers and employed RAFT polymerization to develop a family of fluorescently-labeled glycopolymers capable of macrophage-specific targeting.

3.2. MATERIALS AND METHODS

3.2.1. Materials

Materials were purchased from Sigma-Aldrich unless otherwise specified. 4,4′-Azobis(4-cyanovaleric acid) (V501) was obtained from Wako Chemicals USA, Inc. 4-Cyano-4-(ethylsulfanylthiocarbonyl) sulfanylvpentanoic acid (ECT) and Pyridyl disulfide ethyl methacrylamide (PDSEMA) was synthesized as described previously [38].

3.2.2. General synthesis of glycomonomers

TMSOTf (cat.) was added to a mixture of trichloroacetimidate sugar donor [39] (1g, 2.0 mmol) and 2-hydroxyethyl methacrylate (1.2 eq) in dichloromethane at room temperature. The reaction mixture was stirred at room temperature for 20 min and then quenched by the addition of triethylamine. The protected sugar-hydroxyethyl methacrylate was obtained after removal of solvent under reduced pressure, followed by purification via flash silica column chromatography (82-89% yield). For deprotection, sugar-hydroxyethyl methacrylate was added to 1% sodium methoxide in methanol and the mixture was stirred at 25 $^{\circ}$C for 15 min. The reaction mixture was neutralized with glacial acetic acid. The fully deprotected glycomonomer was obtained after evaporation of solvent under reduced pressure, followed by purification via flash silica column chromatography (70-82% yield).

3.2.2. Synthesis of glycopolymers

The RAFT polymerization of glycopolymers was conducted in a heterogeneous solvent system of dH$_2$O/ethanol (3:1 vol:vol) at 70°C with 15 wt% monomer under a nitrogen atmosphere for 4h using ECT and V501 as the chain transfer agent (CTA) and radical

initiator, respectively. The initial CTA to monomer molar ratio ($[CTA]_0:[M]_0$) was 50:1, the initial CTA to initiator molar ratio ($[CTA]_0:[I]_0$) was 20:1, and the initial molar feed ratios of glycomonomer to PDSEMA was 9:1. The resultant glycopolymer was isolated by dilution into dH_2O followed by lyophilization. The glycopolymer was further purified by redissolution into dH_2O, chromatographic separation with a PD-10 desalting column (GE Healthcare), and further lyophilization to obtain the final polymer.

3.2.3. Glycopolymer characterization

Monomer conversion and incorporation were determined by ^{1}H-NMR (500 MHz, D_2O). Conversion was determined to be greater than 99% due to the absence of resonances associated with vinyl protons on the glycomonomer (δ 6.07) and PDSEMA (δ 5.77) following polymerization. Copolymer composition was calculated from an aromatic PDSEMA proton (δ 8.40) and a methylene proton vicinal to the ester group (δ 4.15 Man) or methine proton on the pyranose ring (δ 4.36 Gal and δ 4.51 GlcNAc). Molecular weights (M_n) and polydispersity indices (PDI) were determined by gel permeation chromatography (GPC) using a Viscotek GPCmax VE2001 and refractometer VE3580 (Viscotek) with Tosoh TSK-GEL α-3000 (2X) and α-4000 columns connected in series (Tosoh Bioscience). HPLC-grade N,N-dimethylacetamide (DMAc; 0.03% w/v LiBr; 0.05% w/v BHT) was used as the eluent at a flow rate of 0.85 mL/min while column temperature was maintained at 50°C. Absolute number average molecular weights were calculated from dn/dc values that were determined for each glycopolymer (pManEMA: 0.101, pGalEMA: 0.100, pGlcNAcEMA: 0.130). PDSEMA incorporation was further validated by reduction of the glycopolymers in the presence of Bond-Breaker TCEP solution (~150 molar excess per polymer at 50 mM; Thermo Scientific) followed by spectroscopic measurement of liberated pyridine-2-thione ($\varepsilon_{343} = 8080$ M cm^{-1}).

3.2.4. Fluorophore labeling of glycopolymers

Glycopolymers (~10 mg mL^{-1}, in 0.1 M sodium phosphate pH 7.4 with 0.15 M NaCl buffer) were incubated in immobilized TCEP disulfide reducing gel (~10 molar excess per polymer; Thermo Scientific) for 2h followed by elution with PBS. Alexa Flour 488 (AF488) C5 maleimide (10 mg mL^{-1} in DMSO) was added to the reduced polymer in solution resulting in an approximately equimolar amount of fluorophore to reduced PDS groups and an overall polymer concentration of ~2 mg mL^{-1}. The reaction proceeded overnight at room temperature followed by removal of excess fluorophore by a PD-10 desalting column and

lyophilization. Fluorophore labeling efficiency was determined by spectroscopic measurement of the trithiocarbonate species on the glycopolymer end group (ε_{310} = 20,000 M cm^{-1}) and the Alexa Fluor [48]8 (ε_{495} = 73,000 M cm^{-1}).

3.2.5. Lectin agglutination assay

The ability of the glycopolymers to bind a mannose-specific lectin, Concanavalin A (ConA), was assessed by an agglutination assay. 1 µM ConA was mixed with 10 µM glycopolymer (based on number of carbohydrate repeats) and the solution turbidity was measured by UV-Vis spectroscopy at 350 nm at one minute intervals for 30 minutes.

3.2.6. In vitro glycopolymer uptake assay

Animal protocol was approved by University of Washington Institutional Animal Care and Use Committee. Primary mouse lung fibroblasts (MLF) were isolated and cultured as previously described (Choi 2009). The murine lung epithelial cell line MLE12 was obtained from American Type Culture Collection (ATCC). MLF and MLE12 uptake assays were performed in colorless DMEM supplemented with Glutamax (Life Technologies) and Nutridoma-SP (Roche). Bone marrow derived macrophages (BMDM) were isolated from femurs and tibias of 8-12 week-old C57BL6 mice as previously described [40] and cultured in RPMI-1640 containing 10% Fetal Bovine Serum and 30% L929-conditioned medium for 7-10 days. To obtain differentiated macrophages, BMDMs (M0) were treated with 50 ng mL^{-1} *E. coli* 0111:B4 LPS (Sigma) for 24 hours (M1) or 20 ng mL^{-1} each of IL-4 and IL-13 (Life Technologies) for 48 hours (M2). Cells were seeded in 12-well plates and allowed to adhere overnight. Cells were rinsed with DPBS, and then incubated with indicated concentration of Alexa488-labeled glycopolymers in colorless RPMI supplemented with Glutamax and Nutridoma-SP. For competition experiments, unlabeled glycopolymer was added 15 min prior to addition of labeled glycopolymer. At the end of incubation, the cells were washed and lifted with cold DPBS aided by cell scrapers. Internalized polymer was measured as fluorescence intensity of the cells using Guava EasyCyte Plus System (Millipore) and data analyzed using CellQuest 2.0 (BD Biosciences). All experiments were performed in triplicate and repeated at least 3 times.

3.2.7. In vivo glycopolymer uptake assay

8-12 week-old C57BL6 mice (Jackson Laboratories) underwent intratracheal instillation with 10 µM Alexa-488 glycopolymers or control (unlabeled) polymer in 50 µL DPBS. After 15-30 min, the lungs were lavaged with 1 mL of DPBS containing 0.6 mM EDTA. Bronchoalveolar lavage cells were centrifuged and rinsed to remove unincorporated polymers and resuspended in PBS for flow analysis by Guava as above [41]. In some cases, BAL cells were spun onto microslides, and nuclei were counterstained with DAPI. Images were obtained using a Nikon Eclipse 80i microscope with a DS Camera Head DS-5M for fluorescent microscopy.

3.2.8. Statistical analysis

Means of more than two groups of data were compared using one-way analysis of variance (ANOVA) for analysis of one independent variable or two way ANOVA, for analysis of two independent variables, followed by Tukey's honestly significant difference (HSD) post hoc test. Student T-test was used for comparison of paired parametric data. For non-parametric data, Mann-Whitney's U test was performed. All tests were two-tailed and p values ≤ 0.05 were considered significant.

3.3. RESULTS AND DISCUSSION

3.3.1. Glycopolymer synthesis and characterization

Carbohydrates are attractive ligands for imparting biological targeting functionality to polymeric systems. Carbohydrate-ligands can be easily synthesized in large scale [42], are stable to indefinite storage at ambient temperatures [43], and can leverage low-affinity binding interactions through multivalency [44]. Well-defined glycopolymers were prepared via the RAFT polymerization of synthesized glycomonomers (**Scheme 3.1**). We selected mannose (Man) and *N*-acetylglucosamine (GlcNAc) because of their known mannose receptor binding and galactose (Gal) due to its lack of mannose receptor interactions [16,45]. Each monosaccharide was functionalized with ethyl methacrylate (EMA), yielding the glycomonomers: ManEMA, GlcNAcEMA, and GalEMA. These glycomonomers were polymerized via the RAFT technique. A pyridyl disulfide comonomer, pyridyl disulfide ethyl methacrylamide (PDSEMA), was incorporated into the polymerization (at a 10% molar feed ratio) to provide a conjugatable handle for a maleimide-containing fluorophore.

Glycopolymers (subsequently referred to as pManEMA, pGlcNAcEMA, and pGalEMA) were successfully synthesized under controlled conditions with consistent size and composition as determined by gel permeation chromatography (GPC) and ^{1}H-NMR spectroscopy (**Table 3.1** and **Figure 3.1**). The glycopolymers exhibited narrow molecular weight distributions with polydispersity indices (PDI) of 1.2 and resultant block lengths of 11400 – 13400 g mol^{-1}. The monomer incorporations of pyridyl disulfide groups per polymer were also similar between the glycopolymers (3.3 – 5.2). These findings demonstrate the first direct RAFT polymerization of the ManEMA and GlcNAcEMA glycomonomers used here while the GalEMA glycomonomer has been previously polymerized via this technique [28,46].

A maleimide-functionalized fluorophore (Alexa Fluor 488, AF488) was conjugated to the glycopolymers through the pyridyl disulfide (PDS) groups following reduction with tris(2-carboxyethyl)phosphine (TCEP). Labeling efficiency was similar among the three glycopolymers as determined by UV-Vis spectroscopy: 0.93 – 1.2 fluorophores/polymer, and there was no measurable increase in solution turbidity suggestive of a lack of glycopolymer aggregation. Moreover, dynamic light scattering (DLS) measurements of the glycopolymers following labeling demonstrated there is no significant aggregation of the materials into larger, macromolecular assemblies as mean particle diameters of less than 8 nm were observed (approximately 4 – 7 nm; Supplementary Fig. S5). To initially determine lectin-binding activity, each glycopolymer was incubated with Concanavalin A (ConA) [47], a mannose-specific-binding lectin known to bind mannose and glucose, but not galactose or N-aceltylglucosamine [48]. pManEMA was found to agglutinate ConA, as measured by an increase in solution turbidity, showing that the material is capable of multivalent CRD-binding, a prerequisite for mannose receptor engagement (**Figure 3.2**). pGlcNAcEMA and pGalEMA did not induce ConA agglutination, demonstrating that the glycopolymer binding activity is carbohydrate-specific.
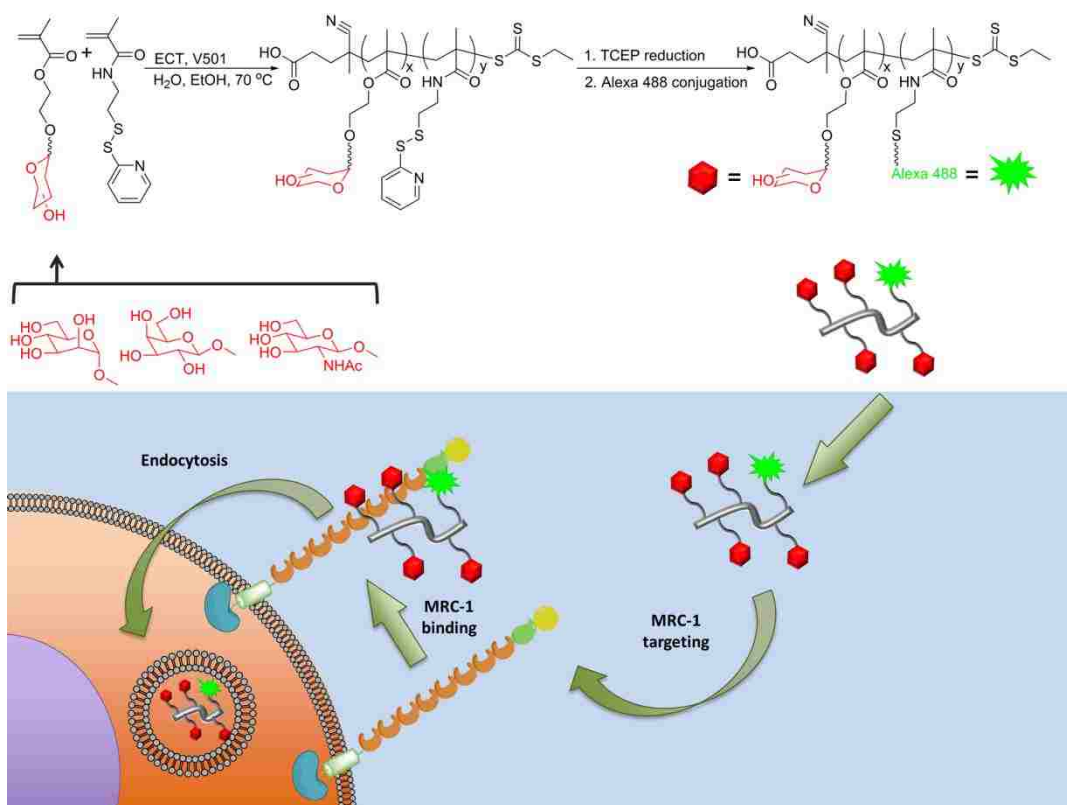
Scheme 3.1. RAFT-mediated glycopolymer synthesis and subsequent fluorophore conjugation and proposed mechanism of MRC-1-mediated macrophage uptake of the glycopolymers.

Table 3.1.

Molecular weights, compositions, conversions, and labeling efficiency of glycopolymers.

Glycopolymer	$M_n{}^a$ (g/mol)	PDI^a	%Conversion^b	PDS/ polymer^c	Alexa488/ polymer^c
pManEMA	11400	1.2	>99	5.2	0.93
pGalEMA	12200	1.2	>99	4.5	0.95
pGlcNAcEMA	13100	1.2	>99	3.3	1.2

[a] Absolute number average molecular weights and polydispersity index (PDI) as determined by gel permeation chromatography (GPC).
[b] Determined by 1H-NMR
[c] Determined by UV-Vis spectroscopy; ratio represents number of pyridyl disulfide (PDS) groups per polymer chain
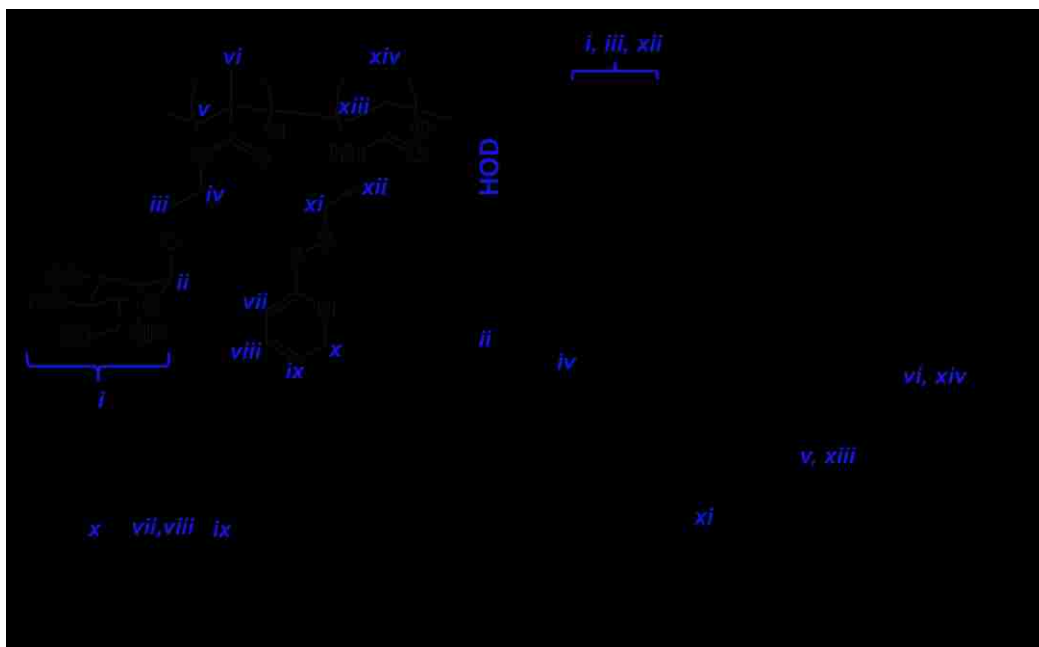
Figure 3.1. ^{1}H NMR of mannose glycopolymer [poly(ManEMA-*co*-PDSMA)] at 500 MHz in D$_2$O.
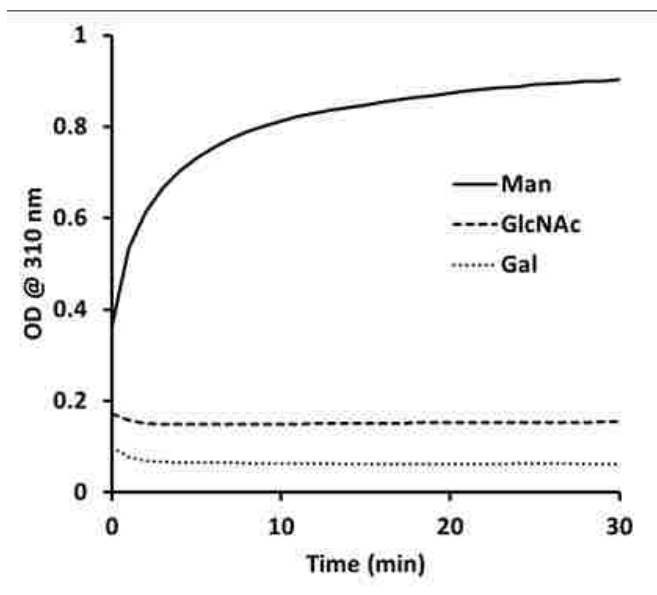
Figure 3.2. Time-dependent agglutination of ConA mediated by glycopolymers. ConA is at 1 µM and glycopolymers are at 10 µM (based on number of carbohydrate repeats).

3.3.2. In vitro macrophage uptake of glycopolymers

We first examined whether the glycopolymers were differentially internalized by murine bone marrow-derived macrophages (BMDMs), a cell type known to express the mouse mannose receptor, MRC-1. BMDMs were incubated with increasing doses of AF488-labeled glycopolymers for varying lengths of time and cell uptake was assessed by flow cytometry and fluorescent microscopy (**Figure 3.3** and **3.4**). We found that pManEMA and pGlcNAcEMA, but not pGalEMA, were internalized efficiently by BMDMs in a time dependent fashion. The uptake of pManEMA and pGlcNAcEMA were 30- and 19-fold higher than pGalEMA, respectively. Significant uptake occurred by 15 min and increased up to 6 hours (**Figure 3.4** and data not shown). Mannose-binding protein, a soluble multi-domain C-type lectin in the same family as MRC-1, is known to exhibit carbohydrate-binding specificities defined by interactions with the vicinal, equatorial hydroxyl groups, C-3 and C-4, that are shared between several sugars [49]. Therefore, the ability of polymerized Man and GlcNAc to target macrophages is not surprising. BMDMs demonstrated a cytoplasmic punctate distribution of internalized pManEMA and pGlcNAcEMA, consistent with localization in the endosome/lysosome vesicles. No cell fluorescence above background was observed with pGalEMA. We also observed a dose-dependent response on uptake for both pManEMA and pGlcNAcEMA with saturation of pManEMA uptake occurring at 0.5 µM (**Figure 3.4**); no significant dose-dependent effects were observed for pGalEMA uptake.

The effect of glycopolymer competition on uptake was assessed by incubating BMDMs with labeled glycopolymer in the presence of excess unlabeled glycopolymer. Competition with unlabeled pManEMA was more efficient than pGlcNAcEMA at attenuating uptake of labeled pManEMA and pGlcNAcEMA, suggesting that the binding affinity of MRC-1 towards pManEMA is higher than pGlcNAcEMA (**Figure 3.5**). This finding is consistent with the mannose receptor's stronger affinity for Man residues over GlcNAc [8]. We presume the minimal uptake of pGalEMA by BMDMs was due to nonspecific macropinocytosis, supported by the lack of competition from any of the glycopolymers.
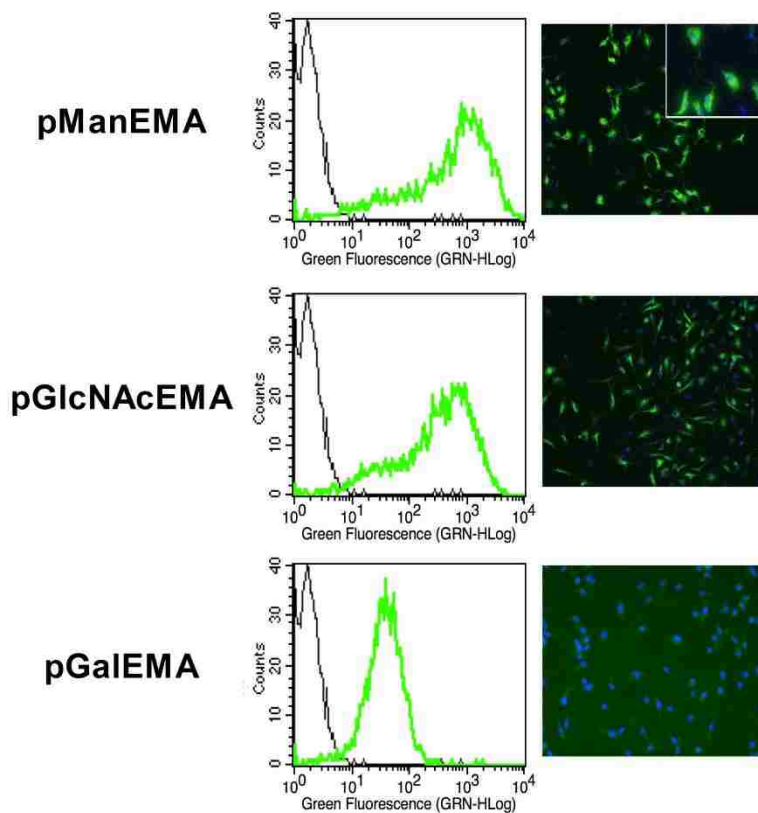
Figure 3.3. In vitro BMDM glycopolymer uptake. Representative histograms (left) and fluorescence microscopy images (right) of BMDMs incubated in vitro with indicated AF488-glycopolymer (1.5 µM) for 4 hr. Black line in histograms represents no polymer control. Inset shows a higher magnification image of the AF488-pManEMA treated cells.
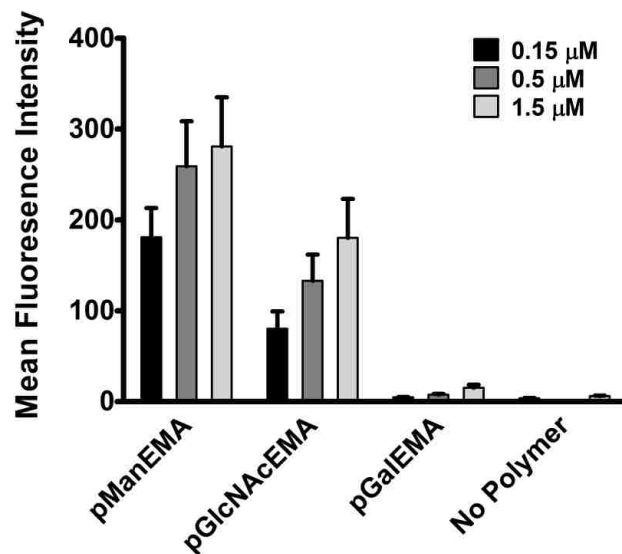
Figure 3.4. Dose dependent internalization. BMDMs were incubated with AF488-glycopolymers for 15 min at 37°C. Data are reported as mean fluorescence intensity ± standard deviation from three independent experiments.
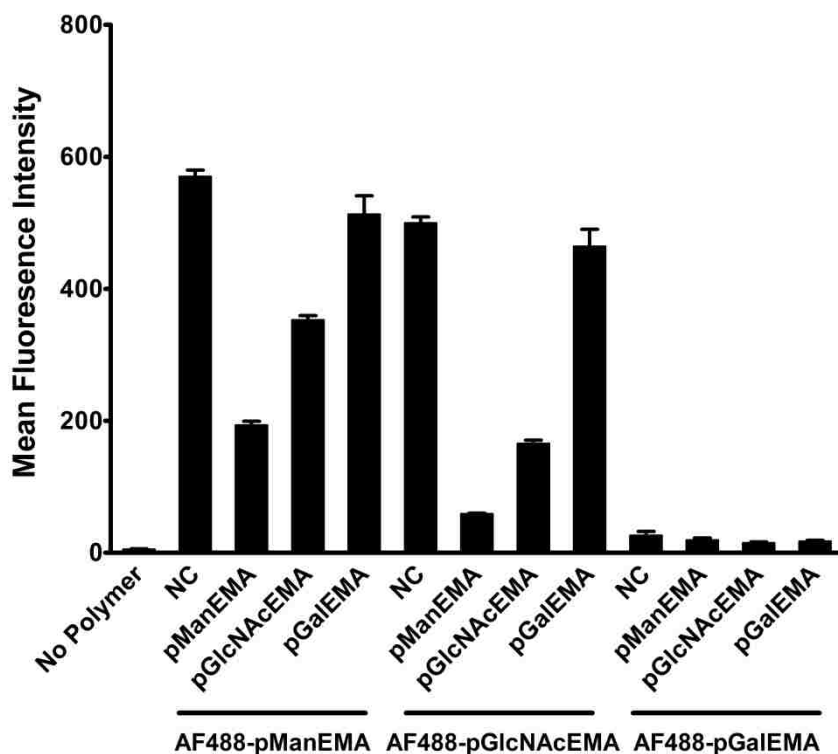
Figure 3.5. Competitive glycopolymer uptake. BMDMs were preincubated with 15 µM unlabeled glycopolymer for 15 min followed by 1 µM AF488-glycopolymer for 30 min at 37°C. NC represents no competition. Data are reported as mean fluorescence intensity ± standard deviation from three independent experiments.

3.3.3. In vitro glycopolymer uptake by polarized macrophages.

We tested whether the polarization state of macrophages altered the uptake of pManEMA. Macrophages can be polarized into a classic "pro-inflammatory" (M1) or alternative "pro-resolution" (M2) state, depending on the local environment of cytokines and other immune-stimulating compounds. Macrophages can be differentiated in vitro by LPS to the M1, "classically" activated state which results in the secretion of pro-inflammatory cytokines. Incubation with IL-4 and IL-13 leads to differentiation into M2, or "alternatively" activated macrophages, which are considered a pro-resolution and anti-inflammatory phenotype [50]. M2 macrophages secrete pro-fibrotic cytokines, such as tumor growth factor β (TGFβ) and platelet-derived growth factor (PDGF), that act on nearby fibroblasts to promote a fibroproliferative response. M2 macrophages also secrete matrix metalloproteases (MMPs) and tissue inhibitor of metalloproteinases (TIMPs) that regulate matrix remodeling. Additionally, they produce chemokines that attract other inflammatory cells (e.g. monocytes and dendritic cells) that subsequently clear apoptotic cells and debris, dampening the inflammatory response [51,52]. Due to the orthogonal roles played by the M1 and M2 macrophage phenotype, differential targeting of activated macrophages is attractive for therapeutic drug delivery applications. Human alveolar macrophages adopting a M2 polarization are believed to play an important role in the pathogenesis of pulmonary fibrosis, highlighting this phenotype as a potential clinical target [5].

BMDMs were cultured in either LPS or IL-4/IL-13 to obtain either the M1 or M2 polarization, respectively. Macrophages activated by the alternative pathway (M2) showed increased internalization of pManEMA whereas classically activated macrophages (M1) had similar internalization of pManEMA as naïve macrophages (M0) (**Figure 3.6**). These differences were retained over a two-hour time course. At this later time point, M2 macrophages had internalized pManEMA at an approximately 3- and 5-fold higher level than M0 and M1 macrophages, respectively. M2 macrophages have higher expression of mannose receptor [53], providing further support that this receptor is facilitating glycopolymer uptake.
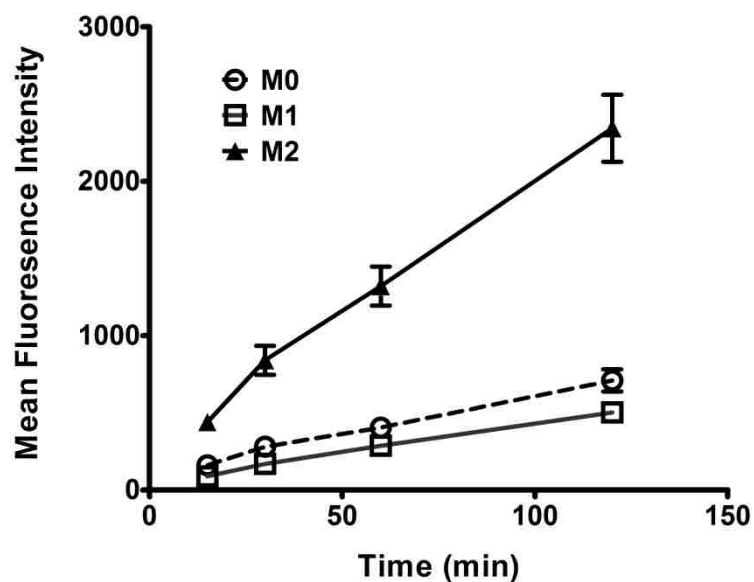
Figure 3.6. Time course of mannose uptake in stimulated macrophages. AF488-pManEMA (1 µM) uptake by unstimulated (M0), LPS-stimulated (M1), or IL-4/IL-13 stimulated (M2) BMDM's (n=3).

3.3.4. In vitro cell-specific glycopolymer uptake

To determine cell-type specificity, we compared uptake and internalization of labeled glycopolymers by BMDMs, primary mouse lung fibroblasts (MLF) and the murine lung epithelial cell line, MLE-12. The latter two cell-types were selected as they are representative of the cell phenotypes encountered in the lung, the target site of our in vivo study. Neither MLF nor MLE-12 had significant internalization of any of the glycopolymers at any timepoint examined (**Figure 3.7**), whereas BMDMs had significant uptake of pManEMA and pGlcNAcEMA. These results are consistent with mannose receptor-mediated uptake of the glycopolymers by macrophages.
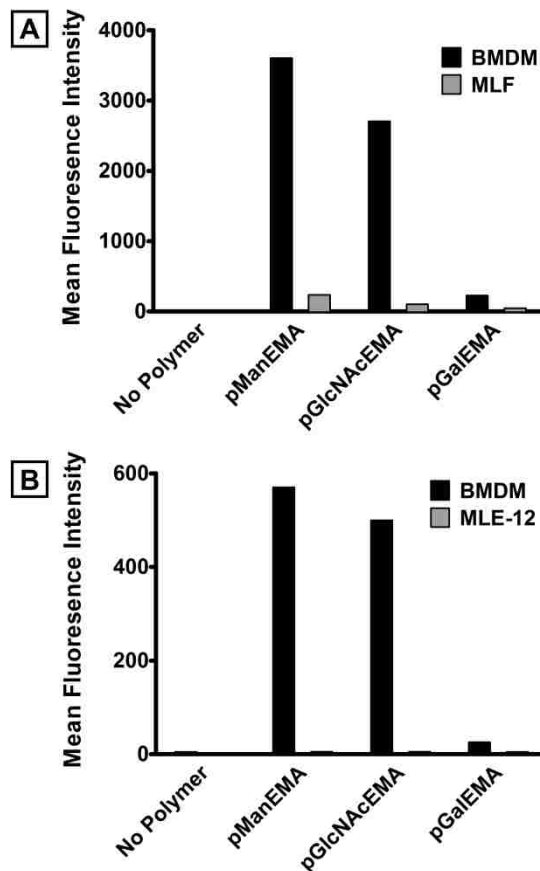
Figure 3.7. Cell specificity of glycopolymer internalization. Internalization of AF488-glycopolymers (1.5 µM) by BMDMs, mouse lung epithelial cells (MLE-12), or primary mouse lung fibroblasts (MLF) after 2h (**A**) or 24h (**B**) incubation.

3.3.5. In vivo macrophage uptake of glycopolymers

To determine whether macrophage internalization of glycopolymers retained the same carbohydrate specificity in vivo, we administered Alexa 488-labeled glycopolymers intratracheally in normal mice and measured uptake by alveolar macrophages. Bronchoalveolar lavage (BAL) was performed at different timepoints following administration, and BAL cells were analyzed for uptake of the glycopolymers. We verified that greater than 90% of the BAL cells were alveolar macrophages by staining with a macrophage cell surface marker (F4/80, data not shown). We found that alveolar macrophages had similar in vivo uptake of glycopolymers as BMDM uptake in vitro: pManEMA and pGlcNAcEMA were readily internalized by alveolar macrophages as early as 30 minutes after instillation whereas pGalEMA had minimal internalization (**Figure 3.8**). Flow cytometric analysis showed that uptake of pManEMA was up to 6-folds higher than the

pGalEMA at 15 min (data not shown). Ex vivo examination of alveolar macrophage demonstrated a similar punctate distribution pattern as observed in BMDMs (**Figure 3.8** inset). These findings are consistent with previous work examining the uptake of mannosylated liposomes by alveolar macrophages following intratracheal administration in rats. Chono et al. demonstrated that adding mannose to liposomes resulted in a 2.2 fold increase in uptake over a 24 hour period as compared to bare liposomes [35]. Wijagkanalan et al. supported these findings by showing a significant increase in the internalization of mannosylated liposomes versus unmodified liposomes after two hours [36]. The results presented here demonstrate that these functional glycopolymers are active within the complex biological milieu found within the lung. Local delivery via intratracheal instillation also has the advantage of less systemic toxicity and off target effects, lower doses, and better drug stability. For example local delivery of therapeutics to the lung is a feasible option in intubated patients suffering from acute respiratory distress syndrome.
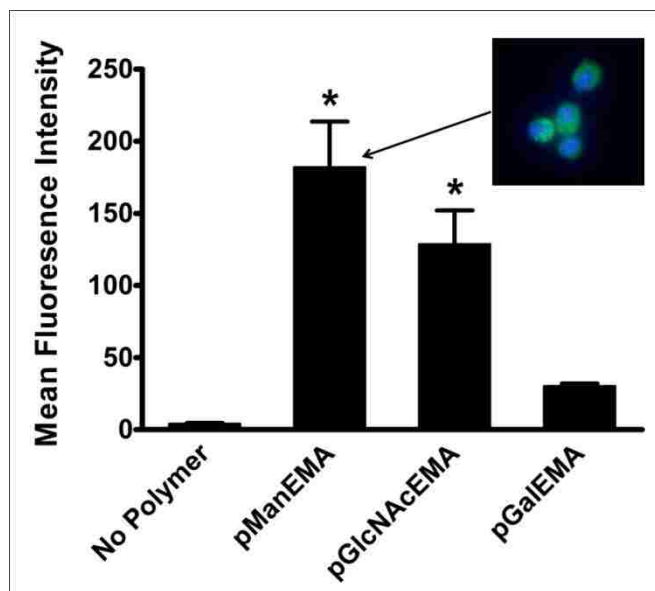
Figure 3.8. Internalization of glycopolymers by alveolar macrophages in vivo. Mice were given 10 µM AF488-glycopolymers intratracheally. Bronchoalveolar lavage (BAL) was performed after 30 min and BAL cells were analyzed by flow cytometry. Data are reported as mean fluorescence intensity ± standard deviation from three independent experiments. *p<0.01 compared to no polymer.

3.4. CONCLUSIONS

Synthetic glycopolymers provide a promising platform to leverage mannose receptor-mediated endocytosis for the intracellular delivery of therapeutic cargo into macrophage populations in the lung. In this study, structurally well-defined glycopolymers were

synthesized via RAFT polymerization and shown to specifically engage macrophages both in vitro and in vivo in a carbohydrate-dependent manner. We demonstrate for the first time that macrophages activated by the alternative pathway (M2) showed increased internalization of mannose glycopolymers and, to a lesser degree, *N*-acetylglucosamine glycopolymers, whereas classically activated macrophages (M1) exhibit similar internalization of glycopolymers as naïve macrophages (M0). Demonstration of specific uptake of pManEMA by alveolar macrophages in vivo is promising for future therapeutic applications. While not explored in this work, the pyridyl disulfide handle on these glycopolymers could be conjugated to other maleimide- or thiol-functionalized compounds, e.g. small molecule drugs and biological macromolecules. Coupled with the versatility of RAFT-based polymer synthesis, glycopolymers are a promising strategy for the design of targeted polymeric drug delivery systems.

3.5. ACKNOWLEDGEMENTS

3.6. REFERENCES

[1]   Allen TM. Ligand-targeted therapeutics in anticancer therapy. Nat Rev Cancer 2002;2:750-63.

[2]   Ting SRS, Chen G, Stenzel MH. Synthesis of glycopolymers and their multivalent recognitions with lectins. Polym Chem 2010;1:1392-412.

[3]   Fleming C, Maldjian A, Da Costa D, Rullay AK, Haddleton DM, St John J, et al. A carbohydrate-antioxidant hybrid polymer reduces oxidative damage in spermatozoa and enhances fertility. Nature 2005;1:270-4.

[4]   Murray PJ, Wynn TA. Protective and pathogenic functions of macrophage subsets. Nat Rev Immunol 2011;11:723-37.

[5]   Pechkovsky DV, Prasse A, Kollert F, Engel KMY, Dentler J, Luttmann W, et al. Alternatively activated alveolar macrophages in pulmonary fibrosis--mediator production and intracellular signal transduction. Clin Immunol 2010;137:89-101.

[6]   Zhang-Hoover J, Sutton A, Van Rooijen N, Stein-Streilein J. A critical role for alveolar macrophages in elicitation of pulmonary immune fibrosis. Immunology 2000;101:501-11.

[7]   Esko J, Kimata K, Lindahl U, Varki A, Cummings V, Esko J, et al. Essentials of glycobiology. 2nd ed. Cold Spring Harbor (NY): Cold Spring Harbor Laboratory Press; 2009.

[8]   Taylor M, Bezouska K, Drickamer K. Contribution to ligand binding by multiple carbohydrate-recognition domains in the macrophage mannose receptor. J Biol Chem 1992;267:1719-26.

[9]   Ezekowitz R, Williams D, Koziel H, Armstrong M, Warner A, Richards F, et al. Uptake of Pneumocystis carinii mediated by the macrophage mannose receptor. Nature 1991;351:155-8.

[10]   Stahl PD, Rodman JS, Miller MJ, Schlesinger PH. Evidence for receptor-mediated binding of glycoproteins, glycoconjugates, and lysosomal glycosidases by alveolar macrophages. Proc Natl Acad Sci U S A 1978;75:1399-403.

[11]   Stahl P, Schlesinger PH, Sigardson E, Rodman JS, Lee.YC. Receptor-mediated pinocytosis of mannose glycoconjygates by macrophages: characterization and evidence for receptor recycling. Cell 1980;19:207-15.

[12]   Taylor PR, Martinez-Pomares L, Stacey M, Lin HH, Brown GD, Gordon S. Macrophage receptors and immune recognition. Annu Rev Immunol 2005;23:901-44.

[13]   Lee RT, Ichikawa Y, Kawasaki T, Drickamer K, Lee YC. Multivalent ligand binding by serum mannose-binding protein. Arch Biochem Biophys 1992;299:129-36.

[14]   Mammen M, Choi SK, Whitesides GM. Polyvalent interactions in biological systems: implications for design and use of multivalent ligands and inhibitors. Angew Chem Int Ed 1998;37:2755-94.

[15]   Lee RT, Lee YC. Affinity enhancement by multivalent lectin-carbohydrate interaction. Glycoconj J 2000;17:543-51.

[16]   Shepherd VL, Lee Y, Schlesinger PH, Stahl PD. L-Fucose-terminated glycoconjugates are recognized by pinocytosis receptors on macrophages. Proc Natl Acad Sci U S A 1981;78:1019-22.

[17]   Hoppe CA, Lee YC. Accumulation of a nondegradable mannose ligand within rabbit alveolar macrophages. Receptor reutilization is independent of ligand degradation. Biochemistry 1984;23:1723-30.

[18]   Bernard J, Hao X, Davis TP, Barner-Kowollik C, Stenzel MH. Synthesis of various glycopolymer architectures via RAFT polymerization: from block copolymers to stars. Biomacromolecules 2006;7:232-8.

[19]   Lowe AB, Sumerlin BS, McCormick CL. The direct polymerization of 2-methacryloxyethyl glucoside via aqueous reversible addition-fragmentation chain transfer (RAFT) polymerization. Polymer 2003;44:6761-5.

[20]   Ladmiral V, Melia E, Haddleton DM. Synthetic glycopolymers: an overview. Eur Polym J 2004;40:431-49.

[21]   Miura Y. Design and synthesis of well-defined glycopolymers for the control of biological functionalities. Polym J 2012;doi:10.1038/pj.2012.4.

[22]   Moad G, Rizzardo E, Thang SH. Living radical polymerization by the RAFT process. Aust J Chem 2005;58:379-410.

[23]   Abdelkader O, Moebs-sanchez S, Queneau Y, Bernard J, Fleury E, Lyon D. Generation of well-defined clickable glycopolymers from aqueous RAFT polymerization of isomaltulose-derived acrylamides. Polymer 2011;49:1309-18.

[24]   Boyer C, Davis TP. One-pot synthesis and biofunctionalization of glycopolymers via RAFT polymerization and thiol-ene reactions. Chem Commun (Camb) 2009:6029-31.

[25]   Xiao N-Y, Li A-L, Liang H, Lu J. A well-defined novel aldehyde-functionalized glycopolymer: synthesis, micelle formation, and its protein immobilization. Macromolecules 2008;41:2374-80.

[26]   Wang Y, Li X, Hong C, Pan C. Synthesis and micellization of thermoresponsive galactose-based diblock copolymers. J Polym Sci, Part A: Polym Chem 2011;49:3280-90.

[27]   Deng Z, Li S, Jiang X, Narain R. Well-defined galactose-containing multi-functional copolymers and glyconanoparticles for biomolecular recognition processes. Macromolecules 2009;42:6393-405.

[28]   Spain SG, Albertin L, Cameron NR. Facile in situ preparation of biologically active multivalent glyconanoparticles. Chem Commun (Camb) 2006:4198-200.

[29]   Hetzer M, Chen G, Barner-Kowollik C, Stenzel MH. Neoglycopolymers based on 4-vinyl-1,2,3-triazole monomers prepared by click chemistry. Macromol Biosci 2010;10:119-26.

[30]   Slavin S, Burns J, Haddleton DM, Becer CR. Synthesis of glycopolymers via click reactions. Eur Polym J 2011;47:435-46.

[31]   Kumar J, McDowall L, Chen G, Stenzel MH. Synthesis of thermo-responsive glycopolymers via copper catalysed azide–alkyne 'click' chemistry for inhibition of ricin: the effect of spacer between polymer backbone and galactose. Polym Chem 2011:1879-86.

[32]   Albertin L, Kohlert C, Stenzel M, Foster LJR, Davis TP. Chemoenzymatic synthesis of narrow-polydispersity glycopolymers: poly(6-O-vinyladipoyl-D-glucopyranose). Biomacromolecules 2004;5:255-60.

[33]   Albertin L, Stenzel M, Barner-kowollik C, Foster LJR, Davis TP. Well-defined glycopolymers from RAFT polymerization : poly (methyl 6-O-methacryloyl-α-D-glucoside) and its block copolymer with 2-hydroxyethyl methacrylate. Macromolecules 2004:7530-7.

61

[34]   Lowe AB, Wang R. Synthesis of controlled-structure AB diblock copolymers of 3-O-methacryloyl-1,2:3,4-di-O-isopropylidene-D-galactopyranose and 2-(dimethylamino)ethyl methacrylate. Polymer 2007;48:2221-30.

[35]   Chono S, Tanino T, Seki T, Morimoto K. Uptake characteristics of liposomes by rat alveolar macrophages: influence of particle size and surface mannose modification. J Pharm Pharmacol 2007;59:75-80.

[36]   Wijagkanalan W, Kawakami S, Takenaga M. Efficient targeting to alveolar macrophages by intratracheal administration of mannosylated liposomes in rats. J Control Release 2008;125:121-30.

[37]   Wijagkanalan W, Kawakami S, Higuchi Y, Yamashita F, Hashida M. Intratracheally instilled mannosylated cationic liposome/NFκB decoy complexes for effective prevention of LPS-induced lung inflammation. J Control Release 2011;149:42-50.

[38]   Moad G, Chong YK, Postma A, Rizzardo E, Thang SH. Advances in RAFT polymerization: the synthesis of polymers with defined end-groups. Polymer 2005;46:8458-68.

[39]   Upreti M, Ruhela D, Vishwakarma RA. Synthesis of the tetrasaccharide cap domain of the antigenic lipophosphoglycan of Leishmania donovani parasite. Tetrahedron 2000;56:6577-84.

[40]   Manicone AM, Birkland TP, Lin M, Betsuyaku T, van Rooijen N, Lohi J, et al. Epilysin (MMP-28) restrains early macrophage recruitment in Pseudomonas aeruginosa pneumonia. J Immunol 2009;182:3866-76.

[41]   Choi JE, Lee S, Sunde DA, Huizar I, Haugk KL, Thannickal VJ, et al. Insulin-like growth factor-I receptor blockade improves outcome in mouse model of lung injury. Am J Respir Crit Care Med 2009;179:212-9.

[42]   Zhang J, Wu B, Liu Z, Kowal P, Chen X, Shao J, et al. Large-scale synthesis of carbohydrates for pharmaceutical development. Curr Org Chem 2001;5:1169-76.

[43]   Kallin E, Lönn H, Norberg T. New derivatization and separation procedures for reducing oligosaccharides. Glycoconj J 1986;3:311-9.

[44]   Wolfenden ML, Cloninger MJ. Multivalency in carbohydrate binding. Carbohydrate recognition: biological problems, methods, and applications. 1st ed. John Wiley & Sons Inc; 2011;349-70.

[45]   Taylor ME, Bezouska K, Drickamer K. Contribution to ligand binding by multiple carbohydrate-recognition domains in the macrophage mannose receptor. J Biol Chem 1992;267:1719-26.

[46]   Cameron NR, Spain SG, Kingham JA, Weck S, Albertin L, Barker CA, et al. Synthesis of well-defined glycopolymers and some studies of their aqueous solution behaviour. Faraday Discuss 2008;139:359-68; discussion 399-417, 419-20.

[47]   Edelman GM, Cunningham BA, Reeke GN, Becker JW, Waxdal MJ, Wang JL. The covalent and three-dimensional structure of concanavalin A. Proc Natl Acad Sci U S A 1972;69:2580-84.

[48]   Glycan binding protein database. Available from: http://wwwfunctionalglycomicsorg.

[49]   Weis WI, Drickamer K, Hendrickson WA. Structure of a C-type mannose-binding protein complexed with an oligosaccharide. Nature 1992;360.

[50]   Mosser DM, Edwards JP. Exploring the full spectrum of macrophage activation. Nat Rev Immunol 2008;8:958-69.

[51]   Wynn TA, Barron L. Macrophages: master regulators of inflammation and fibrosis. Semin Liver Dis 2010;30:245-57.

[52]   Duffield JS. The inflammatory macrophage: a story of Jekyll and Hyde. Clin Sci (Lond) 2003;104:27-38.

[53]   Gordon S. Alternative activation of macrophages. Nat Rev Immunol 2003;3:23-35.

CHAPTER 4 – BIOMOLECULAR RECOGNITION OF LECTINS BY GLYCOPOLYMER MICELLES

Matthew J. Manganiello, Eun-Ho Song, Anthony J. Convertine, Daniel M. Ratner, Patrick S. Stayton

ABSTRACT

Reversible addition-fragmentation chain transfer (RAFT) polymerization was employed to generate a series of well-defined glycopolymers which differed in pendent carbohydrate (mannose vs. galactose) and morphology (unimer vs. micelle). Acetylated mannose and galactose ethyl methylacrylate (AcManEMA and AcGalEMA) were homopolymerized and used as macro chain transfer agents (macroCTAs) for the copolymerization of diethylaminoethyl methacrylate (DEAEMA) and butyl methacrylate (BMA). Protective acetyl groups were successfully removed from these materials by base-catalyzed hydrolysis to liberate the native carbohydrate conformation as validated by ^{1}H-NMR. Diblock glycopolymers were shown to assemble into micelles (13 ± 2 nm diameters) at physiological pH driven by the hydrophobic segment of DEAEMA and BMA. This copolymer unit is also responsible for promoting micelle destabilization into unimers at pH values less than 6.6 which was validated by dynamic light scattering (DLS) measurements and a hemolysis assay. The glycopolymer micelles were found to be stable in buffer with low critical micelle concentrations (CMCs) of 10 and 13 µg/mL and aggregation numbers (N_{agg}) of 39 and 36 for mannose and galactose, respectively. Next the ability of these materials to engage the C-type lectin, Concanavalin A (ConA), was investigated by agglutination, precipitation, and surface plasmon resonance imaging (SPRi) assays. In these experiments, the deprotected macroCTAs (unimers) were compared to the diblock glycopolymer micelles. In all cases, the galactose analogs were unable to bind the lectin, demonstrating that this interaction is carbohydrate-specific. The mannose unimer was found to more efficiently bind ConA than the micelle morphology by examining the initial clustering rate ($k_{cluster}$ = 0.17 ± 0.01 vs. 0.10 ± 0.03 AU/min) and the ConA/glycopolymer stoichiometry (1.9 ± 0.2 vs 1.4 ± 0.1). These materials inhibited ConA binding to immobilized α-D-mannose at IC50 values of 0.34 µM and 1.07 µM for the unimer and micelle, respectively, as determined by SPRi.

4.1. INTRODUCTION

Carbohydrates play an essential role in myriad biological functions including the maintenance of immunological activity through mediating cell-cell interactions as well as providing defined motifs for pathogenic detection and elimination [1]. By mimicking the glycosidic structures on pathogens, delivery platforms can be created which shuttle therapeutic cargo to specific immune cells [2]. This strategy can be employed to modulate inflammatory responses, promote wound healing, and develop infectious disease and cancer vaccines, among others [3], [4]. Recent advances in synthetic techniques have given researches the opportunity to both generate complex carbohydrate architectures that resemble those found in nature and to incorporate these structures into delivery systems, greatly expanding upon the clinical utility of carbohydrate-based therapeutics [5–7].

Immune cells identify glycosylated segments by displaying C-type lectins on their surface [8], [9]. These proteins consist of one or more carbohydrate recognition domains (CRDs) that bind specific saccharides. The complex carbohydrate structures found on pathogens are often capable of engaging multiple CRDs simultaneously, thereby raising the overall binding affinity of the interaction. This multivalent binding activity is essential to effectively target cell surface lectins as the interaction of a monosaccharide with a single CRD is typically weak, with mM K_d values [10]. A synthetic approach to overcome this low affinity involves polymerizing glyco-functionalized monomers to generate a polymer displaying multiple pendent carbohydrate residues along its backbone [11]. By utilizing controlled polymerization techniques, such as reversible addition-fragmentation chain transfer (RAFT) polymerization, well-defined polymeric structures can be generated and subsequently incorporated into architectures that allow for the delivery of small molecules and biological macromolecules [12]. RAFT-mediated glycopolymer designs have included glycopolymer micelles [13], glycopolymer stars [14], multi-functional glyconanoparticles [15], and "clickable" glycopolymers [16], demonstrating the versatility of this technique.

While linear glycopolymer segments have been shown to mediate multivalent engagement of C-type lectins [17], there is evidence that displaying carbohydrate moieties on a particulate platform has several advantages [18]. Particles can provide for a higher density of carbohydrate residues, engage a larger number of CRDs, package therapeutics, and more closely resemble pathogenic organisms as nanoparticles can be made the size of

viruses. To achieve a particulate morphology, glycopolymers can be incorporated into block copolymers in which the glycosylated segment stabilizes a hydrophobic unit which drives the spontaneous assembly of core-shell micelles in an aqueous environment [19–21]. Block copolymer micelles have been extensively investigated as drug delivery vehicles with a current emphasis on how researchers can control their interactions with cells, specifically through the use of targeting moieties [22–25]. Instilling the corona of block copolymer micelles with carbohydrate residues is a promising approach for extending these polymer designs into immunotherapeutic applications [5], [26]. There has been significant interest and success recently in the synthesis of glycopolymer micelles and demonstration of their ability to bind lectins and deliver therapeutic cargo [18]. For example, Suriano et al. synthesized amphiphilic glycopolymer micelles and validated galactose-mediated hepatocyte targeting in vitro while also delivering the chemotherapeutic, doxorubicin [27].

Here we describe the synthesis and characterization of glycopolymer micelles prepared via RAFT displaying either pendent mannose or galactose residues in the corona. We studied the ability of these diblock glycopolymers to self-assemble into stable micelles and exhibit a mode of pH-responsive activity. Additionally we evaluated how effectively they can bind a C-type lectin, Concanavalin A (ConA), in a carbohydrate-specific manner and compared the binding activity of the micelle to the unimeric, linear analog. The ability of these materials to recognize lectins as a function of polymeric conformation was evaluated with respect to related glycopolymer [17], [28] and glycodendritic [26], [29] structures.

4.2. MATERIALS AND METHODS

4.2.1. Materials

Chemicals and all materials were supplied by Sigma-Aldrich (St Louis, MO) unless otherwise specified. 2,2′-Azobis(4-methoxy-2.4-dimethyl valeronitrile) (V70) and 1,1'-Azobis(cyclohexane-1-carbonitrile) (V40) were obtained from Wako Chemicals USA, Inc. (Richmond, VA). Spectra/Por 7 standard regenerated cellulose dialysis tubing was obtained from Spectrum Labs (Rancho Dominguez, CA). ECT was synthesized as previously described [30], [31]. Diethylaminoethyl methacrylate (DEAEMA) and butyl methacrylate (BMA) were distilled prior to use. Acetylated mannose and galactose ethyl methylacrylate (AcManEMA and AcGalEMA) was synthesized according to previous methods (see Chapter 3) [32], [33].

4.2.2. Synthesis of pAcManEMA and pAcGalEMA macro chain transfer agents

The RAFT polymerizations of the AcManEMA and AcGalEMA were conducted in dioxane at 30°C with 40 wt% monomer under a nitrogen atmosphere for 18h using ECT and V70 as the chain transfer agent (CTA) and radical initiator, respectively. The initial monomer to CTA molar ratio ($[M]_0$:$[CTA]_0$) was 25:1 and the initial CTA to initiator molar ratio ($[CTA]_0$:$[I]_0$) was 20:1. The resultant polymers were isolated by precipitation into cold hexanes. The polymers were then redissolved in acetone and subsequently precipitated into cold hexanes (×3) followed by drying overnight in vacuo.

4.2.3. Diblock copolymerization of DEAEMA and BMA from pAcManEMA and pAcGalEMA macroCTAs

DEAEMA and BMA were added to either pAcManEMA or pAcGalEMA macroCTA dissolved in dioxane at 40 wt%. The initial molar feed ratio of DEAEMA:BMA was 3:2 (40 mol% BMA). $[M]_0$/$[CTA]_0$ and $[CTA]_0$/$[I]_0$ were 100:1 and 20:1, respectively. Following the addition of V40 the solutions were purged with nitrogen for 30 min and allowed to react at 90 °C for 6 h. The resultant diblock copolymers were isolated by precipitation into cold hexanes. The precipitated polymers were then redissolved into acetone and precipitated into cold hexanes (x3) and dried overnight in vacuo.

4.2.4. Gel permeation chromatography (GPC)

GPC was used to determine molecular weights and polydispersities (M_w/M_n, PDI) of the macroCTA and diblock copolymers. SEC Tosoh TSK-GEL R-3000 and R-4000 columns (Tosoh Bioscience, Montgomeryville, PA) were connected in series to a Agilent 1200 series (Agilent Technologies, Santa Clara, CA), refractometer Optilab-rEX and triple-angle static light scattering detector miniDAWN TREOS (Wyatt Technology, Dernbach, Germany). HPLC-grade DMF containing 0.1 wt.% LiBr at 60 °C was used as the mobile phase at a flow rate of 1 ml/min. The molecular weights of each polymer were determined using a multi-detector calibration based on dn/dc values calculated separately for each homopolymer and copolymer composition assuming 100% mass recovery.

4.2.5. Saponification of glycopolymers

To display native pendent glycomoieties on the homopolymers and diblock copolymers, protective acetyl groups were removed via base-catalyzed hydrolysis. The homopolymers (pAcManEMA and pAcGalEMA) were added to a solution of 1 wt% sodium methoxide in dimethylformamide at a concentration of 25 mg/mL while the diblock copolymers (p(AcManEMA-*b*-[DEAEMA-*co*-BMA]) and p(AcGalEMA-*b*-[DEAEMA-*co*-BMA])) were added to a solution of 1 wt% sodium methoxide in anhydrous methanol at a copolymer concentration of 50 mg/mL. After 1 hour incubation at room temperature, the solutions were neutralized with acetic acid to a pH of ~7 and dialyzed against deionized water using 1000 MWCO tubing. The solutions were then lyophilized to obtain the final deprotected glycopolymers: pManEMA, pGalEMA, p(ManEMA-*b*-[DEAEMA-*co*-BMA]), and p(GalEMA-*b*-[DEAEMA-*co*-BMA]). Aqueous stocks of the deprotected glycopolymers were formulated from the lyophilized material at 2 mg/mL in 1X DPBS, pH 7.4. The diblock glycopolymers were pre-dissolved at 40 mg/mL in methanol prior to addition into buffer to promote micelle formation.

4.2.6. Concanavalin A (ConA) agglutination assay

A stock solution of ConA was initially prepared in HEPES buffered saline (supplemented with $MgCl_2$ and $CaCl_2$). ConA was added to diluted glycopolymer solutions to obtain the following final concentrations: [ConA] = 1 μM and [polymer] = 2 μM. At this point, the mixture was quickly vortexed and measured by UV/Vis spectroscopy at 350 nm and 0.1 Hz for 15 min. To determine the initial rate of cluster formation, $k_{cluster}$, a linear curve was fit to the data in the first 1 min. This kinetic parameter was the average of triplicate samples.

4.2.7. Dynamic light scattering (DLS) and static light scattering (SLS) measurements

The diblock glycopolymer micelles were analyzed by DLS to determine particle mean diameter and by SLS to evaluate particle molecular weight using a Malvern Zetasizer Nano equipped with a 5 mW He-Ne laser operating at 633 nm (Worcestershire, UK) for both techniques. DLS measurements were performed in 1X DPBS at 200 μg/mL with mean diameters reported as the number average ± peak half-width. Prior to SLS measurements, the micelle solutions were dialyzed against 1X DPBS using a Slide-A-Lyzer® MINI Dialysis Device with a 3.5K MWCO (Thermo Scientific, Rockford, IL) to remove methanol. Serial dilutions of these solutions (0.5 – 0.1 mg/mL) were manually injected into a refractometer

(Wyatt Optilab-rEX, Dernbach, Germany) to determine a dn/dc value for each glycopolymer micelle. Micelle molecular weight (M_w) and second virial coefficient (A_2) were determined from a Debye plot generated by SLS measurements at a constant scattering angle of 173° using the Rayleigh equation: $KC/R_\theta = (1/M_w + 2A_2C)$, in which C was varied from 1 – 0.125 mg/mL, K is an optical constant, and R_θ is the Rayleigh ratio of the scattered to incident light intensity. The parameter K can be represented by the following relationship: $K = 4\pi^2 n_0^2(dn/dc)^2/N_A\lambda^4$, in which n_0 is the refractive index of the solvent, N_A is Avogadro's number, and λ is the wavelength of the light source. From the M_w, an aggregation number (N_{agg}) was determined using the molecular weight of the unimeric species ($M_{w,unimer}$) measured by GPC: $N_{agg} = M_{w,micelle}/M_{w,unimer}$. Each data point represents triplicate measurements.

4.2.8. Hemolysis assay

The potential for the diblock glycopolymers to disrupt endosomal membranes was assessed by a hemolysis assay. The protocol followed here has been described previously [34]. Briefly, polymer was incubated in the presence of erythrocytes at 20 µg/mL in 100 mM sodium phosphate buffers (supplemented with 150 mM NaCl) of varying pH (7.4, 7.0, 6.6, 6.2, and 5.8) intended to mimic the acidifying pH gradient that endocytosed material is exposed to. The extent of cell lysis (i.e. hemolytic activity) was determined by detecting the amount of released hemoglobin via absorbance measurements at 492 nm.

4.2.9. Critical micelle concentration (CMC) determination via ANS fluorescence

The CMC value for each diblock glycopolymer was determined using 1-anilino-8-naphthalene sulfonate (ANS) as a hydrophobically-sensitive, fluorescence probe. Serial dilutions of each micelle solution were prepared from 200 – 1 µg/mL and to these was added ANS from a methanol stock to obtain a final ANS concentration of 3 µM. Following a 1 hr incubation at room temperature in the dark, the fluorescence of each solution was measured at an excitation and emission wavelength of 390 and 550 nm, respectively. The CMC value was assigned as the curve inflection point which was determined by the intercept between a linear regression at the lower concentrations and a logarithmic regression at the higher concentrations.

4.2.10. ConA precipitation assay

The experimental procedure for this assay was adapted from similar protocols from Wolfenden et al. [29] and Kumar et al. [26]. Briefly, ConA was added to a series of glycopolymer solutions to achieve a final ConA concentration of 16.7 μM and glycopolymer concentrations of 100, 75, 50, and 25 μM per mannose residue, at a total volume of 1 mL. Each material was diluted into 0.1 M Tris-HCl, 0.15 M NaCl, 1 mM $CaCl_2$, 1 mM $MnCl_2$, pH 7.2 buffer and the solutions were incubated for 20 h at 22 °C. After this time, the solutions were centrifuged at 7000 rpm for 15 min and the residual buffer was aspirated. The resultant pellet was washed three times with cold buffer (1 mL) with centrifugation steps between each wash. The final pellet was resuspended in 500 μL of 0.1 M methyl-α-D-mannopyranoside in Tris-HCl buffer with brief vortexing then diluted with an additional 500 μL buffer. Due to observed turbidity in a number of samples, additional 0.1 M methyl-α-D-mannopyranoside was added to each sample and the solutions were incubated for 30 min at 37 °C. Final ConA concentration was determined by UV-Vis spectroscopy, using an extinction coefficient of 142,000 $M^{-1}cm^{-1}$ at 280 nm.

4.2.11. Surface plasmon resonance (SPR) measurements

Analysis of ConA binding to immobilized glycopolymers was performed on a Biacore T100 (GE Healthcare Life Sciences, Piscataway, NJ) following a modified protocol from Cheng et al. [35]. Briefly, the SPR was operated at 25 °C using a syringe pump at 30 μL/min. Glycopolymers were immobilized to the chip surface by incubation at 50 μM in DPBS for 30 min, exploiting the affinity of gold for the trithiocarbonate functionality of the glycopolymers. Following this functionalization, the surfaces were passivated with 0.1% BSA in PBS for 30 min and equilibrated with HEPES buffered saline (HBS; 10 mM HEPES, 150 mM NaCl, 1 mM Ca^{2+}, 1 mM Mn^{2+}, pH 7.4). To investigate the ability of ConA to bind to each glycopolymer surface, ConA at 500 nM in HBS was pumped over each chip. Data analysis was performed using Biacore evaluation software.

4.2.12. Surface plasmon resonance imaging (SPRi)

Determination of IC50 values for mannose glycopolymer binding to ConA was performed on a SPRimagerII (GWC Technologies, Madison, WI) with α-D-mannose-modified surfaces using a modified protocol from Cheng et al. [35]. The instrument was operated at room temperature using a standard flow cell and a peristaltic pump (EconoPump, Bio-Rad,

Hercules, CA) at 100 µL/min. All surfaces were passivated with 0.1% BSA in PBS buffer for 30 min and equilibrated in HBS prior to binding studies. ConA concentration was fixed at 500 nM in HBS while glycopolymer concentration was varied from 0.2 to 10 µM. Data acquisition consisted of the averaging of 30 images over a short duration to create an average image. The SPR signal given by the average image (in pixel intensity) was subsequently converted to normalized percentage change in reflectivity according to the GWC protocol. For sensogram acquisition, a 500 µM x 500 µM of the image was selected as the region of interest (ROI). For visual clarity, the contrast and brightness of SPR difference image was adjusted by ImageJ (U.S. National Institutes of Health, Bethesda, MD). Two spots on two or more duplicate samples were analyzed. Reported changes in SPR reflectivity (Δ %R) were averaged over multiple spots and background subtracted.

4.3. RESULTS AND DISCUSSION

4.3.1. Glycopolymer synthesis and characterization

Homopolymers of AcManEMA and AcGalEMA were synthesized via RAFT and acted as macroCTAs for the copolymerization of a DEAEMA-co-BMA block (henceforth referred to as EB40 with 40 representing the molar feed ratio of BMA) (**Scheme 4.1**). The resultant homopolymers and diblock copolymers exhibited low polydispersities (PDI ≤ 1.30) and consistent size and monomer compositions between the two glycomonomers investigated (**Table 4.1** and **Figure 4.1**). To liberate the native sugar conformation, each glycopolymer underwent base-catalyzed saponification. Complete removal of pendent acetyl groups was validated by ^{1}H-NMR (**Figure 4.2** and **4.3**).
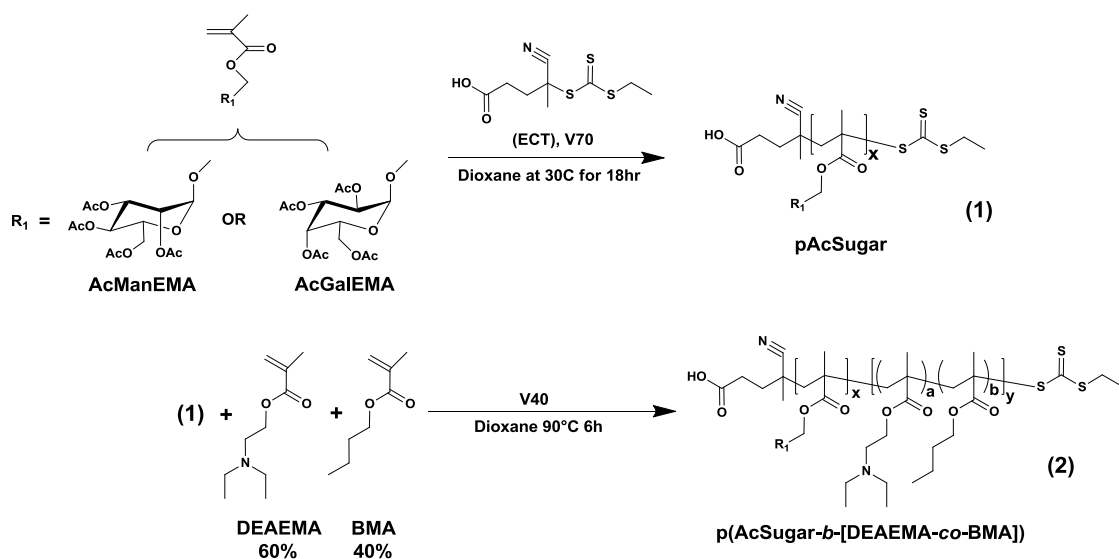
Scheme 4.1. RAFT-mediated synthesis of glycopolymer macroCTAs and subsequent DEAEMA-*co*-BMA (EB40) copolymerization.

Table 4.1.
Molecular weights[a], polydispersities[a], and monomer compositions[b] for polymer designs. Target DPs of 25 and 100 were chosen for the glycomonomer macroCTAs and EB40 polymerizations, respectively.

Polymer	M_n Glyco Block (g/mol)	M_n EB40 Block (g/mol)	Mol% BMA in 2nd block	Total M_n (g/mol)	PDI (M_w/M_n)
pAcManEMA	12000	---	---	12000	1.28
p(AcManEMA-*b*-EB40)	12000	13200	47	25200[c]	1.08
pAcGalEMA	11900	---	---	11900	1.30
p(AcGalEMA-*b*-EB40)	11900	11300	45	23200[c]	1.07

[a] As determined by GPC
[b] As determined by ^{1}H-NMR (CD$_3$OD) spectroscopy (Bruker AV 500)
[c] Following saponification, the glycopolymer macroCTA molecular weights were assumed to be 7600 for both ManEMA and GalEMA, respectively, and the diblock copolymer molecular weights were assumed be 20600 and 18800 g/mol for ManEMA and GalEMA, respectively, due to removal of acetyl groups
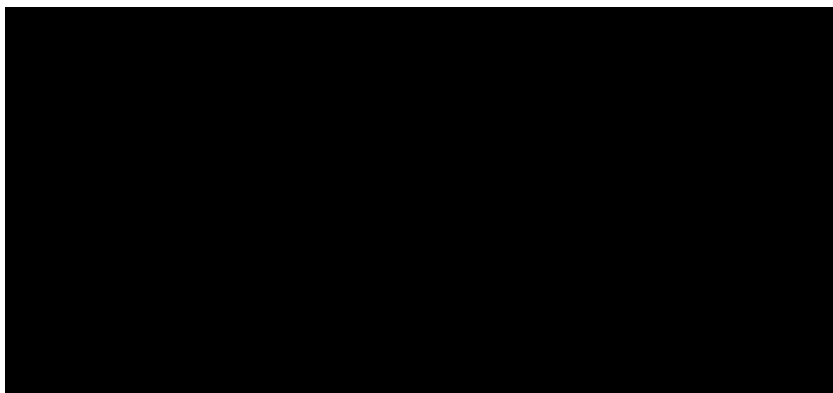
Figure 4.1. GPC traces of polymers in DMF.
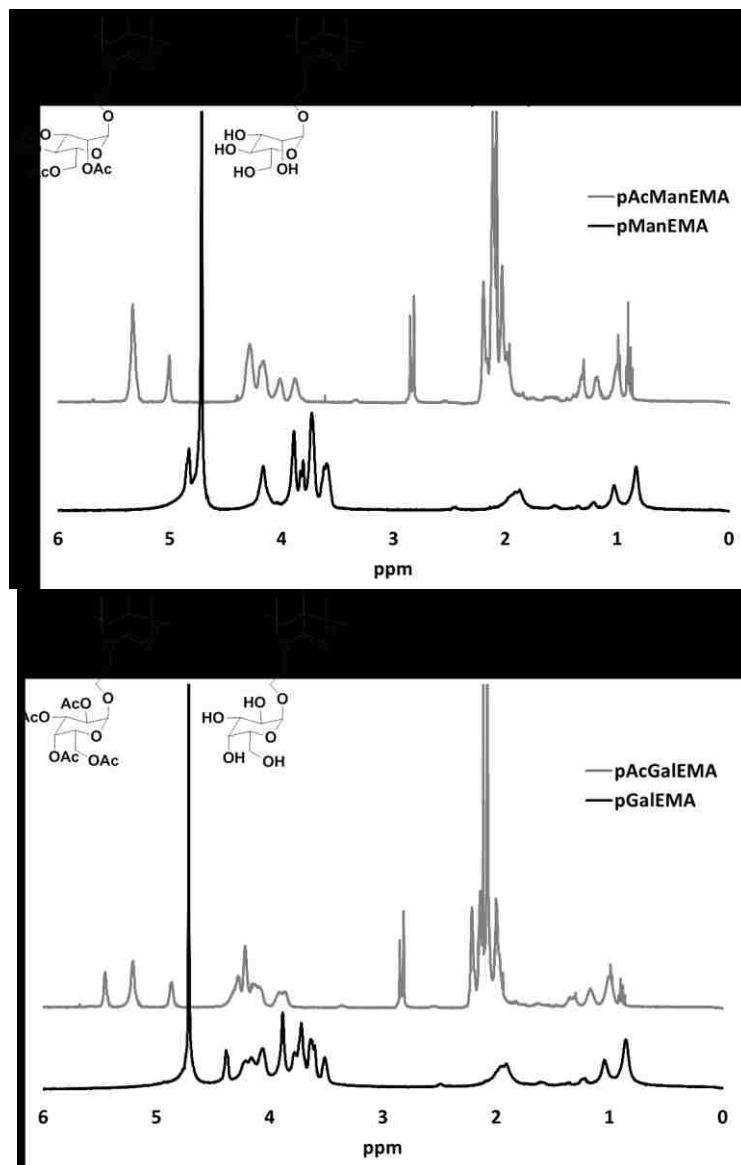
Figure 4.2. ^{1}H-NMR of acetylated (pAcManEMA and pAcGalEMA) and deacetylated (pManEMA and pGalEMA) glycopolymers in $(CD_3)_2CO$ and D_2O, respectively. Resonances associated with the acetyl groups are in the range of δ = ~2.2-1.8.
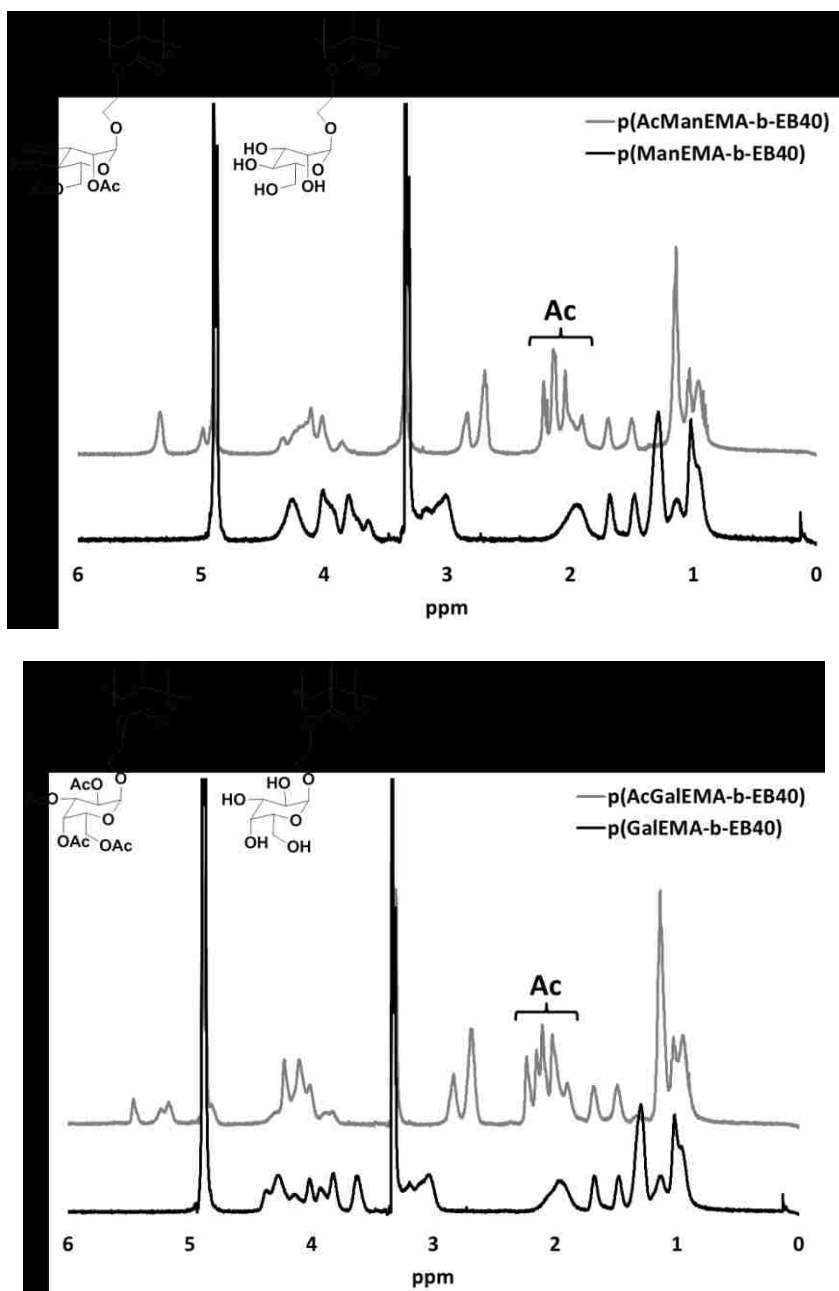
Figure 4.3. ^{1}H-NMR of diblock glycopolymers in CD$_3$OD before and after saponification. Resonances associated with the acetyl groups are in the range of δ = ~2.2-1.8.

4.3.2. pH-responsive activity of diblock glycopolymer micelles

The pH-responsive behavior of the diblock glycopolymer micelles in aqueous solution was measured by dynamic light scattering (DLS) and a hemolytic assay. While differing in the structure of pendent glycomoiety comprising the corona, each glycopolymer micelle contains the same hydrophobic segment which exhibits a phase transition upon a decrease in pH. Based upon similar studies (see **Figure 2.1** and **2.2**), the incorporation of 40% BMA within

73

this segment was anticipated to promote micellization of diblock copolymer architectures at pH 7.4 while mediating destabilization into an unimeric conformation at pH 6.6 and below. This structural transition is promoted by protonation of DEAEMA tertiary amines upon acidification which allows for solvation of this block once a sufficient charge density is reached. At this transition point, entropically driven sequestration of this polymer segment is no longer energetically favorable. DLS measurements of the glycopolymer micelles at pH 7.4 yielded particle sizes of 13 ± 2 nm for both Man and Gal (**Figure 4.4**), similar to those values obtained for p(DMAEMA-*b*-EB40) micelles (18 ± 4 nm) (**Figure 2.1**). For each glycopolymer micelle, an apparent drop in particle size was observed at pH 6.6 and below, confirming evolution of an unimer species in this pH regime. This transition point was also observed in a hemolysis assay as hemolytic activity was only measured at these pH values. An important distinction is the lower hemolytic activity for the Gal micelle at pH 6.6 despite exhibiting the same DLS trends as Man and similar extents of hemolysis at pH 6.2 and 5.8. While this phenomena may be carbohydrate-based, this finding likely highlights the importance of fine-tuning the composition of BMA within the core-forming segment to ensure proper pH transition of the resultant material. Small differences in BMA incorporation between the two micelles and slight differences in buffer pH between the two assays may account for the discrepancy in the data. These two datasets demonstrate that changing the corona chemistry of the diblock copolymer design from a cationic to carbohydrate species does not significantly alter the micelle pH-responsive behavior and that this activity is not largely affected by the stereochemistry of pendent carbohydrates.
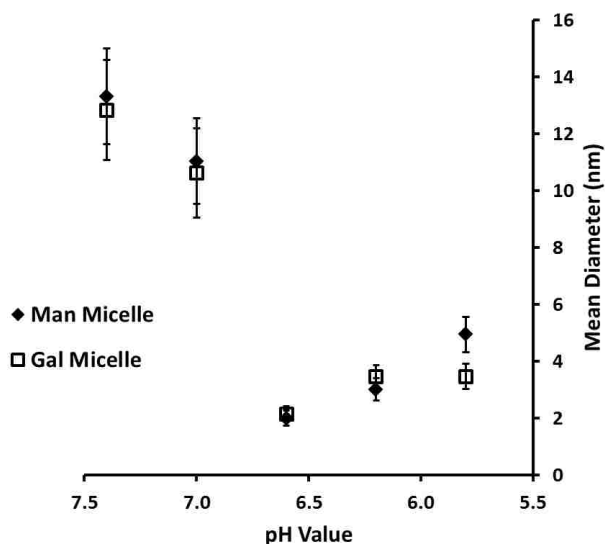
Figure 4.4. Particle size measurements of diblock glycopolymer micelles as a function of pH via DLS. All measurements were performed at a copolymer concentration of 0.2 mg/mL in 100 mM sodium phosphate buffer with 150 mM NaCl. Mean diameter was determined from the number particle size distribution while error bars represent the average peak half-width.
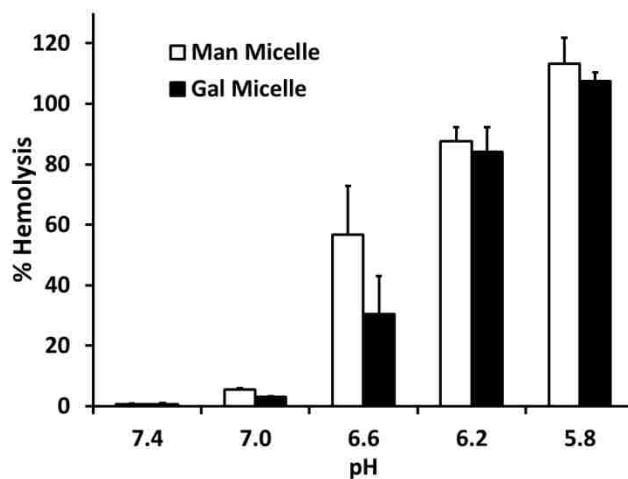
Figure 4.5. Hemolytic activity of diblock glycopolymers at a concentration of 20 µg/mL. Hemolytic activity is normalized relative to a positive control, 1% v/v Triton X-100, and the data represent a single experiment conducted in triplicate ± standard deviation.

4.3.3. Physicochemical properties of diblock glycopolymer micelles

To understand the stability and assembly of these micelles in an aqueous environment, both the critical micelle concentration (CMC) and aggregation number (N_{agg}) were determined via two independent measurements. The concentration at which the unimeric conformation of a polymeric species saturates both the bulk solvent and the solvent-air interface leading to the spontaneous assembly of micellar particles is known as the CMC [36]. This parameter is

75

important to understanding the stability of polymeric micelles towards dilution effects since below the CMC, micelles will dissemble into their constituent unimeric components. Surfactants exhibit relatively high CMCs with values often in the mM-range [37] while synthetic polymer-based micelles can achieve sub-µM CMCs allowing for retention of this particulate conformation following in vivo administration and subsequent dilution into biological fluids [24]. There exist a number of techniques to determine this parameter including the use of probes which exhibit polarity-sensitive, fluorescent properties, such as pyrene and 1-anilino-8-naphthalene sulfonate (ANS) [38]. Upon interaction with hydrophobic components, ANS experiences a significant blue shift in its emission maximum. This activity can be utilized to probe for the formation of hydrophobic domains within micellar structures as ANS will readily incorporate into these areas due to its poor aqueous solubility [39].

Using ANS, the CMC was determined to be 10 and 13 µg/mL for the Man and Gal micelles, respectively (**Figure 4.6** and **Table 4.2**). These values are comparable to those reported for related polymer-based micelle systems. For example, Convertine et al. reported on a pH-responsive diblock copolymer micelle incorporating BMA into the core segment and obtained a CMC value of 2 µg/mL using pyrene as a probe [40]. Li et al. reported on diblock copolymer micelles with BMA homopolymer cores that had 0.5 – 6 µg/mL CMCs [41]. PEG-stabilized BMA copolymer micelles were also shown to exhibit sub-10 µg/mL CMC values [42]. As a comparison, the thoroughly-studied Pluronic compositions (triblock copolymers composed of poly(ethylene oxide) coronas and poly(propylene oxide) cores) can provide CMC values from 1 – 50 µg/mL depending on the relative block sizes and method of analysis [43], [44]. While the CMCs determined for these glycopolymer micelles are slightly higher than some values reported for BMA-containing polymers, they are still low enough for these materials to be suitable for downstream biological studies. For instance, Suriano et al. demonstrated cell-specific in vitro cytotoxicitiy for doxorubicin-loaded, glycopolymer micelles with CMC values of 5 – 7 µg/mL [27].
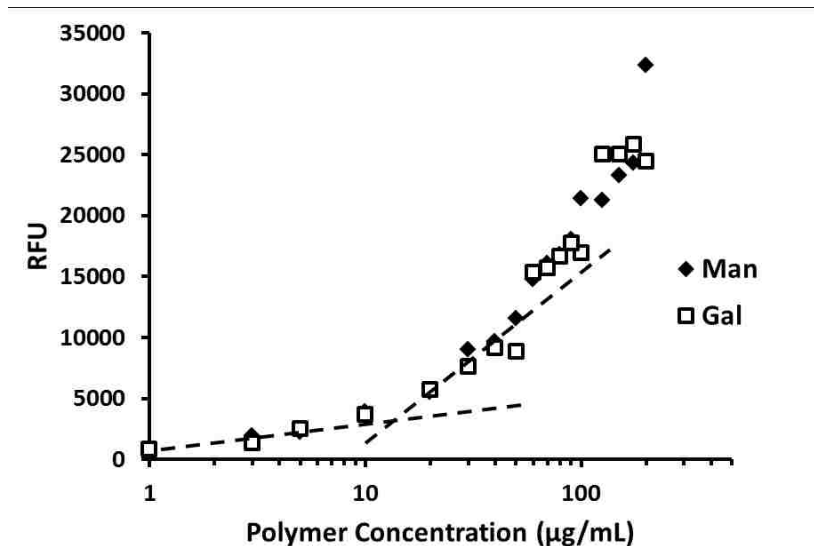
Figure 4.6. Determination of critical micelle concentration (CMC) of diblock copolymer micelles in 1X DPBS using 8-anilino-1-napthalenesulfonic acid (ANS) as a hydrophobic-sensitive fluorescent probe. CMC values were determined from the inflection point of each curve, as illustrated for Gal.

Next, the aggregation numbers of the micelles were determined using static light scattering (SLS) (**Figure 4.7**). This technique calculates the absolute molecular weight of a species by measuring the scattering intensity at a fixed angle as a function of the solute concentration. Factoring in the molecular weight of the unimeric diblock glycopolymer from GPC, the number of individual polymer chains which comprise a micellar particle (N_{agg}) could additionally be calculated (**Table 4.2**). An important parameter to include in this analysis is the dn/dc value of the material which had to be determined separately using a refractometer. The N_{agg} for the two glycopolymer micelles were found to be similar (39 and 36 for Man and Gal, respectively) suggesting that there is minimal effect of the type of carbohydrate residue on the stabilization of the EB40 core segment. These aggregation numbers are consistent with those reported for related copolymer micelle systems: 30-40 for poly[(*N*-acryloylmorpholine)-*b*-BMA] [41] and 34 for poly[(dimethylaminoethyl methacrylate)-*b*-(butyl acrylate)] [45] as well as compared to Pluronic systems with N_{agg} values dependent upon relative and absolute block sizes, reaching values of low 30s for optimally stable formulations [43].

An additional parameter that can be extracted from the SLS measurements is the second virial coefficient, A2. This variable is a measure of solution nonideality as it represents, in this case, micelle-micelle interactions [43], [46]. Micelles with high A2 values exhibit

77

substantial inter-aggregate attraction leading to particles with larger aggregation numbers [41]. Both glycopolymer micelles gave similar A2 values (2.86 and 2.36 · 10^{-4} mL·mol/g^2 for Man and Gal, respectively) demonstrating that each carbohydrate moiety has the same likelihood for self-interaction when incorporated onto a micellar platform. These A2 values are comparable to polymeric systems with similar N_{agg} values. Li et al. reported $1 - 3 · 10^{-4}$ mL·mol/g^2 A2 values for diblock copolymer micelles consisting of morpholine coronas and BMA cores [41] while Nolan et al. showed that Pluronic compositions exhibit smaller A2 values of $2 - 5 · 10^{-5}$ mL·mol/g^2
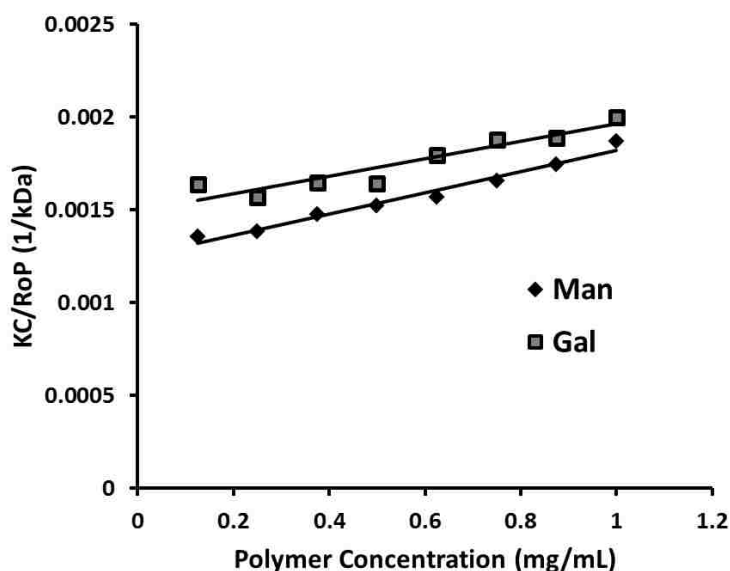
Figure 4.7. Debye plot of diblock glycopolymer micelles in 1X DPBS.

Table 4.2.
Physical properties of diblock glycopolymer micelles in 1X DPBS as determined by dynamic light scattering[a], refractometry[b], static light scattering[c], and ANS fluorescence[d].

Polymer	Diameter[a] (nm)	dn/dc[b]	MW[c] (kDa)	Aggregation number (N_{agg})[c]	A2[c] (mL·mol/g^2)/10^4	CMC[d] (µg/mL)
Man	13 ± 2	0.123	800 ± 20	39	2.86	10
Gal	14 ± 2	0.134	670 ± 20	36	2.36	13

4.3.4. ConA recognition by glycopolymers using UV/Vis spectroscopy

Concanavalin A (ConA) is a C-type lectin composed of four distinct subunits each possessing a carbohydrate recognition domain (CRD) [47]. This CRD has specificity for saccharides possessing vicinal, equatorial hydroxyl groups at the C-3 and C-4 positions, such as mannose and glucose [48]. Due to the tetrameric structure of this soluble protein,

CRD engagement with multivalent ligands can facilitate aggregation to occur, resulting in clustering of bound protein and ligand [17]. Spectroscopic assays can measure this activity as a function of solution turbidity, monitoring the formation of agglutinated complexes over time. Such an assay was performed comparing the two polymeric conformations (micelle vs. unimer) for each of the carbohydrate compositions (Man vs. Gal) at fixed polymer (and carbohydrate) concentrations (**Figure 4.8**). Unsurprisingly, only the polymers displaying pendent mannose moieties were able to engage ConA, as the CRD of this lectin is unable to recognize galactose due to the axial positioning of the saccharide's C-4 hydroxyl group.
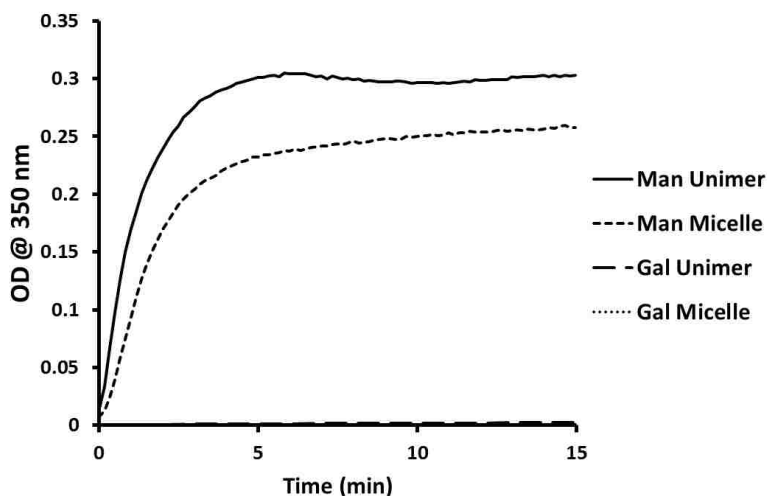
Figure 4.8. Time-dependent agglutination of ConA mediated by glycopolymers. ConA is at 1 µM and glycopolymers are at 2 µM (52 µM per pendent glyco-residues). The Man unimer and micelle solutions were run in triplicate with the curves displayed being representative.

From these data, a kinetic parameter can be extracted which identifies the initial rate of ConA/glycopolymer cluster formation. By applying a linear regression to the early time points, an initial clustering rate constant, $k_{cluster}$, was determined: 0.17 ± 0.01 and 0.10 ± 0.03 AU/min for the Man unimer and micelle, respectively. These data suggest that the unimeric glycopolymer conformation is better able to display its carbohydrate groups for CRD recognition compared to the micellar structure, thereby promoting enhanced multivalent lectin engagement and therefore, lectin clustering. It is possible that packing of glycopolymer segments within a micellar corona restricts chain mobility and sterically hinders interactions which could explain the decreased rate of agglutination at this carbohydrate concentration. However, these results contradict those found for glycodendrimer structures. These assemblies display branched, terminal monosaccharides

on a dendrimer platform. The aforementioned steric hindrance issue is thought to mediate enhanced multivalent ligand engagement in these materials by displaying saccharides on the surface of a macromolecular structure as opposed to confining pendent saccharides to a polymer matrix in linear glycopolymers [49]. Kumar et al. demonstrated that a glucose-functionalized glycodendrimer exhibits a higher initial ConA clustering rate when compared to a linear glycopolymer analog [26]. In a similar study, Hetzer et al. determined that promoting micellization of a temperature-responsive diblock glycopolymer resulted in enhanced ConA clustering over the unassembled, unimeric conformation [50].

A precipitation assay was then employed to determine how efficient these materials are at binding ConA on a per mannose residue basis. Each glycopolymer was incubated with an excess of lectin at different mannose residue concentrations leading to precipitation of ConA/glycopolymer complexes, with the amount of protein in these aggregates determined by UV/Vis spectroscopy (**Figure 4.9**). For all concentrations investigated, the unimer bound more ConA than the micelle at the same mannose concentration. The relative concentrations and trends from this dataset are similar to those generated by Kumar et al. for a glucose-dendrimer except those researchers observed an opposite effect when comparing a linear vs. particulate structure [51]. From these data, the stoichiometry of ConA/glycopolymer within the precipitate complexes was determined to be 1.9 ± 0.2 and 1.4 ± 0.1 for the Man unimer and micelle, respectively. Wolfenden et al. calculated approximately 5 – 25 ConA tetramers bound per mannosylated/glucosylated dendrimer (with molecular weight values ~5-fold higher than the Man and Gal diblock copolymers), dependent on the relative carbohydrate composition of the material [29]. It is important to note the distinct structural differences between glycodendrimers and the polymeric micelles investigated in the presented studies. Glycodendrimers present carbohydrates on their surface, creating a brush-like configuration which provides a crew-cut morphology, while these spherical micelles likely adapt a more star-like conformation which is speculated due to their relative block sizes and low CMCs and aggregation numbers [24], [41], [51], [52]. For the polymer micelles described in this chapter, it is likely that incorporation of the glycopolymer segment into a macromolecular assembly is reducing accessibility of the mannose residue towards lectin engagement when compared to the linear conformation.
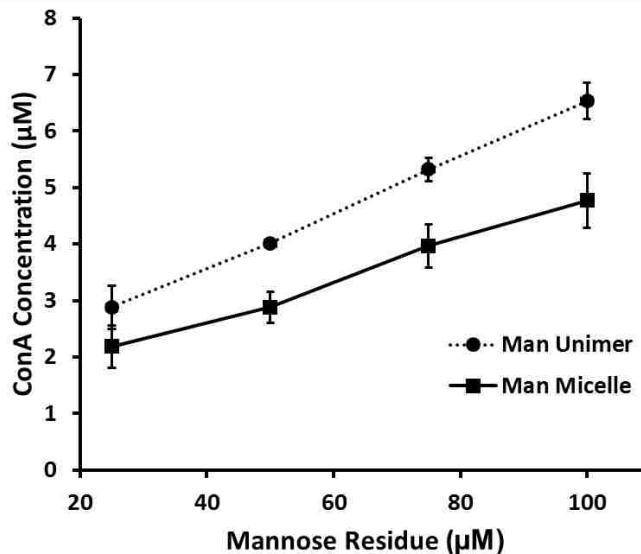
Figure 4.9. Concentration of bound ConA as a function of mannose residue concentration for both the Man unimer and micelle via a precipitation assay. Each data point represents triplicate samples.

The ConA binding stoichiometry can also be represented as the ratio of mannose residues per ConA: 14.0 ± 1.4 and 19.1 ± 1.8 for the Man unimer and micelle, respectively. Cairo et al. found this ratio to be 9 for a fully mannosylated linear glycopolymer, suggesting that the Man unimer has comparable efficiency at binding ConA [17]. They also found that increasing the carbohydrate density on a scaffold enhances the rate of lectin engagement while also reducing inter-receptor distance. One additional parameter that can be obtained from this data is the stoichiometry of ConA/micelle based upon the previously determined Man micelle aggregation number. This ratio was determined to be 54 ± 5 which illustrates that a micellar platform provides the advantage of engaging a large number of lectins on a per particle basis, a characteristic which mimics pathogenic organisms and can be exploited for therapeutic applications [1].

4.3.4. ConA recognition by glycopolymers using surface plasmon resonance (SPR) techniques

Surface plasmon resonance (SPR) is a powerful analytical tool for probing biomolecular binding events at an interface [53]. Due to the high sensitivity of instrumentation which measures this phenomenon, quantitative parameters can be generated that describe both the equilibrium and kinetic aspects of a given interaction [54]. In the simplest sense, SPR works by measuring changes in the reflection of polarized incident light (either by intensity or

angle) upon a surface. When mass is deposited onto a surface, e.g. due to ligand binding to an immobilized receptor, the frequency of oscillating free electrons (surface plasmons) within that surface changes and at a specific incident angle the electrons will resonate with the light leading to absorption. This response can then be correlated to the quantity of adsorbed material, providing the basis for modeling biomolecular interactions at this interface. Based upon these known concepts, SPR was employed to initially determine whether the technique could measure these ConA/glycopolymer interactions (**Figure 4.10**). Surfaces were separately functionalized with each glycopolymer by exploiting the affinity of gold for sulfur-containing compounds, namely the trithiocarbonate moiety at the glycopolymer ω end. It is important to consider that particle morphology is lost in this approach as the ω end is typically sequestered in the micelle core and that this experiment is simply a screen to evaluate the SPR technique for the given application. Much like the agglutination data, neither the Gal unimer or micelle were able to generate a significant response while the Man unimer and micelle both mediated rapid ConA deposition and saturation. In this configuration, the mannose on both the unimer and micelle should be equally accessible to the lectin resulting in similar responses.
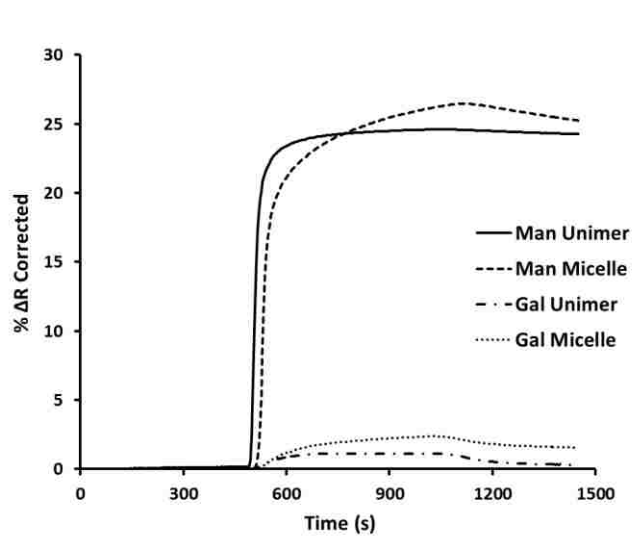
Figure 4.10. SPR measurements of ConA (500 nM) binding to immobilized glycopolymers (50 µM).

To make quantitative lectin binding affinity comparisons between the Man glycopolymer morphologies, a related technique known as SPR imaging (SPRi) was utilized. This technique exploits the same general principles which govern SPR but allows for multiple experimental conditions, e.g. ligand concentration, to be monitored simultaneously. SPRi

has been previously validated for studying protein-carbohydrate interactions [55], [56]. For the experiments presented in this section, an indirect measure of lectin binding affinity was determined. Solutions of ConA at a fixed concentration were mixed with varying amounts of glycopolymer and added to mannoside-functionalized surfaces. This competitive assay then measured the deposition of accessible ConA onto the surface. The concentration of glycopolymer at which half the ConA was able to bind to the mannosylated surface, the half maximal inhibitory concentration (IC50), was determined and used as a measurement of lectin binding affinity (**Figure 4.11**). IC50 values were found to be 0.34 µM and 1.07 µM for the Man unimer and micelle, respectively. These findings demonstrate that the unimeric conformation is more efficient than the micelle at inhibiting α-D-mannose/ConA interactions. To give a reference for these concentrations, α-D-mannose inhibits ConA binding to dextran at an IC50 value of 2.0 mM using a classical precipitation assay [57] while via SPR this value was found to be 6.5 mM for the monosaccharide inhibiting ConA binding to a mannosylated surface [28], both of the values being over a 1000-fold higher than these glycopolymers. The inhibitory effects of the described glycopolymers are similar to those presented by Ponader et al. who determined an IC50 of 1 µM for ConA inhibition by a glycopolymer segment [28]. Additional studies have demonstrated the inhibitory activity of ConA binding by mannosylated clusters (IC50 = 7 µM [58]) and polyvalent mannosides (IC50 = 17 µM [59]). The ability of mannosylated dendritic polymers to inhibit lectin binding has also been studied, with Tabarani et al. determining an IC50 value in the µM-range for the inhibition of DC-SIGN binding to the HIV glycoprotein gp120 [60].
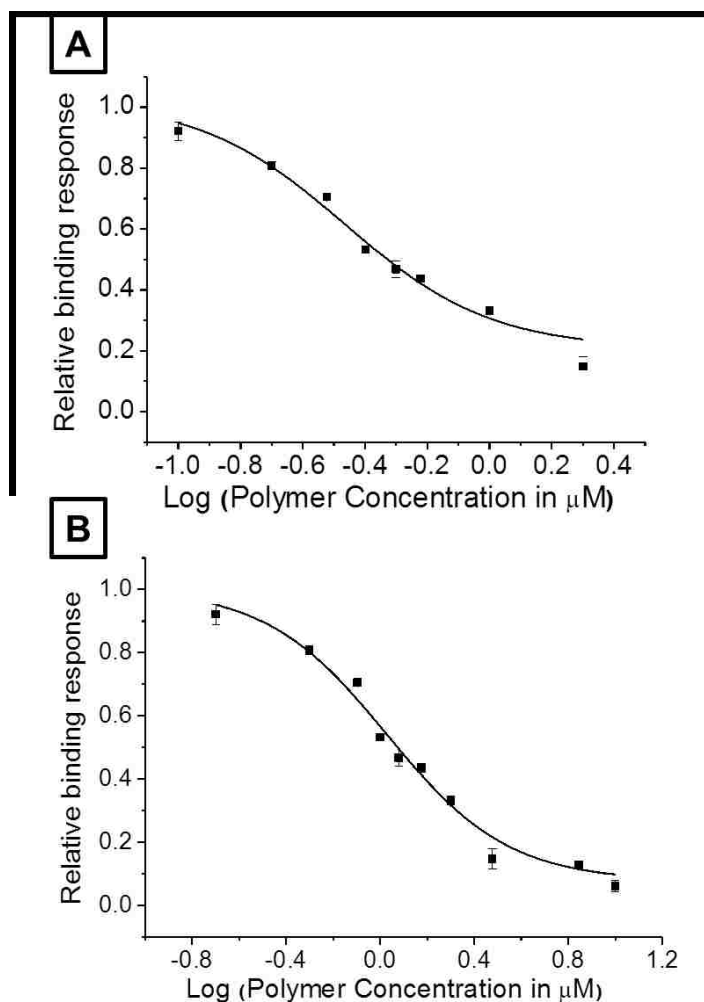
Figure 4.11. SPRi measurement for Man unimer (**A**) and diblock (**B**) inhibiting ConA binding to immobilized α-D-mannose. Data were fit using a dose response curve in Origin software (OriginLab, Northampton, MA).

4.4. CONCLUSIONS

A family of multivalent glycopolymers was successfully prepared via RAFT which differed in carbohydrate (mannose vs. galactose) and conformation (micelle vs. unimer). The micellar morphology was achieved by polymerizing a discrete, acetylated glycopolymer segment and blocking on a hydrophobic, endosomolytic copolymer. Following saponification to remove protective acetyl groups, the resultant diblock glycopolymers were shown to assemble into micelles in a physiological environment while exhibiting a unique pH-responsive destabilization mode of activity as demonstrated by DLS measurements and a hemolysis assay. The micelles were found to be stable in buffer with low CMC values and aggregation numbers with no significant differences between the mannose and galactose coronas. Both

84

the mannose micelle and unimer were able to engage the C-type lectin, Concanavalin A (ConA), while the galactose analogs were unable to do so. Compared to the mannose micelle, the mannose unimer was able to bind ConA at a faster rate (initial clustering rate = 0.17 ± 0.01 vs. 0.10 ± 0.03 AU/min) and higher stoichiometry (ConA/glycopolymer = 1.9 ± 0.2 vs 1.4 ± 0.1). These data are contradictory to what other researchers have found when comparing particulate and linear morphologies for multivalent carbohydrates and suggests that incorporation of this glycopolymer segment into a micellar platform slightly inhibits lectin engagement on a per carbohydrate basis. Additionally, IC50 values for ConA binding to immobilized α-D-mannose were determined via SPRi for the mannose unimer (0.34 µM) and micelle (1.07 µM) which are consistent with materials displaying a high density of pendent carbohydrates.

4.5. REFERENCES

[1] C. R. Bertozzi and L. L. Kiessling, "Chemical Glycobiology," *Science*, vol. 291, no. 5512, pp. 2357–2364, Mar. 2001.

[2] H. Zhang and Y. Ma, "Recent developments in carbohydrate-decorated targeted drug/gene delivery," *Medicinal Research Reviews*, vol. 30, no. 2, pp. 270–289, 2010.

[3] P. J. Murray and T. a Wynn, "Protective and pathogenic functions of macrophage subsets.," *Nature reviews. Immunology*, vol. 11, no. 11, pp. 723–37, Nov. 2011.

[4] K. Palucka, H. Ueno, and J. Banchereau, "Recent developments in cancer vaccines.," *Journal of immunology (Baltimore, Md. : 1950)*, vol. 186, no. 3, pp. 1325–31, Feb. 2011.

[5] E. W. Adams, D. M. Ratner, P. H. Seeberger, and N. Hacohen, "Carbohydrate-mediated targeting of antigen to dendritic cells leads to enhanced presentation of antigen to T cells.," *Chembiochem : a European journal of chemical biology*, vol. 9, no. 2, pp. 294–303, Jan. 2008.

[6] W. Wijagkanalan, S. Kawakami, Y. Higuchi, F. Yamashita, and M. Hashida, "Intratracheally instilled mannosylated cationic liposome/NFκB decoy complexes for effective prevention of LPS-induced lung inflammation.," *Journal of controlled release : official journal of the Controlled Release Society*, vol. 149, no. 1, pp. 42–50, Jan. 2011.

[7] S. Chono, T. Tanino, T. Seki, and K. Morimoto, "Uptake characteristics of liposomes by rat alveolar macrophages: influence of particle size and surface mannose modification.," *The Journal of pharmacy and pharmacology*, vol. 59, no. 1, pp. 75–80, Jan. 2007.

[8] C. G. Figdor, Y. van Kooyk, and G. J. Adema, "C-type lectin receptors on dendritic cells and Langerhans cells.," *Nature reviews. Immunology*, vol. 2, no. 2, pp. 77–84, Feb. 2002.

[9] E. P. McGreal, J. L. Miller, and S. Gordon, "Ligand recognition by antigen-presenting cell C-type lectin receptors.," *Current opinion in immunology*, vol. 17, no. 1, pp. 18–24, Feb. 2005.

[10] R. T. Lee, K. Drickamer, and Y. C. Lee, "Multivalent Ligand Binding by Serum Protein '," *Archives of Biochemistry and Biophysics*, vol. 299, no. 1, 1992.

[11] S. R. S. Ting, G. Chen, and M. H. Stenzel, "Synthesis of glycopolymers and their multivalent recognitions with lectins," *Polymer Chemistry*, vol. 1, no. 9, p. 1392, 2010.

[12]   A. B. Lowe, B. S. Sumerlin, and C. L. McCormick, "The direct polymerization of 2-methacryloxyethyl glucoside via aqueous reversible addition-fragmentation chain transfer (RAFT) polymerization," *Polymer*, vol. 44, no. 22, pp. 6761–6765, Oct. 2003.

[13]   N.-Y. Xiao, A.-L. Li, H. Liang, and J. Lu, "A Well-Defined Novel Aldehyde-Functionalized Glycopolymer: Synthesis, Micelle Formation, and Its Protein Immobilization," *Macromolecules*, vol. 41, no. 7, pp. 2374–2380, Apr. 2008.

[14]   J. Bernard, X. Hao, T. P. Davis, C. Barner-Kowollik, and M. H. Stenzel, "Synthesis of various glycopolymer architectures via RAFT polymerization: from block copolymers to stars.," *Biomacromolecules*, vol. 7, no. 1, pp. 232–8, Jan. 2006.

[15]   Z. Deng, S. Li, X. Jiang, and R. Narain, "Well-Defined Galactose-Containing Multi-Functional Copolymers and Glyconanoparticles for Biomolecular Recognition Processes," *Macromolecules*, vol. 42, no. 17, pp. 6393–6405, Sep. 2009.

[16]   O. Abdelkader, S. Moebs-sanchez, Y. Queneau, J. Bernard, E. Fleury, and D. Lyon, "Generation of Well-Defined Clickable Glycopolymers from Aqueous RAFT Polymerization of Isomaltulose-Derived Acrylamides," *Polymer*, vol. 49, pp. 1309–1318, 2011.

[17]   C. W. Cairo, J. E. Gestwicki, M. Kanai, and L. L. Kiessling, "Control of multivalent interactions by binding epitope density.," *Journal of the American Chemical Society*, vol. 124, no. 8, pp. 1615–9, Feb. 2002.

[18]   S. Pearson, N. Allen, and M. H. Stenzel, "Core-Shell Particles with Glycopolymer Shell and Polynucleoside Core via RAFT : From Micelles to Rods," *Polymer*, pp. 1706–1723, 2009.

[19]   G. M. Whitesides and B. Grzybowski, "Self-assembly at all scales.," *Science (New York, N.Y.)*, vol. 295, no. 5564, pp. 2418–21, Mar. 2002.

[20]   H. Ringsdorf, "Molecular architecture and function of polymeric oriented systems: models for the study of organization, surface recognition, and dynamics of biomembranes," *… International Edition in …*, vol. 27, no. 1, pp. 113–158, 1988.

[21]   J.-M. Lehn, "Supramolecular polymer chemistry-scope and perspectives," *Polymer International*, vol. 51, no. 10, pp. 825–839, Oct. 2002.

[22]   P. L. Soo, L. Luo, D. Maysinger, and A. Eisenberg, "Micelles : Implications for Drug Delivery," *Langmuir*, no. 21, pp. 9996–10004, 2002.

[23]   Y. Kakizawa and K. Kataoka, "Block copolymer micelles for delivery of gene and related compounds.," *Advanced drug delivery reviews*, vol. 54, no. 2, pp. 203–22, Feb. 2002.

[24]   R. Savić, A. Eisenberg, and D. Maysinger, "Block copolymer micelles as delivery vehicles of hydrophobic drugs: micelle-cell interactions.," *Journal of drug targeting*, vol. 14, no. 6, pp. 343–55, Jul. 2006.

[25]   M. H. Stenzel, "RAFT polymerization: an avenue to functional polymeric micelles for drug delivery.," *Chemical communications (Cambridge, England)*, no. 30, pp. 3486–503, Aug. 2008.

[26]   J. Kumar, A. Bousquet, and M. H. Stenzel, "Thiol-alkyne chemistry for the preparation of micelles with glycopolymer corona: dendritic surfaces versus linear glycopolymer in their ability to bind to lectins.," *Macromolecular rapid communications*, vol. 32, no. 20, pp. 1620–6, Oct. 2011.

[27]   F. Suriano, R. Pratt, J. P. K. Tan, N. Wiradharma, A. Nelson, Y.-Y. Yang, P. Dubois, and J. L. Hedrick, "Synthesis of a family of amphiphilic glycopolymers via controlled ring-opening polymerization of functionalized cyclic carbonates and their application in drug delivery.," *Biomaterials*, vol. 31, no. 9, pp. 2637–45, Mar. 2010.

[28]   D. Ponader, F. Wojcik, F. Beceren-Braun, J. Dernedde, and L. Hartmann, "Sequence-defined glycopolymer segments presenting mannose: synthesis and lectin binding affinity.," *Biomacromolecules*, vol. 13, no. 6, pp. 1845–52, Jun. 2012.

[29]   M. L. Wolfenden and M. J. Cloninger, "Carbohydrate-functionalized dendrimers to investigate the predictable tunability of multivalent interactions.," *Bioconjugate chemistry*, vol. 17, no. 4, pp. 958–66, 2006.

[30]   G. Moad, Y. K. Chong, A. Postma, E. Rizzardo, and S. H. Thang, "Advances in RAFT polymerization: the synthesis of polymers with defined end-groups," *Polymer*, vol. 46, no. 19, pp. 8458–8468, Sep. 2005.

[31]   A. J. Convertine, D. S. W. Benoit, C. L. Duvall, A. S. Hoffman, and P. S. Stayton, "Development of a novel endosomolytic diblock copolymer for siRNA delivery.," *Journal of Controlled Release*, vol. 133, no. 3, pp. 221–9, Feb. 2009.

[32]   L. E. Iters, T. Ren, and D. Liu, "Synthesis of targetable cationic amphiphiles," *Tetrahedron Letters*, vol. 40, pp. 7621–7625, 1999.

[33]   S. Kitazawa, M. Okumura, K. Kinomura, and T. Sakakibara, "Syntheses and properties of novel vinyl monomers bearing a glycoside residue," *Chemistry Letters*, vol. 19, no. 9, pp. 1733–1736, 1990.

[34]   V. Bulmus, "A new pH-responsive and glutathione-reactive, endosomal membrane-disruptive polymeric carrier for intracellular delivery of biomolecular drugs," *Journal of Controlled Release*, vol. 93, no. 2, pp. 105–120, Dec. 2003.

[35]   F. Cheng, J. Shang, and D. M. Ratner, "A versatile method for functionalizing surfaces with bioactive glycans.," *Bioconjugate chemistry*, vol. 22, no. 1, pp. 50–7, Jan. 2011.

[36]   V. P. Torchilin, "Structure and design of polymeric surfactant-based drug delivery systems.," *Journal of controlled release : official journal of the Controlled Release Society*, vol. 73, no. 2–3, pp. 137–72, Jun. 2001.

[37]   P. Mukerjee and K. Mysels, *Critical micelle concentrations of aqueous surfactant systems*. 1970.

[38]   J. A. N. Slavik, "ANILINONAPHTHALENE SULFONATE AS A PROBE OF MEMBRANE COMPOSITION AND FUNCTION," *Biochimica et Biophysica Acta*, vol. 694, pp. 1–25, 1982.

[39]   K. Dan and S. Ghosh, "pH-Responsive Aggregation of Amphiphilic Glyco-Homopolymer.," *Macromolecular rapid communications*, vol. 1, pp. 127–132, Nov. 2011.

[40]   A. J. Convertine, C. Diab, M. Prieve, A. Paschal, A. S. Hoffman, P. H. Johnson, P. S. Stayton, W. H. Street, and S. Washington, "pH-Responsive Polymeric Micelle Carriers for siRNA Drugs," *Biomacromolecules*, pp. 2904–2911, 2010.

[41]   W. Li, M. Nakayama, J. Akimoto, and T. Okano, "Effect of block compositions of amphiphilic block copolymers on the physicochemical properties of polymeric micelles," *Polymer*, vol. 52, no. 17, pp. 3783–3790, 2011.

[42]   P. Satturwar, M. N. Eddine, F. Ravenelle, and J.-C. Leroux, "pH-responsive polymeric micelles of poly(ethylene glycol)-b-poly(alkyl(meth)acrylate-co-methacrylic acid): influence of the copolymer composition on self-assembling properties and release of candesartan cilexetil.," *European journal of pharmaceutics and biopharmaceutics : official journal of Arbeitsgemeinschaft für Pharmazeutische Verfahrenstechnik e.V*, vol. 65, no. 3, pp. 379–87, Mar. 2007.

[43]   S. Nolan, R. Phillips, P. Cotts, and S. Dungan, "Light Scattering Study on the Effect of Polymer Composition on the Structural Properties of PEO-PPO-PEO Micelles," *Journal of colloid and interface science*, vol. 191, no. 2, pp. 291–302, Jul. 1997.

[44]   M. Y. Kozlov, N. S. Melik-nubarov, E. V Batrakova, and A. V Kabanov, "Relationship between Pluronic Block Copolymer Structure , Critical Micellization Concentration and Partitioning Coefficients of Low Molecular Mass Solutes," pp. 3305–3313, 2000.

[45]   A. M. Alhoranta, J. K. Lehtinen, A. O. Urtti, S. J. Butcher, V. O. Aseyev, and H. J. Tenhu, "Cationic amphiphilic star and linear block copolymers : synthesis , self-assembly and in vitro gene transfection," *Polymer*, 2011.

[46]   D. J. Winzor, M. Deszczynski, S. E. Harding, and P. R. Wills, "Nonequivalence of second virial coefficients from sedimentation equilibrium and static light scattering studies of protein solutions.," *Biophysical chemistry*, vol. 128, no. 1, pp. 46–55, Jun. 2007.

[47]   G. M. Edelman, B. a Cunningham, G. N. Reeke, J. W. Becker, M. J. Waxdal, and J. L. Wang, "The covalent and three-dimensional structure of concanavalin A.," *Proceedings of the National Academy of Sciences of the United States of America*, vol. 69, no. 9, pp. 2580–4, Sep. 1972.

[48]   V. Sharma and a Surolia, "Analyses of carbohydrate recognition by legume lectins: size of the combining site loops and their primary specificity.," *Journal of molecular biology*, vol. 267, no. 2, pp. 433–45, Mar. 1997.

[49]   A. L. Martin, B. Li, and E. R. Gillies, "Surface functionalization of nanomaterials with dendritic groups: toward enhanced binding to biological targets.," *Journal of the American Chemical Society*, vol. 131, no. 2, pp. 734–41, Jan. 2009.

[50]   M. Hetzer, G. Chen, C. Barner-Kowollik, and M. H. Stenzel, "Neoglycopolymers based on 4-vinyl-1,2,3-triazole monomers prepared by click chemistry.," *Macromolecular bioscience*, vol. 10, no. 2, pp. 119–26, Feb. 2010.

[51]   J. Kumar, L. McDowall, G. Chen, and M. H. Stenzel, "Synthesis of thermo-responsive glycopolymers via copper catalysed azide–alkyne 'click' chemistry for inhibition of ricin: the effect of spacer between polymer backbone and galactose," *Polymer Chemistry*, pp. 1879–1886, 2011.

[52]   I. LaRue, M. Adam, E. B. Zhulina, M. Rubinstein, M. Pitsikalis, N. Hadjichristidis, D. a. Ivanov, R. I. Gearba, D. V. Anokhin, and S. S. Sheiko, "Effect of the Soluble Block Size on Spherical Diblock Copolymer Micelles," *Macromolecules*, vol. 41, no. 17, pp. 6555–6563, Sep. 2008.

[53]   K. M. Bolles, F. Cheng, J. Burk-Rafel, M. Dubey, and D. M. Ratner, "Imaging Analysis of Carbohydrate-Modified Surfaces Using ToF-SIMS and SPRi," *Materials*, vol. 3, no. 7, pp. 3948–3964, Jul. 2010.

[54]   J. Homola, S. Yee, and G. Gauglitz, "Surface plasmon resonance sensors: review," *Sensors and Actuators B: Chemical*, vol. 54, pp. 3–15, 1999.

[55]   E. a Smith, W. D. Thomas, L. L. Kiessling, and R. M. Corn, "Surface plasmon resonance imaging studies of protein-carbohydrate interactions.," *Journal of the American Chemical Society*, vol. 125, no. 20, pp. 6140–8, May 2003.

[56]   M. Dhayal and D. M. Ratner, "XPS and SPR analysis of glycoarray surface density.," *Langmuir : the ACS journal of surfaces and colloids*, vol. 25, no. 4, pp. 2181–7, Mar. 2009.

[57]   R. D. Poretzt and I. J. Goldstein, "An Examination of the Topography of the Saccharide Binding Sites of Concanavalin," *Biochemistry*, no. 14, pp. 2890–2896, 1970.

[58]   D. Pagé and R. Roy, "Synthesis of divalent Î±-D-mannopyranosylated clusters having enhanced binding affinities towards concanavalin A and pea lectins," *Bioorganic & Medicinal Chemistry Letters*, vol. 6, no. 15, pp. 1765–1770, 1996.

[59]   S. Dimick and S. Powell, "On the meaning of affinity: cluster glycoside effects and concanavalin A," *Journal of the …*, no. 12, pp. 10286–10296, 1999.

[60]   G. Tabarani, J. J. Reina, C. Ebel, C. Vivès, H. Lortat-Jacob, J. Rojo, and F. Fieschi, "Mannose hyperbranched dendritic polymers interact with clustered organization of DC-SIGN and inhibit gp120 binding.," *FEBS letters*, vol. 580, no. 10, pp. 2402–8, May 2006.

CHAPTER 5 – PHYSICOCHEMICAL PROPERTIES AND STABILITY OF DIBLOCK COPOLYMER MICELLES AS A FUNCTION OF CORONA COMPOSITION

Matthew J. Manganiello, John P. Sumida, Eun-Ho Song, Carlos E. Catalano, Anthony J. Convertine, Daniel M. Ratner, Patrick S. Stayton

ABSTRACT

Polymeric micelles were prepared from diblock copolymers synthesized by reversible addition-fragmentation chain transfer (RAFT) polymerization. The micelles consisted of a core copolymer segment of diethylaminoethyl methacrylate (DEAEMA) and butyl methacrylate (BMA), and homopolymer coronas of fixed molecular weights but varying chemistries: dimethylaminoethyl methacrylate (DMAEMA), N,N-dimethylacrylamide (DMA), and mannose ethyl methacrylate (ManEMA). These materials were designed to examine the influence of a cationic, neutral, and carbohydrate corona on micelle assembly and stability in buffer and serum. Each diblock copolymer was shown to form particles of different sizes (21 ± 2, 32 ± 4, and 16 ± 2 nm mean diameters for DMA, DMAEMA, and ManEMA, respectively) as determined by dynamic light scattering (DLS). Transmission electron microscopy (TEM) of the ManEMA diblock demonstrated that the material adopts a spherical morphology in buffer. The pH-responsive activity of the copolymer core segment was found to be unaffected by the corona composition as shown by a hemolysis assay. A polarity-sensitive probe was used to demonstrate that the critical micelle concentrations (CMCs) were consistent among the materials (13 – 14 ug/mL). Static light scattering (SLS) measurements showed distinct differences in the aggregation number (N_{agg}) of each micelle: N_{agg}(DMA) = 40, N_{agg}(DMAEMA) = 70, and N_{agg}(ManEMA) = 21, a trend that correlates with particle mean diameter. Analytical ultracentrifugation (AUC) was employed to study the stability of micelles in buffer, mouse serum, and recombinant human serum albumin (rHSA). Preliminary AUC analyses demonstrate trends in N_{agg} consistent with data from SLS and show that the ManEMA micelle does not significantly interact with either mouse serum or rHSA.

5.1. INTRODUCTION

Block copolymer micelles have garnered interest as nanoscale delivery vehicles for small molecule drugs and biological macromolecules [1]. These synthetic materials adopt a core-

shell morphology at physiological conditions, with a hydrophobic segment that self-associates to minimize solvent interactions stabilized by a hydrophilic block. When designing these systems, proper selection of the hydrophilic component is essential to not only micelle stability but affects how the resultant micelle interacts with exogenous materials. For biological applications, the interaction of micelles with extracellular proteins and cellular membranes becomes an important design consideration [2]. Changes in the chemical composition of the micelle corona can affect the particle's affinity towards a given soluble protein, membrane lipid, or cell-surface receptor, altering the in vivo behavior of the material [3]. Additionally, intra-particle repulsion of the soluble segments comprising the corona impacts micelle assembly [4]. Through better understanding on how to control these interactions, the clinical utility of this class of synthetic polymers can be greatly improved.

In vivo administration of polymeric micelles can proceed through a variety of routes. Intravenous delivery is commonly employed as it allows for access to multiple organs and can exploit the enhanced permeability and retention (EPR) effect for tumor targeting [5]. Proteins found in the blood present an obstacle to efficacious systemic delivery as they can act to destabilize micelles through nonspecific adsorption. Serum proteins can also be found outside the bloodstream, e.g. residing in subcutaneous tissue fluid, highlighting the importance of elucidating polymer/protein interactions for multiple routes of delivery [6]. Numerous methods exist for probing these binding events including Forster resonance energy transfer (FRET) [7], surface plasmon resonance (SPR) [8], dynamic light scattering (DLS) [9], static light scattering (SLS) [10], transmission electron microscopy (TEM) [11], and photon correlation spectroscopy [12]. While these techniques provide inherent advantages, difficulties still exist in isolating the behavior of individual species within a complex biological media. Measuring the interactions of biological macromolecules in heterogeneous and non-ideal solutions has presented analytical challenges that are actively being addressed by new techniques and approaches [7], [9].

Analytical ultracentrifugation (AUC) has been extensively applied to study the hydrodynamic and thermodynamic properties of macromolecules in solution [13], [14]. AUC monitors the sedimentation of compounds in a centrifugal field by fluorescence, absorbance, or interference detection, relating sedimentation velocity or equilibrium data to physical properties of the studied material. This technique generates a rich dataset with high

precision and sensitivity that can be analyzed to produce size distribution profiles of macromolecules. Recent advances in the mathematical treatment of these data have allowed for the deconvolution of complex, non-ideal solutions thereby isolating individual species within a heterogeneous system [15]. Through application of these approaches, characterization of novel materials exhibiting unique physicochemical properties, e.g. polysaccharides and macromolecular assemblies, is achievable [16], [17].

Here we endeavor to apply both AUC and light scattering experiments to evaluate diblock copolymer micelle assembly and stability in both buffer and complex media. The core composition of these micelles was fixed while the corona chemistry was varied through incorporation of one of three monomer units: dimethylaminoethyl methacrylate (DMAEMA), N,N-dimethylacrylamide (DMA), and mannose ethyl methacrylate (ManEMA). Each of these compounds displays a unique pendent, hydrophilic functionality: cation (DMAEMA), neutral (DMA), and saccharide (ManEMA). The effect of these corona chemistries on micelle assembly/stability in buffer and in the presence of serum proteins was investigated. AUC was employed to both validate the technique for micelle characterization and to measure the interactions of these particles with serum components.

5.2. MATERIALS AND METHODS

5.2.1. Materials

Chemicals and all materials were supplied by Sigma-Aldrich (St Louis, MO) unless otherwise specified. 2,2′-Azobis(4-methoxy-2.4-dimethyl valeronitrile) (V70), 1,1'-*Azobis*(cyclohexane-1-carbonitrile) (V40), and 2-2'-Azobis(isobutyronitrile) (AIBN) were obtained from Wako Chemicals USA, Inc. (Richmond, VA). Spectra/Por 7 standard regenerated cellulose dialysis tubing was obtained from Spectrum Labs (Rancho Dominguez, CA) and Slide-A-Lyzer® MINI Dialysis Device with a 3.5K MWCO were obtained from Thermo Scientific (Rockford, IL). ECT was synthesized as previously described [18], [19]. Dimethylaminoethyl methacrylate (DMAEMA), diethylaminoethyl methacrylate (DEAEMA), butyl methacrylate (BMA), and N,N-dimethylacrylamide (DMA) were distilled prior to use. Methacryloxyethyl thiocarbamoyl rhodamine B (RhodMA) was obtained from Polysciences, Inc. (Warrington, PA). Acetylated mannose ethyl methylacrylate (AcManEMA) was synthesized according to previous methods (see Chapter

4) [20], [21].   Recombinant human serum albumin (rHSA) was obtained from Albumin Biosciences (Huntsville, AL).

5.2.2. Synthesis of poly(DEAEMA-co-BMA-co-RhodMA) macro chain transfer agent (pEB40r macroCTA)

The RAFT copolymerization of DEAEMA, BMA, and RhodMA was conducted in dioxane at 90 °C with 50 wt% monomer under a nitrogen atmosphere for 6 h using ECT and V40 as the chain transfer agent (CTA) and radical initiator, respectively.   The initial monomer to CTA molar ratio ($[M]_0$:$[CTA]_0$) was 100:1, the initial CTA to initiator molar ratio ($[CTA]_0$:$[I]_0$) was 20:1, and the initial molar feed ratios (%) of DEAEMA, BMA, and RhodMA was 60, 40, and 0.04, respectively.   The resultant macroCTA was isolated by dialysis (6000 – 8000 MWCO) against methanol followed by rotary evaporation and drying in vacuo.

5.2.3. Diblock polymerization of DMA, DMAEMA, and AcManEMA from pEB40r macroCTA

Three separate diblock copolymers were polymerized from the same pEB40r macroCTA in dioxane.   The DMA copolymer (p(EB40r-*b*-DMA)) was polymerized at 60 °C for 6 h at 30 wt% monomer with AIBN as the radical source, the initial monomer to CTA ratio ($[M]_0$:$[CTA]_0$) at 150:1, and the initial CTA to initiator molar ratio ($[CTA]_0$:$[I]_0$) at 20:1.   The DMAEMA copolymer p(EB40r-*b*-DMAEMA) was polymerized at 30 °C for 18 h at 40 wt% monomer with V70 as the radical source, the initial monomer to CTA ratio ($[M]_0$:$[CTA]_0$) at 100:1, and the initial CTA to initiator molar ratio ($[CTA]_0$:$[I]_0$) at 20:1.   The AcManEMA copolymer (p(EB40r-*b*-AcManEMA)) was polymerized at 30 °C for 18 h at 40 wt% monomer with V70 as the radical source, the initial monomer to CTA ratio ($[M]_0$:$[CTA]_0$) at 50:1, and the initial CTA to initiator molar ratio ($[CTA]_0$:$[I]_0$) at 20:1.   The resultant diblock copolymers were isolated by precipitation into cold petroleum ether.   The copolymers were then redissolved into acetone and further precipitated into cold petroleum ether (×4) followed by drying overnight in vacuo.   Aqueous solutions of the DMA and DMAEMA diblock copolymers were prepared by dissolving the materials at 200 mg/mL in methanol then immediately diluting into pH 7.4 1X DPBS at 20 mg/mL.   These solutions were then dialyzed against DPBS using 3.5K MWCO.

5.2.4. Saponification of p(EB40r-b-AcManEMA)

To display native pendent glycomoieties on the AcManEMA diblock copolymer, protective acetyl groups were removed via base-catalyzed hydrolysis. p(EB40r-*b*-AcManEMA) was added to a solution of 1 wt% sodium methoxide in anhydrous methanol at a copolymer concentration of 50 mg/mL. After 1 hour incubation at room temperature, the solution was neutralized with acetic acid to a pH of ~7 and dialyzed against deionized water using 1000 MWCO tubing. The solution was then lyophilized to obtain the final deprotected glycopolymer: p(EB40r-b-ManEMA). An aqueous solution of this diblock copolymer was then prepared in the same manner as described for the DMA and DMAEMA diblock copolymers (see above).

5.2.5. Gel permeation chromatography (GPC)

GPC was used to determine molecular weights and polydispersities (M_w/M_n, PDI) of the macroCTA and diblock copolymers. SEC Tosoh TSK-GEL R-3000 and R-4000 columns (Tosoh Bioscience, Montgomeryville, PA) were connected in series to a Agilent 1200 series (Agilent Technologies, Santa Clara, CA), refractometer Optilab-rEX and triple-angle static light scattering detector miniDAWN TREOS (Wyatt Technology, Dernbach, Germany). HPLC-grade DMF containing 0.1 wt.% LiBr at 60 °C was used as the mobile phase at a flow rate of 1 ml/min. The molecular weights of each polymer were determined using a multi-detector calibration based on dn/dc values calculated separately for each copolymer composition.

5.2.6. Dynamic light scattering (DLS) and static light scattering (SLS) measurements

The diblock glycopolymer micelles were analyzed by DLS to determine particle mean diameter and by SLS to evaluate particle molecular weight using a Malvern Zetasizer Nano equipped with a 5 mW He-Ne laser operating at 633 nm (Worcestershire, UK) for both techniques. DLS measurements were performed in 1X DPBS at 200 μg/mL with mean diameters reported as the number average ± peak half-width. Prior to SLS measurements, the micelle solutions were dialyzed against 1X DPBS using a Slide-A-Lyzer® MINI Dialysis Device with a 3.5K MWCO (Thermo Scientific, Rockford, IL) to remove methanol. Serial dilutions of these solutions (0.5 – 0.1 mg/mL) were manually injected into a refractometer (Wyatt Optilab-rEX, Dernbach, Germany) to determine a dn/dc value for each diblock copolymer micelle. Micelle molecular weight (M_w) and second virial coefficient (A_2) were

determined from a Debye plot generated by SLS measurements at a constant scattering angle of 173° using the Rayleigh equation: $KC/R_\theta = (1/M_w + 2A_2C)$, in which C was varied from 1 – 0.125 mg/mL, K is an optical constant, and R_θ is the Rayleigh ratio of the scattered to incident light intensity. The parameter K can be represented by the following relationship: $K = 4\pi^2 n_0^2 (dn/dc)^2/N_A\lambda^4$, in which n_0 is the refractive index of the solvent, N_A is Avogadro's number, and λ is the wavelength of the light source. From the M_w, an aggregation number (N_{agg}) was determined using the molecular weight of the unimeric species ($M_{w,unimer}$) measured by GPC: $N_{agg} = M_{w,micelle}/M_{w,unimer}$. Each data point represents triplicate measurements.

5.2.7. Hemolysis assay

The potential for the diblock copolymers to disrupt endosomal membranes was assessed by a hemolysis assay. The protocol followed here has been described previously [22]. Briefly, polymer was incubated in the presence of erythrocytes at 20 µg/mL in 100 mM sodium phosphate buffers (supplemented with 150 mM NaCl) of varying pH (7.4, 7.0, 6.6, 6.2, and 5.8) intended to mimic the acidifying pH gradient that endocytosed material is exposed to. The extent of cell lysis (i.e. hemolytic activity) was determined by detecting the amount of released hemoglobin via absorbance measurements at 492 nm.

5.2.8. Critical micelle concentration (CMC) determination via ANS fluorescence

The CMC value for each diblock copolymer was determined using 1-Anilino-8-Naphthalene Sulfonate (ANS) as a hydrophobically-sensitive, fluorescence probe. Serial dilutions of each micelle solution were prepared from 200 – 1 µg/mL and to these was added ANS from a methanol stock to obtain a final ANS concentration of 3 µM. Following a 1 hr incubation at room temperature in the dark, the fluorescence of each solution was measured at an excitation and emission wavelength of 390 and 550 nm, respectively. The CMC value was assigned as the curve inflection point which was determined by the intercept between a linear regression at the lower concentrations and a logarithmic regression at the higher concentrations.

5.2.9. Transmission electron microscopy (TEM)

The ManEMA diblock copolymer was applied to a carbon coated copper grid for 30 min from a 1X DPBS stock at 0.5 mg/mL. The polymer-treated grid was fixed in Karnovsky's solution

and washed in cacodylate buffer once and then water eight times. The grid was then negatively stained for 15 min with a 6% uranyl acetate solution and then allowed to dry until analysis. Imaging was performed on a JEOL 1230 microscope.

5.2.10. Analytical ultracentrifugation (AUC)

All experiments were performed on a Proteome XLI instrument equipped with fluorescence optics (Beckman Coulter, Palo Alto, CA). Two sector charcoal Epon sedimentation velocity (SV) cells were loaded with 440 µL 1X DPBS spiked with diblock copolymer solutions. No reference sector was required as fluorescence measurements were taken. An 8-hole titanium rotor was loaded with 3 cells, a counterweight, a fluorescence calibration cell, and run at 30,000 rpm and 20 °C at 260 scans for each sector. For all measurements, diblock copolymer concentrations ranged from 0.25 – 1.0 mg/mL. For samples in serum, clarified mouse serum was spiked into the buffer samples. For samples in rHSA, protein concentration was varied from 0 – 1.0 mg/mL. Partial specific volume (v-bar) measurements were made for each diblock copolymer micelle using a DMA5000 densitometer/viscometer (Anton Paar, Ashland, VA). Measurements in only buffer were analyzed using SEDFIT software [13] while all measurements were analyzed by globally fitting the data using SEDANAL software [15].

5.3. RESULTS AND DISCUSSION

5.3.1. Diblock copolymer synthesis and characterization

The purpose of these studies was to evaluate the effect of corona composition on the assembly and stability of core-shell micelles. To this end, a series of diblock copolymers were synthesized via reversible addition-fragmentation chain transfer (RAFT) polymerization in which three different homopolymer segments (DMA, DMAEMA, and AcManEMA) were separately blocked onto an endosomolytic copolymer macroCTA (**Scheme 5.1** and **Table 5.1**). The macroCTA (EB40r) is similar to the copolymer composition described in **Chapter 2** with a 40% BMA molar feed except an additional monomer, rhodamine B methacrylate (RhodMA), was incorporated into this synthesis. This monomer resulted in relatively uniform fluorescent labeling of the resultant diblock materials (**Table 5.2**) which allowed for fluorescent detection by analytical ultracentrifugation (AUC). Each monomer successfully blocked off the EB40r macroCTA producing diblock copolymers with low polydispersities (PDI ≤ 1.16) confirming that the polymerizations were controlled (**Figure 5.1**). Target DP

values for each homopolymerization were selected to achieve similar block sizes which was validated by GPC. To obtain a mannosylated micelle, protective acetyl groups had to first be removed from the p(EB40r-*b*-AcManEMA) diblock copolymer by saponification. Complete removal of these pendent groups was confirmed by ^{1}H-NMR (**Figure 5.2**).
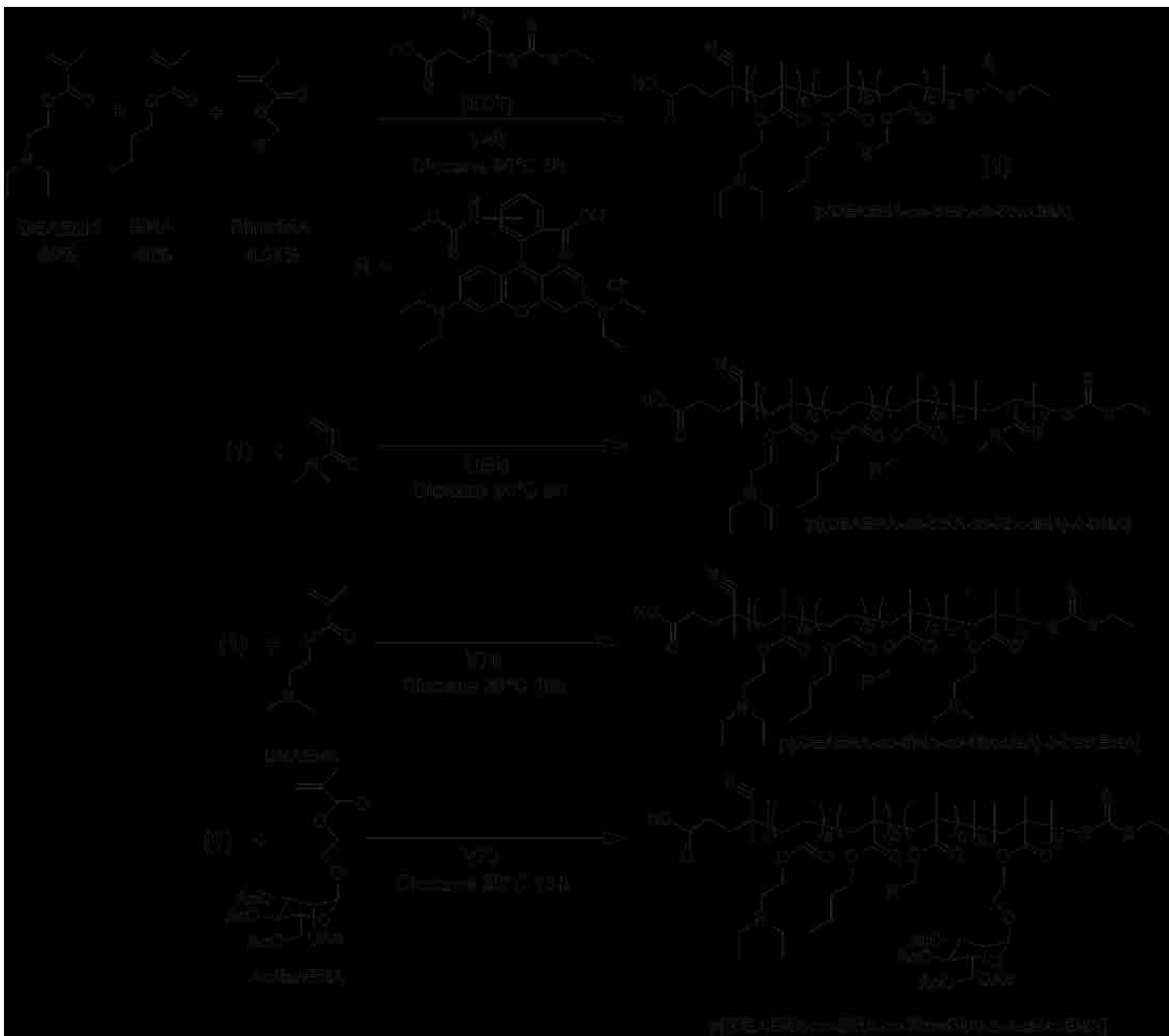
Scheme 5.1. RAFT-mediated polymerization of three diblock copolymers from a shared macroCTA. The following are the abbreviated monomer names: diethylaminoethyl methacrylate (DEAEMA), butyl methacrylate (BMA), rhodamine B methacrylate (RhodMA), dimethyl acrylamide (DMA), dimethylaminoethyl methacrylate (DMAEMA), and acetylated mannose ethyl methacrylate (AcManEMA).

Table 5.1.
Molecular weights[a], polydispersities[a], and monomer compositions[b] for copolymer designs.

Polymer	M_n EB40 Block (g/mol)	M_n 2nd Block (g/mol)	Experimental DP 2nd block	Total M_n (g/mol)	PDI (M_w/M_n)
p(EB40r) macroCTA[b]	14700	---	---	14700	1.09
p(EB40r-*b*-DMA)	14700	13200	133	27900	1.06
p(EB40r-*b*-DMAEMA)	14700	15800	84	30500	1.05
p(EB40r-*b*-AcManEMA)	14700	25200	55	39900[c]	1.16

[a] As determined by GPC
[b] 39% BMA as determined by ^{1}H-NMR (CD$_3$OD) spectroscopy (Bruker AV 500); total DP of block is approximately 87 (32 BMA and 55 DEAEMA)
[c] Following saponification, the diblock copolymer molecular weight was assumed to be 30700 g/mol due to removal of acetyl groups
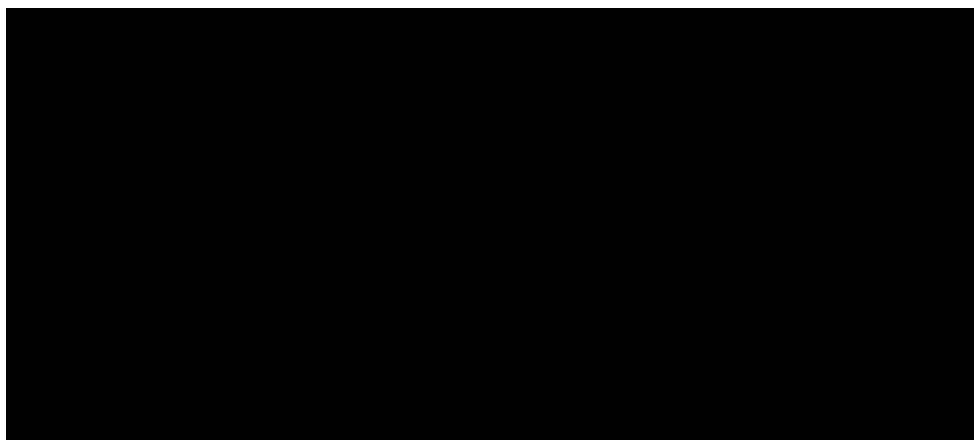
Figure 5.1. GPC traces of three diblock copolymers and macroCTA in DMF.
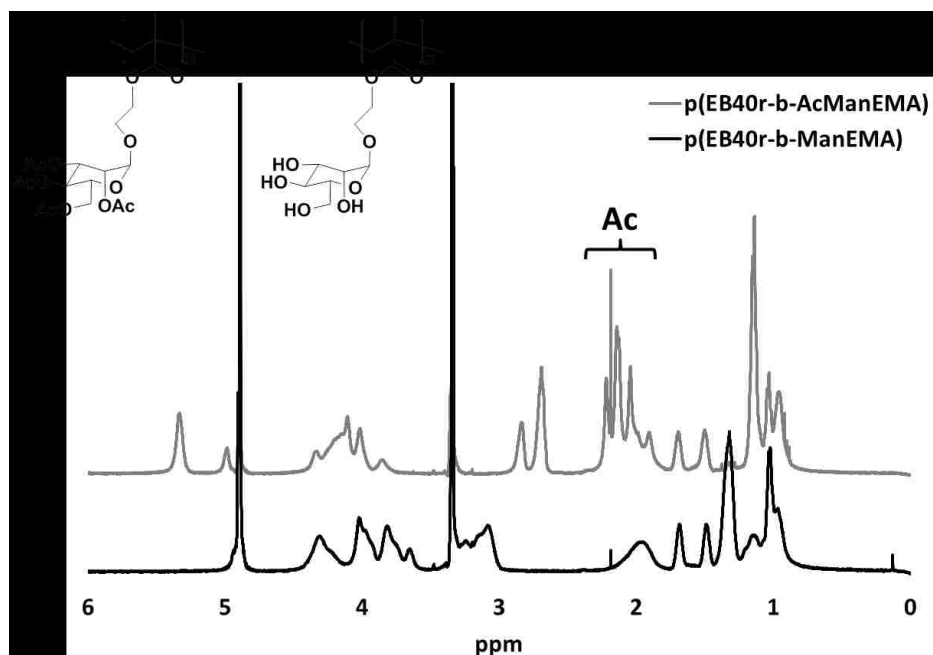
Figure 5.2. ^{1}H-NMR of mannosylated diblock copolymer in CD$_3$OD before and after saponification. Resonances associated with the acetyl groups are in the range of δ = ~2.2-1.8.

5.3.2. Characterization of diblock copolymer micelles in buffer

All diblock copolymers were shown to assemble into particles at physiological pH: 21 ± 2, 32 ± 4, 16 ± 2 nm mean diameters for DMA, DMAEMA, ManEMA, respectively (**Table 5.2**). A transmission electron microscope (TEM) image was taken of the ManEMA micelle which confirmed a spherical morphology, consistent with the architecture expected for block copolymers with these block sizes (**Figure 5.3**) [23]. While each of the three micelles displays unique corona chemistries, the composition of the core was fixed. To study if these different coronas affected the pH-responsive activity of the copolymer segment, a hemolysis assay was performed (**Figure 5.4**). For each micelle, there was minimal hemolytic activity at pH values of 7.4 and 7.0 while significant red blood cell lysis was observed for values 6.6 and below. This critical transition point has been confirmed for copolymer compositions incorporating 40% BMA (see **Chapter 2**) and is related to micelle destabilization into membrane-interactive unimers at this pH value. This study confirms that corona composition does not have a significant effect on the pH-responsive activity of the core segment.

98

Table 5.2.
Physical properties of diblock copolymer micelles in 1X DPBS as determined by dynamic light scattering[a], refractometry[b], static light scattering[c], ANS fluorescence[d], and UV/Vis spectroscopy[e].

Polymer	Diameter[a] (nm)	dn/dc[b]	MW[c] (kDa)	Aggregation number[c]	A2[c] (mL·mol/g^2)/10^4	CMC[d] (μg/mL)	Mol% Rhodamine[e]
DMA	21 ± 2	0.122	1120 ± 20	40	1.34	13	0.39
DMAEMA	32 ± 4	0.157	2140 ± 30	70	2.20	14	0.38
ManEMA	16 ± 2	0.169	660 ± 20	21	3.09	13	0.46
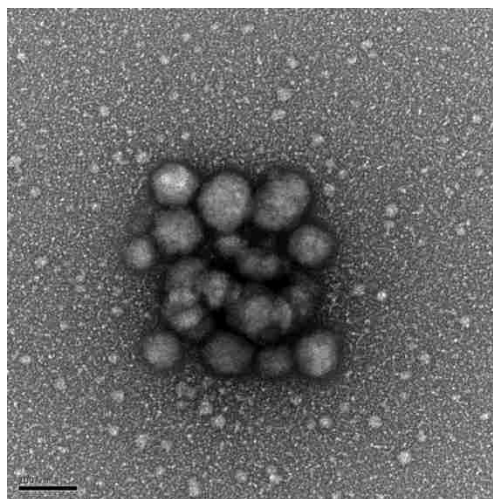
Figure 5.3. Transmission electron microscopy (TEM) image of ManEMA diblock copolymer immobilized on a carbon coated copper grid. Scale bar represents 100 nm.
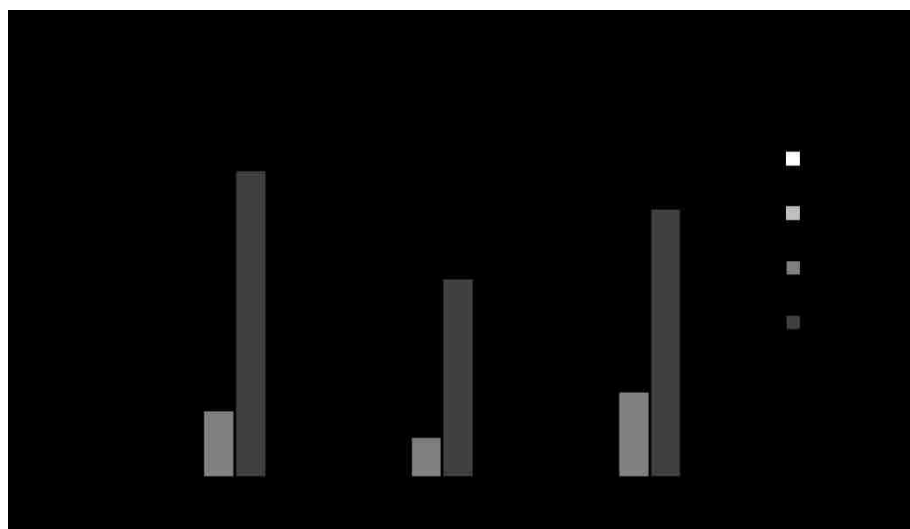
Figure 5.4. Hemolytic activity of diblock copolymers at a concentration of 20 μg/mL. Hemolytic activity is normalized relative to a positive control, 1% v/v Triton X-100, and the data represent a single experiment conducted in triplicate ± standard deviation.

Next, micelle assembly and stability in buffer were assessed by determining the critical micelle concentration (CMC) and aggregation number (N_{agg}) for each of the three diblock copolymers via two independent measurements. The concentration at which the unimeric conformation of a polymeric species saturates both the bulk solvent and the solvent-air interface leading to the spontaneous assembly of micellar particles is known as the CMC [24]. This parameter is important to understanding the stability of polymeric micelles towards dilution effects since below the CMC, micelles will dissemble into their constituent unimeric components. The CMC was determined using a fluorescent polarity-sensitive probe, 1-anilino-8-naphthalene sulfonate (ANS), that exhibits a blue shift in its emission maximum upon incorporation into hydrophobic domains, e.g. micelle core [25], [26]. CMC values of 13, 14, and 13 µg/mL were determined for DMA, DMAEMA, and ManEMA micelles, respectively, confirming that corona composition does not affect micelle stability towards dilution (**Figure 5.5** and **Table 5.2**). These CMCs are slightly higher but comparable to related methacrylate-based block copolymer micelles. Convertine et al. reported on a pH-responsive diblock copolymer micelle incorporating BMA into the core segment and obtained a CMC value of 2 µg/mL using pyrene as a probe [27]. Li et al. described diblock copolymer micelles with BMA homopolymer cores that had 0.5 – 6 µg/mL CMCs [28]. PEG-stabilized BMA copolymer micelles were also shown to exhibit sub-10 µg/mL CMC values [29]. The presence of DEAEMA residues within the core of the micelles described in this chapter may account for the increased CMC when compared to BMA homopolymer-based micelles.
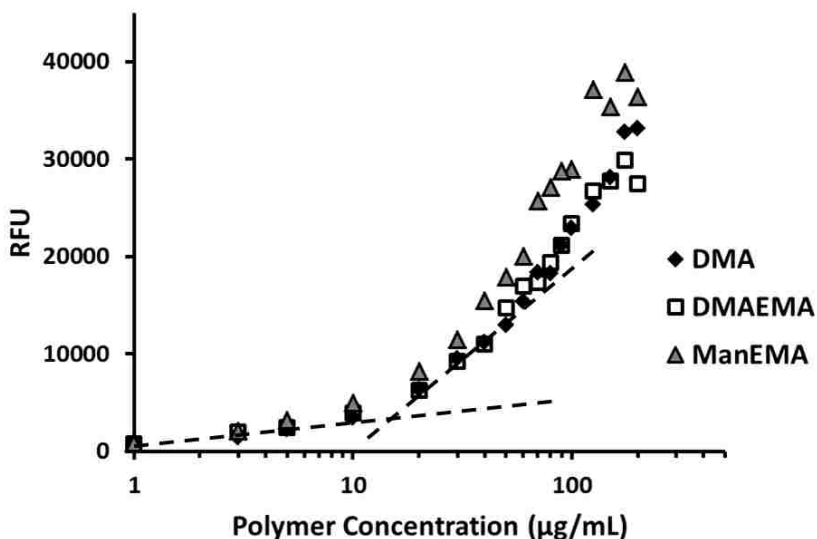
Figure 5.5. Determination of critical micelle concentration (CMC) of diblock copolymer micelles in 1X DPBS using 8-anilino-1-napthalenesulfonic acid (ANS) as a hydrophobic-sensitive fluorescent probe. CMC values were determined from the inflection point of each curve, as illustrated for DMA.

Micelle aggregation numbers (N_{agg}) were determined by measuring light scattering intensity across a range of copolymer concentrations via static light scattering (SLS) (**Figure 5.6**). N_{agg} values were calculated to be 40, 70, and 21 for the DMA, DMAEMA, and ManEMA micelles, respectively. Researchers have demonstrated a strong dependence of N_{agg} on the length of hydrophilic corona segments for Pluronics, a thoroughly-studied triblock copolymer composed of a poly(ethylene oxide) (PEO) corona and poly(propylene oxide) (PPO) core [30], [31]. An increase in the PEO length has been shown to lead to a decrease in N_{agg} which is attributed to steric hindrance of the PEO head groups preventing dense chain packing in the corona. The monomers investigated here vary in not only chemical functionality but also size (MW_{DMA} = 99.1 g/mol, MW_{DMAEMA} = 157.2 g/mol, MW_{ManEMA} = 292.1 g/mol). The bulky, pendent saccharide groups of the ManEMA micelle may limit corona chain packing due to steric hindrance, leading to a lower N_{agg}. The values for N_{agg} also scale with mean diameter suggesting that particle size may dominate this trend. The DMAEMA segment is expected to adopt an extended chain conformation in physiological conditions as a result of charge group repulsion, thereby creating a larger corona that increases particle size [32]. The N_{agg} values reported for these micelles are consistent with those found for related methacrylate-based block copolymers: 30-40 for poly[(*N*-acryloylmorpholine)-*b*-BMA] [28] and 34 for poly[DMAEMA-*b*-(butyl acrylate)] [33].

101

The second virial coefficient, A2, was also determined from the SLS experiments and provides a measure of micelle-micelle interactions [34]. The ManEMA micelle was found to have the highest A2 value (3.09· 10^{-4} mL·mol/g^2) compared to DMA (1.34 · 10^{-4}) and DMAEMA (2.20 · 10^{-4}). A possible explanation for this finding is the hydroxyl groups of the pendent saccharides promote hydrogen bonding between adjacent chains [35], [36]. These A2 values are consistent with similar polymeric materials: 1 – 3 · 10^{-4} mL·mol/g^2 for diblock copolymer micelles consisting of morpholine coronas and BMA cores [28] while Pluronic compositions exhibited slightly smaller A2 values of 2 – 5 · 10^{-5} mL·mol/g^2 [31].
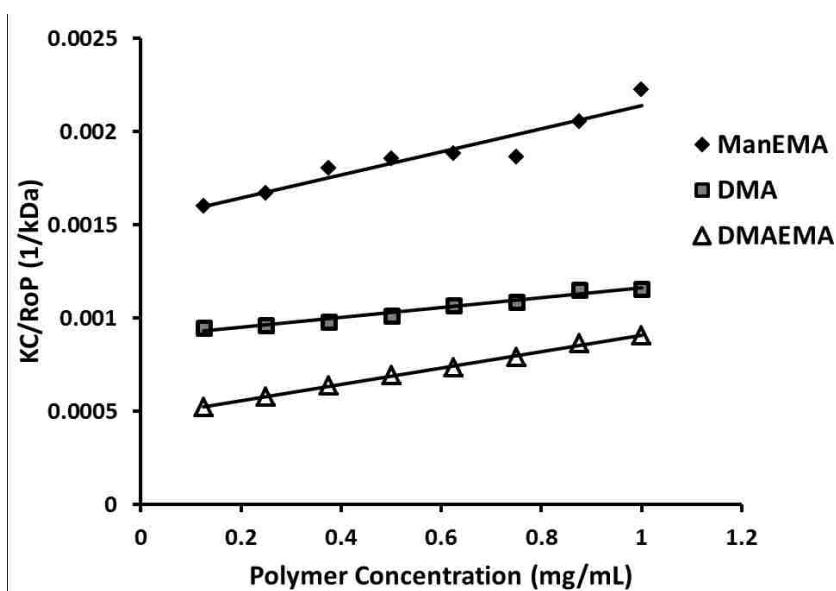
Figure 5.6. Debye plot of diblock copolymers in 1X DPBS.

5.3.3. Analytical ultracentrifugation (AUC) analysis of diblock copolymer micelles

Each diblock copolymer micelle was studied in buffer and in the presence of mouse serum and recombinant human serum albumin (rHSA) by AUC sedimentation velocity experiments using fluorescence detection. This approach monitors the sedimentation of species as a function of time and radial position within the instrument, allowing for the determination of absolute molecular weight by solving the Lamm and Svedberg equations [13]. Size distribution profiles for each micelle in buffer were determined using the program SEDFIT (NIH, Bethesda, MD) (**Figure 5.7**). Only the DMA micelle behaved as a single, discrete component while both DMAEMA and ManEMA micelles exhibited peak asymmetry for the dominant species with larger, although less prevalent, species also present. For all

materials, a low molecular weight fraction was found close to the meniscus that did not migrate throughout the duration of the experiment. This finding may be attributed to unincorporated dye that was not removed during dialysis.
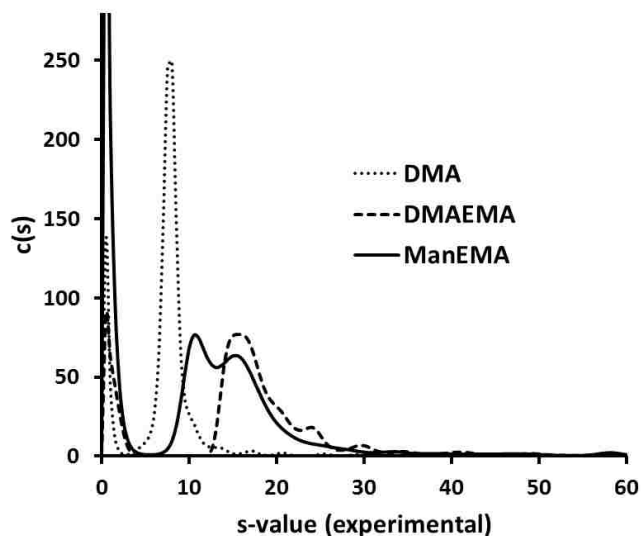
Figure 5.7. c(S) distribution analysis of the boundary data performed by SEDFIT for the three diblock copolymer micelles in buffer at approximately 1 mg/mL.

Using v-bar values calculated from a related polymer micelle, absolute molecular weights of the dominant species from the c(s) distributions were determined for each diblock copolymer (**Table 5.3**). A similar trend in aggregation number is observed when compared to the SLS data: N_{agg}(DMAEMA) > N_{agg}(DMA) > N_{agg}(ManEMA). Following this analysis, densitometry measurements were made to yield the following v-bar values: 0.986, 0.832, and 0.730 mL/g for the DMA, DMAEMA, and ManEMA micelles, respectively. Discrepancies in the absolute molecular weight values between SLS and AUC may be less apparent when using the correct v-bar values during SEDFIT analysis; these experiments are currently ongoing.

Table 5.3.
Summary of the main components determined by c(s) distribution analysis using a v-bar value (mL/g) of 0.866 for all diblock copolymers.

Polymer	s20w	MW (kDa)	N_{agg}
DMA	8.4 ± 0.2	790 ± 40	28 ± 2
DMAEMA	18.2 ± 0.2	1950 ± 70	63 ± 3
ManEMA[*]	11.4 ± 0.4	380 ± 10	12 ± 1

[*]Secondary component exhibits a s20w of 18.0 ± 0.7, MW of 750 ± 30 kDa, and N_{agg} of 24 ± 1.

While SEDFIT is able to fit AUC data of the micelles in buffer and generate molecular weight distributions, the program cannot account for the non-ideality that exists for the sedimentation of complex media containing serum components. These non-idealities affect determination of frictional ratios and diffusion constants which arise primarily due to charge effects in crowded media, a phenomenon known as the Johnston-Ogsten effect. To account for this behavior, algorithms within the program SEDANAL [15] were employed to measure the sedimentation of micelles in buffer alone and buffer spiked with rHSA and mouse serum.

SEDANAL analysis of ManEMA micelles in buffer yielded two components with similar aggregation numbers (N_{agg} of 13 and 14) (**Figure 5.8**). Neither of these species exhibited a change in N_{agg} upon increasing concentrations of rHSA, suggesting that the polymer does not significantly interact with this protein. Conversely, the N_{agg} of the DMA micelle increased from 18 in buffer only to 26 with 1 mg/mL rHSA present. rHSA is an anionic protein at physiological pH (pI = 5.0 [37]) so it is capable of electrostatically interacting with cationic materials. As the pendent moieties of DMA and ManEMA are both neutral they are unable to participate in this type of interaction. However, tertiary amines from DEAEMA residues in the core may be able to bind electrostatically with anionic amino acid residues if they are not properly shielded by the corona. These data suggest that ManEMA better stabilizes the micelle towards anionic protein interactions and that this activity may be due to enhanced protection of cationic components present in the core. The DMAEMA micelle was not investigated in this study due to its predominantly cationic character at physiological pH (pK_a of DMAEMA residues is approximately 7.4 [38]).
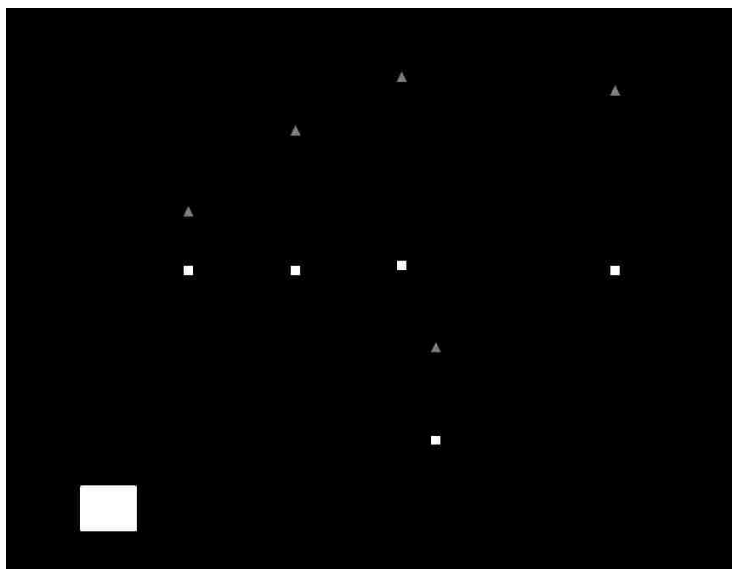
Figure 5.8. Aggregation number (N_{agg}) as a function of rHSA concentration for both DMA and ManEMA diblock copolymer micelles at a polymer concentration of 1 mg/mL. Both the primary and secondary component from the ManEMA micelle sedimentation profile are reported.

Next, the stability of these micelles in complete mouse serum was investigated. In buffer alone, each diblock copolymer sedimented at a different rate (DMAEMA > ManEMA > DMA) with the DMAEMA micelles exhibiting the most complex sedimentation profile with multiple boundaries observed (**Figure 5.9**). In the presence of mouse serum, both the DMA and DMAEMA micelles display non-ideal concentration fluctuations at the top of the boundary in the plateau region, suggesting that there is significant interaction of these materials with serum components. However, perturbations in the plateau region are absent in the ManEMA micelle sedimentation profile, providing further evidence that the ManEMA corona is better able to stabilize these micelles towards non-specific protein binding. Preliminary SEDANAL analysis was performed to generate absolute molecular weight values of the dominant species in these profiles (**Table 5.4**). From these data, there are significant changes in aggregation number for the DMA and DMAEMA micelles between buffer and serum while these values remain relatively unchanged for the ManEMA micelle between these two media (6 ± 2 in buffer only and 6 ± 3 in serum). For a more accurate determination of these values, SEDANAL analysis needs to be performed using the correct v-bar values for each diblock copolymer.
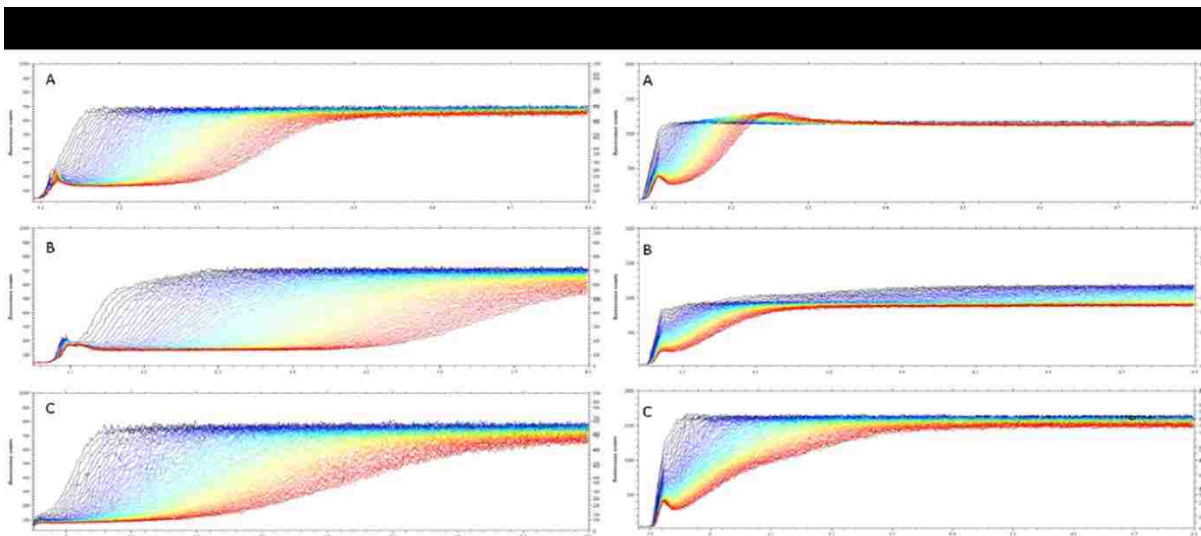
Figure 5.9. Sedimentation profiles of DMA (**A**), DMAEMA (**B**), and ManEMA (**C**) diblock copolymer micelles in buffer or mouse serum at approximately 1 mg/mL polymer.

Table 5.4.
Summary of SEDANAL fitting results for the main components of the three diblock copolymers in buffer and serum.

Polymer	v-bar (mL/g)	s20w	MW (kDa)	N_{agg}
DMA (buffer)	0.986	7.9 ± 0.1	440 ± 20	16 ± 1
DMA (serum)	0.986	3.7	310	11
DMAEMA (buffer)	0.866*	16.4 ± 0.6	350 ± 40	11 ± 1
DMAEMA (serum)	0.866*	4.1 ± 1.5	600 ± 390	20 ± 13
ManEMA (buffer)	0.866*	14.3 ± 0.1	190 ± 60	6 ± 2
ManEMA (serum)	0.866*	5.6 ± 2.2	170 ± 90	6 ± 3

*v-bar value calculated previously for a related diblock copolymer material.

5.4. CONCLUSIONS

A series of diblock copolymers were successfully prepared via reversible addition-fragmentation chain transfer (RAFT) polymerization and shown to assemble into micellar nanoparticles. These materials consist of an endosomolytic copolymer core and homopolymer coronas with various pendent chemical functionalities: neutral (N,N-dimethylacrylamide, DMA), cationic (dimethylaminoethyl methacrylate, DMAEMA), and saccharide (mannose ethyl methacrylate, ManEMA). Dynamic light scattering (DLS) measurements of the micelles in buffer confirmed a trend in mean particle size (DMAEMA > DMA > ManEMA) which was consistent with the aggregation numbers determined by both static light scattering (SLS) and analytical ultracentrifugation (AUC) experiments. AUC studies additionally demonstrated that the ManEMA micelles did not significantly interact

106

with either recombinant human serum albumin (rHSA) or mouse serum, suggesting that carbohydrate-based coronas may be optimal for systemically administered micelle-based therapeutics.

5.5. REFERENCES

[1]   K. Kataoka, A. Harada, and Y. Nagasaki, "Block copolymer micelles for drug delivery: Design, characterization and biological significance.," *Advanced drug delivery reviews*, Sep. 2012.

[2]   R. Savić, A. Eisenberg, and D. Maysinger, "Block copolymer micelles as delivery vehicles of hydrophobic drugs: micelle-cell interactions.," *Journal of drug targeting*, vol. 14, no. 6, pp. 343–55, Jul. 2006.

[3]   D. Velluto, S. N. Thomas, E. Simeoni, M. a Swartz, and J. a Hubbell, "PEG-b-PPS-b-PEI micelles and PEG-b-PPS/PEG-b-PPS-b-PEI mixed micelles as non-viral vectors for plasmid DNA: tumor immunotoxicity in B16F10 melanoma.," *Biomaterials*, vol. 32, no. 36, pp. 9839–47, Dec. 2011.

[4]   C. Giacomelli, V. Schmidt, K. Aissou, and R. Borsali, "Block Copolymer Systems: From Single Chain to Self-Assembled Nanostructures.," *Langmuir : the ACS journal of surfaces and colloids*, vol. 26, no. 7, pp. 15734–15744, Apr. 2010.

[5]   U. Kedar, P. Phutane, S. Shidhaye, and V. Kadam, "Advances in polymeric micelles for drug delivery and tumor targeting.," *Nanomedicine : nanotechnology, biology, and medicine*, vol. 6, no. 6, pp. 714–729, Jun. 2010.

[6]   H. Haljam and E. H. Fredbn, "intentionally altering the capillary permeability an attempt was also made to determine if the permeability is affected by the sampling procedure due to liberation of vaso-," vol. 71, pp. 163–171, 1970.

[7]   J. Lu, S. C. Owen, and M. S. Shoichet, "Stability of Self-Assembled Polymeric Micelles in Serum.," *Macromolecules*, vol. 44, no. 15, pp. 6002–6008, Aug. 2011.

[8]   R. J. Green, M. C. Davies, C. J. Roberts, and S. J. Tendler, "A surface plasmon resonance study of albumin adsorption to PEO-PPO-PEO triblock copolymers.," *Journal of biomedical materials research*, vol. 42, no. 2, pp. 165–71, Nov. 1998.

[9]   L. Yin, M. C. Dalsin, A. Sizovs, T. M. Reineke, and M. a. Hillmyer, "Glucose-Functionalized, Serum-Stable Polymeric Micelles from the Combination of Anionic and RAFT Polymerizations," *Macromolecules*, vol. 45, no. 10, pp. 4322–4332, May 2012.

[10]   A. Valstar, M. Almgren, W. Brown, and M. Vasilescu, "The interaction of bovine serum albumin with surfactants studied by light scattering," *Langmuir*, no. 11, pp. 922–927, 2000.

[11]   J. Liu, F. Zeng, and C. Allen, "Influence of serum protein on polycarbonate-based copolymer micelles as a delivery system for a hydrophobic anti-cancer agent.," *Journal of controlled release*, vol. 103, no. 2, pp. 481–97, Mar. 2005.

[12]   M. E. Norman, P. Williams, and L. Illum, "Human serum albumill as a probe for surface conditioning (opsonization) of block copolymer-coated microspheres aces," *Biomaterials*, vol. 13, no. 12, 1992.

[13]   P. Schuck, "Size-distribution analysis of macromolecules by sedimentation velocity ultracentrifugation and lamm equation modeling.," *Biophysical journal*, vol. 78, no. 3, pp. 1606–19, Mar. 2000.

[14]   J. Lebowitz, M. S. Lewis, and P. Schuck, "Modern analytical ultracentrifugation in protein science : A tutorial review," *Protein Science*, pp. 2067–2079, 2002.

[15]   W. F. Stafford and P. J. Sherwood, "Analysis of heterologous interacting systems by sedimentation velocity: curve fitting algorithms for estimation of sedimentation coefficients, equilibrium and kinetic constants.," *Biophysical chemistry*, vol. 108, no. 1–3, pp. 231–43, Mar. 2004.

[16] S. E. Harding, A. S. Abdelhameed, and G. a Morris, "Molecular weight distribution evaluation of polysaccharides and glycoconjugates using analytical ultracentrifugation.," *Macromolecular bioscience*, vol. 10, no. 7, pp. 714–20, Jul. 2010.

[17] C. Wandrey, U. Hasegawa, A. J. van der Vlies, C. O'Neil, N. Angelova, and J. a Hubbell, "Analytical ultracentrifugation to support the development of biomaterials and biomedical devices.," *Methods (San Diego, Calif.)*, vol. 54, no. 1, pp. 92–100, May 2011.

[18] G. Moad, Y. K. Chong, A. Postma, E. Rizzardo, and S. H. Thang, "Advances in RAFT polymerization: the synthesis of polymers with defined end-groups," *Polymer*, vol. 46, no. 19, pp. 8458–8468, Sep. 2005.

[19] A. J. Convertine, D. S. W. Benoit, C. L. Duvall, A. S. Hoffman, and P. S. Stayton, "Development of a novel endosomolytic diblock copolymer for siRNA delivery.," *Journal of Controlled Release*, vol. 133, no. 3, pp. 221–9, Feb. 2009.

[20] L. E. Iters, T. Ren, and D. Liu, "Synthesis of targetable cationic amphiphiles," *Tetrahedron Letters*, vol. 40, pp. 7621–7625, 1999.

[21] S. Kitazawa, M. Okumura, K. Kinomura, and T. Sakakibara, "Syntheses and properties of novel vinyl monomers bearing a glycoside residue," *Chemistry Letters*, vol. 19, no. 9, pp. 1733–1736, 1990.

[22] V. Bulmus, "A new pH-responsive and glutathione-reactive, endosomal membrane-disruptive polymeric carrier for intracellular delivery of biomolecular drugs," *Journal of Controlled Release*, vol. 93, no. 2, pp. 105–120, Dec. 2003.

[23] P. L. Soo, L. Luo, D. Maysinger, and A. Eisenberg, "Micelles : Implications for Drug Delivery," *Langmuir*, no. 21, pp. 9996–10004, 2002.

[24] V. P. Torchilin, "Structure and design of polymeric surfactant-based drug delivery systems.," *Journal of controlled release : official journal of the Controlled Release Society*, vol. 73, no. 2–3, pp. 137–72, Jun. 2001.

[25] J. A. N. Slavik, "ANILINONAPHTHALENE SULFONATE AS A PROBE OF MEMBRANE COMPOSITION AND FUNCTION," *Biochimica et Biophysica Acta*, vol. 694, pp. 1–25, 1982.

[26] K. Dan and S. Ghosh, "pH-Responsive Aggregation of Amphiphilic Glyco-Homopolymer.," *Macromolecular rapid communications*, vol. 1, pp. 127–132, Nov. 2011.

[27] A. J. Convertine, C. Diab, M. Prieve, A. Paschal, A. S. Hoffman, P. H. Johnson, P. S. Stayton, W. H. Street, and S. Washington, "pH-Responsive Polymeric Micelle Carriers for siRNA Drugs," *Biomacromolecules*, pp. 2904–2911, 2010.

[28] W. Li, M. Nakayama, J. Akimoto, and T. Okano, "Effect of block compositions of amphiphilic block copolymers on the physicochemical properties of polymeric micelles," *Polymer*, vol. 52, no. 17, pp. 3783–3790, 2011.

[29] P. Satturwar, M. N. Eddine, F. Ravenelle, and J.-C. Leroux, "pH-responsive polymeric micelles of poly(ethylene glycol)-b-poly(alkyl(meth)acrylate-co-methacrylic acid): influence of the copolymer composition on self-assembling properties and release of candesartan cilexetil.," *European journal of pharmaceutics and biopharmaceutics : official journal of Arbeitsgemeinschaft für Pharmazeutische Verfahrenstechnik e.V*, vol. 65, no. 3, pp. 379–87, Mar. 2007.

[30] F. Gadelle, W. J. Koros, and R. S. Schechter, "Solubilization of Aromatic Solutes in Block Copolymers," *Macromolecules*, vol. 28, no. 14, pp. 4883–4892, Jul. 1995.

[31] S. Nolan, R. Phillips, P. Cotts, and S. Dungan, "Light Scattering Study on the Effect of Polymer Composition on the Structural Properties of PEO-PPO-PEO Micelles," *Journal of colloid and interface science*, vol. 191, no. 2, pp. 291–302, Jul. 1997.

[32] V. Bulmus, "Biomembrane-Active Molecular Switches as Tools for Intracellular Drug Delivery," *Australian Journal of Chemistry*, no. January 2004, pp. 411–422, 2005.

[33] A. M. Alhoranta, J. K. Lehtinen, A. O. Urtti, S. J. Butcher, V. O. Aseyev, and H. J. Tenhu, "Cationic amphiphilic star and linear block copolymers : synthesis , self-assembly and in vitro gene transfection," *Polymer*, 2011.

[34]   D. J. Winzor, M. Deszczynski, S. E. Harding, and P. R. Wills, "Nonequivalence of second virial coefficients from sedimentation equilibrium and static light scattering studies of protein solutions.," *Biophysical chemistry*, vol. 128, no. 1, pp. 46–55, Jun. 2007.

[35]   L. You and H. Schlaad, "An easy way to sugar-containing polymer vesicles or glycosomes.," *Journal of the American Chemical Society*, vol. 128, no. 41, pp. 13336–7, Oct. 2006.

[36]   A. Gress, A. Heilig, B. M. Smarsly, M. Heydenreich, and H. Schlaad, "Hydrogen-Bonded Polymer Nanotubes in Water," *Macromolecules*, vol. 42, no. 12, pp. 4244–4248, Jun. 2009.

[37]   C. C. Gyenge, O. Tenstad, and H. Wiig, "In vivo determination of steric and electrostatic exclusion of albumin in rat skin and skeletal muscle.," *The Journal of physiology*, vol. 552, no. Pt 3, pp. 907–16, Nov. 2003.

[38]   P. van de Wetering, N. J. Zuidam, M. J. van Steenbergen, O. a. G. J. van der Houwen, W. J. M. Underberg, and W. E. Hennink, "A Mechanistic Study of the Hydrolytic Stability of Poly(2-(dimethylamino)ethyl methacrylate)," *Macromolecules*, vol. 31, no. 23, pp. 8063–8068, Nov. 1998.

Chapter 6 – In Vivo DNA Delivery Mediated by Glycopolymer Micelles

Matthew J. Manganiello, Connie Cheng, Eun-Ho Song, John T. Wilson, Anthony J. Convertine, James D. Bryers, Daniel M. Ratner, Patrick S. Stayton

Abstract

Polymeric micelles were prepared via reversible-addition fragmentation chain transfer (RAFT) polymerization consisting of two discrete copolymer segments with unique functions: an endosomolytic, core-forming block of diethylaminoethyl methacrylate (DEAEMA) and butyl methacrylate (BMA) and a hydrophilic, corona-forming block of dimethylaminoethyl methacrylate (DMAEMA) and mannose ethyl methacrylate (ManEMA) with varying molar feed ratios (0 to 100% ManEMA). Using dynamic light scattering (DLS) and hemolysis assays, these materials were shown to adopt a membrane-inert, micellar morphology at physiological pH that destabilized into membrane-disruptive unimers at endosomal pH values (≤ 6.6). Micelles incorporating ManEMA into their corona were able to engage the C-type lectin, Concanavalin A, as demonstrated by an agglutination assay. All micelles condensed plasmid DNA (pDNA) into 140 – 200 nm complexes with zeta potentials that decreased upon increasing mannosylation; the 100% ManEMA diblock copolymer yielded near-neutral polyplexes (-1 ± 0.5 mV). The in vitro pDNA transfection activity of these complexes was highly dependent on ManEMA incorporation: greater than 25% ManEMA produced inactive polyplexes while the 0% ManEMA (100% DMAEMA) diblock copolymer performed better than the liposomal commercial reagent. However, subcutaneous administration of luciferase-encoding pDNA polyplexes demonstrated that the 0% ManEMA polyplex was unable to mediate expression while the 100% ManEMA polyplex produced detectable luminescence at the site of injection. In vivo monitoring of fluorescently-labeled pDNA showed that the pDNA from the 100% ManEMA polyplex distributes out of the subcutaneous tissue after 24 hours while the 0% ManEMA polyplex sequesters pDNA in a punctate depot for up to 72 hours. Evaluation of fluorescently-labeled diblock copolymers further suggests depot formation for the 0% ManEMA polyplex. Lymph node trafficking studies revealed that the 100% ManEMA polyplex significantly enhances pDNA uptake by CD11c^{+}/MHCII^{+} dendritic cells (10.8 ± 4.1% cells positive for pDNA) when compared to free pDNA (2.5 ± 10%) while the 0% and 50% ManEMA polyplexes did not mediate uptake above background levels.

6.1. INTRODUCTION

The safe, efficacious delivery of DNA requires the use of carriers to facilitate cellular entry and nuclear localization while protecting the nucleic acid from enzymatic degradation [1]. While polycation-based delivery systems are capable of exhibiting high transfection activities in vitro, their primary mode of cellular internalization, nonspecific adsorptive pinocytosis, limits their utility as in vivo nucleic acid carriers [2]. Electrostatic interactions with extracellular matrix proteins can also lead to deleterious effects following intradermal or subcutaneous administration of polycations [3–5]. Imparting carbohydrate-mediated targeting, termed "glycotargeting", to delivery systems can overcome these shortcomings [6]. Cell-surface lectins are capable of recognizing carbohydrates with high specificity and can internalize adsorbed material through receptor-mediated endocytosis following multivalent engagement of carbohydrate recognition domains (CRDs) [7]. By directly targeting these lectins through the glycosylation of nucleic acid carriers, the uptake of genetic cargo can be enhanced in specific cell populations while minimizing interaction with off-target cells and extracellular matrix components.

Functionalizing polymeric gene delivery systems with mannose has generated much interest due to the ability of the carbohydrate to recognize a range of immunologically relevant C-type lectins, notably the macrophage mannose receptor (MMR) found on the surfaces of macrophages and dendritic cell (DC) subsets [8], [9]. Mannosylation as a tool to enhance cell-specific uptake of synthetic polymers was first demonstrated by direct conjugation of mannose to poly(L-lysine) (PLL) with the resultant material exhibiting preferential uptake by alveolar macrophages [10]. This work was extended by Ferkol et al. who delivered DNA to murine macrophages using a mannosylated PLL carrier [11]. Polyamidoamine-based dendrimers modified with mannose also have been shown to display high DNA transfection activity across multiple cell types [12], [13]. Hashimoto et al. developed mannosylated chitosan carriers which were able to mediate high pDNA expression levels in murine peritoneal macrophages [14]. An important note from this work was the mitigation of nonspecific, polycation-mediated toxicity; this finding is often observed with reports of cationic materials that have been modified with carbohydrates [6], [15], [16]. Mannosylation has also been utilized to functionalize liposomal gene delivery systems which are capable of in vivo DC targeting upon carbohydrate modification [17], [18].

111

DCs are a promising target for gene therapy as they are pivotal mediators of adaptive immune responses, acting as antigen presentation cells (APCs) by priming T cells to elicit antigen-specific effector functions. Delivering antigenic material to these APCs represents a promising strategy to initiate potent immune responses in a variety of vaccine applications [19]. To access these relevant immune cell populations, carriers must be able to overcome barriers in the extracellular space to avoid accumulation in off-target cells and potentially navigate through lymphatic vessels to encounter APCs within the draining lymph nodes [4], [20], [21].

Despite the reported successes of achieving DNA transfection in APCs in vitro with mannose-modified synthetic polymers, there has been limited progress in translating these systems in vivo. One approach to overcome these obstacles is to develop materials that mimic the multivalent, carbohydrate-mediated binding capabilities of pathogenic organisms [22], [23]. Advances in the field of controlled radical polymerizations have allowed the synthesis of structurally well-defined glycopolymers to meet these ends, namely through the application of the reversible addition-fragmentation chain transfer (RAFT) process [24], [25]. These constructs contain pendent carbohydrate functionalities and can be incorporated into a variety of complex polymer architectures, including block copolymers [26], glycopolymer micelles [27], glycopolymer stars [28], multi-functional glyconanoparticles [29], and "clickable" glycopolymers [30]. Herein we report the development of mannosylated diblock copolymer micelles prepared via RAFT. This approach is based upon previous diblock copolymer designs which transition from micelles into membrane-interactive unimers at low pH, thereby facilitating release from endosomes following cellular internalization. We examined the ability of these materials to deliver DNA in vivo as a function of mannose incorporation in the micelle corona.

6.2. MATERIALS AND METHODS

6.2.1. Materials

Chemicals and all materials were supplied by Sigma-Aldrich (St Louis, MO) unless otherwise specified. 2,2′-Azobis(4-methoxy-2.4-dimethyl valeronitrile) (V70) and 1,1'-Azobis(cyclohexane-1-carbonitrile) (V40) were obtained from Wako Chemicals USA, Inc. (Richmond, VA). Spectra/Por 7 standard regenerated cellulose dialysis tubing was obtained from Spectrum Labs (Rancho Dominguez, CA) and Amicon Ultra centrifugal filters were

obtained from EMD Millipore (Billerica, MA). ECT was synthesized as previously described [31], [32]. Dimethylaminoethyl methacrylate (DMAEMA), diethylaminoethyl methacrylate (DEAEMA), butyl methacrylate (BMA) were distilled prior to use. Acetylated mannose ethyl methylacrylate (AcManEMA) was synthesized according to previous methods (see Chapter 3) [33], [34]. gWiz-GFP pDNA was obtained from Aldevron LLC (Fargo, ND) and pCMV-Luc pDNA was obtained from Elim Biopharm (Hayward, CA). Lipofectamine 2000 (LF) was obtained from Invitrogen (Carlsbad, CA). *Label* IT® Tracker™ Intracellular Nucleic Acid Localization Kit, Cy™5 was obtained from Mirus Bio (Madison, WI) and NIR-664-iodoacetamide was obtained from Santa Cruz Biotechnology (Santa Cruz, CA). RAW 264.7 (murine leukaemic monocyte macrophage cell line) (ATCC) cells were maintained in Dulbecco's Modified Eagle Medium (DMEM) High Glucose containing L-glutamine (GIBCO) supplemented with 1% penicillin-streptomycin (GIBCO) and 10% fetal bovine serum (FBS, Invitrogen) at 37 °C and 5% CO_2.

6.2.2. Synthesis of poly(DEAEMA-co-BMA) macro chain transfer agent (EB40 macroCTA)

The RAFT copolymerization of DEAEMA and BMA was conducted in dioxane (50 wt% monomer) at 90 °C under a nitrogen atmosphere for 6 h using ECT and V40 as the chain transfer agent (CTA) and radical initiator, respectively. The initial monomer to CTA molar ratio ($[M]_0:[CTA]_0$) was 100:1, CTA to initiator molar ratio ($[CTA]_0:[I]_0$) was 20:1, and molar feed ratio of DEAEMA:BMA was 3:2 (40 mol% BMA). The resultant EB40 macroCTA was isolated by dialysis against methanol with 1000 MWCO tubing followed by rotary evaporation and drying overnight in vacuo to remove residual solvent.

6.2.3. Diblock copolymerization of DMAEMA and AcManEMA from EB40 macroCTA

DMAEMA and AcManEMA were copolymerized from an EB40 macroCTA in which the initial molar feed of AcManEMA was either 0, 25, 50, 75, or 100%. Each polymerization was conducted in dioxane at 40 wt% monomer for 18 h at 30 °C using V70 as the primary radical source. The initial monomer to CTA molar ratio ($[M]_0:[CTA]_0$) was 65:1 and CTA to initiator molar ratio ($[CTA]_0:[I]_0$) was 20:1. The resultant diblock copolymers were isolated by precipitation into cold hexanes. The precipitated polymers were then redissolved into acetone and precipitated into cold hexanes (x3) and dried overnight in vacuo.

6.2.4. Gel permeation chromatography (GPC)

GPC was used to determine molecular weights and polydispersities (M_w/M_n, PDI) of the macroCTA and diblock copolymers. SEC Tosoh TSK-GEL R-3000 and R-4000 columns (Tosoh Bioscience, Montgomeryville, PA) were connected in series to a Agilent 1200 series (Agilent Technologies, Santa Clara, CA), refractometer Optilab-rEX and triple-angle static light scattering detector miniDAWN TREOS (Wyatt Technology, Dernbach, Germany). HPLC-grade DMF containing 0.1 wt.% LiBr at 60 °C was used as the mobile phase at a flow rate of 1 ml/min. The molecular weights of each polymer were determined using a multi-detector calibration based on dn/dc values calculated separately for copolymer composition assuming 100% mass recovery.

6.2.5 Saponification of diblock copolymers

To display native pendent glycomoieties on the diblock copolymers, protective acetyl groups were removed via base-catalyzed hydrolysis. The diblock copolymers (including the 0% AcManEMA composition) were separately added to a solution of 1 wt% sodium methoxide in anhydrous methanol at a copolymer concentration of 50 mg/mL. After 1 hour incubation at room temperature, the solutions were neutralized with acetic acid to a pH of ~7 and dialyzed against deionized water using 1000 MWCO tubing. The solutions were then lyophilized to obtain the final diblock copolymers. Aqueous stocks of the deprotected diblock copolymers were formulated from the lyophilized material at 2 mg/mL in 1X DPBS, pH 7.4. The copolymers were pre-dissolved at 40 mg/mL in methanol prior to addition into buffer to promote micelle formation. For in vivo studies, copolymer stocks were buffer exchanged into HEPES buffered glucose (HBG; 20 mM HEPES, 5% (w/v) glucose, pH 7.4) via centrifugal filtration with a 3000 MWCO.

6.2.6. Concanavalin A (ConA) agglutination assay

A stock solution of ConA was initially prepared in HEPES buffered saline (supplemented with $MgCl_2$ and $CaCl_2$). Diblock copolymers were added to diluted ConA to obtain the following final concentrations: [ConA] = 100 µg/mL and [polymer] = 50 µg/mL. At this point, the mixture was quickly vortexed and measured by UV/Vis spectroscopy at 350 nm and 0.1 Hz for 15 min. To determine the initial rate of cluster formation, $k_{cluster}$, a linear curve was fit to the data in the first 1 min. This kinetic parameter was the average of triplicate samples.

6.2.7. Formation of diblock copolymer/pDNA polyplexes and lipoplexes

Diblock copolymer/pDNA polyplexes were prepared by first diluting pDNA (at 1 mg/mL molecular biology grade water) into 1X pH 7.4 DPBS followed by addition of the diblock copolymers from a 2 mg/mL aqueous stock with a minimum incubation time of 30 min at room temperature. The total formulation volume was 20 μL per 1 μg pDNA. Polyplexes were formulated at fixed weight ratios of polymer/DNA (w_{poly}/w_{pDNA}). Lipoplexes were formed by combining pDNA with Lipofectamine 2000 at a 3:1 v/w L2K:DNA ratio in serum-free media in accordance with the manufacturer's protocol.

6.2.8. Dynamic light scattering (DLS) and zeta potential measurements

The sizes of free diblock copolymer micelles and copolymer/pDNA polyplexes in 1X DPBS were determined by DLS measurements using a Malvern Zetasizer Nano ZS (Worcestershire, UK). Free copolymer measurements were performed at a polymer concentration of 200 μg/mL while polymer/pDNA particles were analyzed at a pDNA concentration of 5 μg/mL. Free copolymer mean diameters are reported as the number average ± peak half-width while polyplex mean diameters are reported as the Z-average ± standard deviation. For zeta potential measurements, polyplexes were diluted into water to achieve a final pDNA concentration of 5 μg/mL

6.2.9. Hemolysis assay

The potential for the diblock copolymers to disrupt endosomal membranes was assessed by a hemolysis assay. The protocol followed here has been described previously [35]. Briefly, polymer was incubated in the presence of erythrocytes at 20 μg/mL in 100 mM sodium phosphate buffers (supplemented with 150 mM NaCl) of varying pH (7.4, 7.0, 6.6, 6.2, and 5.8) intended to mimic the acidifying pH gradient that endocytosed material is exposed to. The extent of cell lysis (i.e. hemolytic activity) was determined by detecting the amount of released hemoglobin via absorbance measurements at 492 nm.

6.2.10. In vitro transfections

RAW 264.7 were seeded in 24-well plates at $1 \cdot 10^5$ cells/well in 0.5 mL DMEM/10% FBS/antibiotics and cultured for 18 h to approximately 50% confluency. Polyplexes and lipoplexes were formulated as described above using GFP-encoding pDNA and added to the cells at 1 μg pDNA/well. Cell media was added to each well to obtain a total volume 1

mL/well and the poly/lipoplexes were allowed to incubate for 24 h. After this time, the cells were washed once with DPBS and then lysed with 300 µL RIPA lysis buffer (Pierce) for 1 h at 4 °C. Lysates were transferred to a black 96-well plate (150 µL/well) and fluorescence intensity was measured at an excitation and emission wavelength of 470 and 510 nm, respectively.

6.2.12. Fluorescent labeling of pDNA and diblock copolymers

gWiz-GFP pDNA was fluorescently labeled using *Label* IT® kit by following the manufacturer's protocol. The resultant material is referred to as Cy5-pDNA. Diblock copolymers were labeled by quaternizing tertiary amines with an iodoacetamide-functionalized near-IR dye (NIR-664-iodoacetamide). Briefly, diblock copolymer (50 mg/mL) and dye (70 – 170 µg/mL) were reacted for 18 h in methanol in the dark. This reaction mixture was dialyzed against methanol using a 6000 – 8000 MWCO followed by dissolution into dH_2O and lyophilization. The reconstituted NIR-664-diblock copolymer was then characterized by measuring fluorescence intensity at an excitation and emission wavelength of 640 and 700 nm, respectively, and via UV-Vis spectroscopy using the copolymer and NIR-664 absorbance at 310 and 664 nm, respectively.

6.2.13. In vitro pDNA uptake

Bone barrow-derived dendritic cells (BMDCs) were isolated from 6-8 week BALB/c mice (Jackson Laboratories, Bar Harbor, MA) using standard procedures [36]. Briefly, bone marrow cells were collected from mouse femurs and tibias and treated with ACK lysis buffer to remove red blood cells. These cells were washed and cultured at $2 \cdot 10^6$ cells/mL in 3 mL of complete RPMI media (2% HEPES buffer, 0.1 mM 2-mercaptoethanol, 100 U/mL penicillin, 100 µg/mL streptomycin, 2 mM glutamine, 10% fetal calf serum) supplemented with 10 ng/mL granulocyte-colony-stimulating factor (GM-CSF) and interleukin-4 (IL-4) (BD Biosciences, San Jose, CA) in six-well plates. At day 6 of this culture method, the cells were plated in 24-well non tissue culture-treated polystyrene plates at $7.5 \cdot 10^4$ cells/well in 0.5 mL complete RPMI media. After overnight incubation, diblock copolymer/Cy5-pDNA treatments were added at 0.5 µg pDNA/well. After 15 min, media was removed and cells were washed with 1X DPBS. Cells were then incubated for 10 min at room temperature in 100 µL/well PBS-based cell dissociation buffer (GIBCO) and collected by vigorous washing. These solutions were then diluted 1:2 with 1X DPBS containing 2% FBS. Fluorescence data was

116

acquired on a BD FACscan flow cytometer (BD Biosciences) with 10,000 events gated on forward/side scatter collected per sample and analyzed in FlowJo (TreeStar, Ashland, OR).

6.2.14. In vivo transfections and polyplex tissue distribution

6-8 week-old female BALB/c mice were administered treatments subcutaneously in the lower right abdominal quadrant using a 29.5-gauge needle. Polyplexes were formulated in HBG with 5 µg pDNA at +/- 4 and diluted to a total volume of 200 µL prior to injection. pCMV-Luc pDNA was selected for transfection studies while tissue distribution studies used either unlabeled diblock copolymer/Cy5-pDNA or NIR-664-diblock copolymer/gWiz-GFP pDNA polyplexes. For transfection studies, 24 hours post-injection luciferin solutions were prepared at 15 mg/mL in DPBS, filter sterilized, and injected intraperitoneally in the lower right abdominal quadrant at 150 mg/kg luciferin. Mice were subsequently anesthetized with isoflurane and imaged with the IVIS200 imaging system (Xenogen Corp., Alameda, CA) using the luminescence setting and a 3 min exposure time. For the tissue distribution studies, mice were imaged at various time points post-injection (0, 4, 24, and 72 h) following the same protocol as described above except via fluorescent measurements at excitation and emission wavelengths of 640 and 700 nm, respectively, with exposure time determined automatically in Living Image analysis software (Caliper Life Sciences, Hopkinton, MA).

6.2.15. Lymph node trafficking

6-8 week-old female C57BL/6 mice (Jackson Laboratories, Bar Harbor, MA) were administered treatments subcutaneously in the lower right abdominal quadrant using a 29.5-gauge needle. Polyplexes were formulated in HBG with 5 µg Cy5-pDNA at +/- 4 and diluted to a total volume of 200 µL prior to injection. 24 hours post-injection, animals were euthanized and inguinal lymph nodes were isolated. Lymph nodes were subsequently digested in 1mL of RPMI 1640 supplemented with 0.34 mg/mL Liberase TL and 2 mg/mL DNaseI (Roche, Indianapolis, IN) for 20 min at 37 °C and then ground through a 40 µm cell strainer with 1X DPBS and cell dissociation buffer (enzyme-free, PBS; Life Technologies, Carlsbad, CA) washes. Following an additional incubation at 37 °C, the cell solutions were quenched with media (RPMI 1640 supplemented with 10% heat-inactivated FBS) and centrifuged for 5 min at 1500 rpm. Cell pellets were aspirated then resuspended in 3 mL of red blood cell lysis buffer (eBioscience, San Diego, CA) for 5 min at room temperature, diluted with 10 mL 1X DPBS, centrifuged, aspirated, and resuspended in FACS buffer (1X

DPBS supplemented with 2% heat-inactivated FBS) to an approximate concentration of 1 - 3 · 10^6 cells/mL. These solutions were then incubated with 2 µL purified rat anti-mouse CD16/32 antibody (BD Biosciences, San Jose, CA) diluted 1:5 for 5 min at 4 °C. Following this Fc receptor blocking step, cells were double stained with 2 µL APC anti-mouse CD11c (BioLegend, San Diego, CA) and PE anti-mouse I-Ab (BD Biosciences) diluted 1:5 and 1:10, respectively, for 30 min at 4 °C. After staining, cells were washed twice with FACS buffer with centrifugation steps at 300 g for 5 min in between. The final cell pellets were resuspended in FACS buffer and analyzed by flow cytometry using the FACSCantoII (BD Biosciences).

6.2.16. Intracellular cytokine (ICC) staining and flow cytometry

Splenocytes were isolated as described previously and characterized using the following modified protocol [37], [38]. Briefly, splenocytes were cultured on a 96-well plate and treated with and without antigenic stimulation from the peptide mixture (100 µg/mL) for six hours with 2 M monensin (GolgiStop; BD Biosciences, San Jose, CA) present. The cells were washed and stained with either FITC-anti-CD4 or FITC-anti-CD8 monoclonal antibody (mAb). Following an additional wash, the cells were fixed with paraformaldehyde in the presence of a permeabilization agent, saponin, and stained with PE-anti-IFN-γ mAb. Cells were washed a final time and suspended in PBS supplemented with 2% FBS, counted using a FACSCanto (BD Biosciences), and analyzed in FlowJo (TreeStar).

6.2.17. Statistical Analysis

ANOVA was used to test for treatment effects, and Tukey's test was used for post hoc pairwise comparisons between individual treatment groups.

6.3. RESULTS AND DISCUSSION

6.3.1. Diblock copolymer synthesis and characterization

A series of diblock copolymers were synthesized according to **Scheme 6.1** consisting of two discrete statistical copolymer segments: a hydrophobic, endosomolytic unit with monomer feed ratios of 60% DEAEMA and 40% BMA (EB40) and cationic/targeting unit of DMAEMA and AcManEMA at varying monomer feed ratios of AcManEMA (0, 25, 50, 75, and 100%). The isolated EB40 copolymer acted as a macroCTA for the subsequent copolymer synthesis (**Table 6.1** and **Figure 6.1** and **6.2**). The diblock copolymer series exhibited

unimodal size distributions with low polydispersities (1.09 ≤ PDI ≤ 1.27) with monomer incorporations close to the initial feed ratios. Subsequent saponification yielded diblock copolymers lacking protective acetyl groups (δ = ~2.2-1.8), revealing the native mannose sugar conformation (representative demonstration of acetyl group removal in **Figure 6.3**).
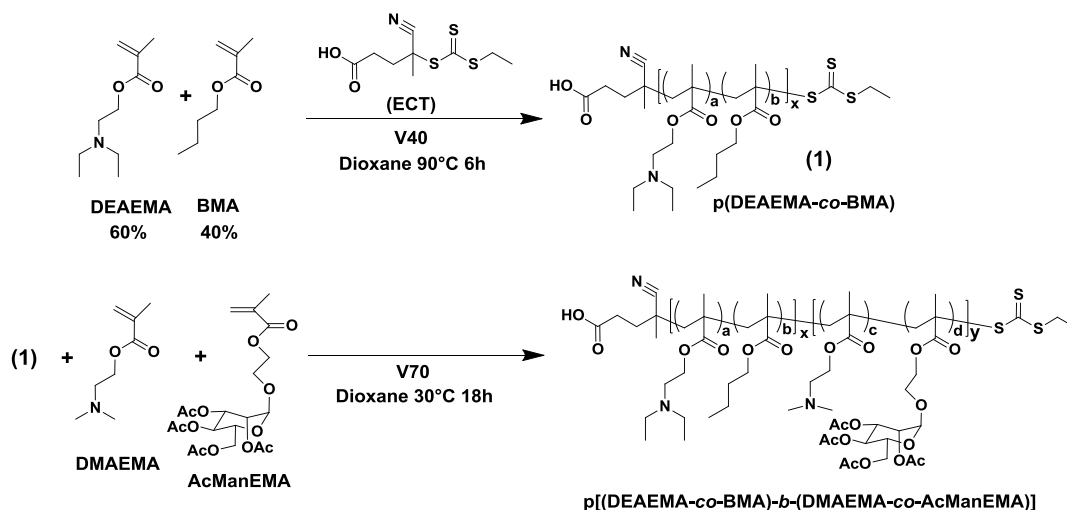
Scheme 6.1. RAFT-mediated synthesis of diblock copolymers consisting of an endosomolytic hydrophobic block (DEAEMA-*co*-BMA) which acted as a macroCTA for the copolymerization of DMAEMA and AcManEMA at varying molar feed ratios.

Table 6.1.
Molecular weights, polydispersities, and monomer compositions for polymer designs.

Polymer	Theoretical[a] % Man 2nd block	Exp.[b] % ManEMA 2nd block	2nd block M_n[c] (g/mol)	Total M_n[c] (g/mol)	Total M_n[d] (g/mol)	PDI[c] (M_w/M_n)
EB40 mCTA[e]	---	---	---	15600	15600	1.16
0% Man	0	0	11700	27300	27300	1.09
25% Man	25	29	13300	28900	26300	1.11
50% Man	50	57	18100	33700	28400	1.19
75% Man	75	79	27700	43300	34000	1.14
100% Man	100	100	34700	50300	37600	1.27

[a] Calculated molar feed ratio
[b] As determined by ^{1}H-NMR (CD$_3$OD) spectroscopy (Bruker AV 500)
[c] As determined by GPC
[d] Molecular weight estimation following saponification based upon complete removal of acetyl groups
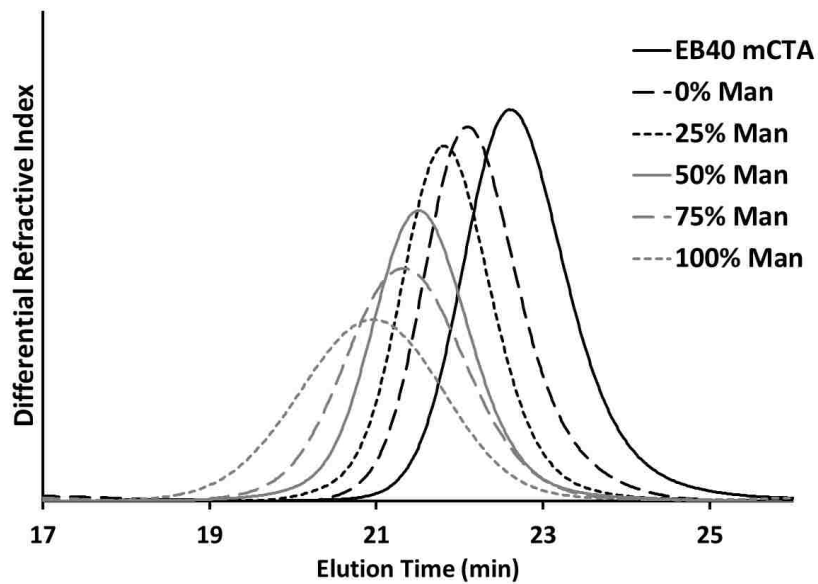[e] 43% BMA as determined by ^{1}H-NMR spectroscopy

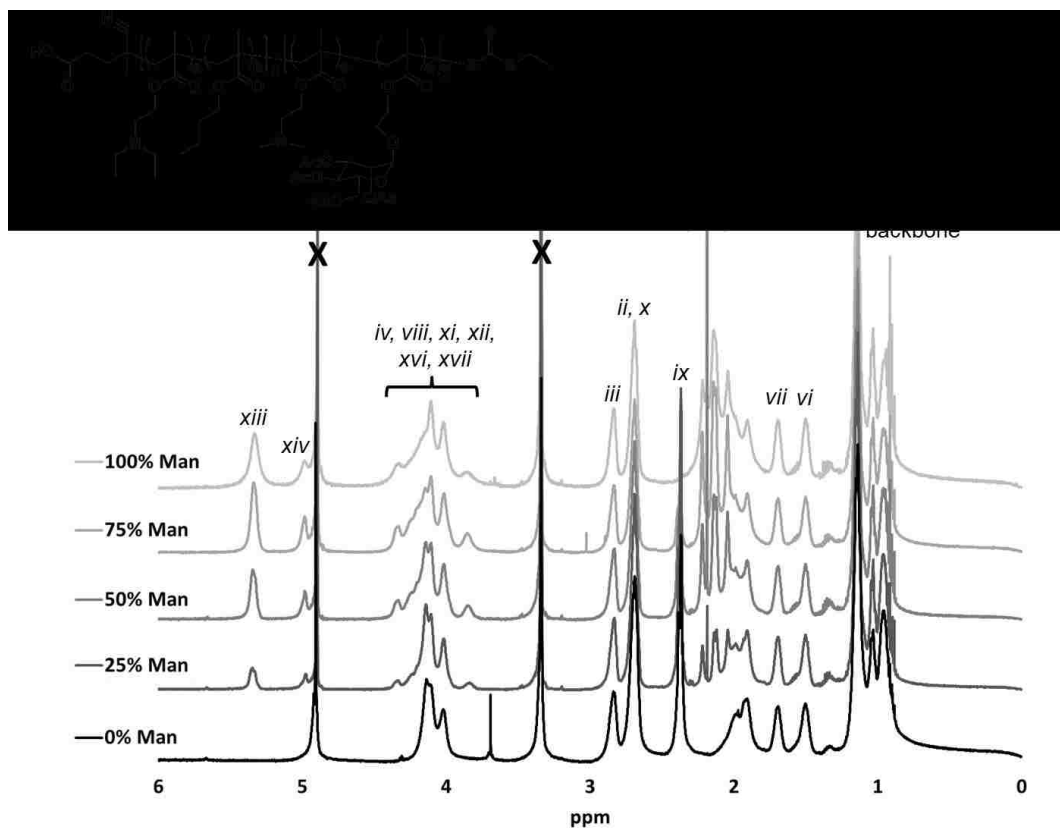**Figure 6.1**. GPC traces of diblock copolymer series and macroCTA in DMF.

Figure 6.2. ¹H-NMR of diblock copolymers in CD₃OD.
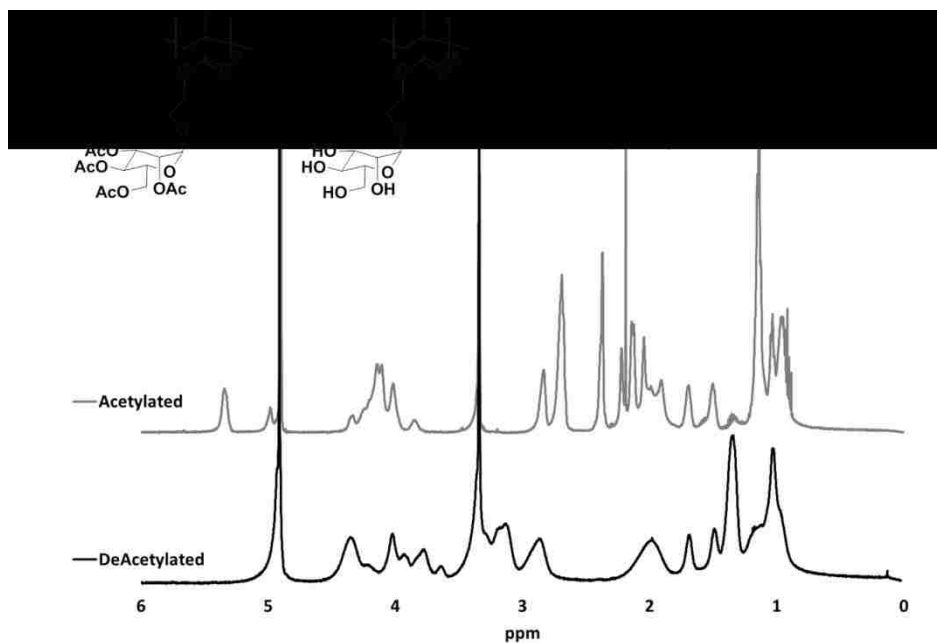
Figure 6.3. ^{1}H-NMR of acetylated and deacetylated 50% Man diblock copolymer in CD$_3$OD.

6.3.2. Aqueous properties of diblock copolymer micelles

The diblock copolymers consist of two discrete segments intended to impart different structural and biological activity to the resultant materials when exposed to aqueous conditions. The p(DEAEMA-*co*-BMA) unit is predominantly hydrophobic at physiological pH but becomes increasingly hydrophilic when the pH is decreased into the endosomal/lysosomal regime (pH 5.8 – 6.6) due to protonation of tertiary amines from pendent DEAEMA residues. The p(DMAEMA-*co*-ManEMA) unit, independent of ManEMA incorporation, is hydrophilic at physiological pH. When a diblock copolymer comprising these two segments is introduced into a physiological environment, it is expected to self-assemble into micellar particles due to entropically-driven sequestration of the hydrophobic p(DEAEMA-*co*-BMA) block stabilized by the hydrophilic p(DMAEMA-*co*-ManEMA) block. This activity was validated by dynamic light scattering (DLS) as particle sizes of approximately 12 – 17 nm mean diameter were observed for the entire series of diblock copolymers (**Table 6.2**). The pH-responsive activity was confirmed by a hemolysis assay in which each copolymer was able to disrupt red blood cell membranes upon a decrease of solution pH to 6.6 (**Figure 6.4**). This activity is correlated to a structural transition from micelle-to-unimer due to solvation of the hydrophobic core block at a pH value specific to the copolymer composition (see **Chapter 2**; **Figure 2.2**).

121

Table 6.2.
Dynamic light scattering measurements (DLS) of diblock copolymers and diblock copolymer/pDNA polyplexes. Polyplexes were formulated at fixed weight ratios of polymer/pDNA (w_{poly}/w_{pDNA}).

Polymer (% Man)	Polymer Mean Diameter (nm)	(w_{poly}/w_{pDNA}) = 4.5		(w_{poly}/w_{pDNA}) = 9	
		Mean Diameter (nm)	Zeta Potential (mV)	Mean Diameter (nm)	Zeta Potential (mV)
0	17 ± 2	370 ± 40	18 ± 3	190 ± 5	28 ± 2
25	12 ± 2	180 ± 10	14 ± 2	200 ± 20	22 ± 3
50	13 ± 2	190 ± 10	6 ± 3	140 ± 10	16 ± 3
75	13 ± 2	170 ± 10	7 ± 2	140 ± 10	10 ± 2
100	15 ± 2	140 ± 10	-2 ± 3	140 ± 5	-1 ± 2
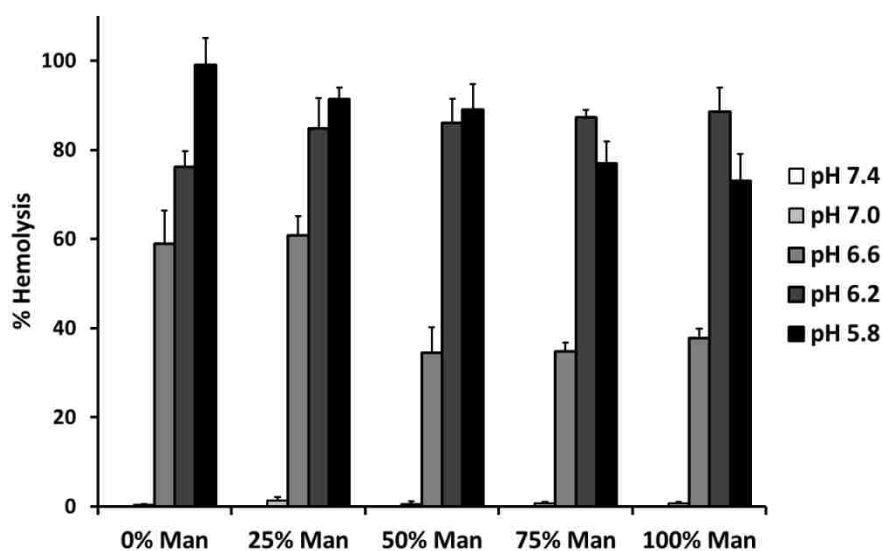
Figure 6.4. Hemolytic activity of diblock copolymers at a concentration of 20 µg/mL. Hemolytic activity is normalized relative to a positive control, 1% v/v Triton X-100, and the data represent a single experiment conducted in triplicate ± standard deviation.

To investigate the lectin-binding potential of the p(DMAEMA-*co*-ManEMA) block, an agglutination assay with Concanavalin A (ConA) was performed. All diblock copolymers incorporating ManEMA, but not the composition lacking ManEMA, were able to bind ConA as measured by an increase in solution turbidity (**Figure 6.5**). From these data, a kinetic parameter which identifies the initial rate of ConA/glycopolymer cluster formation ($k_{cluster}$) can be determined by applying a linear regression to the early time points: 0.08 ± 0.01, 0.10 ± 0.01, 0.07 ± 0.01, and 0.02 ± 0.01 AU/min for the 100%, 75%, 50%, and 25% Man diblock copolymers, respectively. These findings demonstrate that glycopolymer micelles are functionally active in binding lectins (see **Chapter 4**) and that copolymer segments with as

little as 29 mol% mannose can recognize these proteins. Additionally, there appears to be an optimal mannose incorporation for both inducing rapid lectin binding and achieving saturation of lectin binding sites.
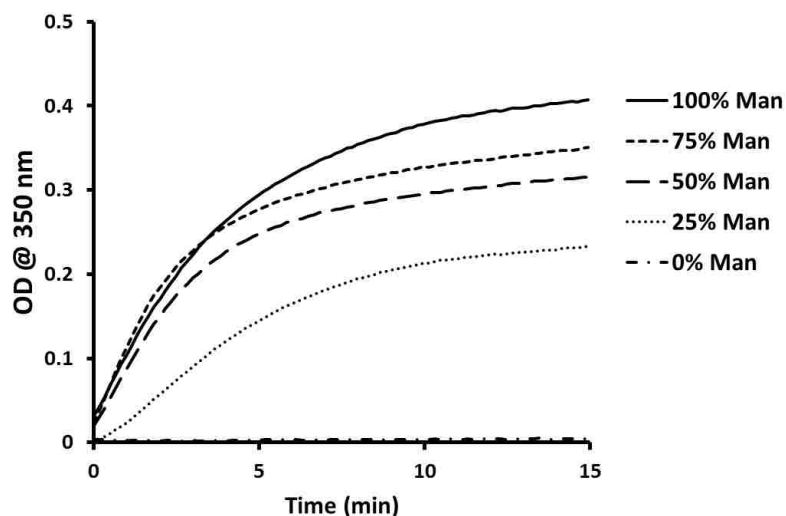
Figure 6.5. Time-dependent agglutination of ConA (100 µg/mL) mediated by diblock copolymers (50 µg/mL).

6.3.3. Characterization and in vitro activity of diblock copolymer/pDNA polyplexes

The diblock copolymers investigated in this study are based upon a previous design for pDNA delivery to immune cells (see **Chapter 2**). Through copolymerization of ManEMA into the corona segment, the intent of this new synthetic strategy was to both impart lectin-specific targeting functionality and dilute out the cationic charge which is attributed to deleterious effects in vivo [4]. To initially study the potential for this series of diblock copolymers to act as pDNA delivery vehicles, DLS measurements on diblock/pDNA polyplexes were performed (**Table 6.2**). With the exception of polyplexes formed between the 0% Man copolymer and pDNA at a mass ratio of polymer to pDNA (w_{poly}/w_{pDNA}) equal to 4.5, all polyplex formulations exhibited mean diameters sub-200 nm (140 – 200 nm) suggestive of successful pDNA complexation. These findings were further validated with a gel retardation assay (data not shown) which demonstrated complete association of copolymer and pDNA at the weight ratios investigated. For diblock copolymer compositions incorporating DMAEMA, these data are unsurprising as the pendent tertiary amines on this monomer unit were previously implicated in electrostatic complexation with the anionic phosphate groups on the pDNA backbone, an activity which has been routinely exploited for polymer-based nucleic acid delivery [39].

123

An unexpected finding is that the diblock copolymer composition lacking DMAEMA, 100% Man, was not only able to form polyplexes, but produced the smallest particle sizes (mean diameter of 140 ± 5 nm). This result suggests that these diblock copolymers do not retain their micelle morphology in the presence of pDNA and are likely exposing core DEAEMA residues to participate in pDNA complexation. To investigate the role of ManEMA incorporation on the shielding of cationic charge, zeta potential measurements were performed for each polyplex formulation. A general trend can be observed in which an increase in ManEMA content leads to a decrease in polyplex zeta potential, culminating in near-neutral particles for polyplexes formulated with the fully mannosylated diblock copolymer at $w_{poly}/w_{pDNA} = 9$ (-1 ± 0.5 mV).

Following polyplex characterization, the in vitro gene transfection activity of these materials was investigated using GFP-encoding pDNA in RAW264.7 (macrophage-like murine) cells (**Figure 6.6**). The diblock copolymer composition lacking ManEMA, 0% Man, produced similar or better levels of GFP expression as compared to the commercial liposomal transfection reagent, Lipofectamine 2000, a finding supported by previous cell culture experiments (see **Chapter 2**). The 25% Man diblock copolymer was able to mediate expression levels above background at the higher w_{poly}/w_{pDNA} ratios (9 and 18) while all other compositions resulted in fluorescence values similar to baseline. These findings demonstrate that dilution of the DMAEMA component in these diblock copolymer designs significantly attenuates in vitro pDNA transfection activity, confirming that DMAEMA plays a crucial role in facilitating pDNA delivery in culture.
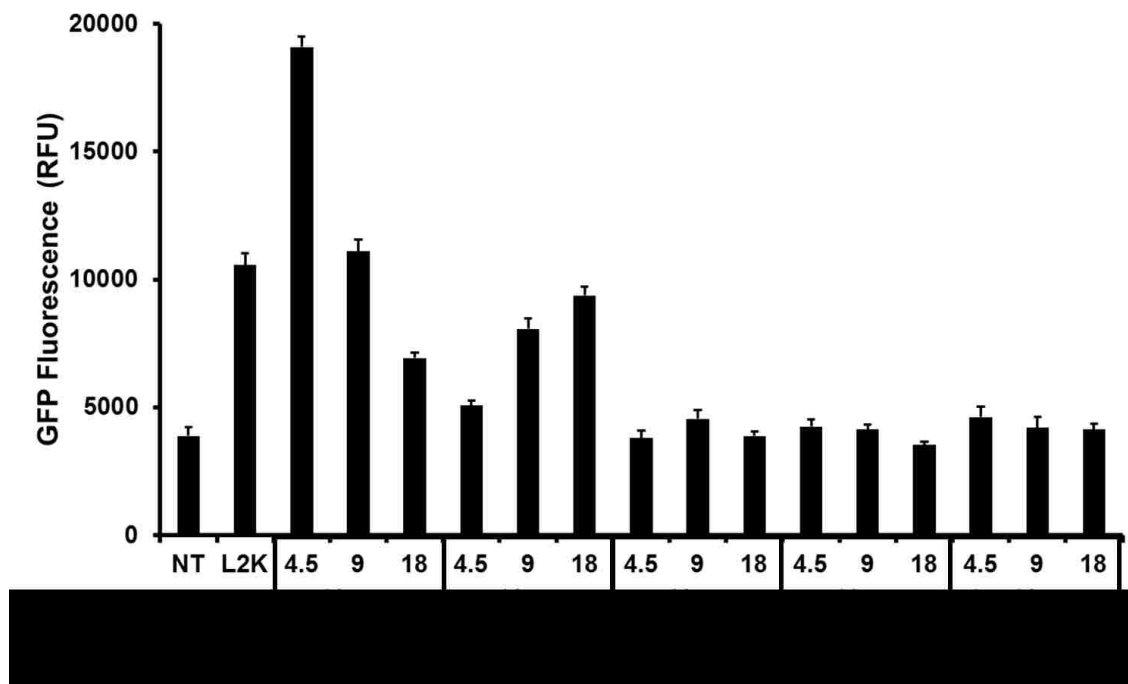
Figure 6.6. In vitro transfection efficiencies in RAW 264.7 cells. L2K corresponds to treatment with Lipofectamine/pDNA. Data are from a single experiment run in triplicate with the error bars representing the standard deviation.

While DMAEMA was found to not be essential in polyplex formation, the monomer likely promotes pDNA transfection in vitro through two possible mechanisms: the cationic charge mediates enhanced levels of nonspecific internalization and/or the tertiary amines participate in endosomal escape through the proton sponge effect [40–43]. While the latter possibility may be a factor, the sharp drop in transfection levels at compositions of 75% DMAEMA and below suggests this is not a dominant effect since every composition contains the same quantity of DEAEMA residues that should be able to participate in this activity. However, a critical tertiary amine concentration in these polymer systems may be an important parameter in facilitating the proton sponge effect [44]. The effect of cell uptake attenuation due to dilution of DMAEMA has been investigated in bone marrow-derived dendritic cells (BMDCs) and initial studies have demonstrated that 0% Man polyplexes exhibit significantly higher levels of uptake as compared to 50% Man and 100% Man at short incubation times (**Figure 6.7**). Based upon zeta potential measurements, the polyplexes with greater mannosylation exhibit lower surface charges (near neutral at 100% Man) so a decrease in charge-mediated modes of uptake would be anticipated. Since these

routes of nonspecific uptake often dominate in vitro, it is unsurprising that overall uptake would decrease upon charge neutralization of the polyplexes.
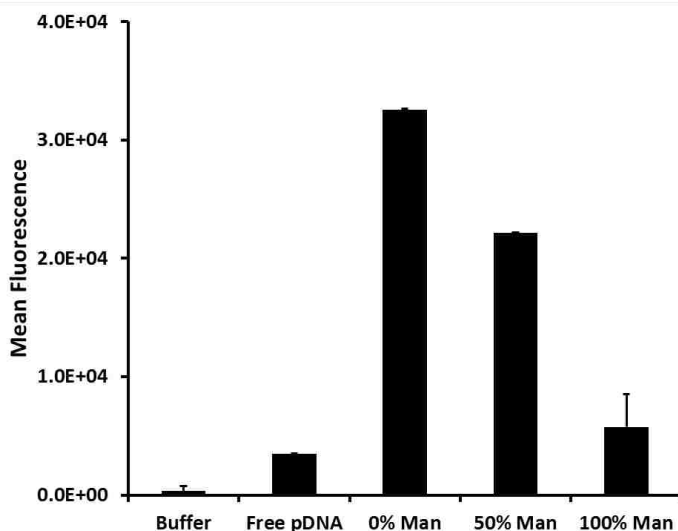
Figure 6.7. In vitro uptake of Cy5-labeled pDNA in bone marrow-derived dendritic cells (BMDCs) after 15 min by flow cytometry. Diblock copolymer/pDNA polyplexes were formulated at (W_{POLY}/W_{PDNA}) = 9. Data are from a single experiment run in triplicate with the error bars representing the standard deviation.

The intended effect of introducing mannose residues into these polymer designs is to divert the primary mode of cell uptake from these nonspecific mechanisms towards C-type lectin-mediated endocytosis. This specific route of internalization has been demonstrated for our glycopolymers in the unimeric, linear conformation (see **Chapter 3**) but has not yet been confirmed in vitro for these glycopolymer micelles and polyplexes. If these mannosylated systems are being internalized by cell surface receptors, their intracellular fate will be dependent upon the specific receptor and cell type. For example, the mannose receptor on dendritic cells was found to traffic only to early endosomes following receptor engagement [45] while endocytosed compartments of DEC-205 can mature into late endosomes/lysosomes [46]. These findings allude to the possibility that selection of the right cell type may result in significant pDNA transfection for the 100% Man diblock copolymer in vitro.

6.3.4. In vivo pDNA expression

Polyplexes formulated with luciferase-encoding pDNA were administered subcutaneously to visually observe expression at the site of injection after 24 hours. Free pDNA administration resulted in the largest distribution of transfected cells as well as the highest luminescence levels (**Figure 6.8**). These results are consistent with initial studies examining intradermal administration of free luciferase-encoding pDNA in which luminescent tissue was detected up to 14 days post-injection [47]. The polyplexes lacking mannose, 0% Man, did not produce significant luminescence. Polyethylenimine (PEI) polyplexes were also investigated and did not produce detectable luminescence (data not shown). The fully mannosylated polyplex, 100% Man, was able to facilitate pDNA transfection at the injection site, albeit at levels lower than the free pDNA ($3.9 \cdot 10^6$ vs. $5.2 \cdot 10^5$ p/s). It is important to note from these studies the high animal-to-animal variability, likely a result of slight differences in administration technique. The stark contrast in expression levels between the mannosylated and non-mannosylated material highlight an important discordance often observed between in vitro and in vivo gene delivery studies. As an example, van den Berg et al. found that cationic lipoplexes dramatically outperformed free pDNA in vitro while this trend was reversed for intradermally administered material [4]. Additionally, these researchers found that in vivo and ex vivo activity of a cationic polymer was only observed following polymer PEGylation. This latter finding demonstrates the detrimental effect of polycations in vivo despite the high transfection these materials promote in vitro. This discordance is highlighted in this chapter's findings as the near-neutral, mannosylated polyplexes were ineffective in vitro (as measured by transfection in RAW264.7 cells and uptake in BMDCs) yet were capable of mediating pDNA expression in subcutaneous tissue (dissections revealed that expression was localized to the skin, data not shown).
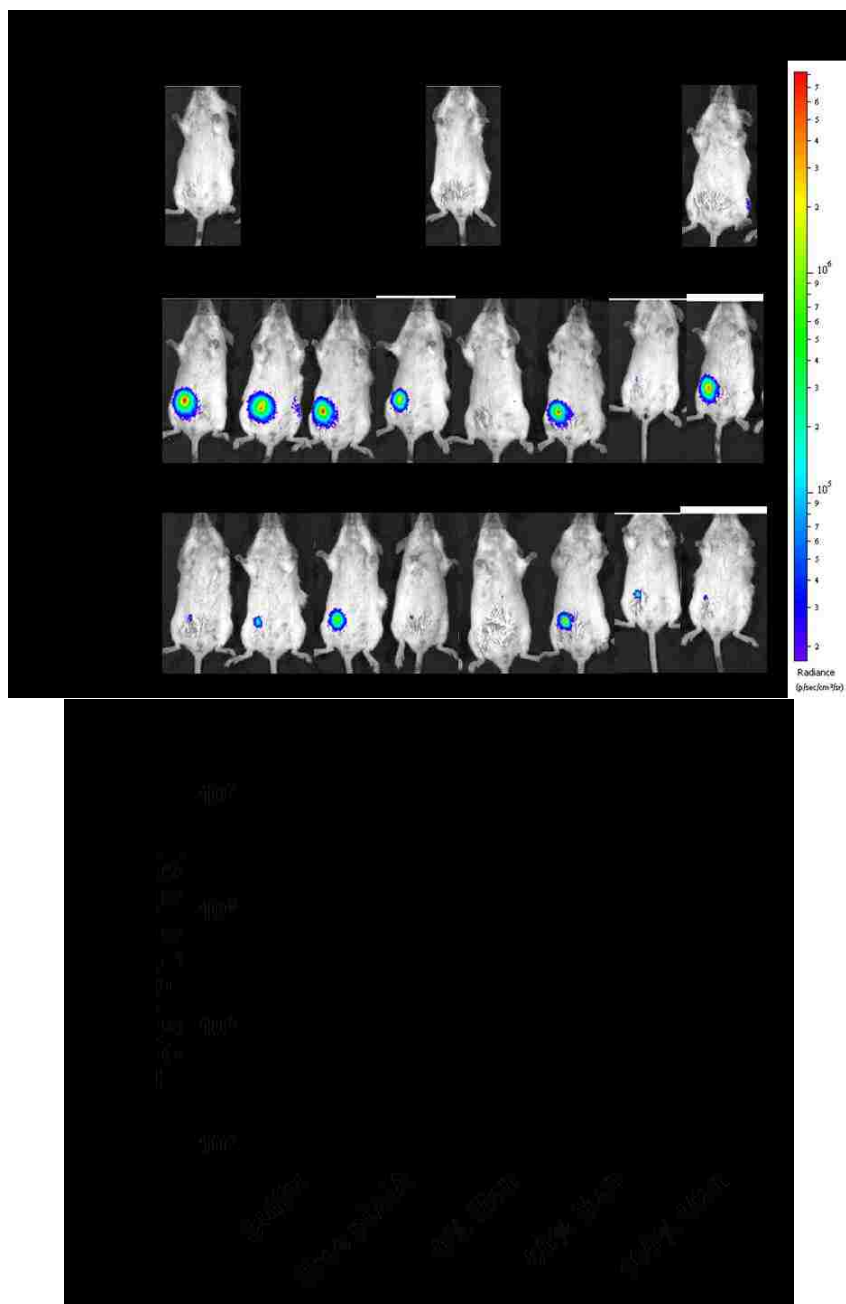
Figure 6.8. Representative in vivo visualization (**A**) and total flux (**B**) of luciferin bioluminescence due to luciferase-encoding pDNA expression. The total flux of the free pDNA and 100% Man treatments is $3.9 \cdot 10^6$ and $5.2 \cdot 10^5$ p/s, respectively. Polyplexes were formulated at $W_{POLY}/W_{PDNA} = 9$.

It is important to consider what cell types are internalizing and expressing the delivered pDNA. Material administered via a subcutaneous route primarily accesses the hydodermis which consists of fibroblasts, adipocytes, and mononuclear cells. These cells also comprise

the dermis which is targeted by intradermal injections. Drabick et al. found that free pDNA administered intradermally via electroporation was expressed in fibroblasts, endothelial cells, adipocytes, and mononuclear cells which could include dermal dendritic cells [48]. Another study which examined free pDNA uptake after intradermal administration (without electroporation) showed that the nucleic acid predominantly co-localized with dermal fibroblasts and not antigen presenting cells (APCs) [5]. This same study demonstrated that cationic polyplexes were unable to significantly transfect fibroblasts due to the formation of insoluble depots. After 4 hours post-injection, dendritic cells were observed at the periphery of these depots internalizing pDNA. Neutral polyplexes were shown to better infiltrate tissue around the injection site, allowing for delivery of DNA to both fibroblasts and dendritic cells. The data reported here are consistent with these previous findings as the neutral, mannosylated polyplex was able to produce detectable luminescence in the subcutaneous tissue while the cationic, mannosylated polyplex was not. This finding is likely due to the neutral particles being able to access dermal fibroblasts while cationic particles are sequestered in depots, a supposition which will be investigated in the following sections.

These materials were designed to directly transfect APCs, ultimately to prime the immune system to an antigen encoded in the pDNA. An alternative pathway of antigen delivery to APCs involves transfecting fibroblasts and other off-target cells, or "bystander cells", in the dermal/hypodermal tissue [49]. Through a combination of antigen expression and cell death by these bystander cells, dendritic cells are able to both mature and present antigen leading to robust T cell activation. This phenomenon is one possible mechanism in which the polyplexes presented here could be capable of eliciting an antigen-specific immune response.

6.3.5. In vivo polyplex tissue distribution

To determine the tissue distribution of mannosylated (100% Man) and non-mannosylated (0% Man) polyplexes following subcutaneous administration, polyplexes incorporating both fluorescently-labeled pDNA (**Figure 6.9**) and diblock copolymer (**Figure 6.10**) were investigated. Free pDNA was found to largely disperse away from the injection site by 24 hours with very little persisting at 72 hours. Treatment with the mannosylated polyplex produced a similar finding as free pDNA with complete clearance of the nucleic acid around 24 – 72 hours. The cationic, non-mannosylated polyplex was the only treatment which had

detectable pDNA fluorescence in all animals at 72 hours. Additionally, the bulk of the fluorescent intensity was confined to a punctate region which differed from the distributed pattern of the free pDNA and mannosylated polyplex groups. These findings for the non-mannosylated polyplex are consistent with depot formation as discussed previously.

Figure 6.9. In vivo visualization of tissue distribution (**A**) and average radiant efficiency (**B**) of diblock copolymer polyplexes (formulated at W_{POLY}/W_{pDNA} = 9) with Cy5-labeled pDNA. Average radiant efficiency was determined using automatic detection of regions of interest with Living Image analysis software and error bars representing standard deviation (n = 3). There was a significant difference in the average radiant efficiency of DMAEMA polyplexes as compared to free pDNA and ManEMA polyplexes at 24 and 72 h ($p < 0.05$).

When examining polyplexes in which polymer was fluorescently labeled, both the mannosylated and non-mannosylated polymers were visually found to persist at the injection site after 72 hours. However, when examining the average radiant efficiency of these regions, there is a sharp decline in fluorescence for the 100% Man polyplex between 0 and 72 hours ([$3.7 \cdot 10^9 \pm 6.7 \cdot 10^8$] vs. [$4.7 \cdot 10^8 \pm 6.8 \cdot 10^7$] (p/s/cm^2/sr)/($\mu$W/cm^2)) with only 13% remaining by this latter time point. For the 0% Man polyplex, 57% of the initial fluorescence is detectable at 72 hours. These results are unsurprising for the non-mannosylated polyplex as pDNA was also found to be sequestered in a discrete region throughout the duration of the experiment, suggesting that polyplexes remain relatively intact (or at least the two components comprising these complexes co-localize) within a depot. While the mannosylated polymer was present at later time points, fluorescence levels were substantially lower than those for the initial administered material, suggesting that the majority of polymer is able to traffic out of the injection site by 72 hours. When formulating polyplexes, an excess of polymer is used and this residual, non-pDNA-associated material may account for the signal measured at these latter time points.
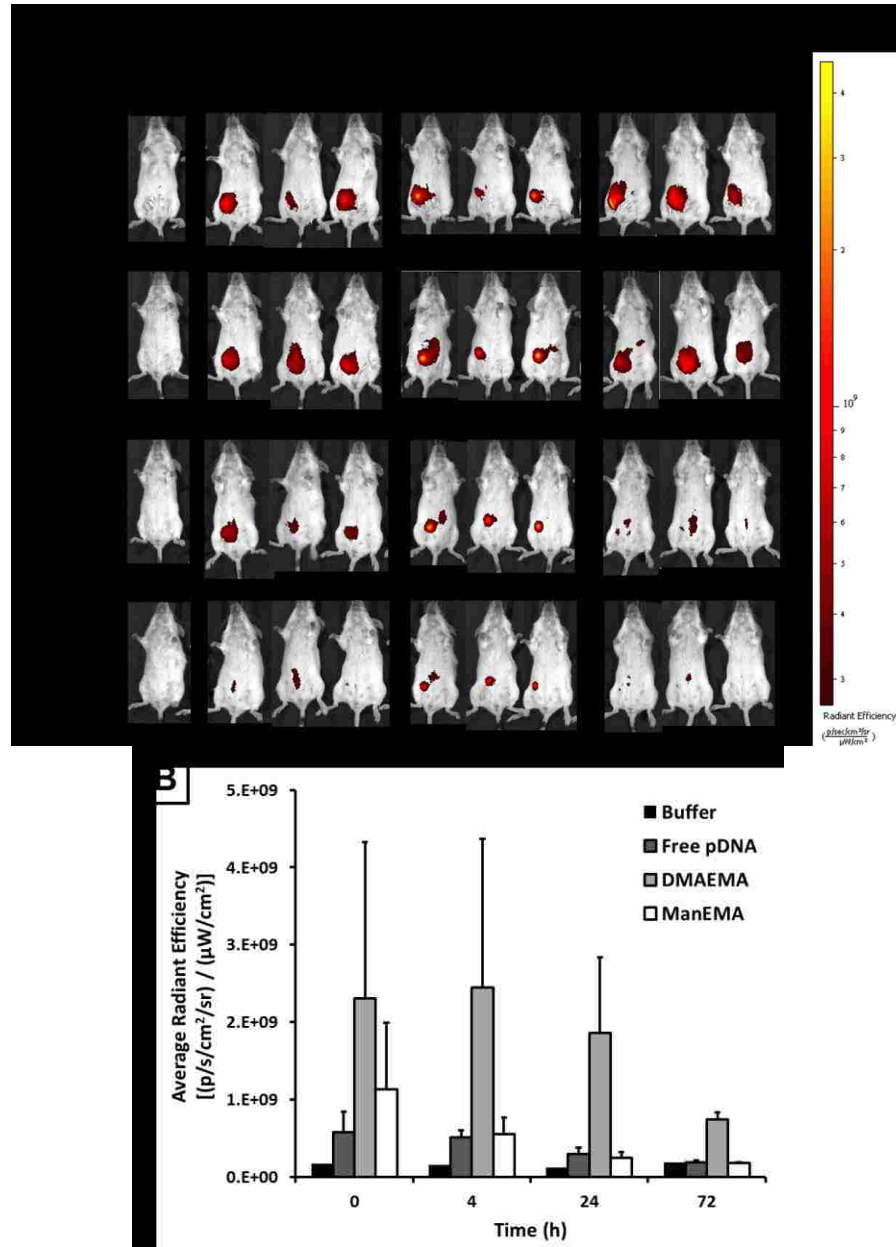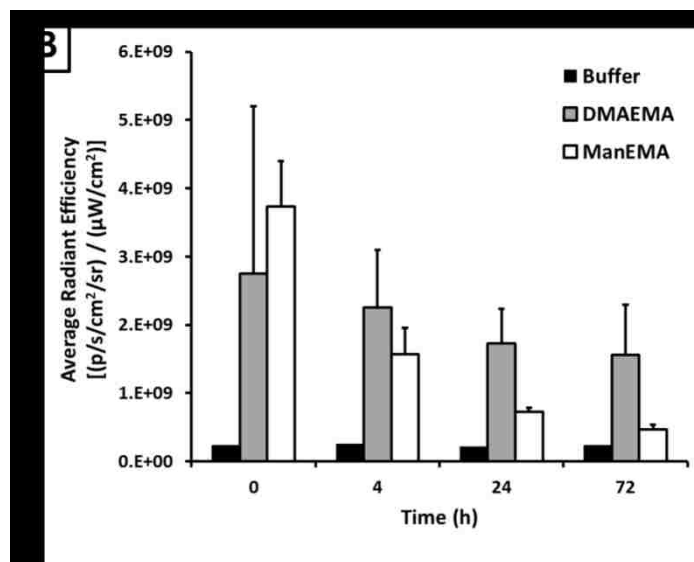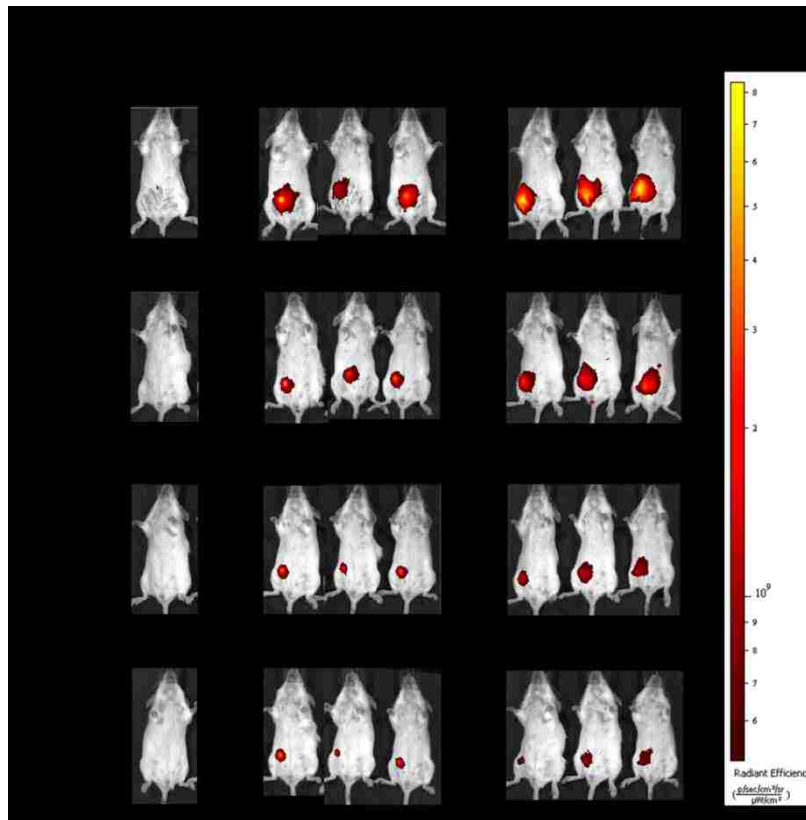
Figure 6.10. In vivo visualization of tissue distribution (**A**) and average radiant efficiency (**B**) of diblock copolymer polyplexes (formulated at $W_{POLY}/W_{PDNA} = 9$) with near-IR fluorophore (NIR-664)-labeled polymer. Average radiant efficiency was determined using automatic detection of regions of interest with Living Image analysis software and error bars representing standard deviation (n = 3). There was a significant difference in the average radiant efficiency of DMAEMA polyplexes as compared to ManEMA polyplexes at 24 but not 72 h ($p < 0.05$).

6.3.5. Lymph node trafficking

To obtain an efficacious cancer vaccine which is capable of generating a robust antigen-specific T cell population, antigenic material must be delivered to the lymph nodes and presented by DCs. This requisite activity can be achieved via two distinct pathways: passive transport through the lymphatics and subsequent uptake by lymph node-resident DCs or active transport by migratory DCs at the injection site. For particles administered by either intradermal or subcutaneous routes, particle size has been found to be a key parameter determining which route of lymph node trafficking is preferred or even possible. Manolova et al. found that following intradermal administration of polystyrene particles, those with 500 – 2000 nm diameters were associated with injection site DCs while smaller 20 – 200 nm particles had been internalized by lymph node-resident macrophages and DCs [50]. When investigating the behavior of this latter group of nanoparticles, researchers demonstrated that smaller 25 nm particles readily transport through the lymphatics to draining lymph nodes via interstitial flow after intradermal injection [21]. Approximately 50% of lymph node-resident DCs had internalized this material compared to 10% for nanoparticles with 100 nm diameters. Migratory DCs can additionally hone to an injection site up to four days post-administration and actively traffic material to the draining lymph node [5], [51].

To investigate the effect of carrier mannosylation on lymph node trafficking, 0%, 50%, and 100% Man polyplexes incorporating labeled pDNA were administered subcutaneously and after 24 hours, DCs were analyzed from isolated inguinal lymph nodes (**Figure 6.11**). 24 hours was selected as a time point as both free pDNA and pDNA associated with mannosylated polymer were found to distribute out of the injection site by this point. Additionally, Rush et al. demonstrated that free pDNA administered subcutaneously accumulated in draining lymph DCs by this time [52]. In our study, nominal pDNA uptake by CD11c$^+$/MHCII$^+$ DCs was observed for the free pDNA treatment (2.5 ± 1.0%) while significant uptake was found for the mannosylated polyplex (10.8 ± 4.1%). These findings are consistent with DC uptake of 100 nm polystyrene particles administered intradermally, as discussed above [21]. 0% (1.0 ± 0.4%) and 50% Man (1.0 ± 0.2%) polyplexes did not mediate uptake of pDNA by DCs above background levels (1.0 ± 0.1%).
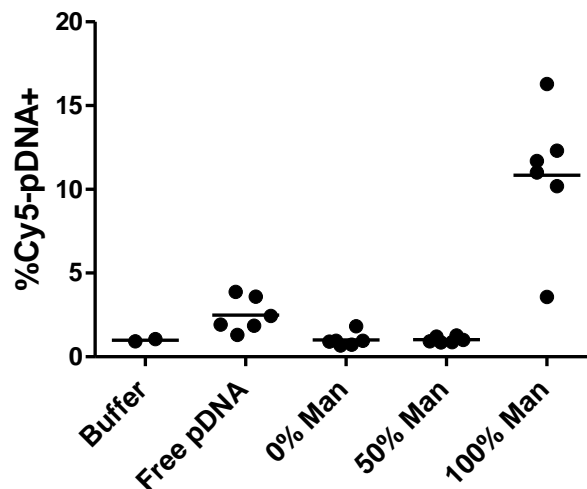
Figure 6.11. Uptake of Cy5-labeled pDNA by CD11c$^+$/MHCII$^+$ dendritic cells in the inguinal lymph node 24-hr post-injection. 5 µg pDNA was administered subcutaneously in the lower right abdominal quadrant. Polyplexes were formulated at $W_{POLY}/W_{PDNA} = 9$. Percent uptake of pDNA by DCs was found to be significantly different for the 100% Man polyplexes as compared to free pDNA, 0% Man polyplexes, and 50% Man polyplexes ($p < 0.05$).

The results of this study highlight the therapeutic potential of this mannosylated material in priming the immune system to an antigen encoded in pDNA. When compared to free pDNA, mannosylated polyplexes produce less expression at the injection site and appear to distribute pDNA through subcutaneous tissue in a similar spatiotemporal manner. However, there is a distinct enhancement in the extent of DC pDNA uptake in the draining lymph nodes which could potentially lead to an increase in downstream T cell activation. While these results are encouraging, it is important to highlight a recent report by Carstens et al. [53]. These researchers found that PEGylated liposomal DNA vaccines enhanced DC uptake of pDNA in the draining lymph nodes when compared to non-modified liposomes but the immune responses were dampened. Nonetheless, these findings are highly encouraging as they are the first to demonstrate the substantial accumulation of pDNA in lymph node DCs by a synthetic polymer carrier. Further studies need to be performed to assess the clinical utility of these mannosylated materials.

6.4. CONCLUSIONS AND FUTURE DIRECTIONS

A series of diblock copolymer micelles were synthesized in which the corona chemistry was varied to incorporate different ratios of pendent tertiary amine (DMAEMA) or mannose (ManEMA) functionalities. Each composition consisted of the same hydrophobic,

endosomolytic core segment (DEAEMA-*co*-BMA) that led to similar pH-responsive behavior for each copolymer in the series, as determined by a hemolytic assay. Diblock copolymers that contained ManEMA were found to agglutinate the C-type lectin, Concanavalin A, demonstrating that the mannose residues are capable of binding to carbohydrate recognition domains (CRDs). Each copolymer was able to condense pDNA into polyplexes with diameters of 100 – 200 nm and surface charges that decreased as a function of ManEMA composition with the 100% ManEMA diblock copolymer producing near-neutral particles (-1 ± 0.5 mV). In vitro gene transfection studies examining diblock/pDNA polyplexes demonstrated a negative trend of pDNA expression with increasing ManEMA incorporation; at 50% ManEMA and greater, no significant expression activity was observed.

For in vivo studies, only the 100% ManEMA (fully mannosylated), 50% ManEMA, and 0% ManEMA (100% DMAEMA) polyplexes were investigated. Free pDNA and the 100% ManEMA polyplex were capable of mediating pDNA expression in subcutaneous tissue, albeit the latter at lower levels, while the 0% and 50% ManEMA polyplex was unable to produce gene expression levels above background. Tissue distribution experiments demonstrated that the majority of free pDNA and pDNA in mannosylated polyplexes disperses out of the injection site by 24 hours while non-mannosylated polyplexes sequester pDNA in a depot for up to 72 hours. The majority of the non-mannoslyated polymer also persists at the injection site for this same period of time.

To generate a robust antigen-specific immune response, these materials first need to deliver their genetic cargo to relevant APC populations. When compared to free pDNA, 0%, and 50% ManEMA polyplexes, the fully mannosylated polymer was found to significantly enhance pDNA uptake by DCs in draining lymph nodes. Further studies would need to be performed to demonstrate whether a polymer component is associated with the pDNA that traffics through the lymphatics. If this is not found to be case, an additionally possibility exists in which mannose is conferring an adjuvant effect leading to enhanced DC uptake [54]. To elucidate whether mitigation of cationic charge is leading to this improved trafficking behavior, non-glycosylated, neutral PEGylated polyplexes (i.e. p(PEGMA-*b*-[DEAEMA-*co*-BMA])/pDNA complexes) were also studied. Intermediate pDNA DC uptake was observed for these materials (6.7 ± 1.1%), significantly different than both 0% and 100% ManEMA polyplexes, demonstrating that charge neutralization does have a positive effect on this

activity. Substitution of galactose ethyl methacrylate (GalEMA), or another glycomonomer that does not exhibit APC affinity, into the micelle corona could demonstrate if this enhanced trafficking is carbohydrate-specific.

Ultimately, these materials would need to be evaluated in an in vivo vaccine model. Previously, we examined the immune response generated by a cationic, non-mannosylated polymer complexed to ovalbumin-encoding pDNA by subcutaneous administration following a prime/boost protocol over one month. We found that free pDNA was able to elicit a significant antigen-specific CD8+ T cell population while the polyplex produced levels similar to background for both CD4+ and CD8+ T cells (**Figure 6.12**). Based upon the poor performance of the cationic polyplex investigated in this chapter and the promising gene expression and lymph node trafficking results from the mannosylated polyplex, there is justified motivation to pursue vaccine studies with this new material. Alternative modes of administration could also be explored to improve the therapeutic efficacy of these delivery vehicles, e.g. gene gun, DNA tattoo, and transcutaneous microneedles [55], [56]. The latter approach is particularly advantageous as it deposits material in epidermal tissue, accessing Langerhans cells which are potent mediators of CD4+ and CD8+ T cell responses [57], [58].
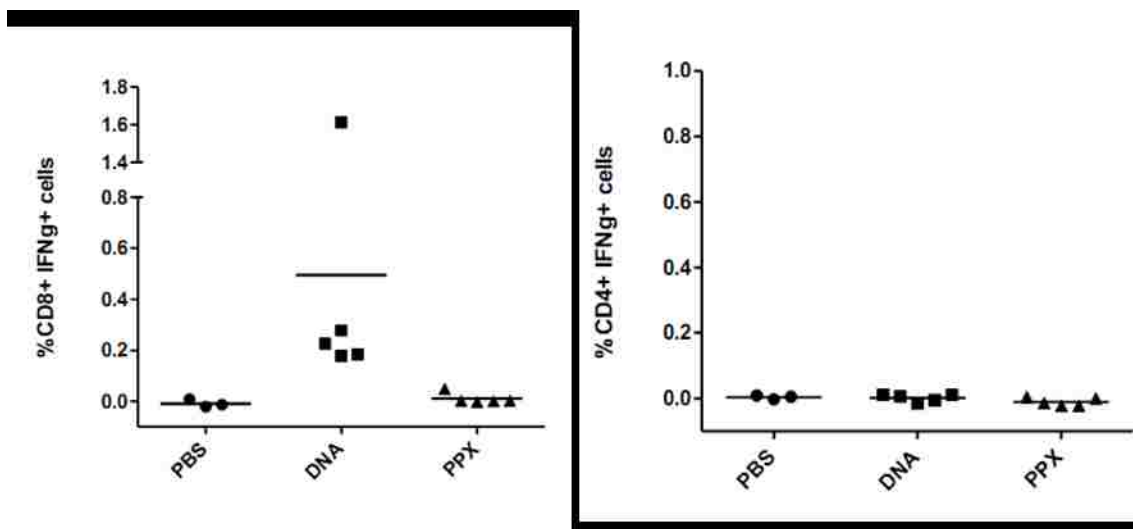
Figure 6.12. Intracellular cytokine staining for ovalbumin-specific T cells after one month prime/boost DNA vaccine study (prime at day 0, boost at day 14, and sacrifice at day 28). 100 μg pDNA was administered by two 200 μL subcutaneous injections in the base of tail for each prime and boost. DNA represents free pDNA treatment while PPX represents p(DMAEMA-*b*-[DEAEMA-*co*-BMA])/pDNA polyplexes at +/- 2. Splenocytes were restimulated in vitro with ovalbumin epitope peptides for 1 h, then incubated with Brefeldin A for 8 h prior to staining and analysis. Horizontal line represents group mean. Note y-axis break.

6.5. MANNOSYLATED TRIBLOCK COPOLYMERS AS pDNA CARRIERS

Prior to studying diblock copolymer micelles with mannose-containing coronas, mannosylated triblock copolymers were investigated. The rationale behind these designs was to preserve the active diblock copolymer structure from **Chapter 2** while incorporating a discrete glycopolymer targeting segment. This work extends upon a series of triblock copolymers synthesized by Cheng et al. in which blocks of PEG were systematically introduced into an architecture containing poly(DMAEMA) and poly(DEAMEA-*co*-BMA) segments [59]. An optimal blocking order and relative block sizes were found to mediate the highest mRNA expression levels. Triblock copolymers have also been investigated as nonviral DNA vectors [60–64]. Notable among these designs is the use of an ABC triblock copolymer consisting of targeting lactosylated poly(ethylene glycol), pH-responsive polyamine, and DNA-condensing polyamine segments developed by Oishi et al. [62]. These DNA carriers demonstrated specific cell uptake in hepatocytes via the asialoglycoprotein receptor and higher transfection efficiencies as compared to related diblock copolymers.

With these studies in mind, a series of mannosylated triblock copolymers were synthesized and their general design (**Table 6.3**) and characterization data (**Table 6.4**) are presented below. Only four of the seven triblocks (MT2,4,6,7) were able to mediate detectable levels of pDNA expression in vitro. Preliminary in vivo transfections were performed by monitoring luminescence after separate subcutaneous administration of each of these four triblocks complexed to luciferase-encoding pDNA. None of the triblock copolymers were able to elicit significant expression in the subcutaneous tissue. The cause of the poor in vivo activity for these materials is unclear but likely stems from the presence of solvated DMAEMA residues leading to unfavorable depot formation, as observed for the cationic, non-mannosylated polyplex investigated above. The PEGylated polyplexes studied by Cheng et al. still exhibit a significant surface charge and one would speculate these mannosylated triblock polyplexes do as well, which could be the cause of the low in vivo activity that is often observed for other cationic systems [4], [5].

Table 6.3.
Summary of mannose triblock (MT) copolymers with target DP values for each block.

Mannose Triblock (MT)	Polymer Design	In vitro activity	ConA Agglutination
1	ManEMA 25 — DMAEMA 75 — EB40 100	-	Yes
2	DMAEMA 75 — EB40 100 — ManEMA 25	+	Yes
3	DMAEMA 75 — EB40 100 — ManEMA 75	-	Yes
4	DMAEMA 75 — EB40 200 — ManEMA 25	++	No*
5	DMAEMA 75 — EB40 200 — ManEMA 75	-	Yes
6	DMAEMA 75 — ManEMA 75 — EB40 100	++	Yes
7	DMAEMA 75 — ManEMA 75 — EB40 200	++	Yes

For in vitro activity, "**+**" signifies activity significantly above background while "**++**" refers to activity comparable to non-mannosylated, diblock copolymers. EB40 represents (DEAEMA-*co*-BMA) copolymer segments with a molar feed ratio of 40% for BMA. *MT4 was unable to agglutinate ConA by a UV/Vis turbidity assay but demonstrated ConA binding by SPR.

Table 6.4.
Molecular weights[a], polydispersities[a], and monomer compositions[b] of mannose triblock copolymers.

MT	M_n DMAEMA Block (g/mol)	M_n EB40 Block (g/mol)	M_n AcManEMA Block (g/mol)	Total M_n (g/mol)	PDI (M_w/M_n)	Mol% BMA in EB40 Block
1	5100	14200	11000	30300	1.10	45
2	5600	12400	11000	29000	1.08	45
3	9200	14300	31400	54900	1.27	45
4	9200	21900	10000	41100	1.08	45
5	9200	21900	24100	55200	1.09	45
6	9300	3300	36300	48900	1.09	49
7	9300	12800	36300	58400	1.06	51

[a] As determined by GPC
[b] As determined by ^{1}H-NMR (CD$_3$OD) spectroscopy (Bruker AV 500)

6.5. REFERENCES

[1] D. W. Pack, A. S. Hoffman, S. Pun, and P. S. Stayton, "Design and development of polymers for gene delivery.," *Nature reviews. Drug discovery*, vol. 4, no. 7, pp. 581–93, Jul. 2005.

[2] J. C. Perales, T. Ferkol, H. Beegen, O. D. Ratnoff, and R. W. Hanson, "Gene transfer in vivo: sustained expression and regulation of genes introduced into the liver by receptor-targeted uptake.," *Proceedings of the National Academy of Sciences of the United States of America*, vol. 91, no. 9, pp. 4086–90, Apr. 1994.

[3] P. van de Wetering, N. M. Schuurmans-Nieuwenbroek, W. E. Hennink, and G. Storm, "Comparative transfection studies of human ovarian carcinoma cells in vitro, ex vivo and in vivo with poly(2-(dimethylamino)ethyl methacrylate)-based polyplexes.," *The journal of gene medicine*, vol. 1, no. 3, pp. 156–65, 1999.

[4] J. H. van den Berg, K. Oosterhuis, W. E. Hennink, G. Storm, L. J. van der Aa, J. F. J. Engbersen, J. B. a G. Haanen, J. H. Beijnen, T. N. Schumacher, and B. Nuijen, "Shielding the cationic charge of nanoparticle-formulated dermal DNA vaccines is essential for antigen expression and immunogenicity.," *Journal of Controlled Release*, vol. 141, no. 2, pp. 234–40, Jan. 2010.

[5] R. N. Palumbo, X. Zhong, D. Panus, W. Han, W. Ji, and C. Wang, "Transgene expression and local tissue distribution of naked and polymer-condensed plasmid DNA after intradermal administration in mice.," *Journal of controlled release : official journal of the Controlled Release Society*, vol. 159, no. 2, pp. 232–9, Apr. 2012.

[6] H. Yan and K. Tram, "Glycotargeting to improve cellular delivery efficiency of nucleic acids.," *Glycoconjugate journal*, vol. 24, no. 2–3, pp. 107–23, Apr. 2007.

[7] K. Drickamer, "Two distinct classes of carbohydrate-recognition domains in animal lectins.," *The Journal of biological chemistry*, vol. 263, no. 20, pp. 9557–60, Jul. 1988.

[8] M. E. Taylor, K. Bezouska, and K. Drickamer, "Contribution to ligand binding by multiple carbohydrate-recognition domains in the macrophage mannose receptor.," *The Journal of biological chemistry*, vol. 267, no. 3, pp. 1719–26, Jan. 1992.

[9] R. T. Lee and Y. C. Lee, "Affinity enhancement by multivalent lectin-carbohydrate interaction.," *Glycoconjugate journal*, vol. 17, no. 7–9, pp. 543–51, 2001.

[10] C. a Hoppe and Y. C. Lee, "Accumulation of a nondegradable mannose ligand within rabbit alveolar macrophages. Receptor reutilization is independent of ligand degradation.," *Biochemistry*, vol. 23, no. 8, pp. 1723–30, Apr. 1984.

[11] T. Ferkol, J. C. Perales, F. Mularo, and R. W. Hanson, "Receptor-mediated gene transfer into macrophages.," *Proceedings of the National Academy of Sciences of the United States of America*, vol. 93, no. 1, pp. 101–5, Jan. 1996.

[12] K. Wada, H. Arima, T. Tsutsumi, Y. Chihara, K. Hattori, F. Hirayama, and K. Uekama, "Improvement of gene delivery mediated by mannosylated dendrimer/alpha-cyclodextrin conjugates.," *Journal of controlled release : official journal of the Controlled Release Society*, vol. 104, no. 2, pp. 397–413, May 2005.

[13] H. Arima, Y. Chihara, M. Arizono, S. Yamashita, K. Wada, F. Hirayama, and K. Uekama, "Enhancement of gene transfer activity mediated by mannosylated dendrimer/alpha-cyclodextrin conjugate (generation 3, G3).," *Journal of controlled release : official journal of the Controlled Release Society*, vol. 116, no. 1, pp. 64–74, Nov. 2006.

[14] M. Hashimoto, M. Morimoto, H. Saimoto, Y. Shigemasa, H. Yanagie, M. Eriguchi, and T. Sato, "Gene transfer by DNA/mannosylated chitosan complexes into mouse peritoneal macrophages.," *Biotechnology letters*, vol. 28, no. 11, pp. 815–21, Jun. 2006.

[15] F. Leclercq, "Synthesis of glycosylated polyethylenimine with reduced toxicity and high transfecting efficiency," *Bioorganic & Medicinal Chemistry Letters*, vol. 10, no. 11, pp. 1233–1235, Jun. 2000.

[16] Y. H. Choi, F. Liu, J. S. Park, and S. W. Kim, "Lactose-poly(ethylene glycol)-grafted poly-L-lysine as hepatoma cell-tapgeted gene carrier.," *Bioconjugate chemistry*, vol. 9, no. 6, pp. 708–18, 1998.

[17] Y. Hattori and Y. Lu, "Enhanced DNA vaccine potency by mannosylated lipoplex after intraperitoneal administration," *Journal of Gene Medicine, The*, no. December 2005, pp. 824–834, 2006.

[18] K. Un, S. Kawakami, R. Suzuki, K. Maruyama, F. Yamashita, and M. Hashida, "Suppression of melanoma growth and metastasis by DNA vaccination using an ultrasound-responsive and mannose-modified gene carrier.," *Molecular pharmaceutics*, Jan. 2011.

[19] L. G. Salazar and M. L. Disis, "Cancer vaccines: the role of tumor burden in tipping the scale toward vaccine efficacy.," *Journal of Clinical Oncology*, vol. 23, no. 30, pp. 7397–8, Oct. 2005.

[20] R. S. Burke and S. H. Pun, "Extracellular barriers to in Vivo PEI and PEGylated PEI polyplex-mediated gene delivery to the liver.," *Bioconjugate chemistry*, vol. 19, no. 3, pp. 693–704, Mar. 2008.

[21] S. T. Reddy, A. J. van der Vlies, E. Simeoni, V. Angeli, G. J. Randolph, C. P. O'Neil, L. K. Lee, M. a Swartz, and J. a Hubbell, "Exploiting lymphatic transport and complement activation in nanoparticle vaccines.," *Nature biotechnology*, vol. 25, no. 10, pp. 1159–64, Oct. 2007.

[22] R. T. Lee, K. Drickamer, and Y. C. Lee, "Multivalent Ligand Binding by Serum Protein '," *Archives of Biochemistry and Biophysics*, vol. 299, no. 1, 1992.

[23] Y. Lee, "Carbohydrate-protein interactions: basis of glycobiology," *Accounts of chemical research*, vol. 28, no. 8, 1995.

[24] J. Chiefari, Y. (Bill) Chong,, and F. Ercole, "Living free-radical polymerization by reversible addition-fragmentation chain transfer: the RAFT process," vol. 9297, no. 2, pp. 5559–5562, 1998.

[25] A. B. Lowe, B. S. Sumerlin, and C. L. McCormick, "The direct polymerization of 2-methacryloxyethyl glucoside via aqueous reversible addition-fragmentation chain transfer (RAFT) polymerization," *Polymer*, vol. 44, no. 22, pp. 6761–6765, Oct. 2003.

[26] L. Albertin, M. H. Stenzel, C. Barner-Kowollik, L. J. R. Foster, and T. P. Davis, "Well-Defined Diblock Glycopolymers from RAFT Polymerization in Homogeneous Aqueous Medium," *Macromolecules*, vol. 38, no. 22, pp. 9075–9084, Nov. 2005.

[27] N.-Y. Xiao, A.-L. Li, H. Liang, and J. Lu, "A Well-Defined Novel Aldehyde-Functionalized Glycopolymer: Synthesis, Micelle Formation, and Its Protein Immobilization," *Macromolecules*, vol. 41, no. 7, pp. 2374–2380, Apr. 2008.

[28] J. Bernard, X. Hao, T. P. Davis, C. Barner-Kowollik, and M. H. Stenzel, "Synthesis of various glycopolymer architectures via RAFT polymerization: from block copolymers to stars.," *Biomacromolecules*, vol. 7, no. 1, pp. 232–8, Jan. 2006.

[29] Z. Deng, S. Li, X. Jiang, and R. Narain, "Well-Defined Galactose-Containing Multi-Functional Copolymers and Glyconanoparticles for Biomolecular Recognition Processes," *Macromolecules*, vol. 42, no. 17, pp. 6393–6405, Sep. 2009.

[30] O. Abdelkader, S. Moebs-sanchez, Y. Queneau, J. Bernard, E. Fleury, and D. Lyon, "Generation of Well-Defined Clickable Glycopolymers from Aqueous RAFT Polymerization of Isomaltulose-Derived Acrylamides," *Polymer*, vol. 49, pp. 1309–1318, 2011.

[31] G. Moad, Y. K. Chong, A. Postma, E. Rizzardo, and S. H. Thang, "Advances in RAFT polymerization: the synthesis of polymers with defined end-groups," *Polymer*, vol. 46, no. 19, pp. 8458–8468, Sep. 2005.

[32] A. J. Convertine, D. S. W. Benoit, C. L. Duvall, A. S. Hoffman, and P. S. Stayton, "Development of a novel endosomolytic diblock copolymer for siRNA delivery.," *Journal of Controlled Release*, vol. 133, no. 3, pp. 221–9, Feb. 2009.

[33] L. E. Iters, T. Ren, and D. Liu, "Synthesis of targetable cationic amphiphiles," *Tetrahedron Letters*, vol. 40, pp. 7621–7625, 1999.

[34] S. Kitazawa, M. Okumura, K. Kinomura, and T. Sakakibara, "Syntheses and properties of novel vinyl monomers bearing a glycoside residue," *Chemistry Letters*, vol. 19, no. 9, pp. 1733–1736, 1990.

[35] V. Bulmus, "A new pH-responsive and glutathione-reactive, endosomal membrane-disruptive polymeric carrier for intracellular delivery of biomolecular drugs," *Journal of Controlled Release*, vol. 93, no. 2, pp. 105–120, Dec. 2003.

[36] K.-C. Sheng, D. S. Pouniotis, M. D. Wright, C. K. Tang, E. Lazoura, G. a Pietersz, and V. Apostolopoulos, "Mannan derivatives induce phenotypic and functional maturation of mouse dendritic cells.," *Immunology*, vol. 118, no. 3, pp. 372–83, Jul. 2006.

[37] M. Shi, S. Hao, T. Chan, and J. Xiang, "CD4 ƨ T cells stimulate memory CD8 ƨ T cell expansion via acquired pMHC I complexes and costimulatory molecules , and IL-2 secretion Abstract : The rapid and efficient expansion of CD8 memory T cells after the second encounter undescribed role of active," *Journal of Leukocyte Biology*, 2006.

[38] M. P. Piechocki, S. a Pilon, and W. Z. Wei, "Complementary antitumor immunity induced by plasmid DNA encoding secreted and cytoplasmic human ErbB-2.," *Journal of immunology (Baltimore, Md. : 1950)*, vol. 167, no. 6, pp. 3367–74, Sep. 2001.

[39] M. Ahmed and R. Narain, "Progress of RAFT based polymers in gene delivery," *Progress in Polymer Science*, pp. 1–24, Sep. 2012.

[40] O. Boussif, F. Lezoualc'h, M. a Zanta, M. D. Mergny, D. Scherman, B. Demeneix, and J. P. Behr, "A versatile vector for gene and oligonucleotide transfer into cells in culture and in vivo: polyethylenimine.," *Proceedings of the National Academy of Sciences of the United States of America*, vol. 92, no. 16, pp. 7297–301, Aug. 1995.

[41] P. Dubruel, B. Christiaens, B. Vanloo, K. Bracke, M. Rosseneu, J. Vandekerckhove, and E. Schacht, "Physicochemical and biological evaluation of cationic polymethacrylates as vectors for gene delivery.," *European journal of pharmaceutical sciences : official journal of the European Federation for Pharmaceutical Sciences*, vol. 18, no. 3–4, pp. 211–20, Mar. 2003.

[42] R. A. Jones, M. H. Poniris, and M. R. Wilson, "pDMAEMA is internalised by endocytosis but does not physically disrupt endosomes.," *Journal of Controlled Release*, vol. 96, no. 3, pp. 379–91, May 2004.

[43] Y. Hu, T. Litwin, A. R. Nagaraja, B. Kwong, J. Katz, N. Watson, and D. J. Irvine, "Cytosolic Delivery of Membrane-Impermeable Molecules in Dendritic Cells Using pH-Responsive Core-Shell Nanoparticles," *Nano Letters*, 2007.

[44]   a Kichler, C. Leborgne, E. Coeytaux, and O. Danos, "Polyethylenimine-mediated gene delivery: a mechanistic study.," *The journal of gene medicine*, vol. 3, no. 2, pp. 135–44, 2001.

[45] S. Burgdorf, A. Kautz, V. Böhnert, P. a Knolle, and C. Kurts, "Distinct pathways of antigen uptake and intracellular routing in CD4 and CD8 T cell activation.," *Science (New York, N.Y.)*, vol. 316, no. 5824, pp. 612–6, Apr. 2007.

[46] K. Mahnke, M. Guo, S. Lee, H. Sepulveda, S. L. Swain, M. Nussenzweig, and R. M. Steinman, "The dendritic cell receptor for endocytosis, DEC-205, can recycle and enhance antigen presentation via major histocompatibility complex class II-positive lysosomal compartments.," *The Journal of cell biology*, vol. 151, no. 3, pp. 673–84, Oct. 2000.

[47] Y. H. Jeon, Y. Choi, J. H. Kang, J.-K. Chung, Y. J. Lee, C. W. Kim, J. M. Jeong, D. S. Lee, and M. C. Lee, "In vivo monitoring of DNA vaccine gene expression using firefly luciferase as a naked DNA.," *Vaccine*, vol. 24, no. 16, pp. 3057–62, Apr. 2006.

[48] J. J. Drabick, J. Glasspool-Malone, a King, and R. W. Malone, "Cutaneous transfection and immune responses to intradermal nucleic acid vaccination are significantly enhanced by in vivo electropermeabilization.," *Molecular therapy : the journal of the American Society of Gene Therapy*, vol. 3, no. 2, pp. 249–55, Feb. 2001.

[49] R. N. Palumbo, X. Zhong, and C. Wang, "Polymer-mediated DNA vaccine delivery via bystander cells requires a proper balance between transfection efficiency and cytotoxicity.," *Journal of controlled release : official journal of the Controlled Release Society*, vol. 157, no. 1, pp. 86–93, Jan. 2012.

[50] V. Manolova, A. Flace, M. Bauer, K. Schwarz, P. Saudan, and M. F. Bachmann, "Nanoparticles target distinct dendritic cell populations according to their size," *European journal of immunology*, vol. 38, no. 5, pp. 1404–13, May 2008.

[51]   S. T. Reddy, A. Rehor, H. G. Schmoekel, J. a Hubbell, and M. a Swartz, "In vivo targeting of dendritic cells in lymph nodes with poly(propylene sulfide) nanoparticles.," *Journal of controlled release : official journal of the Controlled Release Society*, vol. 112, no. 1, pp. 26–34, May 2006.

[52]   C. M. Rush, T. J. Mitchell, and P. Garside, "A detailed characterisation of the distribution and presentation of DNA vaccine encoded antigen.," *Vaccine*, vol. 28, no. 6, pp. 1620–34, Feb. 2010.

[53]   M. G. Carstens, M. G. M. Camps, M. Henriksen-Lacey, K. Franken, T. H. M. Ottenhoff, Y. Perrie, J. a Bouwstra, F. Ossendorp, and W. Jiskoot, "Effect of vesicle size on tissue localization and immunogenicity of liposomal DNA vaccines.," *Vaccine*, vol. 29, no. 29–30, pp. 4761–70, Jun. 2011.

[54]   B. Carrillo-Conde, E.-H. Song, A. Chavez-Santoscoy, Y. Phanse, A. E. Ramer-Tait, N. L. B. Pohl, M. J. Wannemuehler, B. H. Bellaire, and B. Narasimhan, "Mannose-functionalized 'pathogen-like' polyanhydride nanoparticles target C-type lectin receptors on dendritic cells.," *Molecular pharmaceutics*, vol. 8, no. 5, pp. 1877–86, Oct. 2011.

[55]   A. D. Bins, A. Jorritsma, M. C. Wolkers, C.-F. Hung, T.-C. Wu, T. N. M. Schumacher, and J. B. a G. Haanen, "A rapid and potent DNA vaccination strategy defined by in vivo monitoring of antigen expression.," *Nature medicine*, vol. 11, no. 8, pp. 899–904, Aug. 2005.

[56]   P. C. DeMuth, X. Su, R. E. Samuel, P. T. Hammond, and D. J. Irvine, "Nano-layered microneedles for transcutaneous delivery of polymer nanoparticles and plasmid DNA.," *Advanced materials (Deerfield Beach, Fla.)*, vol. 22, no. 43, pp. 4851–6, Nov. 2010.

[57]   J. Idoyaga, C. Cheong, K. Suda, N. Suda, J. Y. Kim, H. Lee, C. G. Park, and R. M. Steinman, "Cutting edge: langerin/CD207 receptor on dendritic cells mediates efficient antigen presentation on MHC I and II products in vivo.," *Journal of immunology (Baltimore, Md. : 1950)*, vol. 180, no. 6, pp. 3647–50, Mar. 2008.

[58]   J. Idoyaga, A. Lubkin, C. Fiorese, M. H. Lahoud, I. Caminschi, and Y. Huang, "Comparable T helper 1 (Th1) and CD8 T-cell immunity by targeting HIV gag p24 to CD8 dendritic cells within," *PNAS*, vol. 1, pp. 1–6, 2010.

[59]   C. Cheng, A. J. Convertine, P. S. Stayton, and J. D. Bryers, "Multifunctional triblock copolymers for intracellular messenger RNA delivery.," *Biomaterials*, vol. 33, no. 28, pp. 6868–76, Oct. 2012.

[60]   Z. Zhong, J. Feijen, M. C. Lok, W. E. Hennink, L. V Christensen, J. W. Yockman, Y.-H. Kim, and S. W. Kim, "Low molecular weight linear polyethylenimine-b-poly(ethylene glycol)-b-polyethylenimine triblock copolymers: synthesis, characterization, and in vitro gene transfer properties.," *Biomacromolecules*, vol. 6, no. 6, pp. 3440–8, 2005.

[61]   M. Bello-Roufaï, O. Lambert, and B. Pitard, "Relationships between the physicochemical properties of an amphiphilic triblock copolymers/DNA complexes and their intramuscular transfection efficiency.," *Nucleic acids research*, vol. 35, no. 3, pp. 728–39, Jan. 2007.

[62]   M. Oishi, K. Kataoka, and Y. Nagasaki, "pH-responsive three-layered PEGylated polyplex micelle based on a lactosylated ABC triblock copolymer as a targetable and endosome-disruptive nonviral gene vector.," *Bioconjugate chemistry*, vol. 17, no. 3, pp. 677–88, 2006.

[63]   K. Miyata, M. Oba, M. R. Kano, S. Fukushima, Y. Vachutinsky, M. Han, H. Koyama, K. Miyazono, N. Nishiyama, and K. Kataoka, "Polyplex micelles from triblock copolymers composed of tandemly aligned segments with biocompatible, endosomal escaping, and DNA-condensing functions for systemic gene delivery to pancreatic tumor tissue.," *Pharmaceutical research*, vol. 25, no. 12, pp. 2924–36, Dec. 2008.

[64]   R. Sharma, J. Lee, R. C. Bettencourt, C. Xiao, S. F. Konieczny, and Y.-Y. Won, "Effects of the incorporation of a hydrophobic middle block into a PEG-polycation diblock copolymer on the physicochemical and cell interaction properties of the polymer-DNA complexes.," *Biomacromolecules*, vol. 9, no. 11, pp. 3294–307, Nov. 2008.